UC Santa Barbara

UC Santa Barbara Electronic Theses and Dissertations

Title

Design and Development of Donor-Acceptor Stenhouse Adducts: A New Visible Light Activated Photochromic Compound

Permalink

https://escholarship.org/uc/item/1zv1q6vn

Author

Helmy, Sameh

Publication Date

2015

Peer reviewed|Thesis/dissertation

eScholarship.org Powered by the California Digital Library
University of California

UNIVERSITY OF CALIFORNIA

Santa Barbara

Design and Development of Donor-Acceptor Stenhouse Adducts: A New Visible Light Activated Photochromic Compound

A dissertation submitted in partial satisfaction of the

requirements for the degree Doctor of Philosophy

in Chemistry

by

Sameh Helmy

Committee in charge:

Professor Javier Read de Alaniz, Chair

Professor Mattanjah de Vries

Professor Liming Zhang

Professor Craig Hawker

June 2015

The dissertation of Sameh Helmy is approved.

_____

Craig Hawker

_____

Liming Zhang

_____

Mattanjah de Vries

_____

Javier Read de Alaniz, Committee Chair

April 2015

Design and Development of Donor-Acceptor Stenhouse Adducts:

A New Visible Light Activated Photochromic Compound

Copyright © 2015

by

Sameh Helmy

ACKNOWLEDGEMENTS

This work is dedicated in loving memory of my mother Abia Mohammed El Tayeb.

I would like to first thank my advisor, Javier Read de Alaniz, for his tireless support and guidance. He has taught me far more than chemistry, and helped me develop my beliefs and opinions on education and academic research. I am forever indebted for the opportunity you have provided me, and the wisdom you have passed along. Thank you for everything. And to all of the past and present members of the Read Group: thank you, it has been an honor to work and learn with you.

Second, I would like to thank Dr. Philip Hampton. I have learned more from you over the last seven years then I could have ever imagined. You have provided me with countless opportunities and endless guidance. I have been blessed to have you as a mentor and honored to call you my friend.

I wish to thank the friends who have stood beside me through this experience. Elis, you are the sister of my heart, I may not know what the future holds, but I know I can always count on you. To Saralynn, Zach, Apoorva, Lauren, Eric, Alex, Corey and Alicia, thanks for getting me off the couch and reminding me to have fun, I love you all.

VITA OF SAMEH HELMY

April 2014

EDUCATION

- Doctorate of Philosophy, Chemistry, University of California, Santa Barbara, CA, April 2015

- Bachelors of Science, Chemistry, California State University, Channel Islands, May 2010

PROFESSIONAL EMPLOYMENT

- June 2012-August 2014: Assistant Program Coordinator, California Alliance for Minority Participation-Summer Program, Materials Research Laboratory, University of California, Santa Barbara, CA

- August 2013-March 2015: Teaching Assistant-Organic Chemistry Laboratory, Department of Chemistry and Biochemistry, University of California, Santa Barbara, CA

- August 2012-September 2012: Invited Lecturer, School for Scientific Thought, Center for Science and Engineering Partnerships, University of California, Santa Barbara, CA

- August 2011-September 2011: Research Mentor, Summer Institute in Mathematics and Science, California NanoSystems Institute, University of California, Santa Barbara, CA

- May 2010-June 2010: Research Mentor, CSUCI HSI-STEM Summer Institute, California State University Channel Islands, CA

- May 2010-June 2010: Lecture and Laboratory Instructor, CSUCI HSI-STEM Summer Institute, California State University Channel Islands, CA

- August 2009-May 2010: Chemistry and Mathematics Tutor, CSUCI HSI-STEM, California State University Channel Islands, CA

- May 2009-May 2010: Student Research Assistant, CSUCI Alzheimer's Institute, California State University Channel Islands, CA

PUBLICATIONS AND PRESENTATIONS

- S. Helmy, F. A. Leibfarth, S. Oh, C. Hawker, and J. Read de Alaniz "Visible Light as a Stimulus for Organic Catalyst Recycling" *Manuscript Submitted to RSC Chem. Comm.*

- S. Helmy, S. Oh, F. A. Leibfarth, C. Hawker, and J. Read de Alaniz "Design and Synthesis of Donor-Acceptor Stenhouse Adducts: A Visible Light Photoswitch Derived from Furfural" *Journal of Organic Chemistry (DOI: 10.1021/jo502206g)*

- S. Helmy, F. A. Leibfarth, S. Oh, J. E. Poelma, C. Hawker, and J. Read de Alaniz "Photoswitching Using Visible Light: A New Class of Organic Photochromic Molecules" *Journal of the American Chemical Society (DOI:10.1021/ja503016b)*

- S. Helmy, J. Read de Alaniz "Cascade Rearrangement of Activated Furans Gives Access to an Undiscovered Photochromic Switch" Invited presentation to the Faculty of the Department of Chemistry, Ain Shams University, Cairo, Egypt at the National Institute for Research, Cairo, Egypt; January 5, 2012

- S. Helmy, P. Hampton "Reverse Phase Chromatography of Candy Coatings and the Teaching of the Scientific Method", Presented at the 43rd Western Regional Meeting of the ACS, Pasadena, CA, United States, November 10-12, 2011, WRM343

- S. Helmy, H. Baker, and P. Hampton "VIA-CI Project: Remote instrument operation and its impact on student learning", 239th ACS National Meeting, San Francisco, CA, United States, March 21-25, 2010 (2010), CHED-1606

- S. Helmy, and P. Hampton "Novel Routes to the Synthesis and Purification of Water Soluble Curcumin Derivatives", 239th ACS National Meeting, San Francisco, CA, United States, March 21-25, 2010 (2010), ORGN-310

HONORS AND FELLOWSHIPS

- 2012/13 UCSB MRL Award for Outstanding Service in Undergraduate Mentoring

- 2012/13 UCSB DCB Robert H. DeWolfe Oustanding Teaching Assistant in Organic Chemistry (Winter and Spring)

- 2011/12 UCSB DCB Robert H. DeWolfe Oustanding Teaching Assistant in Organic Chemistry (Fall and Winter)

- 2010-12 LSAMP Bridges to the Doctorate Fellowship

- 2010/11 UCSB Summer Doctoral Research Incentive Fellowship

- 2010/11 CSU Student Research Competition, First Place Award in Undergraduate Physical and Mathematical Sciences

- 2009/10 Sage Student Research Award for Excellence in Chemical Research

- 2009/10 Alzheimer's Institute Research Scholarship Recipient

- 2009/10 Channel Islands Alzheimer's Institute Summer Research Scholar

ABSTRACT

Design and Development of Donor-Acceptor Stenhouse Adducts:

A New Visible Light Activated Photochromic Compound

by

Sameh Helmy

The development of an easily synthesized, modular, and tunable organic photoswitch that responds to visible light has been a long-standing pursuit. Herein we provide a detailed account of the design and synthesis of a new class of photochromes based on furfural, termed donor−acceptor Stenhouse adducts (DASAs). A wide variety of these derivatives are easily prepared from commercially available starting materials, and their photophysical properties are shown to be dependent on the substituents of the push−pull system. Analysis of the switching behavior provides conditions to access the two structural isomers of the DASAs, reversibly switch between them, and use their unique solubility behavior to provide dynamic phase-transfer materials. Overall, these negative photochromes respond to visible light and heat and display an unprecedented level of structural modularity and tunabilty. We demonstrate the considerable potential of DASA photoswitches in two unique and powerful applications. First we have applied DASAs for the visible light-initiated recycling of homogeneous organic catalysts. This catalyst-photoswitch construct effectively polymerized lactide with control over molecular weight and a low PDI. The visible-light mediated phase

transfer and subsequent recovery of the thiourea catalyst allowed recycling of the organocatalyst. Further, the potential of these photoswitches in biological applications is demonstrated through the synthesis of a functional amphiphile that displays on-demand light-mediated disassembly and cargo release. This one-photon visible light-responsive micellar system served as an efficient, on-demand drug delivery system. The efficiency and effectiveness of this system was demonstrated in an in-vitro setting, delivering the chemotherapeutic paclitaxel only on exposure to visible light.

Table of Contents

LIST OF ABBREVIATIONS

Å	–	angstroms
λ_{max}	–	wavelength of maximum absorption
$\tau_{1/2}$	–	half-life of thermal recoloration
Φ_f	–	fluorescence quantum yield
[2.2]PC	–	[2.2]paracyclophane
4-TsOH	–	*para*-toluene sulfonic acid
Ac_2O	–	acetic anhydride
AcOH	–	acetic acid
aq.	–	aqueous
ATRP	–	atom transfer radical polymerization
BID	–	Bridged Imidazole Dimer
Boc_2O	–	di-*tert*-butyl dicarbonate
cat.	–	catalytic
CC	–	*cis*-*cis*
CD	–	circular dichroism
CMC	–	critical micelle concentration
CT	–	*cis*-*trans*
CuAAC	–	copper catalyzed azide-alkyne cycloaddition
CV	–	cyclic voltammetry
DABCO	–	1,4-diazabicyclo[2.2.2]octane
DASA	–	donor-acceptor Stenhouse adduct
DCC	–	*N,N′*-dicyclohexylcarbodiimide

DCE – 1,2-dichloroethane

DCM – dichloromethane

DHP – dihydropyridine

DIPEA – diethyl isopropyl amine

DLS – Dynamic light scattering

DMAP – 4-dimethylamino pyridine

DMF – dimethylformamide

DNA – deoxyribonucleic acid

DP – degree of polymerization

DPC – DASA-PEG conjugate

DPI – diphenylimidazole

DPIR – diphenylimidazoyl radical

Et_3N – triethylamine

Et_2O – diethyl ether

EtOH – ethanol

eq. – equivalents

Fc – ferrocene

FVP – flash vacuum pyrolysis

GFP – green fluorescent protein

GPC – gel permeation chromatography

HABI – hexaarylbiimidazole

HOMO – highest occupied molecular orbital

HPLC – high performance liquid chromatography

HRXPS – high resolution X-ray photoelectron spectroscopy

ImMNPs – imidazoline-functionalized magnetic nanoparticles

LUMO – lowest unoccupied molecular orbital

MCF-7 – Michigan Cancer Foundation-7

MeCN – acetonitrile

MeOH – methanol

MesMgBr – mesityl magnesium bromide

MNPs – magnetic nanoparticles

MS – mass spectrometry

MW – microwave

n-BuLi – *n*-butyllithium

NaOAc – sodium acetate

NH_4OAc – ammonium acetate

NDPI – naphthalene diphenylimidazole

NDPIR – 2-(1-naphthyl)-4,5-diphenylimidazoyl radical

NIR – near infrared

NMR – Nuclear Magnetic Resonance

ODCB – *ortho*-dichlorobenzene

ORTEP – Oak Ridge Thermal Ellipsoid Plot

PDI – polydispersity index

Pd-MNPs – palladium-functionalized magnetic nanoparticles

PEG – poly(ethylene glycol)

PhMe – toluene

PI – phenanthroimidazole

PIR – phenanthroimidazoyl radical

PLA – polylactic acid

PMDETA – pentamethyldiethylenetriamine

PPh_3 – triphenylphosphine

PSB – protonated Schiff base

PSS – photostationary state

RI – refractive index

RP – radical pair

rt – room temperature

SWV – square wave voltammetry

$TBAPF_6$ – tetrabutyl ammonium hexafluorophosphate

t-BuLi – *tert*-butyllithium

TC – *trans-cis*

TFA – trifluoroacetic acid

tF-BDPI-2Y – 1,4-bis(4,5-diphenylimidazol-2-ylidene

TGA – thermogravimetric analysis

THF – tetrahydrofuran

TMDPI – tetramethoxy diphenylimidazole

TPI – triphenylimidazole

TPID – triphenylimidazole dimer

TPIR – 2,4,5-triphenylimidazolyl radical

TT – *trans-trans*

UV – Ultra Violet

V_h – hydrodynamic volume

Vis – visible

XPS – X-ray photoelectron spectroscopy

LIST OF FIGURES

Chapter 1

Chapter 2

Chapter 4

Chapter 5

LIST OF SCHEMES

Chapter 1

Chapter 2

Chapter 3

Chapter 4

Chapter 5

LIST OF TABLES

Chapter 1

Chapter 2

Chapter 3

Chapter 4

Chapter 5

1. Organic Photochromism

1.1. Historical Perspective

The phenomenon of photochromism was first reported by Fritsche in 1867, when he observed that a red solution of tetracene **1** bleached on exposure to sunlight, and recolored when held in the dark (Figure 1). In 1899, Markwald observed the reversible color change of 2,3,4,4-tetrachloronapthalen-1(4*H*)-one **2** in the solid state (Figure 1).[1]

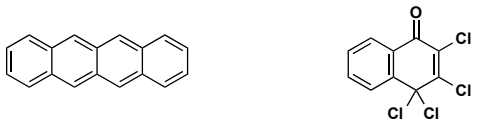

1 2

Figure 1. Organic photochromic molecules reported by Fritsche and Markwald.

In the 150 years since its initial discovery, research in the field of organic photochromism has occurred in waves. Until the 1940s, interest in photochromism was steady yet limited. It would take the development of advanced analytical techniques (UV-visible, NMR, time-resolved spectroscopies and flash photolysis) to drive the boom in synthetic and mechanistic studies on photochromism that occurred through 1940-1960.[1] It would be during this period that Hirshberg, in 1950, coined the term photochromism [from the Greek *phos*(light) and *chroma*(color)], which is used to this day to describe this behavior. Yet, despite this interest, and early applications such as the photochromic micro imaging process, the photodegradation of these compounds limited their potential for applications. While photochromism is a nondestructive process, side reactions (primarily oxidation) can occur, leading to chemical degradation of the material with concomitant loss of performance over time and repeated cycling. A new renaissance of photochromic research was seen in the 1980s, with the discovery of highly fatigue resistant systems, including spirooxazines,[2] diarylethenes,[3]

chromenes,[4] and their derivatives, which led to commercial applications such as photochromic lenses, optical filters, and optical recording.

Photochromism is defined as a "reversible transformation of a chemical species induced in one or both directions by absorption of electromagnetic radiation between two forms, A and B, having different absorption spectra" (Figure 2a). Thus the thermodynamically stable form A is transformed to form B, the back reaction of which can occur thermally (type T photochromism) or photochemically (type P photochromism). The overwhelming majority of organic photochromic systems involve unimolecular processes of a colorless form A converting to a colored form B. This is known as *positive photochromism*. When $\lambda_{max}(A)>\lambda_{max}(B)$ the processes is termed *negative, inverse,* or *reverse photochromism* (Figure 2b).

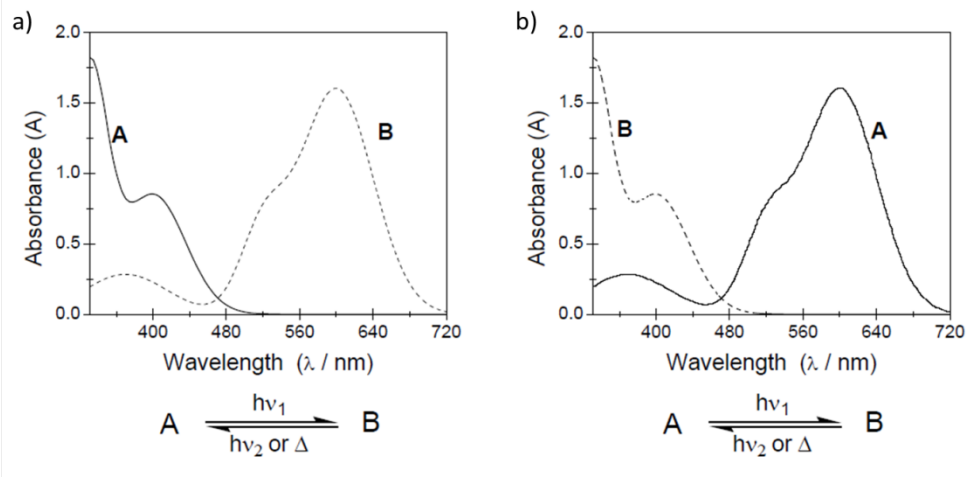

Figure 2. Representative spectra of a) normal and b) reverse photochromism.

Over thirteen classes of organic photochromic compounds have been identified (Figure 3). Of these the preponderance of research has focused on the three 'privileged' classes, spiropyrans/sprioxanzines **3/4**, diarylethenes **9**, and azo-compounds **13**; with efforts primarily focused on derivatizing and tailoring these systems to specific applications. Further, only

two reports disclose negative photochromism in organic systems, with minimal investigation into their properties and no efforts toward application.[5,6]

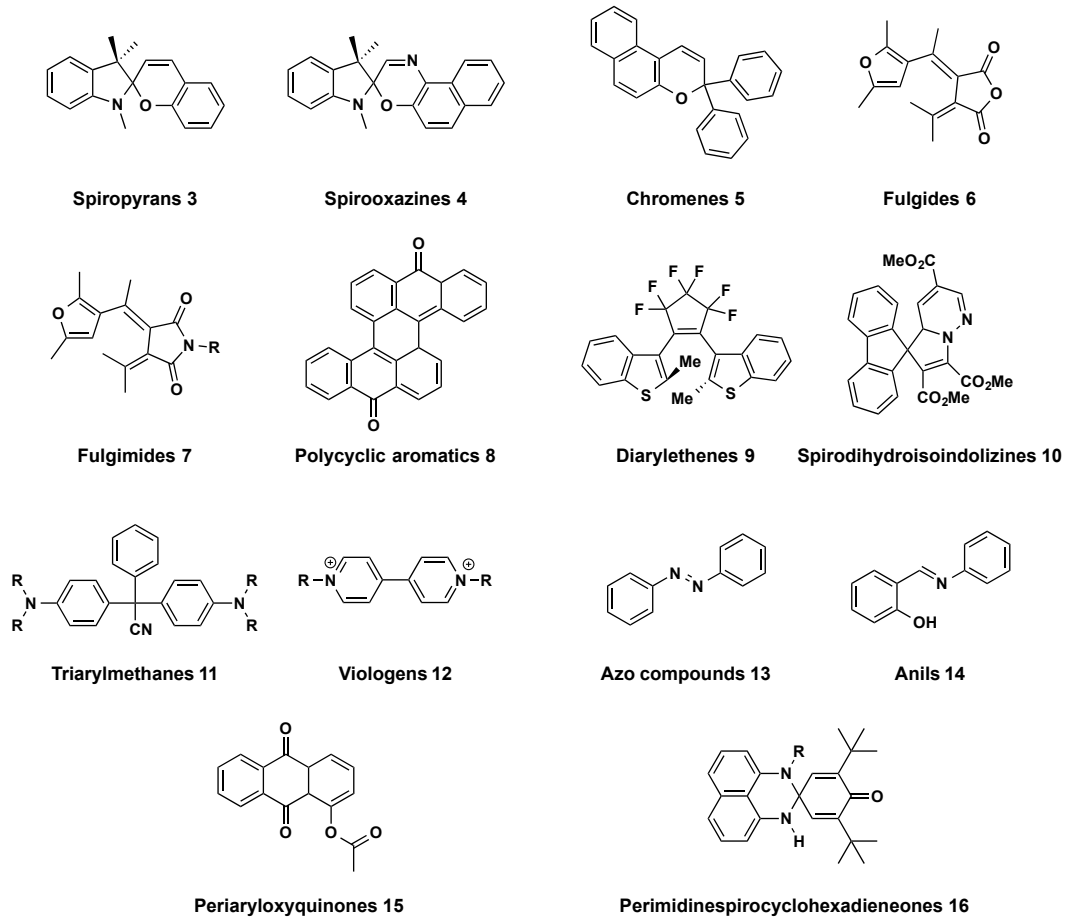

Figure 3. Representative members of known classes of organic photochromic compounds

Interest in adaptable and responsive systems has led to significant effort in the chemistry of organic photochromic compounds. The ability of organic photochromes to undergo reversible spectral and physical property changes has led to applications ranging from energy production, chemical sensing, and molecular actuators to biological systems.[7] These switches are particularly valuable as their property changes are triggered by light, the most widely available, non-invasive and environmentally benign external stimulus. The driving force for this focus is the abundant and versatile nature of light as a stimulus, which provides unique opportunities for spatial and temporal resolution.

Heterocyclic moieties have a rich and potent history in the field of organic photochromism, as demonstrated by the abundance of work devoted to dithienylethenes[3,8] **9**, spiropyrans **3** and spirooxazines **4**.[2,9] Indeed since their discovery, there has been such a boom in the work related to these classes that there exists a plethora of not only primary but also secondary literature covering ongoing developments in the control of their properties and applications. While these two classes have dominated the field of photochromic heterocycles, recent years have seen the introduction and development of several promising new organic photochromes and the revival of known, yet underdeveloped, classes. Because the "privileged" photochromes have been extensively reviewed, the following section will focus on highlighting the new organic photochromes.

1.2. Recent Advances

1.2.1. Bridged Imidazole Dimers

Increasing the switching rates, specifically thermal bleaching, of photochromic systems is critical for their adoption in applications such light modulation or optical data processing. Abe and coworkers have developed a family of bridged imidazole dimers (BIDs), based on the hexaarylbiimidazole (HABI) framework.[10] These materials demonstrate instantaneous coloration, however, through rational molecular design their half-life of thermal back reaction can be reduced to as low as 35μs. This rapid thermal bleaching allows for precise spatial control over coloration, since the bleaching kinetics exceed diffusion of the colored species. As will be discussed, between their ease of synthesis, diverse molecular design and unprecedented bleaching performance this class of photochromic compounds is promising for applications in high performance ophthalmic lenses and revolutionary optical switching devices.

1.2.1.1. Background

Since being first reported in 1960 by Hayashi and Meada, hexaarylbiimidazole (HABI) has garnered great attention due to its unique properties.[10] HABI is cleaved into a pair of 2,4,5-triphenylimidazolyl radicals (TPIRs) by various stimuli (light, pressure, or heat); this radical pair (RP) thermally recombines to regenerate the original dimer (Scheme 1). Hayashi and Meada were the first to specifically observe that in either the solution or solid state, HABI developed a deep red-violet color on irradiation, which faded slowly for the solid and rapidly in solution. This photochromic behavior is a result of the homolytic cleavage of the C-N bond between the two imidazole rings.[11] While the photo-induced cleavage of HABI to TPIRs occurs near instantaneously, the thermal regeneration of HABI by radical recombination of TPIRs in solution requires several minutes as radical-radical reactions generally obey second order kinetics. Thus while these systems have seen widespread adoption as photoinitiators for polymerization or imaging materials, their relatively slow rate of thermal bleaching has limited their use in photochromic applications.[12]

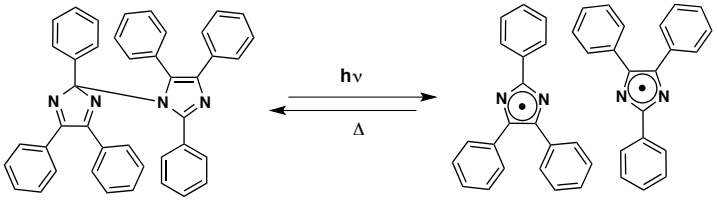

Scheme 1. Photochromism of HABI.

To better understand how this radical recombination could be tamed, Abe and coworkers examined the behavior of the TPIR derivative tF-BDPI-2Y **21** (1,4-bis(4,5-diphenylimidazol-2-ylidene), shown in Figure 4.[13] tF-BDPI-2Y **21** dimerizes to the photochromic tF-BDPI-2YD **20** at room temperature, this dimer cleaves to the original RP **21** on irradiation with 360 nm light (Figure 4). The tF-BDPI-2Y RP **21** is stable in solution at room

temperature and thermal recombination to tF-BDPI-2YD **20** occurs over two days at room temperature in the dark. Thus, a fast thermal bleaching photochromic molecule could be developed on the basis of a virtual one photon reaction of tF-BDPI-2YD **20**, where in this case the TPIR-RP **19** would immediately recombine as the RP is restricted in it its diffusion. Abe and coworkers used this design principle to develop their Bridged Imidazole Dimer (BID) class of photochromic compounds.

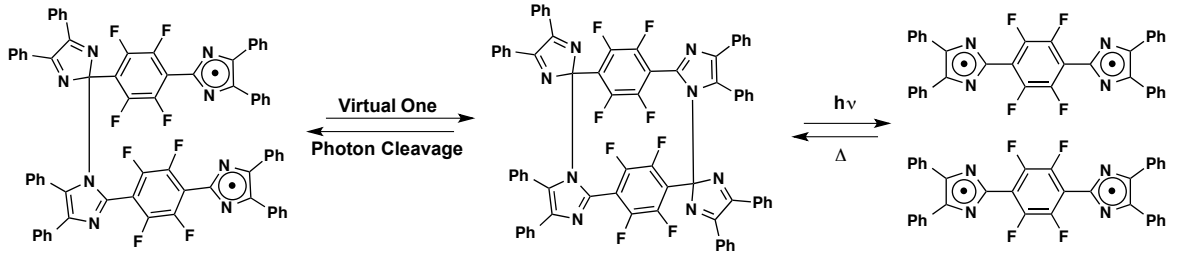

Figure 4. Photochromism and virtual one photon cleavage of tF-BDPI-2Y.

1.2.1.2. Synthesis

Two major subclasses of BIDs have been developed, naphthalene bridged dimers and [2.2]paracyclophane bridged dimers. As outlined in Scheme 2, the synthesis of naphthalene BIDs begins with the cyclocondensation of a 1,2-diaryl-β-diketone **23**, aryl aldehyde **22** and ammonium acetate, to generate the 2,4,5-triarylimiazole **24**.[14] Typically the aryl aldehyde employed bears a boronic acid or ester moiety to facilitate Suzuki coupling to the naphthalene bridge **25**. At this stage the imidazole moieties are oxidized by basic potassium ferricyanide in the absence of light generating the bridged radical pair **27**, which instantly dimerize to the photochromic BID **28**. For naphthalene BIDs, structural diversity is introduced in the choice of aryl aldehyde and 1,2-diaryl-β-diketone, allowing control over thermal bleaching and wavelength of activation.

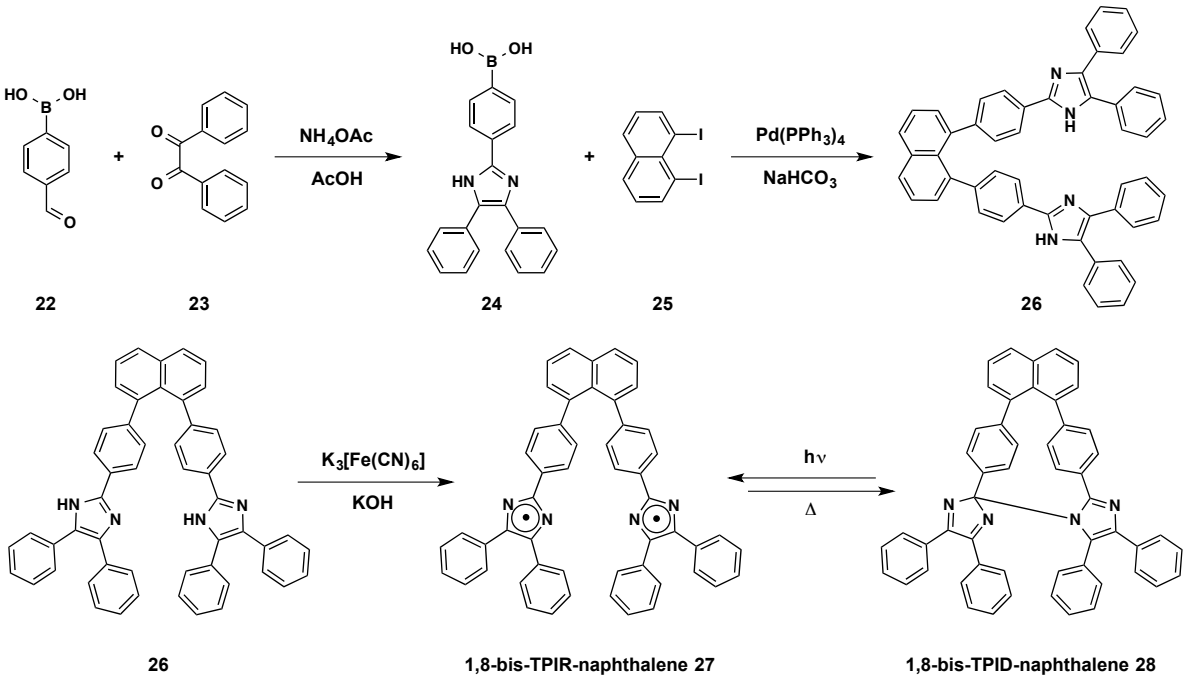

Scheme 2. Synthesis and photochromism of 1,8-bis-TPID-naphthalene.

Further, chiroptical switching can be achieved by using 4-formylnaphthylboronic acid **29** as one of the two aryl aldehydes employed, Scheme 3.[15] Sequential Suzuki coupling of the naphthyldiphenyl imidazole **30** to the naphthalene linker **25**, followed by coupling to a triphenyl imidazole **24**, oxidation and dimerization, provides 1-NDPI-8-TPI-napthalene **34**. The BIDs produced in this fashion exhibit axial chirality due to the binaphthyl moiety generated in their synthesis.

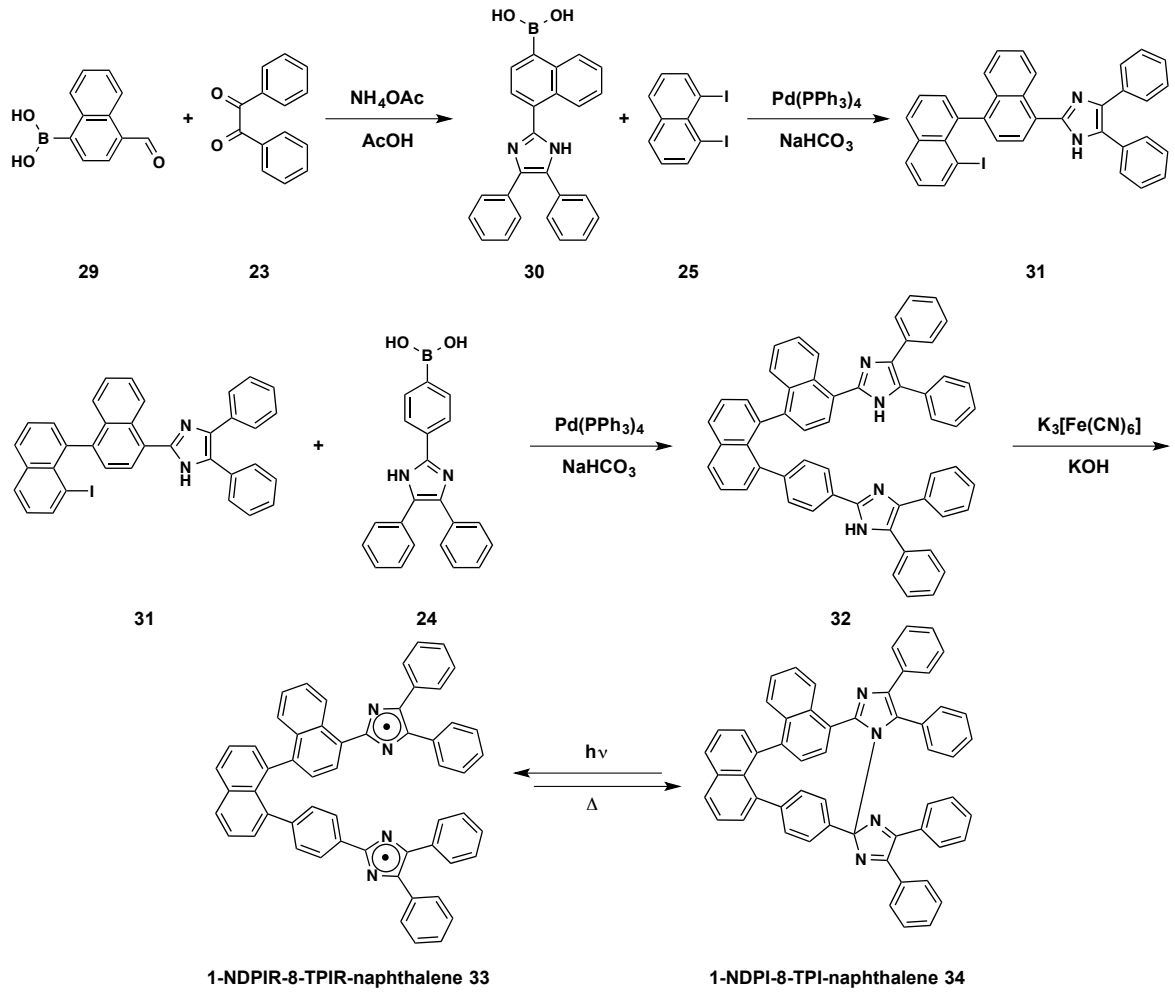

Scheme 3. Synthesis and photochromism of 1-NDPI-8-TPI-napthalene.

Alternately a di-aldehyde bridging linker can be employed directly in the cyclocondensation reaction, as is the case with [2.2]paracyclophane bridged derivative *pseudogem*-bis-DPI[2.2]PC, Scheme 4.[16] Here the synthetic path is highly streamlined compared to the preparation of naphthalene-bridged dimers. The initial cyclocondensation occurs between the paracyclophane linker **35**, 1,2-diaryl-β-diketone **23** and ammonium acetate providing the bridged imidazole pair **36**, which undergoes oxidation and dimerization to provide the desired BID **38**. Here structural diversity is introduced by variations in the 1,2-diaryl-β-diketones employed. Indeed, the cyclocondensation can be performed step-wise to provide asymmetric [2.2]paracyclophane BIDs.[17]

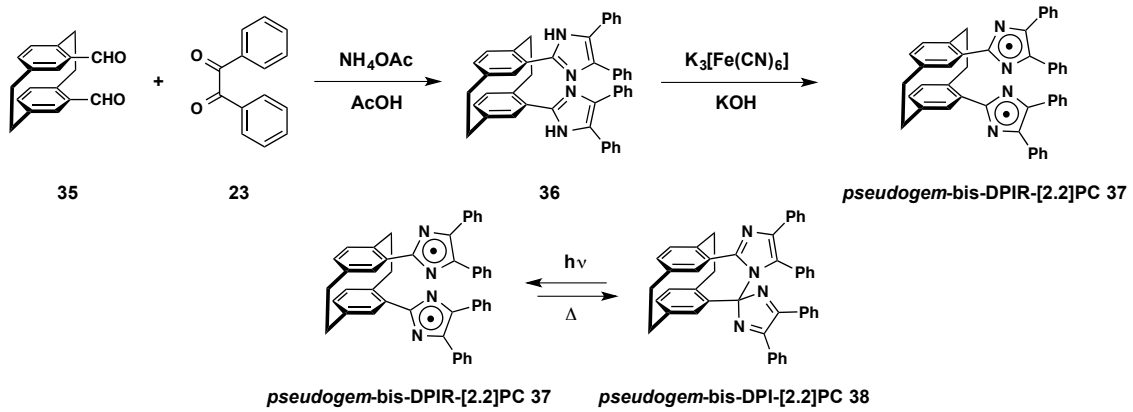

35 23 36 *pseudogem*-bis-DPIR-[2.2]PC 37

pseudogem-bis-DPIR-[2.2]PC 37 *pseudogem*-bis-DPI-[2.2]PC 38

Scheme 4. Synthesis and Photochromism of *pseudogem*-bis-DPI[2.2]paracyclophane.

The inherent modularity of these synthetic pathways enables rapid structural diversification of the BID. Control over thermal bleaching kinetics is affected by the choice of bridging linker, while structural and electronic diversification of the TPID moiety can effect the thermal bleaching rate through steric control and the wavelength of irradiation that triggers formation of the bridged TPIR, respectively.

1.2.1.3. Photochromism and Related Properties

1.2.1.3.1. Naphthalene BIDs

As with all HABI derivatives 1,8-bis-TPID-naphthalene **28** (Scheme 2) is cleaved by light to form 1,8-bis-TPIR-naphthalene **27**, which displays an intense absorption band with λ_{max} = 585 nm and a shoulder band with absorption maximum at ~620 nm extending beyond 750 nm.[14] Combined, these result in a green coloration of the 1,8-bis-TPIR-naphthalene RP **27** in solution. Unlike HABI **17**, the RP of 1,8-bis-TPIR-naphthalene **28** cannot diffuse in solution to give free radicals. Compared to the long thermal recombination rates for HABI **17**, which follow second order kinetics, thermal bleaching of 1,8-bis-TPIR-naphthalene **27** follows first order kinetics with a half-life of 730 ms at room temperature. After this dramatic enhancement, a second type of naphthalene bridged dimer, 1-NDPI-8-TPI-napthalene

34 (Scheme 3), was prepared, bearing two different TPIR moieties, 2-(1-naphthyl)-4,5-diphenylimidazoyl radical (NDPIR) and TPIR.[18] The colored RP of 1-NDPI-8-TPI-napthalene **34** gives superposed absorption spectra covering the entire visible range. The TPIR moiety giving absorbance from 500 to 600 nm and the NDPIR moiety absorbing from 550 to 900 nm, in addition to the sharp band at ~ 460 nm, giving 1-NDPIR-8-TPIR-napthalene **33** a green color in solution. Under continuous UV irradiation 1-NDPI-8-TPI-napthalene **34** achieves the photostationary colored state rapidly. Thermal bleaching of the RP, here again, follows first order kinetics, with a half-life of 230 ms at room temp. Interestingly it is not known why the thermal bleaching kinetics of 1-NDPI-8-TPI-napthalene **34** is accelerated over 1,8-bis-TPI-napthalene **28**. Still, naphthalene-BIDs were the first photochromic compounds to achieve these remarkable thermal bleaching rates.

1-NDPI-8-TPI-napthalene **34** is axially chiral resulting from the 1,1`-binaphthyl framework established in its preparation, and crystallographic analysis confirms that both enantiomers are present in the racemic crystal. Axially chiral binaphthalenes show large optical rotation values and strong circular dichroism (CD), dependent on their dihedral angle. Chiroptical switches are chiral molecules whose chiral properties can be modulated using light.[19] The racemic mixture of 1-NDPI-8-TPI-napthalene **34** was separated by HPLC provided each enantiomer in 96% ee. As the thermal half-life of 1-NDPIR-8-TPIR-napthalene **34** is too short to measure its CD spectrum at room temperature, the CD spectra were collected at 200 K to retard the rate of thermal recombination. Consistent with axially chiral binaphthyls, 1-NDPI-8-TPI-napthalene **34** exhibits the strong Cotton effect at less than 400 nm.[20] Further, the CD spectrum of the colored form of each enantiomer is different from the parent. Each enantiomer of the RP displays mirror image CD bands in the visible region,

where the racemic RP absorbs, indicating that the electronic transitions of the radical pair are optically active.

Chiral RPs generated in close proximity, recombine with high stereoselectivity if diffusion of the radical pair can be inhibited, as Stowell et al. have reported.[21] For 1-NDPI-8-TPI-napthalene **34** photo-racemization does not occur as the radical pair is covalently bridged. Chiral HPLC analysis confirmed that no racemization occurs from the photochromic reaction. This is the first example of a reversible photogenerated chiral RP.

1.2.1.3.2. [2.2]paracyclophane BIDs

While the intensity of coloration and rapid thermal bleaching of naphthalene-BIDs are acceptable for applications such as ophthalmic lenses, these rates are still unsatisfactory for real-time image processing application. Indeed, on cessation of irradiation of naphthalene-BIDs, an afterimage persists for ~1 s and can be observed by the naked eye. Thus to further increase the thermal bleaching rate, the RP must be more closely spaced together. To achieve this a new BID *pseudogem*-bis-DPI[2.2]paracyclophane **38** (Scheme 4) was designed and prepared, with a paracyclophane bridge that more tightly couples the photogenerated RP.[16]

On irradiation with 355 nm light, *pseudogem*-bis-DPI[2.2]PC **38** photochromically transforms to *pseudogem*-bis-DPIR[2.2]PC **37** developing a blue color in both the solid state and in solution. The radical pair displays a sharp absorption band at 400 nm and a broad absorption from 500 to 900 nm. Again here, the thermal bleaching obeys first order kinetics, the RP having a half-life of 33 ms at room temperature. Unlike naphthalene-BIDs, *pseudogem*-bis-DPI[2.2]PC **38** does not suffer from an after-image on cessation of irradiation, as complete bleaching in solution is achieved within 200 ms. While it is difficult for the human eye

to detect a phenomenon faster than 10 ms, the lifetime of *pseudogem*-bis-DPIR[2.2]PC **37** is in the tens of milliseconds, and can potentially applied to real-time image processing applications.

The stability of *pseudogem*-bis-DPIR[2.2]PC **37** is a result of the inhibition of diffusion of the RP. Yet a further acceleration of the thermal bleaching is necessary for practical use in fast light modulators. Here a modular approach can be taken in the synthesis of [2.2]PC-BIDs, allowing for stepwise formation of the imidazole rings. This approach allows for the rational design to control the thermal bleaching rate. To further accelerate thermal bleaching of [2.2]PC-BIDs, the colored state would need to be destabilized. As shown in Scheme 5 (below), *pseudogem*-DPI-PI[2.2]PC **43** couples a diphenylimidazole group with a phenanthroimidazole group bridged by the PC linker.[17] Here steric repulsion between the rigid phenanthroimidazole group and the phenyl rings of the DPI moiety destabilize the RP (**42)**. Indeed on irradiation with UV light no color change is observed for a solution of *pseudogem*-DPI-PI[2.2]PC **43** at room temperature, while at liquid nitrogen temperatures the solution changes from clear to blue when irradiated. Here thermal back reaction of the photogenerated *pseudogem*-DPIR-PIR[2.2]PC **42** exceeds the ability of the naked eye to detect coloration at room temperature. The absorption of *pseudogem*-DPIR-PIR[2.2]PC **42** displays a sharp absorption at 400 nm and broad absorption from 450 to 1000 nm, nearly identical to that of *pseudogem*-bis-DPI[2.2]PC **38**. In contrast the half-life of thermal bleaching for *pseudogem*-DPIR-PIR[2.2]PC **42** is 35 μs at room temperature, a 1000 fold acceleration over *pseudogem*-bis-DPI[2.2]PC **38** while maintaining its optical density in the colored state. This behavior demonstrates that destabilizing the nascent RP can dramatically enhance the

thermal bleaching rate. This approach is not limited to using the steric effect, as an electronic effect can be introduced by substituents in appropriately selected 1,2-diaryl-β-diketones.[22]

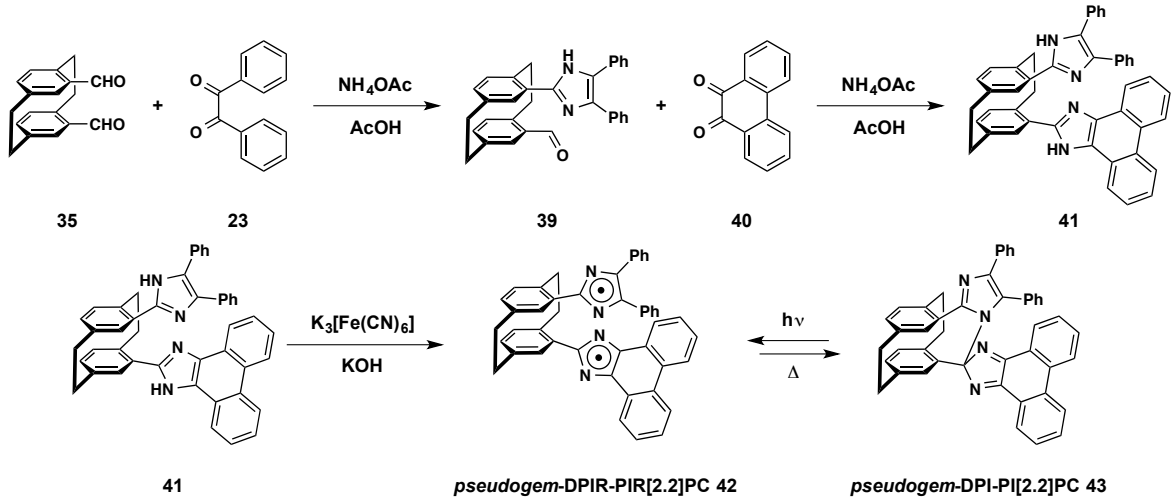

Scheme 5. Synthesis and Photochromism of *pseudogem*-DPIR-PIR[2.2]PC.

While these accelerations are a remarkable achievement, as the thermal bleaching rate increases the color of the photostationary equilibrium becomes lighter, due to the difficulty in increasing the stationary concentration of the colored species. A possible approach to overcome this limitation is to improve the sensitivity of the colorless state to a broader spectrum of irradiation. In regards to the first generation [2.2]PC-BID (**38**), its photosensitivity is poor as it lacks a sufficient absorption band in the UVA region of irradiation. To increase the photosensitivity of [2.2]PC-BIDs, *pseudogem*-bis-TMDPI[2.2]PC **44** was developed which undergoes photochromic reaction under sunlight.[22]

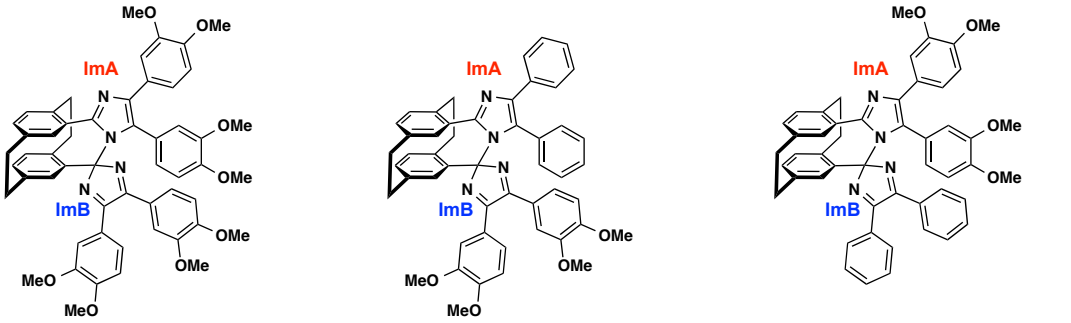

Figure 5. [2.2]PC-BIDs with enhanced photosensitivity.

The two imidazole rings of *pseudogem*-bis-TMDPI[2.2]PC **44**, ImA (red) and ImB (blue), are inequivalent in their electronic nature. As shown in Figure 5, ImA is a planar, resonant moiety with bond lengths typical of a 6π system with electron-donating properties. In contrast, ImB bears an sp^3 carbon connecting to ImA and two localized C=N double bonds. ImB's structure is consistent with a 4π electronic system having electron-withdrawing properties. Based on TDDFT, the absorption of *pseudogem*-bis-TMDPI[2.2]PC **44** is attributed to intramolecular charge-transfer from ImA to ImB. To further understand the nature of the CT characteristics and the photochromic behavior of *pseudogem*-bis-TMDPI[2.2]PC **44**, two related derivatives were prepared and examined to ascertain the molecular design principles for enhancing photosensitivity.[23]

Pseudogem-DPI-TMDPI[2.2]PC **45** and *pseudogem*-TMDPI-DPI[2.2]PC **46** are shown in Figure 5. In *pseudogem*-DPI-TMDPI[2.2]PC **45** the dimethoxyphenyl groups are attached to electron withdrawing ImB and in *pseudogem*-TMDPI-DPI[2.2]PC **46** they are attached to electron donating ImA. *pseudogem*-DPI-TMDPI[2.2]PC **45** exhibits the desired UVA absorption band, where *pseudogem*-TMDPI-DPI[2.2]PC **46** does not. In *pseudogem*-TMDPI-DPI[2.2]PC **46**, the intramolecular CT transition form the electron donating dimethoxyphenyl substituents to electron withdrawing ImB is predicted to have a small oscillator strength, as there is little overlap between the molecular orbitals delocalized over the dimethoxyphenyl rings and ImB. Thus photosensitivity is enhanced by electron donating substituents attached to the phenyl rings of electron withdrawing ImB. Oxidation of the precursor of both *pseudogem*-DPI-TMDPI[2.2]PC **45** and *pseudogem*-TMDPI-DPI[2.2]PC **46** gives a mixture of the two compounds. While both *pseudogem*-DPI-TMDPI[2.2]PC **45** and

pseudogem-TMDPI-DPI[2.2]PC **46** undergo photochromic reaction, repeated cycling of either isomer in its pure state ultimately regenerates a mixture of the two species.

The rapid thermal bleaching of bridged imidazole dimers allows for precise spatial control over coloration, since the bleaching kinetics exceed diffusion of the colored species. Between their ease of synthesis, diverse molecular design and unprecedented bleaching performance Abe and coworkers have used rational design to develop a class of photochromic compounds that are promising for applications in high performance ophthalmic lenses and revolutionary optical switching devices.

1.2.2. Chromene Based Systems

Photochromic benzo and naphthopyrans (Figure 6: **47**-**50**), commonly referred to as chromenes, have been widely applied as reversible coloring agents for ophthalmic lenses since the early 1990s. The studies by several companies to develop benzo and naphthopyrans that offer complementary colors (from yellow to orange) to the more established indolinospironaphthoxazines (blue) led to a great number of patents published through out that decade. In recent years, there has been a renewed interest in this class of organic photochromic compound, specifically, in controlling the rate of thermal bleaching, and improving the synthetic routes to access these materials. Several strategies to meet these ends have been developed and led to unique discoveries regarding this class.

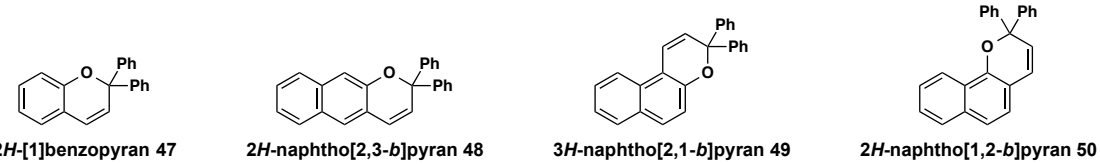

2*H*-[1]benzopyran 47 2*H*-naphtho[2,3-*b*]pyran 48 3*H*-naphtho[2,1-*b*]pyran 49 2*H*-naphtho[1,2-*b*]pyran 50

Figure 6. Photochromic chromenes.

1.2.2.1. Background

From their initial discovery in the 1960s through the mid 1980s, research on photochromic benzo (**47**) and naphthopyrans (**48**-**50**) (Figure 5) was limited and their use in applications rare.[4] These limitations were primarily due to the early literature on chromenes being rife with misinformation. Specifically, Wizinger and Wenning incorrectly reported the synthesis of 3,3-diphenyl-3*H*-naphtho[2,1-*b*]pyran **49** from 2-hydroxy-1-naphthaldehyde **51** and diphenylethylene **52**.[24] This error would be corrected 20 years later when Livingston and coworkers identified the product as 8,8,10,10-tetraphenyl-7a,9,10,10a-tetrahydro-8*H*-cyclopenta[*b*]naphtho[1,2-*d*]furan **53**, Scheme 6.[25]

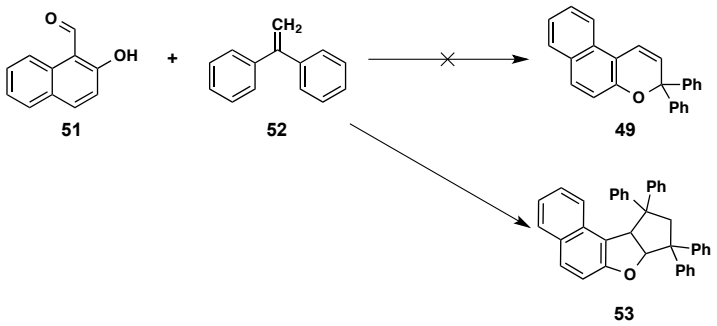

Scheme 6. Synthesis and misidentification of 8,8,10,10-tetraphenyl-7a,9,10,10a-tetrahydro-8*H*-cyclopenta[*b*]naphtho[1,2-*d*]furan.

Unfortunately in 1954, six years prior to this correction, Hirshberg and Fischer would report that naphtho[1,2-*d*]furan **53**, the compound assumed to be 3,3-diphenyl-3*H*-naphtho[2,1-*b*]pyran **49**, was not photochromic.[26] Finally in 1966, Becker and Michl reported the photochromism of 2*H*-1-benzopyrans, investigating over 25 derivatives, and presenting for the first time some of the effects of structural variation on photochromic behavior.[27] In the mid 1970s, Padwa and coworkers would provide valuable insights into the structural considerations that affected fatigue resistance in chromenes.[28]

Traditionally benzopyrans exhibit weak photochromic behavior and have received little attention.[27] Naphthopyrans exhibit more intense color and increased lifetimes, which are further improved by *gem* diaryl substitution adjacent to the pyran oxygen. Of the three isomeric naphthopyrans, the linear 2*H*-naphtho[2,3-*b*]pyran **48** exhibits negligible photochromic behavior at ambient temperature, as the photochromic reaction disrupts the aromaticity of both rings of the naphthalene fragment. The angular isomers, 2*H*-naphtho[1,2-*b*]pyran **50** and 3*H*-naphtho[2,1-*b*]pyran **49**, display good to excellent photochromic response under ambient conditions.[4] The major differences between the two angular isomers being that the open form tautomer of the [1,2-*b*] isomer absorbs more strongly, exhibits two absorption bands in the visible region, and has a significantly longer lifetime after continuous irradiation.

1.2.2.2. Synthesis

The older more traditional synthetic routes for benzopyrans can generally be applied to the synthesis naphthopyrans and will be considered together. The reaction of aryl Grignard reagents with coumarins, while effective, results in significant byproduct formation and low to moderate yields, Scheme 7A.[29] 2,2-Dialkyl and 2-alkyl-2-aryl-benzopyrans are easily prepared by the reduction and dehydration of dihydrobenzopyran-4-ones, which are readily obtained from 2`-hydroxyacetophenones and ketones, Scheme 7B.[30] However, this route is ineffective for the preparation of 2,2-diaryl-benzopyrans as the initial condensation reaction, between the acetophenone and a diaryl-ketone, suffers from extremely low yields even when *t*-butoxide used as the condensing reagent.[31]

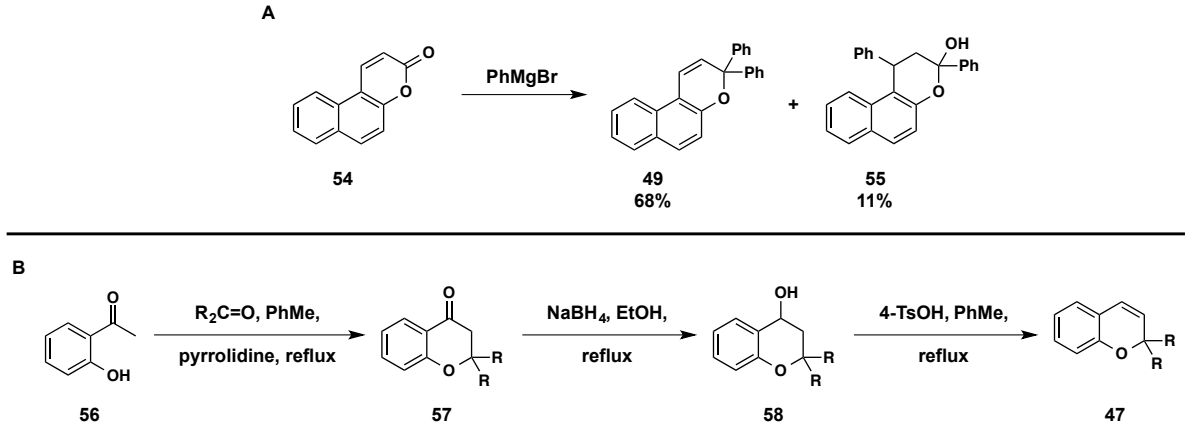

Scheme 7. Classic synthetic routes for the preparation of photochromic chromenes.

The reaction of α,β-unsaturated aldehydes with dilithiated *o*-bromophenols, followed by acid catalyzed cyclization provides photochromic chromenes in moderate to good yield and is only limited by substituent compatibility during the initial lithiation, Scheme 8.[32] Similarly, the reaction between lithiated heterocycles and *o*-hydroxynaphthaldehydes provides facile access to more structurally complex naphthopyrans.[33]

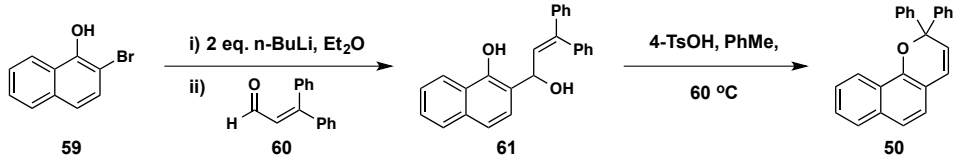

Scheme 8. Lithiation-addition-cyclization strategy for the synthesis of photochromic chromenes

However, the most direct route to naphthopyrans is the thermal rearrangement of naphthyl-propargyl ethers **65** (Scheme 9).[34] A modified, one pot protocol that has dominated the synthesis of diaryl-naphthopyrans is the acid catalyzed reaction between 1,1-diaryl-propargyl alcohols **64** and naphthols **63**, where the naphthyl-propargyl ether **65** is generated *in situ*.[35] This method is also compatible with hydroxyl-substituted heterocycles. Early examples of this synthesis were plagued with byproducts. Interception of the propargyl carbocation by a nucleophilic site on the naphthol generates propenylidenenaphthalenones **67** sometimes as the sole product of the reaction.[36] Additionally, α,β-unsaturated aldehydes are

common byproducts arising from the Meyer-Schuster or Rupe rearrangement of the propargyl alcohol. Gabbutt et al. developed the use of 4-nitrophenol as an additive to suppress these side reactions and increase yields,[36] while Carreira and Zhao have demonstrated that the addition of $(MeO)_3CH$ provides the desired photochromic chromenes in greater the 85% yield.[37]

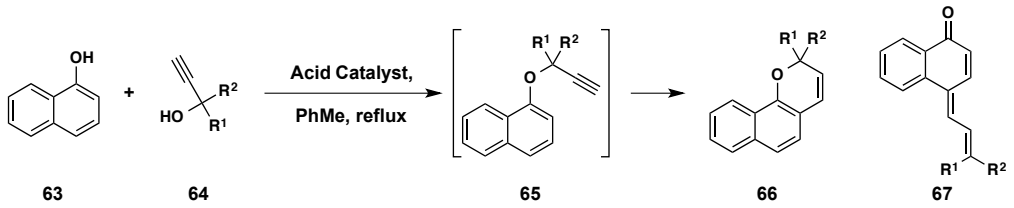

Scheme 9. Acid catalyzed one-pot synthesis of photochromic naphthopyrans.

1.2.2.3. Photochromism and Related Properties

Upon irradiation, chromenes undergo 6π electrocyclic ring opening of the colorless pyran isomer to generate the colored quinoidal isomer which can exist in four isomeric conformations, Figure 7.[38] The heterolytic bond C-O bond cleavage leads to the non-planar *cis-cis* (CC) isomer, **68** or **72**. The CC isomer can either collapse back to the closed form or undergo rotation about the C-C single bond to generate the *trans-cis* (TC) isomer, **69** or **73**. This bond rotation occurs within 10 ps, and thus it is the TC isomer that is accessed on the nanosecond to second time scale. Absorption of a second photon by the TC isomer results in geometrical isomerization to the *trans-trans* (TT) isomer, **70** or **74**, which is the most stable conformation of quinoidal chromene isomers. As the TT isomer is the product of two-photon absorption, its formation is minimal in flash photolysis, but it accumulates to a large degree under continuous irradiation. Rotation of the C-C single bond of the TT isomer leads to formation of the *cis-trans* (CT) isomer, **71** or **75**. Population of the CT isomer is believed to be unlikely as the significant steric interactions dramatically increase energy.

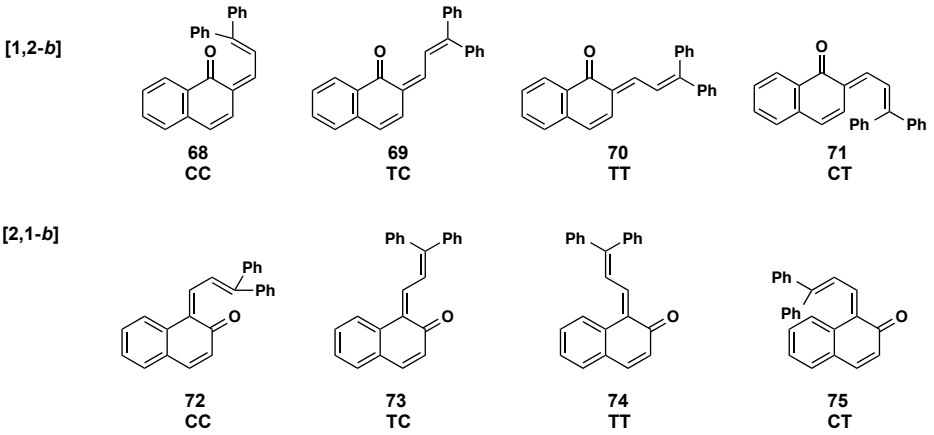

Figure 7. Ring-opened naphthopyran quinoidal isomers.

There is a well-documented difference in the coloration and lifetime of the 2*H*-naphtho[1,2-*b*]pyran **50** relative to the 3*H*-naphtho[2,1-*b*]pyran **49**, with the former having both more intense coloration and a longer lifetime.[4] Analysis of the TC and TT quinoidal structural isomers for each of these derivatives rationalizes this difference. As can be seen in Figure 8, for the [1,2-*b*] isomer **50** there is little to no steric interactions between any 4-H and 5-H in the TC conformation **69** or 3-H and 5-H in the TT conformation **70**, thus permitting both of these states to be readily populated, depending on the length of irradiation. In contrast, in the [2,1-*b*] isomer **49** there is considerable steric interaction between 1-H and 10-H in the TC conformation **73** and 2-H and 10-H in the TT conformation **74**. These steric interactions result in a destabilization of the both states and an overall decrease in there populations during irradiation, with this effect being significantly more pronounced in the TT conformation **74**.

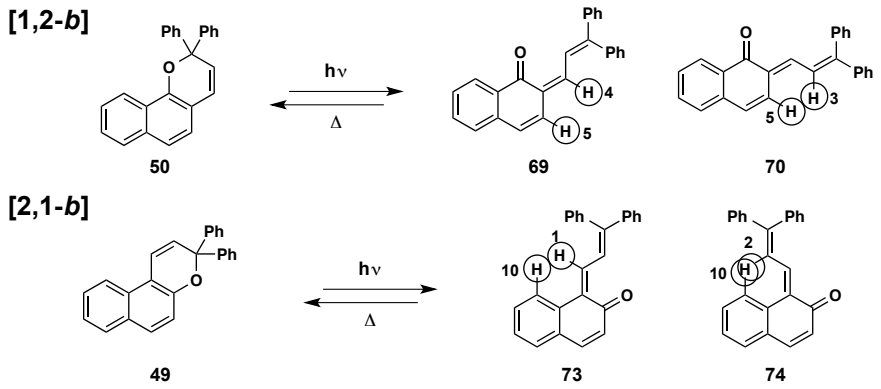

Figure 8. Steric interactions in naphthopyran quinoidal isomers.

The performance of 3*H*-naphtho[2,1-*b*]pyrans **76** can be modulated through the judicious selection of substituents on the aryl groups in position 3.[35] As shown in Table 1, electron-donating groups in the *para* position result in a bathochromic shift in the absorbance of the quinoid, while electron-withdrawing groups cause a hypsochromic shift in absorbance. Further, very precise variation in the absorbance and rate of thermal bleaching can be afforded through the use of amino substituents. Abe and coworkers have show that substitution at position 2 and/or 10 can dramatically accelerate thermal fade rates of 3*H*-naphtho[2,1-*b*]pyrans **76** by increasing steric interactions in the quinoid isomers.[39]

Table 1. Spectroscopic and photochromic properties of some 3*H*-naphtho[2,1-*b*]pyrans

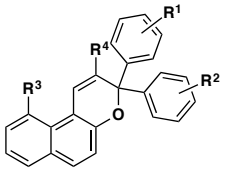

76

R^1	R^2	R^3	R^4	λ_{max} (nm)	$\tau_{1/2}$
H	H	H	H	430	34 min
H	*p*-MeO	H	H	458	-
p-MeO	*p*-MeO	H	H	475	-
p-F	*p*-F	H	H	428	-
H	*p*-CF_3	H	H	422	-
p-MeO	*p*-NMe_2	H	H	512	-
p-NMe_2	*p*-NMe_2	H	H	544	-
H	H	Br	H	455	1.4 min
H	H	H	Br	415	2.5 ms
H	H	Br	Br	415	0.80 ms
H	H	phenyl	phenyl	430	5.1 μs
H	H	H	pyrene	452	46 μs

Under steady state irradiation, similar to that encountered in ophthalmic lens applications, there is a greater equilibrium concentration of the open form of 2*H*-naphtho[1,2-*b*]pyrans **76** compared to 3*H*-naphtho[2,1-*b*]pyrans **77**, as described previously. This results in both increased coloration and slow rates of thermal bleaching. While the former is a beneficial property the later is not. For ophthalmic lenses strong coloration should be coupled with rapid fade rates. One strategy to increase fade rates has been to install substituents at position 5 on the periphery of the naphthopyran, as seen for the derivatives examined in Table 2.[40]

Table 2. Spectroscopic and photochromic properties of some 2*H*-naphtho[1,2-*b*]pyrans.

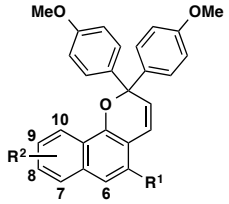

77

R^1	R^2	λ_{max} (nm)	$\tau_{1/2}$ (s)
CO_2Et	H	493	3
CO_2Me	6-OMe	502	73
CO_2Et	7-OMe	508	3
CO_2Me	8-OMe	480	11
CO_2Et	9-OMe	505	3
CO_2Me	10-OMe	485	21

In recent years Moorthy and coworkers have explored the effect of incorporating a chromene into a [2.2]paracyclophane scaffold, Figure 9.[41,42] While the parent benzopyran **47** does not demonstrate photochromism at ambient temperature, benzopyrans constrained to the [2.2]paracyclophane framework exhibit photochromism at room temperature as a result of through space π–π delocalization, the *phane* effect.[43,44] Interestingly, substitution of the second aromatic ring of the [2.2]paracyclophane scaffold increases the lifetime of the colored state over the unsubstituted CPC-H **78**, whether the substituent is electron donating or electron withdrawing. In the case of the electron donating substituent, CPC-OMe **79**, this is a direct result of an enhanced *phane* effect where the electron rich methoxy-substituted ring stabilizes the quinoid via through space π–π delocalization.[41] For CPC-Ac **80**, where the second ring of the paracyclophane scaffold is substituted with an electron withdrawing acyl moiety, two effects operate in concert. As with both CPC-H **78** and CPC-OMe **79**, the *phane* effect stabilizes the quinoid via through space π–π delocalization, additionally the carbonyl oxygen of the *o*-quinoid form functions as a "nucleophile" towards the acetyl carbonyl further stabilizing the open form of CPC-Ac **80**.[42]

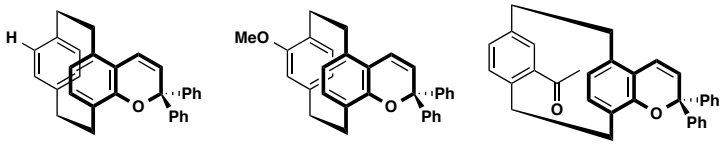

CPC-H 78 CPC-OMe 79 CPC-Ac 80

Figure 9. Photochromic [2.2]paracyclophane constrained benzopyrans.

Coehlo and coworkers have made significant strides in eliminating formation of the long-lived TT conformation of the quinoid.[45,46] As noted previously, the TT isomer is long lived and results in persistence of residual coloration for several minutes after irradiation is ceased. In flash photolysis settings, formation of the TT isomer is indicated by a biexponential decay of the colored species, and thus monoexponential decay indicates that only the short-lived TC isomer is generated. Both a benzopyran **81**[45] and 2*H*-naphtho[1,2-*b*]pyran **83**[46] derivative were prepared that are only capable of generating the TC isomer upon irradiation, Figure 10.

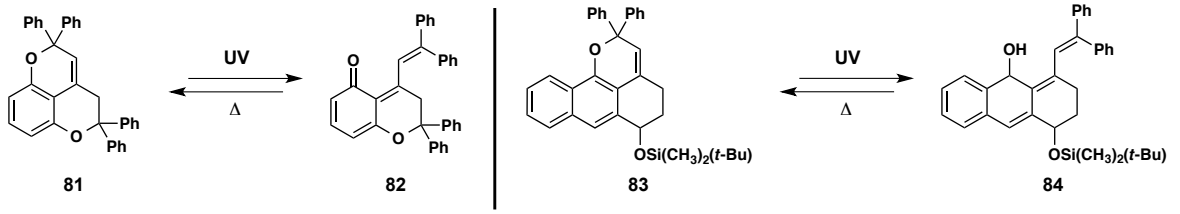

81 82 83 84

Figure 10. Photochromic benzopyran and naphthopyran capable of only generating the TC isomer.

1.2.3. Miscellaneous Classes

While significant strides have been made in regards to the development of the classes presented thus far, it would be remiss to exclude novel architectures whose identification as photoswitches is so recent that they are still being studied and developed. In this section three recently discovered classes will be highlighted. First, oxazolone-based photoswitches that were developed based on the GFP chromophores, second the fused coumarin-heterocycles and finally a borylated dibenzoborepin.

1.2.3.1. Oxazolone-Based Photoswitches

Nature has often inspired chemists and the field of photochromism is no exception. For example, the retinal protonated Schiff base (PSB) chromophores from rhodopsins are very efficient E/Z isomerization switches.[47] In fact several PSB type photoswitches have been prepared and studies on their properties have been reported. Sampedro and coworkers, have drawn inspiration from the chromophore of the green fluorescent protein (GFP) **85**, Figure 11.[48,49]

Figure 11. The GFP chromophore and oxazolone-based photochromic derivatives.

The GFP chromophore **85** is know to undergo *Z/E* isomerization, as a nonradiative relaxation pathway after irradiation, which reduces the luminescence quantum yield.[50] Further, this photoisomerization process has also been reported for intermediates in the synthesis of GFP chromophore derivatives, in particular oxazolone analogs **86**. However, these phenomena have only been slightly investigated, with the primary focus of these studies on the effect of isomerization on fluorescence. To gain a better understanding of the photochromism of these GFP-oxazolone derivatives **86**, Sampedro and coworkers employed classical conditions for the synthesis of azalactones, and prepared a diverse range of these compounds, Table 3, and examined their behavior as photoswitches.

Table 3. Synthesis, spectroscopic and photochromic properties of some oxazolone-based GFP chromophore derivatives.

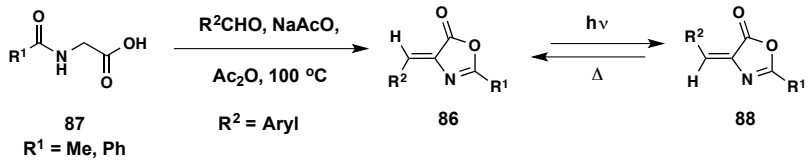

R^1	R^2	% Yield	λ_{max} (nm)	Ratio at PSS	
				% *Z*	% *E*
Ph	Ph	85	360	75	25
Ph	*p*-MeOPh	60	381/404	83	17
Ph	*o*-MeOPh	87	385/403	65	35
Ph	*p*-BrPh	72	366	75	25
Me	Ph	80	327	85	15
Me	*p*-Tol	75	336	85	15
Me	*p*-MeOPh	65	355	85	15
Me	*o*-MeOPh	82	363	64	36
Me	*p*-NO_2Ph	90	350	83	17
Me	*p*-CNPh	80	334	75	25
Me	*p*-$MeCO_2$Ph	60	331	80	20
Me	*p*-BrPh	72	333	85	15
Me	2-naphthyl	61	342	83	17
Me	3-thienyl	74	358	60	40
Me	*o*-BrPh	42	330	60	40
Ph	*p*-NO_2Ph	71	376	80	20
Ph	*p*-CNPh	34	370	45	55

The derivatives are obtained solely as the *Z* isomer (**86**) in greater than 60% yield, the notable exceptions being the incompatibility of 2-carboxybenzaldehyde, 2-cyanobenzaldehyde and ketones, which fail to provide the desired product. Having a range of derivatives, the UV/Vis spectra of the *Z* isomers were obtained. It was found that changing R^1 from a methyl to phenyl group results in a bathochromic shift in the λ_{max}, as a result of the increase in conjugation. Further, a bathochromic shift is also observed when R^1 is maintained as a methyl group and R^2 changed from phenyl to a substituted phenyl, heteroaromatic, or naphthyl group. Finally, those derivatives where R^1 is phenyl exhibit absorbance in the visible region and the photochromic transition can be effected using this low energy

irradiation. This is a highly desirable trait for applications in biological systems where high-energy UV light is often detrimental to the system.

Each of the derivatives was irradiated with >290 nm light to determine the effect of structure on the photoswitching behavior. While none of the materials achieved full switching several notable effects on the photostationary state (PSS) were observed. It was found that R^1 plays a minimal role in the PSS ratio, while R^2 has a pronounced role. When R^1 is held constant as a methyl group and R^2 changed from phenyl to an ortho substituted phenyl or thiophene the ratio of isomers at the PSS is highly enriched in the *E* isomer. If R^1 is maintained as a phenyl group and the substituent on the phenyl ring of R^2 is changed from *para* to *ortho* there is a similar increase in the *E* isomer content of the PSS. Finally, the only instance in which the *E* isomer is dominant in the PSS was for R^2 = *p*-CNPh.

Remarkably the both isomers have incredibly thermal stability. When held in the dark at room temperature the PSS did not change, nor does heating to 50 ^{o}C in the dark effect reversion from the PSS. Only after prolonged refluxing toluene could the E isomer be slowly converted back to the more thermodynamically stable *Z* isomer. In fact these compounds demonstrate such high stability in the PSS that the resulting mixture can be separated by standard flash chromatography.

1.2.3.2. Fused Coumarin-Heterocycles

The coumarin framework is an important class of heterocycle that has wide applications in the fields of functional materials and medicinal chemistry. Yang and coworkers have found that when coumarins are fused with other heterocyclic scaffolds, they resulting systems exhibiting unique and unprecedented properties. In 2011 they reported on the thermochromism of fused coumarin-phenanthridines,[51] this was followed-up by their development

of photochromic pyranocoumarins in 2012,[52] and finally photochromic fused coumarin-pyrroles in 2013[53].

The coumarin and phenanthridine scaffolds constitute two subsets of the heterocycles have found wide application as dyes,[54,55] drugs[56,57] and DNA targeting agents.[58] With interest in the potential biological activity of a fused coumarin-phenanthridine framework, Yang, Li, and Chen developed a highly efficient synthesis of these materials (Figure 12).[51] At room temperature the neutral form **92** produces a light yellow solution in methanol, on cooling to 0 ^{o}C the solution rapidly changes to orange-red as the material converts to the aromatized zwitterion **93**. This discovery represents the first instance of inverse organic thermochromism where the leaving group is an alkoxide. The switching cycle was repeated 10 times without discernable degradation of the system as monitored by UV-Vis spectroscopy indicating excellent fatigue resistance. While the zwitterion **93** could not be isolated for structural characterization, its formation and structure was confirmed by variable temperature NMR.

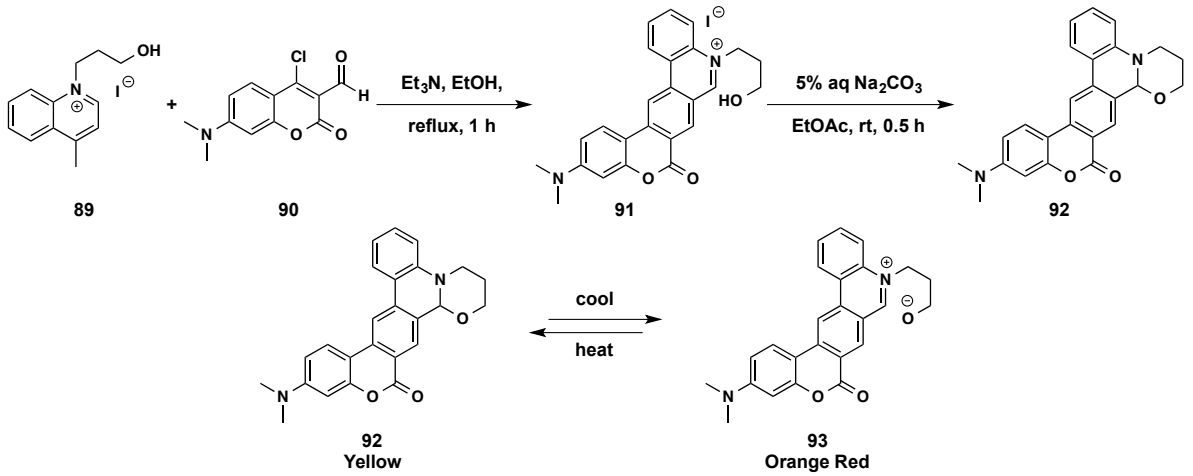

Figure 12. Synthesis and thermochromism of a fused coumarin-phenanthridine.

In the following year, Yang, Lin, and Li reported the microwave synthesis of a quinoline substituted pyranocoumarin **95** (Figure 13).[50] Upon UV irradiation (306 nm), the absorption

band of **95** at 407 nm steadily decreases with the concurrent appearance of an absorption band centered at 507 nm. The photochromic process results in the 6π electrocyclic ring opening of the pyran moiety, and a change in the color of the solution from yellow to red. Interestingly, quinoline substituted pyranocoumarin **95** exhibits only weak fluorescence (λ_{Em} = 450 nm), while the ring opened product is strongly fluorescent (λ_{Em} = 598 nm). Reversion of ring-opened product is induced by the addition of base (DABCO or imidazole).

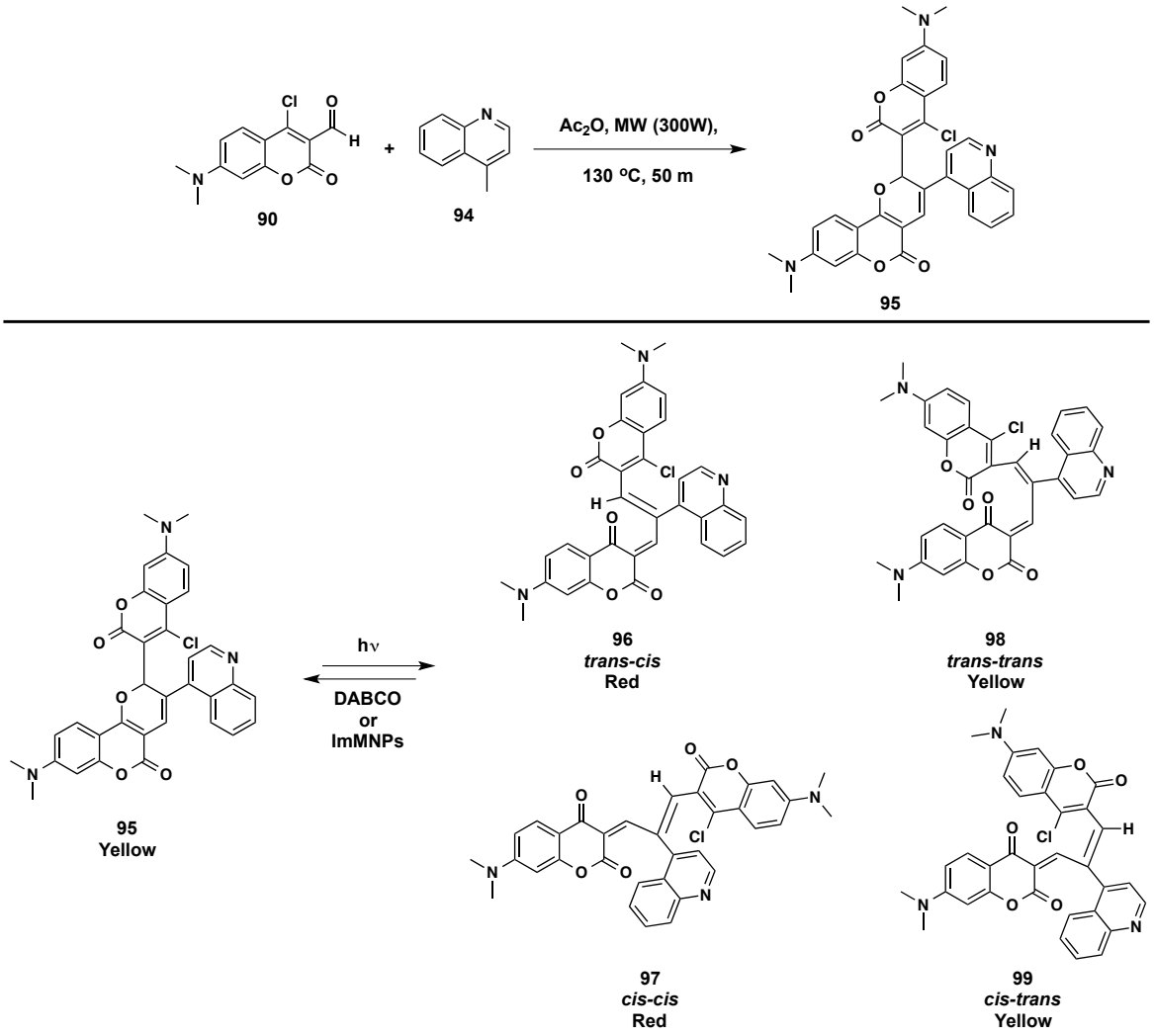

Figure 13. Synthesis and photochromism of a quinoline substituted pyranocoumarin.

As can be seen in Figure 13, the ring opening of the quinoline substituted of pyranocoumarin can lead to four diene configurations **96-99**, as proposed based on ^{1}H NMR spectra

after irradiation. In order to gain a greater understanding of the ring opening process compound **100** was prepared as a model for the *trans-trans* **98** and *cis-trans* **99** ring opening products in which the Cl substituted coumarin and quinoline groups are conjugated through a *trans* olefin (Figure 14).

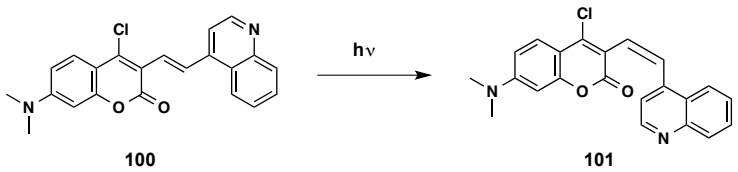

100 101

Figure 14. Model system to evaluate photochromic products of parent quinoline substituted pyranocoumarin.

On irradiation with UV light (306 nm), a chloroform solution of model compound **100** changes in color from yellow to red, and undergoes a similar change in UV-Vis absorption to that observed for the parent quinoline substituted pyranocoumarin. These changes in spectral absorption arise from a trans to cis isomerization, as confirmed by ^{1}H NMR, which enables a donor-acceptor charge transfer from the coumarin to the quinoline in cis conformer **101**. Based on these results the overall photochromic process is believed to be a ring opening followed by olefin isomerization to the *trans-cis* and *cis-cis* isomers **96** and **97**, as the *trans-trans* and *cis-trans* isomers **98** and **99** would be expected to exhibit similar absorption to the parent quinoline substituted pyranocoumarin.

The ring-opened isomers have high stability, and revert by thermal back reaction after prolonged storage in the dark (~ 2 weeks). DABCO was found to efficiently mediate the reversion, presumably through a zwitterionic intermediate. For repeated reversible cycling of the system, the DABCO would have to be removed chemically and thus a mechanically separable alternative would eliminate repeated neutralization. To this end imidazoline-functionalized magnetic nanoparticles (ImMNPs) were evaluated as mediators for the reversion. Reversible switching between the two states using UV irradiation and ImMNPs was

repeated for 10 cycles without noticeable degradation of the photochromes as monitored by UV-Vis spectroscopy. The role of imidazoline as the mediator was confirmed by the failure of the ring-opened isomers to revert when subjected to unfunctionalized MNPs.

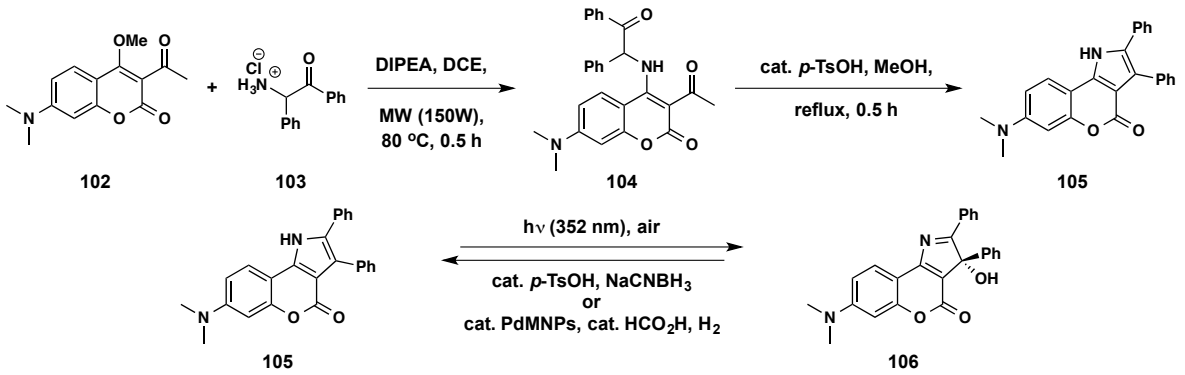

Figure 15. Synthesis and photochromism of a fused coumarin-pyrrole.

Based on the knowledge that certain pyrrole derivatives undergo oxidation when irradiated with UV light[57], Yang and Li designed and prepared a fused coumarin-pyrrole **105** (Figure 15).[51] Upon UV irradiation (352 nm), methylene chloride solutions of the fused coumarin-pyrrole **105** convert from colorless to red, with the expected changes in UV-Vis absorption, to give the tertiary alcohol **106**. In addition to the change in absorbance, upon photo-oxidation the fused coumarin-pyrrole **105** has a nearly complete loss of fluorescence. While the fused coumarin-pyrrole **105** exhibits $\Phi_f = 0.65$, the tertiary alcohol **106** is virtually non-emitting with $\Phi_f = 0.03$. The photo-oxidation product **106** reverts under acidic reducing conditions (Figure 15), presumably via hydrogenation/reduction of the imine followed by acid catalyzed dehydration. The use of mechanically separable and reusable Pd-functionalized magnetic nanoparticles (Pd-MNPs) greatly facilities a reversible process by eliminating the centrifugation and filtration required when employing Pd/C. Finally, the overall redox cycle is 'nearly' perfect since the oxidizing agent is O_2, and the reductant H_2.

Oxygen, an ultimate oxidant, is virtually unlimited and free, while hydrogen is the most atom economical reductant and generates no waste.

1.2.3.3. Borylated Dibenzoborepin

Introduction of boron to π conjugated systems is a useful strategy to generated novel materials with interesting electronic structures.[58] The key design principle being that a tricoordinated boron atom is isosteric with a tricoordinated cationic carbon atom. This substitution permits transformation of a strongly electron accepting system in to an uncharged isolable form. In 2013, Yamaguchi and coworkers sought to employ this principle to prepare novel ladder π systems, specifically borole-fused borole **107** shown in Figure 16.[59] They envisioned that the desired material could be prepared from bisboronic ester **109** via lithium halogen exchange followed by introduction of the aryl substituents with ArMgX. On attempting the synthesis employing *t*BuLi and mesityl magnesium bromide they isolated not the expected product but borylated dibenzoborepin **110** instead.

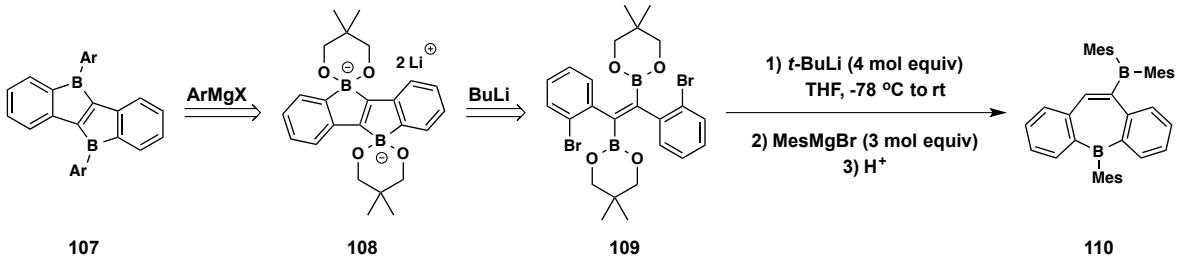

Figure 16. Retrosynthetic plan and synthesis of the photochromic borylated dibenzoborepin.

When irradiated with UV light (320 nm), it was found that a colorless solution of the borylated dibenzoborepin **110** in benzene rapidly turns navy blue. The absorbance bands at 346 and 387 nm in the UV-Vis spectrum of **110** decrease during the photochromic transition with concomitant development of a broad absorption band centered at 634 nm. On cessation of irradiation, the cyclized photoproduct **111** thermally reverts at ambient temperature in the

dark. The structure of the photoproduct **111** was confirmed by X-ray crystallography. As seen in Scheme 10, the photochromic reaction is proposed to proceed through a 4π bora-Nazarov cyclization. It is believed that this unique behavior is possible since the borylated dibenzoborepin is isosteric to the cyclopentadienal cation intermediate of the acid catalyzed Nazarov cyclization. Unlike the Nazarov cyclization and the well-known 6π Nazarov-analogous cyclizations of nitrogen, sulfur and oxygen bearing substrates,[60] which occur under either thermal or photo mediated conditions, the bora-Nazarov only occurs via photoirradiation. This is the first example of a light mediated bora-Nazarov cyclization, and opens the door to novel photochromic materials based on this reversible reaction.

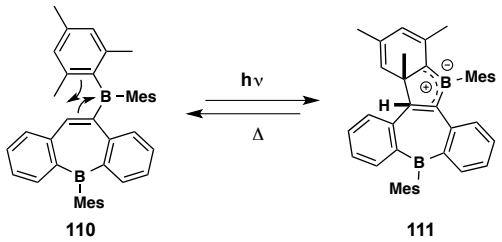

110 111

Scheme 10. Bora-Nazarov photochromism of borylated dibenzoborepin.

1.3. Closing Remarks

As has been shown, in recent decades, significant effort has been devoted to the chemistry of organic photochromic compounds. These efforts have been spread between the design and development of novel systems and efforts towards improving and enhancing the properties of known and established classes. The primary driving force for these works, is the unique ability of these compounds to undergo reversible spectral and physical property changes which has led to their adoption in fields from energy production,[61] chemical sensing,[62] and molecular actuators[63] to biological systems.[7,64–67] While a great many molecular switches are known, the advantage of photochromic systems, those activated by light, over those materials whose reversible transformations are mediated by stimuli such as pH, ionic

concentration, electrical or magnetic field, or humidity is the abundant and versatile nature of light as a stimulus which enables both temporal and spatial resolution.

1.4. References

(1) Bouas-Laurent, H.; Durr, H. In *Pure and Applied Chemistry*; 2001; Vol. 73, pp 639–665.

(2) Minkin, V. I. *Chem. Rev.* **2004**, *104* (5), 2751.

(3) Irie, M.; Fukaminato, T.; Matsuda, K.; Kobatake, S. *Chem. Rev.* **2014**, 141216134227001.

(4) Van Gemert, B. In *Organic Photochromic and Thermochromic Compounds*; Crano, J. C., Guglielmetti, R. J., Eds.; Springer US: Boston, MA, 2002; pp 111–140.

(5) Honda, K.; Komizu, H.; Kawasaki, M. *J. Chem. Soc. Chem. Commun.* **1982**, No. 4, 253.

(6) Inoue, E.; Kokado, H.; Shimizu, I.; Kobayashi, H.; Takahashi, Y. *Bull. Chem. Soc. Jpn.* **1972**, *45* (7), 1951.

(7) *Molecular switches*, 2nd, completely rev. and enl. ed.; Feringa, B. L., Browne, W. R., Eds.; Wiley-VCH: Weinheim, Germany, 2011.

(8) Szalóki, G.; Pozzo, J.-L. *Chem. - Eur. J.* **2013**, *19* (34), 11124.

(9) Klajn, R. *Chem Soc Rev* **2014**, *43* (1), 148.

(10) Hayashi, T.; Maeda, K. *Bull. Chem. Soc. Jpn.* **1960**, *33* (4), 565.

(11) Satoh, Y.; Ishibashi, Y.; Ito, S.; Nagasawa, Y.; Miyasaka, H.; Chosrowjan, H.; Taniguchi, S.; Mataga, N.; Kato, D.; Kikuchi, A.; Abe, J. *Chem. Phys. Lett.* **2007**, *448* (4-6), 228.

(12) Xu, J.; Gao, F.; Yang, Y. *J. Photopolym. Sci. Technol.* **1999**, *12* (2), 343.

(13) Kikuchi, A.; Iwahori, F.; Abe, J. *J. Am. Chem. Soc.* **2004**, *126* (21), 6526.

(14) Iwahori, F.; Hatano, S.; Abe, J. *J. Phys. Org. Chem.* **2007**, *20* (11), 857.

(15) Hatano, S.; Fujita, K.; Tamaoki, N.; Kaneko, T.; Nakashima, T.; Naito, M.; Kawai, T.; Abe, J. *J. Phys. Chem. Lett.* **2011**, *2* (21), 2680.

(16) Kishimoto, Y.; Abe, J. *J. Am. Chem. Soc.* **2009**, *131* (12), 4227.

(17) Harada, Y.; Hatano, S.; Kimoto, A.; Abe, J. *J. Phys. Chem. Lett.* **2010**, *1* (7), 1112.

(18) Fujita, K.; Hatano, S.; Kato, D.; Abe, J. *Org. Lett.* **2008**, *10* (14), 3105.

(19) Feringa, B. L.; van Delden, R. A.; Koumura, N.; Geertsema, E. M. *Chem. Rev.* **2000**, *100* (5), 1789.

(20) Mislow, K.; Glass, M. A. W.; O'Brien, R. E.; Rutkin, P.; Steinberg, D. H.; Weiss, J.; Djerassi, C. *J. Am. Chem. Soc.* **1962**, *84* (8), 1455.

(21) Greene, F. D.; Berwick, M. A.; Stowell, J. C. *J. Am. Chem. Soc.* **1970**, *92* (4), 867.

(22) Muyoh, K.; Hatano, S.; Abe, J. *J. Photopolym. Sci. Technol.* **2010**, *23* (3), 301.

(23) Mutoh, K.; Abe, J. *J. Phys. Chem. A* **2011**, *115* (18), 4650.

(24) Wizinger, R.; Wenning, H. *Helv. Chim. Acta* **1940**, *23* (1), 247.

(25) Livingstone, R.; Miller, D.; Morris, S. *J. Chem. Soc. Resumed* **1960**, 5148.

(26) Hirshberg, Y.; Fischer, E. *J. Chem. Soc. Resumed* **1954**, 3129.

(27) Becker, R. S.; Michl, J. *J. Am. Chem. Soc.* **1966**, *88* (24), 5931.

(28) Padwa, A.; Au, A.; Lee, G. A.; Owens, W. *J. Org. Chem.* **1975**, *40* (8), 1142.

(29) Cotterill, W. D.; Livingstone, R.; Walshaw, M. V. *J. Chem. Soc. C Org.* **1970**, No. 13, 1758.

(30) Kabbe, H.-J.; Widdig, A. *Angew. Chem. Int. Ed. Engl.* **1982**, *21* (4), 247.

(31) Wawzonek, S.; Nagler, R. C.; Carlson, L. J. *J. Am. Chem. Soc.* **1954**, *76* (4), 1080.

(32) Heller, H. G.; Levell, J. R.; Hibbs, D. E.; Hughes, D. S.; Hursthouse, M. B. *Mol. Cryst. Liq. Cryst. Sci. Technol. Sect. Mol. Cryst. Liq. Cryst.* **1997**, *297* (1), 123.

(33) Uchida, M.; Irie, M. *J. Am. Chem. Soc.* **1993**, *115* (14), 6442.

(34) Moghaddam, F.; Matloubi, S. A.; Saidi, M. R. *J. Chem. Res. Synop.* **1996**, No. 7, 338.

(35) Gemert, B. V.; Bergomi, M. P. Preparation of photochromic naphthopyran compounds. US 5066818.

(36) Gabbutt, C. D.; Heron, B. M.; Instone, A. C.; Thomas, D. A.; Partington, S. M.; Hursthouse, M. B.; Gelbrich, T. *Eur. J. Org. Chem.* **2003**, *2003* (7), 1220.

(37) Zhao, W.; Carreira, E. M. *Org. Lett.* **2003**, *5* (22), 4153.

(38) Delbaere, S.; Luccioni-Houze, B.; Bochu, C.; Teral, Y.; Campredon, M.; Vermeersch, G. *J. Chem. Soc. Perkin Trans. 2* **1998**, No. 5, 1153.

(39) Arai, K.; Kobayashi, Y.; Abe, J. *Chem Commun* **2015**, *51* (15), 3057.

(40) Salvador, M. A.; Coelho, P. J.; Burrows, H. D.; Oliveira, M. M.; Carvalho, L. M. *Helv. Chim. Acta* **2004**, *87* (6), 1400.

(41) Moorthy, J. N.; Mandal, S.; Kumar, A. *New J Chem* **2013**, *37* (1), 82.

(42) Mandal, S.; Mukhopadhyay, A.; Moorthy, J. N. *Eur. J. Org. Chem.* **2015**, *2015* (7), 1403.

(43) Bartholomew, G. P.; Bazan, G. C. *Acc. Chem. Res.* **2001**, *34* (1), 30.

(44) Bazan, G. C. *J. Org. Chem.* **2007**, *72* (23), 8615.

(45) Sousa, C. M.; Pina, J.; Seixas de Melo, J.; Berthet, J.; Delbaere, S.; Coelho, P. J. *Eur. J. Org. Chem.* **2012**, *2012* (9), 1768.

(46) Sousa, C. M.; Berthet, J.; Delbaere, S.; Coelho, P. J. *J. Org. Chem.* **2012**, *77* (8), 3959.

(47) Mathies, R. A.; Lugtenburg, J. In *Handbook of Biological Physics*; D.G. Stavenga, W. J. D. and E. N. P., Ed.; North-Holland, 2000; Vol. Volume 3, pp 55–90.

(48) Blanco-Lomas, M.; Campos, P. J.; Sampedro, D. *Org. Lett.* **2012**, *14* (17), 4334.

(49) Blanco-Lomas, M.; Funes-Ardoiz, I.; Campos, P. J.; Sampedro, D. *Eur. J. Org. Chem.* **2013**, *2013* (29), 6611.

(50) Rafiq, S.; Rajbongshi, B. K.; Nair, N. N.; Sen, P.; Ramanathan, G. *J. Phys. Chem. A* **2011**, *115* (47), 13733.

(51) Chen, J.-J.; Li, K.-T.; Yang, D.-Y. *Org. Lett.* **2011**, *13* (7), 1658.

(52) Li, K.-T.; Lin, Y.-B.; Yang, D.-Y. *Org. Lett.* **2012**, *14* (5), 1190.

(53) Lin, C.-H.; Yang, D.-Y. *Org. Lett.* **2013**, *15* (11), 2802.

(54) Hara, K.; Wang, Z.-S.; Sato, T.; Furube, A.; Katoh, R.; Sugihara, H.; Dan-oh Ya-sufumi; Kasada, C.; Shinpo, A.; Suga, S. *J. Phys. Chem. B* **2005**, *109* (32), 15476.

(55) Zhang, J.; Lakowicz, J. R. *J. Phys. Chem. B* **2005**, *109* (18), 8701.

(56) Brühlmann, C.; Ooms, F.; Carrupt, P.-A.; Testa, B.; Catto, M.; Leonetti, F.; Altomare, C.; Carotti, A. *J. Med. Chem.* **2001**, *44* (19), 3195.

(57) Kock, I.; Heber, D.; Weide, M.; Wolschendorf, U.; Clement, B. *J. Med. Chem.* **2005**, *48* (8), 2772.

(58) Bailly, C.; Arafa, R. K.; Tanious, F. A.; Laine, W.; Tardy, C.; Lansiaux, A.; Colson, P.; Boykin, D. W.; Wilson, W. D. *Biochemistry (Mosc.)* **2005**, *44* (6), 1941.

(59) Leete, E. *J. Am. Chem. Soc.* **1961**, *83* (17), 3645.

(60) Jäkle, F. *Chem. Rev.* **2010**, *110* (7), 3985.

(61) Iida, A.; Saito, S.; Sasamori, T.; Yamaguchi, S. *Angew. Chem. Int. Ed.* **2013**, *52* (13), 3760.

(62) Schultz, A. G. *Acc. Chem. Res.* **1983**, *16* (6), 210.

(63) Castagna, R.; Garbugli, M.; Bianco, A.; Perissinotto, S.; Pariani, G.; Bertarelli, C.; Lanzani, G. *J. Phys. Chem. Lett.* **2012**, *3* (1), 51.

(64) Xie, X.; Mistlberger, G.; Bakker, E. *J. Am. Chem. Soc.* **2012**, *134* (41), 16929.

(65) Terao, F.; Morimoto, M.; Irie, M. *Angew. Chem. Int. Ed.* **2012**, *51* (4), 901.

(66) Kienzler, M. A.; Reiner, A.; Trautman, E.; Yoo, S.; Trauner, D.; Isacoff, E. Y. *J. Am. Chem. Soc.* **2013**, *135* (47), 17683.

(67) Kumpfer, J. R.; Rowan, S. J. *J. Am. Chem. Soc.* **2011**, *133* (32), 12866.

(68) Velema, W. A.; Szymanski, W.; Feringa, B. L. *J. Am. Chem. Soc.* **2014**, *136* (6), 2178.

(69) Spruell, J. M.; Hawker, C. J. *Chem Sci* **2011**, *2* (1), 18.

2. Donor-Acceptor Stenhouse Adducts: Design and Discovery

2.1. Design: Background and Historical Perspective

In the field of adaptable and responsive materials, the ability of organic photochromic compounds to reversibly undergo changes in spectral absorption, volume, and solubility is of particular importance for applications in energy storage and chemical sensing and for controlling the conformation and activity of biomolecules.[1–4] These switches are particularly valuable because their property changes are triggered by light, the most widely available, non-invasive, and environmentally benign external stimulus. Significantly, light also provides unique opportunities for spatial and temporal resolution.

Among the classes of organic photochromic materials, azobenzenes, spiropyrans and diarylethenes have received the most attention because of their excellent performance and broad utility. Specifically, azobenzene has been extensively employed for its change in volume, resulting from a *trans* **1** to *cis* **2** isomerization, upon irradiation (Figure 1A).[5,6] Similarly, the change in spectral properties of spiropyrans (**10**) and diarylethenes (**12**) upon photoswitching has been exploited in a number of applications,[7,8] with spiropyran exhibiting the added benefit of a solubility switch, or a conversion from a hydrophobic (**10**) to a hydrophilic form (**11**), upon irradiation.[9,10] Despite their ubiquity and broad utility, these privileged classes of photochromes all typically require the use of high-energy UV light to trigger their photochemical reactions. This hinders their potential use in biomedical applications and material science because UV light can be damaging to healthy cells and results in degradation for many macromolecular systems.[3] Fatigue resistance is also a primary concern for UV-based photochromic switches. A common design principle to address this problem is to

make synthetic modifications to these known classes of photochromic compounds that enable the use of visible light (**3-9**).[11–17]

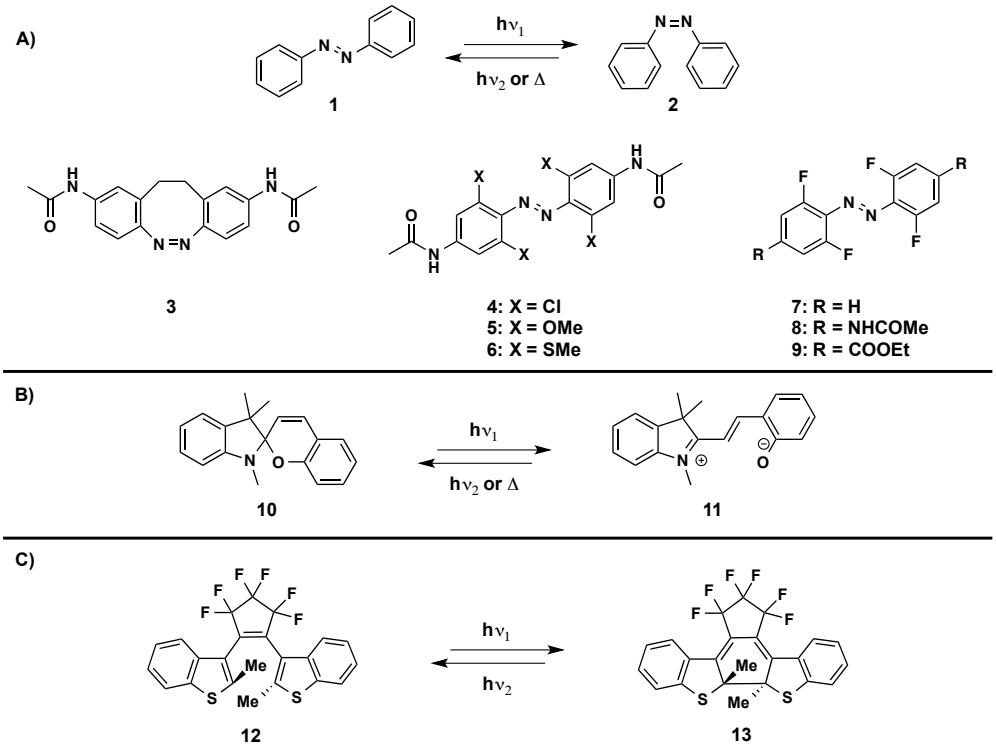

Figure 1. A) Photoswitching of azobenzenes and representative visible light activated derivatives, B) Photoswitching of spiropyrans, C) Photoswitching of diarylethenes.

This is at best a stopgap solution. While effective, this strategy typically results in systems that are limited to specific applications, and necessitates laborious synthetic efforts. The unfortunate consequence being that these derivatives are not widely adopted or employed as their preparation is beyond the abilities of the non-expert. It was our view, inspired by the works of Abe,[15,18–24] Sampedro[25,26], and Yang,[27–29] that the challenge of developing new organic photochromic molecules required a paradigm shift. In addition to the widely employed and accepted practice of tuning known systems, critical analysis of the literature, specifically brief communications of unexpected chemical behavior, should be employed as a starting point for the rational design of novel photochromic compounds that address the limitations of known classes.

After a careful and exhaustive search of the literature surrounding photochromic organic compounds we recognized that two major limitations had been poorly addressed to date. First, there has been a significant deficit in development of organic photochromic molecules that respond to visible light. Overwhelmingly, organic photochromic molecules, both newly developed and known systems, are activated and operate under the irradiation of Ultraviolet light. Second, the scientific community has essentially ignored the field of negative or inverse photochromism, where the stable isomer is colored and reversibly bleaches when irradiated. Indeed the few reports on negative photochromism identify the phenomenon as an accidental discovery. Further, after the initial report, there are rarely any further studies presented. It was with these considerations in mind that we began our efforts towards the design and development of a photochromic organic compound that operates as a negative photochromic system activated by visible light.

Our interest in the cascade rearrangements of activated furans[30–35] and a pioneering report by Honda[36] inspired us to design a novel negative (colored to colorless) photochromic material.[8,15] During the design stage, we established three criteria for an ideal new class of organic photochromic material that helped guide our discovery efforts: (1) intrinsic activation by visible light, (2) significant change in spectral absorption, solubility, and volume, and (3) facile synthetic access, modularity and tunability. A number of important contributions helped us conceive the molecular architecture we would target for study.

In 1870, Stenhouse discovered that in the presence of 2 equiv of a primary or secondary aniline and 1 equiv of protic acid furfural undergoes ring opening to give stable, intensely colored salts whose structure, five-carbon cyanine dyes with an OH group at the second carbon atom, was established by Schiff in 1887 (Figure 2A).[37,38] Initial imine/iminium for-

mation between furfural and the aniline activates the furan nucleus to nucleophilic attack, which then leads to ring opening of furan and formation of the Stenhouse salt. Nearly a century later, in 1982, Honda disclosed the visible light mediated negative photochromism of Stenhouse salts (Figure 2B).[36] Although the mechanism and product of the photochromic reaction was not reported, the enolic OH group was determined to be critical for the photobleaching−thermal recoloration process since the parent cyanine dyes with no OH group (obtained by the Zincke ring opening of pyridinium salts) do not display these properties.[39–41] In Honda's report, the photobleaching-thermal recoloration process was strongly dependent on the concentration of added acid, and in the presence of 100 equiv of HCl photobleaching did not occur. This result is consistent with related studies on Stenhouse salts by Lewis and Mulquiney, even though they did not study the photochromic properties of these systems.[42–44] In the Lewis study, treatment of the Stenhouse salts with base only gave the corresponding colorless cyclopentenone adducts (Figure 2C).[42] Further, in 2000, Safar and co-workers reported a preliminary study on the rearrangement of 5-(furan-2-ylmethylene-)-2,2-dimethyl-1,3-dioxane-4,6-dione **19** with cyclic secondary aliphatic amines (Figure 2D).[45] In contrast to Stenhouse's work, this system exploited the electron-withdrawing nature of the cyclic dicarbonyl to impart the same result as imine/iminium activation. Interestingly, reaction of furan **19** with morpholine or piperidine in a 2:1 or 1:1 molar ratio resulted in a mixture of two compounds; the Stenhouse-based adduct **21** and the corresponding cyclopentenone **22**. All attempts to separate this mixture were unsuccessful; however, treatment of this mixture with excess HBr gave exclusively the cyclopentenone hydrobromide **23**, and presumably the equilibrium was driven to the product by precipitation of the salt.

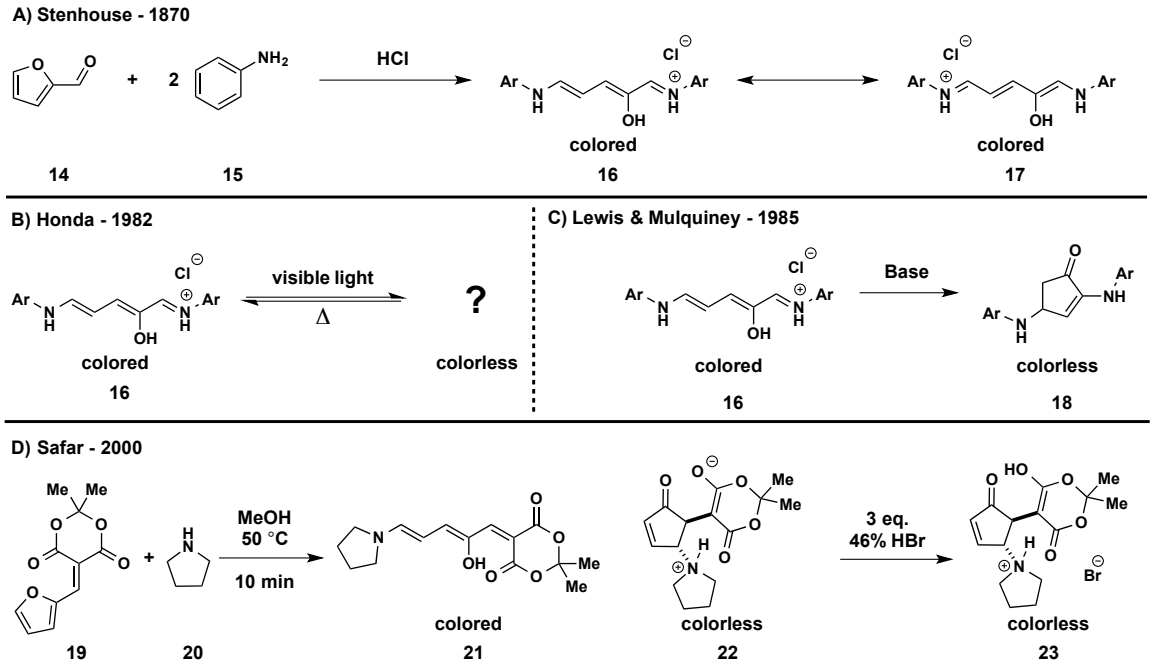

Figure 2. A) Stenhouse's ring opening of furfural by aniline and protic acid, B) photochromism of Stenhouse salts examined by Honda, C) Lewis and Mulquiney's base-mediated cyclization of Stenhouse salts, D) Safar's secondary amine ring opening and rearrangement of activated furans.

Based on these reports we hypothesized that the photochromic behavior observed by Honda was due to a reversible interconversion between the open Stenhouse salt and the closed 4,5-aminocyclopentenone. Combined, these studies also suggest that the ability to tune and control the process by which the open Stenhouse adduct and the closed cyclopentenone adduct interconvert is dependent on the substituents of the push−pull system derived from the amine ring opening of furfural or its derivatives. With these considerations in mind, the donor-acceptor Stenhouse adducts (DASAs) with a general structure **21** were selected for initial studies (Figure 2D).

2.2. Discovery: Synthesis

At the outset, we sought to develop optimal conditions for the selective formation of the colored triene Stenhouse adduct **21** without concomitant generation of the cyclopentenone **22**. The optimal conditions were initially identified using pyrrolidine (Table 1). Reacting an

equimolar ratio of furylidene−Meldrum's acid **19** and pyrrolidine **20** in tetrahydrofuran provided the desired Stenhouse adduct **21** in 95% yield with filtration as the only purification necessary (entry 7). In direct contrast, the use of other solvents required heating to 50 °C and resulted in lower yields (entries 5 and 6) or inseparable mixtures of Stenhouse adduct **21** and cyclopentenone **22** (entries 1−4). While the addition of Lewis acids or bases such as dysprosium triflate or DABCO increased yields, these conditions also produced mixtures of **21** and **22** (entries 2 and 3).

Table 1. Optimization of reaction conditions for the selective formation of Stenhouse-based adducts (DASAs)[a]

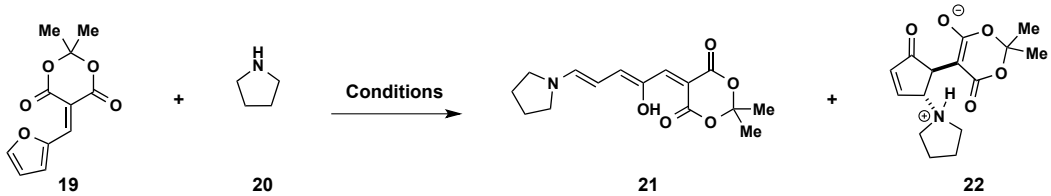

19 **20** **21** **22**

Entry	Solvent	Temp. (°C)	Time (min)	Product	Yield (%)[b]
1	MeCN	50	60	21 + 22	60[c]
2[d]	MeCN	50	60	21 + 22	70[c]
3[e]	MeCN	50	60	21 + 22	80[c]
4	MeOH	50	30	21 + 22	80[c]
5	CH_2Cl_2	23	60	21	50
6	PhMe	50	30	21	50
7	**THF**	**23**	**10**	**21**	**95**

[a]Activated furan **19** (1 equiv) and pyrrolidine **20** (1 equiv) were sequentially added to the solvent and stirred at the temperature indicated. [b]Isolated yields. [c]Inseparable mixture of **21** and **22**. [d]10 mol % of dysprosium triflate added. [e]10 mol % of DABCO added.

With our success in employing Meldrum's acid as an activating group, we were curious if other 1,3-dicarbonyl moieties would be equally effective. Five motifs were selected for examination: 2,4-pentanedione **24**, malonic acid diethyl ester **28**, dimedone **31**, and *N,N`*-dimethylbarbituric acid **34** (Figure 3). Diethyl amine **26** was employed as the nucleophile in testing the susceptibility of the activated furans, obtained by condensation of these dicarbonyls with furfural, towards ring opening. Neither 2,4-pentanedione **24** nor malonic acid diethyl ester **28** sufficiently activated furfural, implicating the importance of the cyclic na-

ture of Meldrum's acid. Similarly, the dimedone activated furan **32** failed to produce the desired Stenhouse adduct, indicating that 1,3-diketones, whether cyclic or acyclic are not capable of activating furfural for the desired ring opening under the described conditions (attempts to overcome this limitation were not pursued). Gratifyingly, *N,N`*-dimethylbarbituric acid **34** was an effective activating group, providing the Stenhouse adduct **36** in excellent yield, 81%.

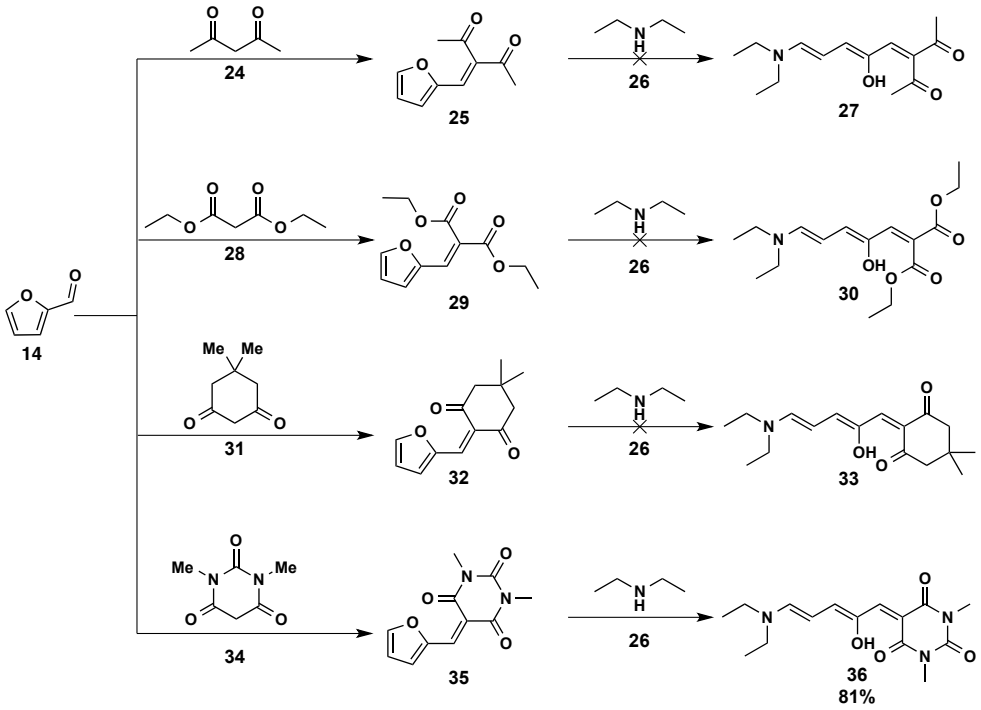

Figure 3. Initial evaluation of the scope of 1,3-dicarbonyl activating groups.

Inherent in the versatility and overall usefulness of these DASA photoswitches is the high yielding and simple nature of the synthetic procedures, which allows non-experts easy access to more complex or functional substrates that are attractive for tailored applications in materials science. Having efficient access to the triene derivatives, the photophysical properties were examined with diethyl amine derived adducts as model systems (Scheme 1).

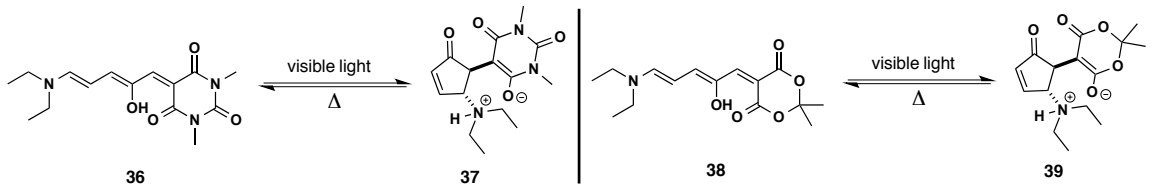

Scheme 1. DASAs selected as model systems for examining photophysical and photochromic properties.

2.3. Discovery: Photophysical and Photochromic Properties

We began by examining the unidirectional conversion of the colored triene **38** to its colorless zwitterionic cyclopentenone isomer **39** using NMR spectroscopy in a deuterated methanolic solution (Figure 4A). Exposure of **38** to a standard incandescent bulb or hand-held fluorescent lamp results in a decrease over the course of 4 h in the NMR peaks corresponding to **38** and a concomitant increase in the peaks for **39**. Similarly, this process was also studied using UV−Vis spectroscopy for **36** in methanol (Figure 4B). Again, irradiation with visible light leads to a decrease of the absorption of **36** as it is converted to **37** over 50 min. The difference in the rate of conversion between the triene and the zwitterionic cyclopentenone isomers was governed by concentration (^{1}H NMR required high concentration to obtain adequate data, dilute conditions were used for UV−vis experiment) and not the nature of the derivative or solvent employed. The isosbestic point was determined to occur at 280 nm for both compounds.

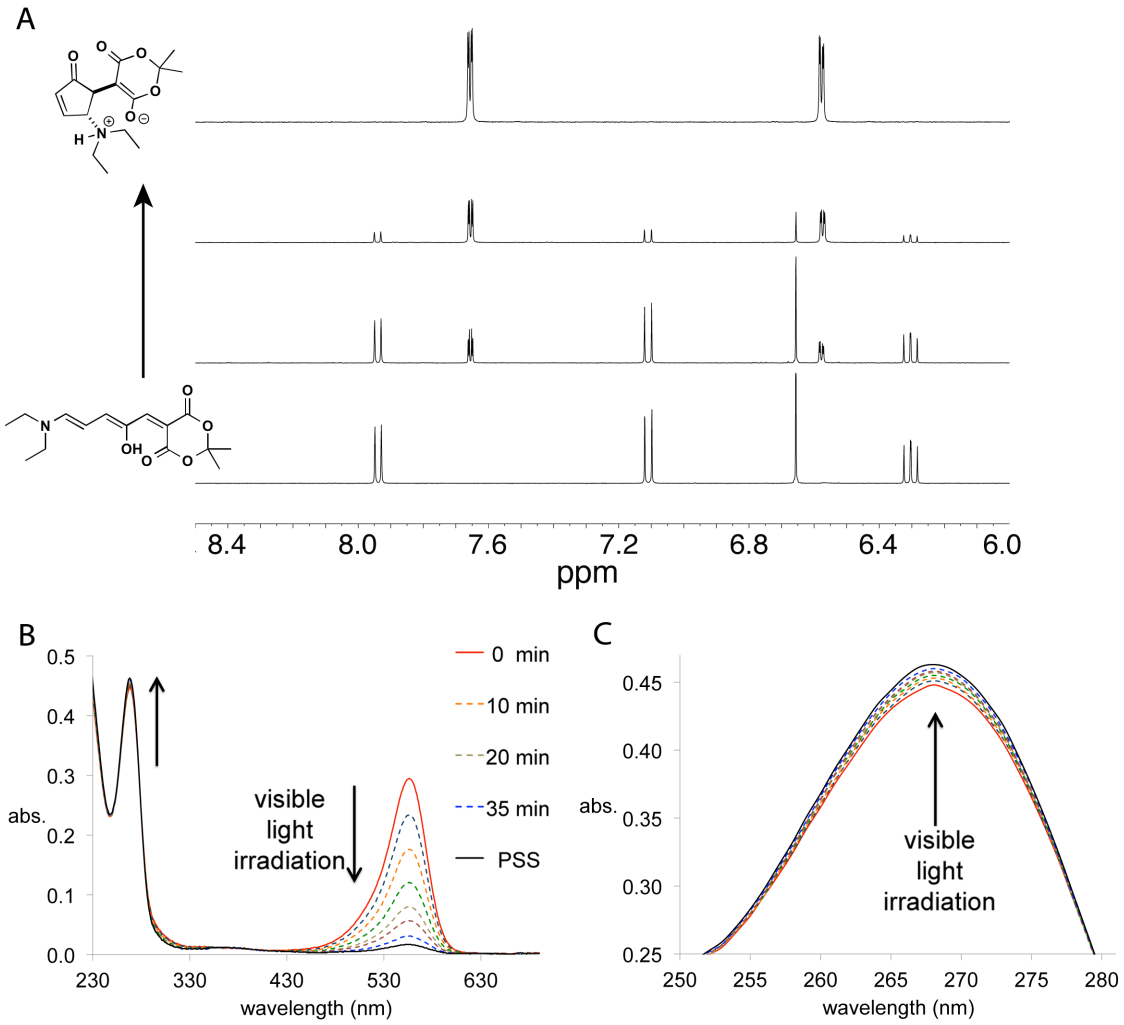

Figure 4. A) Conversion of **38** to **39** by ^{1}H NMR in CD_3OD over 4 h. B) Absorption spectra of **36** to **37** on irradiation with visible light in CH_3OH. C) Expanded view of absorption spectra of **36** to **37** between 250 and 280 nm.

Having controlled access to both structural forms, we next determined conditions that would facilitate rapid, quantitative, and fully reversible switching between the triene and cyclopentenone forms. Similar to spiropyrans and diarylethenes, reversible photoswitching of DASAs was found to be solvent dependent.[46,47] We found aromatic solvents to be ideal, providing conversion of the triene to cyclopentenone upon irradiation with visible light with thermal reversion from the meta-stable cyclopentenone back to the triene when irradiation is stopped.

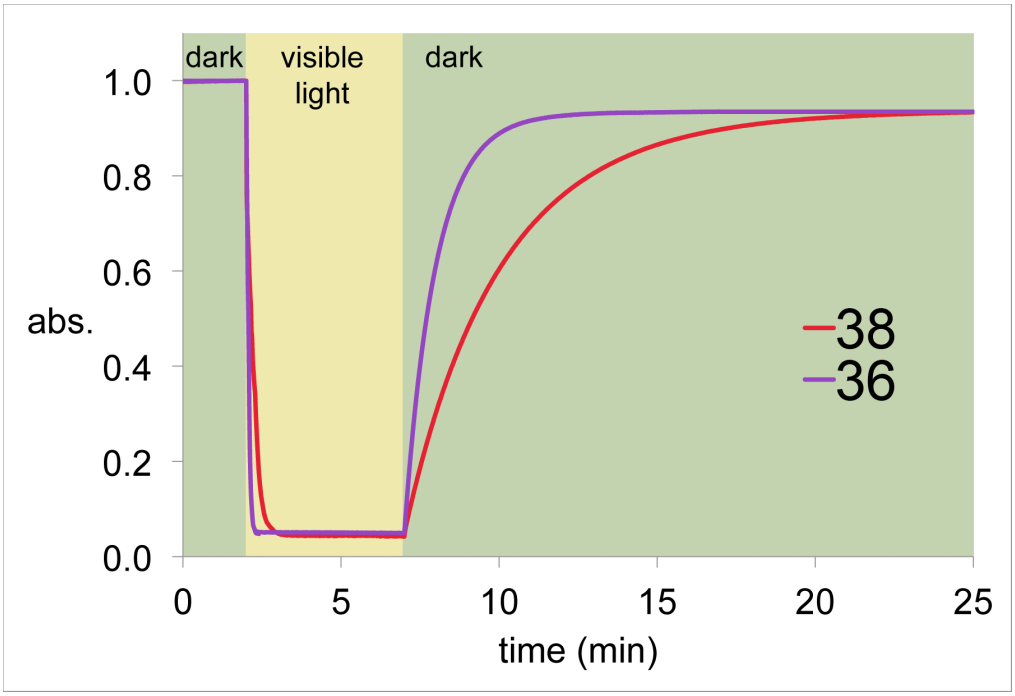

Figure 5. Relative rates of interconversion for derivatives **36** and **38**.

With reversible conditions identified, the relative rates of interconversion between the triene and cyclopentenone isomer were evaluated in toluene for the two photoswitches (**36** and **38**, illustrated in Scheme 1) bearing different acceptor groups. As illustrated in Figure 5 both derivatives undergo conversion from the open triene isomer (**36** and **38**) to the closed zwitterionic cyclopentenone isomer (**37** and **39**) at approximately the same rate. A more dramatic rate difference was observed in the thermal recoloration, upon cessation of irradiation, where the 1,3-dimethyl barbituric acid derivative (**36**) reverted back approximately twice as fast. This process is solvent (Figure 6) and temperature dependent (Figure 7), but it is worth noting that in polar protic solvent thermal reversion was not observed.

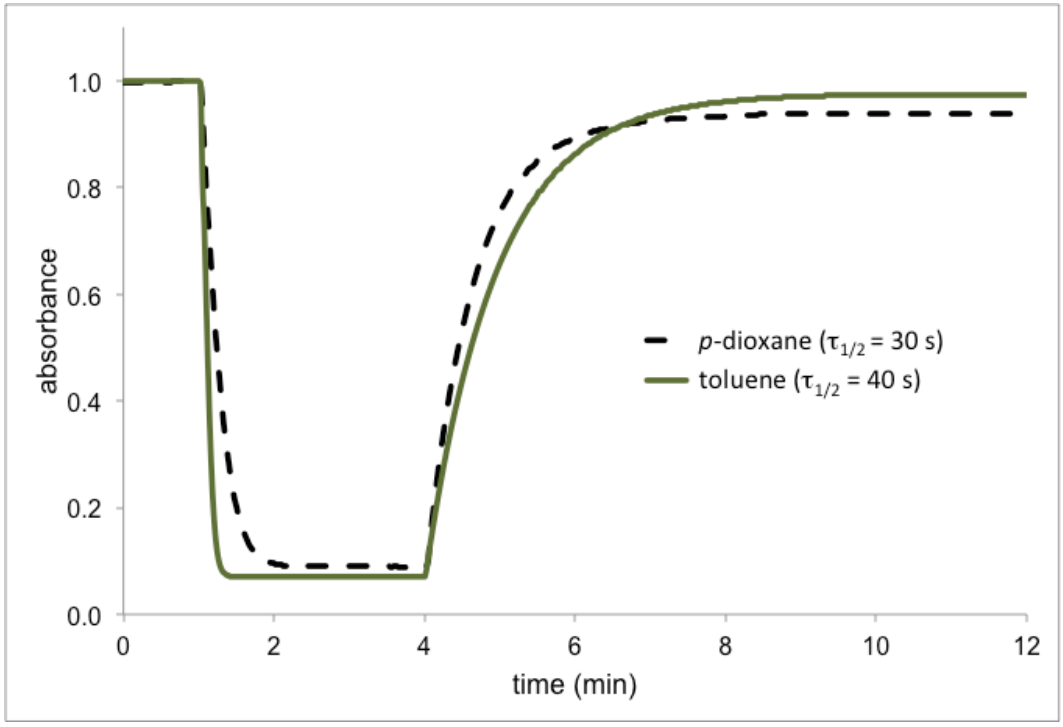

Figure 6. Effect of solvent on photoswitching of **36**, half-life of thermal recoloration ($\tau_{1/2}$) denoted in legend adjacent to solvent. Irradiations were performed with un-filtered high intensity light.

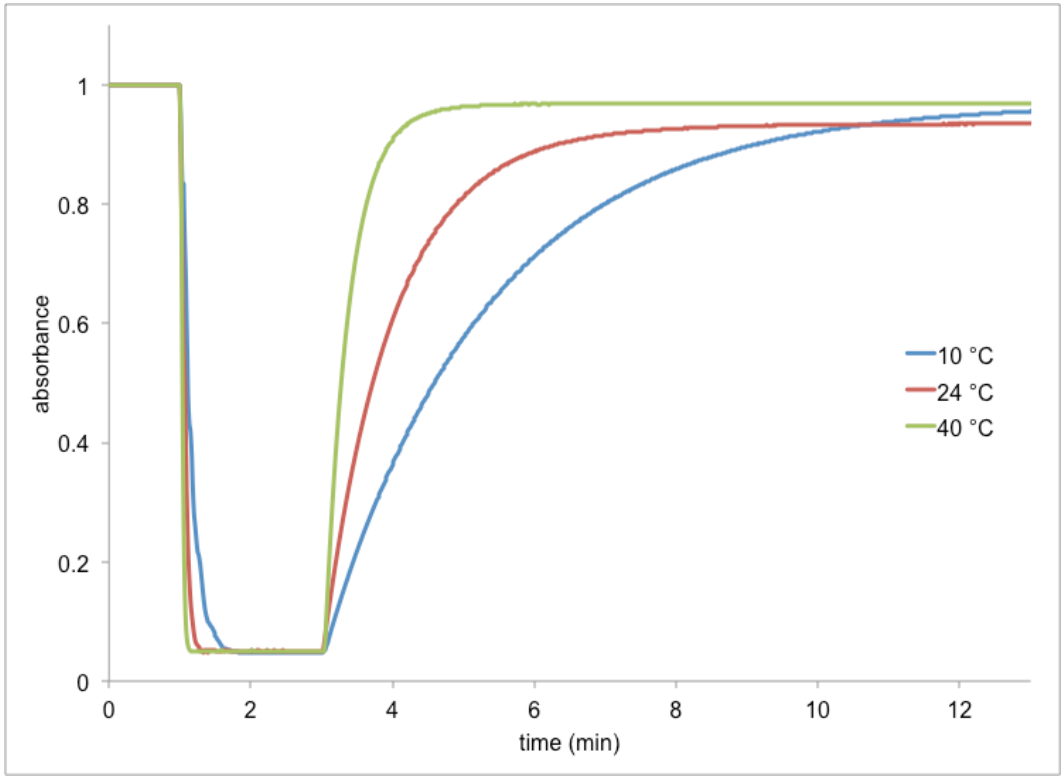

Figure 7: Effect of temperature on photoswitching of **36**. Experiments performed in reagent grade toluene, irradiating with unfiltered high intensity light.

The reversible conversion between the colored triene and the colorless cyclopentenone adduct is most dramatically effected by solvent (Figure 8). This is similar to spiropyran[47] and diarylethene[46] systems, which have also been shown to be highly solvent dependent. In protic solvents (methanol or water), the colored triene can be triggered by visible light and converted into the colorless zwitterionic cyclopentenone form; however, thermal reversion to the triene does not occur. In contrast, thermal reversion to the colored triene form is facile in halogenated solvents (dichloromethane, chloroform, or chlorobenzene), but photoisomerization to the cyclopentenone does not occur. For reversible photocyclization of the triene to cyclopentenone with thermal reversion of the cyclopentenone back to the triene, aromatic solvents (toluene, benzene, or xylenes) are ideal.

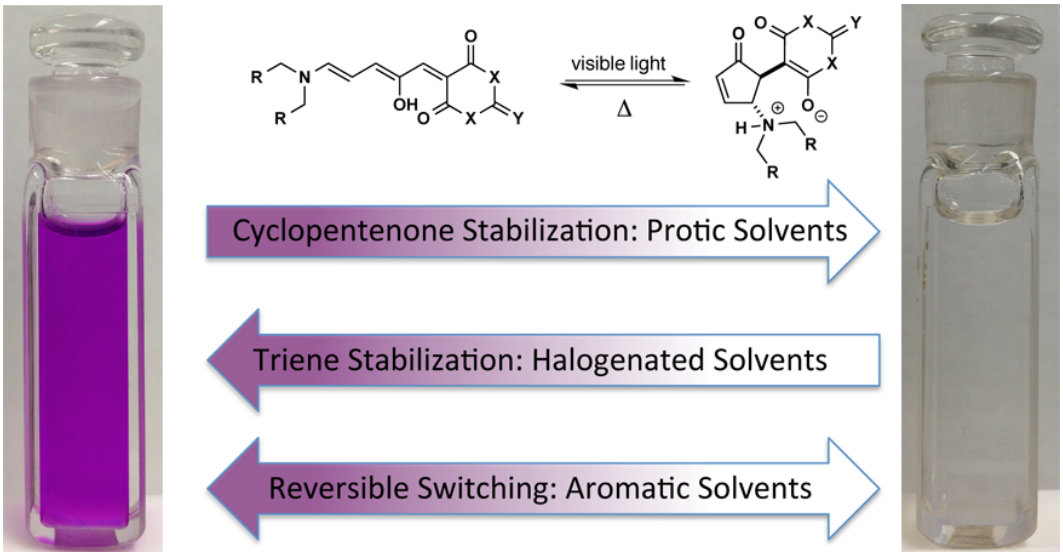

Figure 8. Solvent effects on the solution state switching behavior of DASAs.

We also found that the choice of acceptor group has an effect on the λ_{max} and associated color of the triene. For example, in toluene the Meldrum's acid derived triene **38** displays a λ_{max} of 545 nm, changing the acceptor to the more electron-withdrawing 1,3-dimethyl barbituric acid, **36**, results in a bathochromic shift to 570 nm. In both cases these derivatives are excellent organic dyes with extinction coefficients determined to be ~100,000 M^{-1} cm^{-1} for

the triene form. Further, we have found that these trienes display appreciable solvatochromism similar to other merocyanine-type materials (Figures 9 and 10).[48,49]

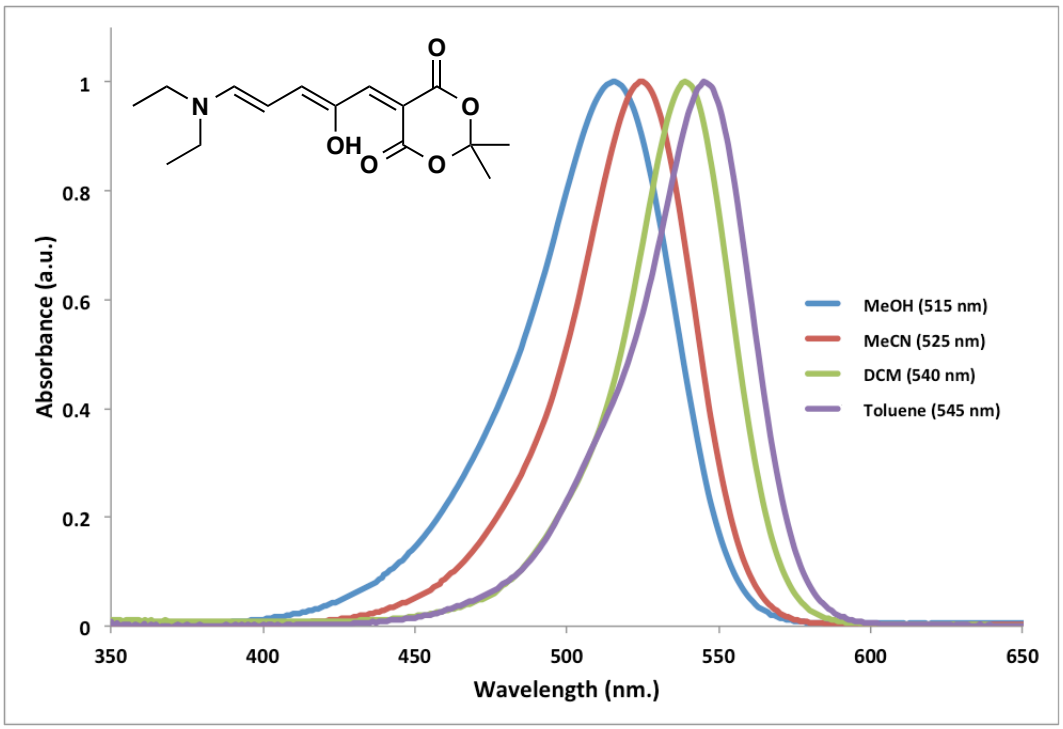

Figure 9 Solvent dependent spectral absorption of **38.**

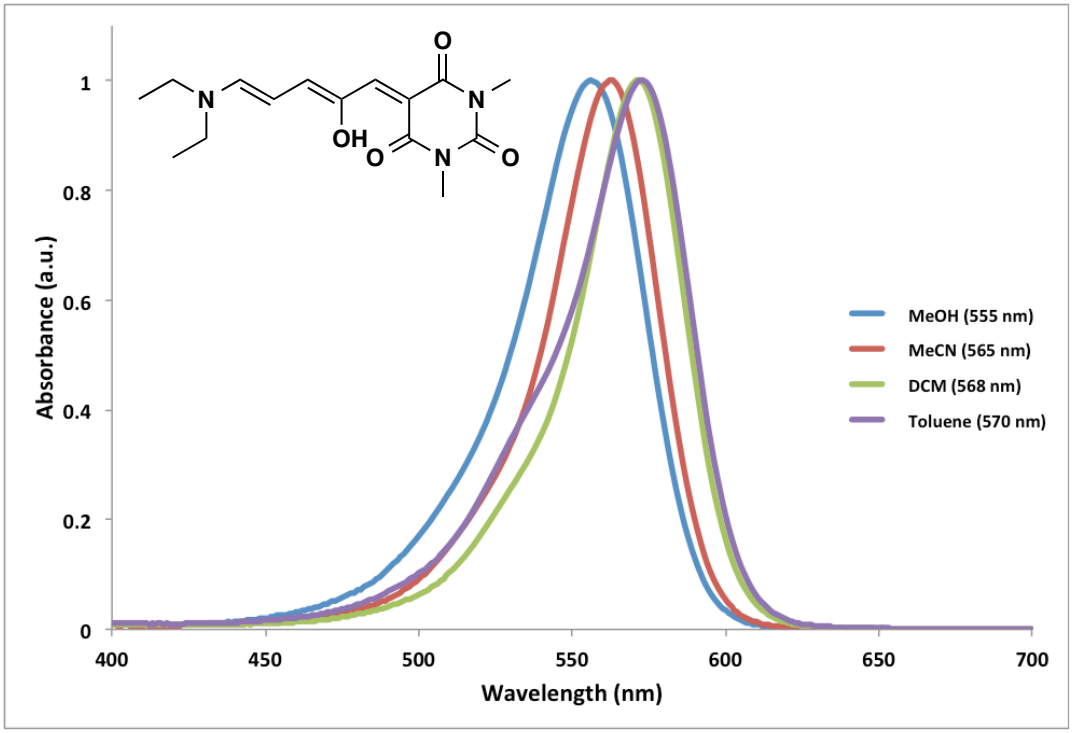

Figure 10. Solvent dependent spectral absorption of **36.**

From related studies, the mechanism of switching is proposed to occur via a reversible Nazarov-type 4π electrocyclization.[30–35] Importantly, conversion to the zwitterionic cyclopentenone (**37** and **39**) results in bleaching of all derivatives studied, providing colorless, water-soluble materials. Intrigued by the solution-state behavior of our DASA materials, we reasoned that these compounds could engage in dynamic phase transfer. If true, this enables applications of these compounds as visible light activated phase-transfer tags.[50–55] To probe the potential of this avenue, we layered toluene solutions of a variety od DASAs over water (Table 2). Upon irradiation of these biphasic systems with visible light, the DASAs were observed to cyclize with transfer of the DASA to the aqueous layer being quantified by UV−Vis and NMR spectroscopy.

Table 2. Schematic representation of DASA dynamic phase transfer and results.

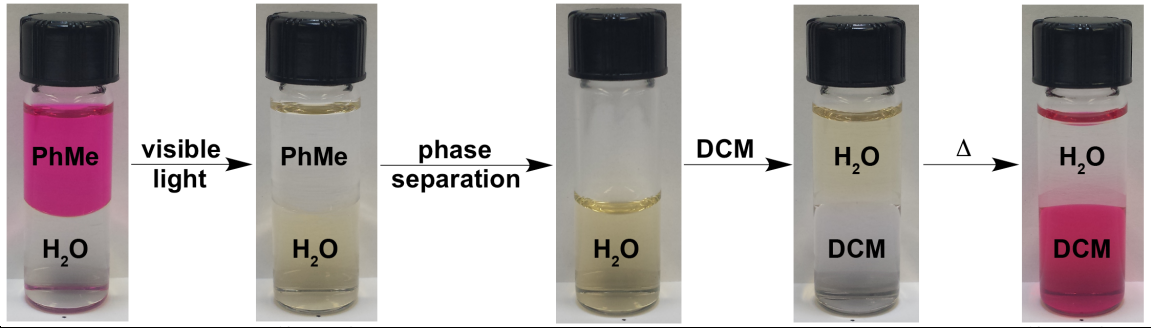

Entry	Acceptor	Donor	% Transferred to Aqueous	% Recovered from Aqueous
1	Meldrum's acid	Diethylamine	100	10
2	Meldrum's acid	Dibutylamine	>99	98
3	Meldrum's acid	Dihexylamine	80	77(96)
4	Meldrum's acid	Dioctylamine	0	NA
5	Dimethyl Barbituric acid	Diethylamine	100	5
6	Dimethyl Barbituric acid	Dibutylamine	85	81(95)
7	Dimethyl Barbituric acid	Dihexylamine	67	60(90)
8	Dimethyl Barbituric acid	Dioctylamine	0	NA

We found that the amine donor plays a dramatic role in the efficacy of transfer to the aqueous phase. Employing short alkyl chain amine donors (entries 1, 2, 5 and 6) results in near quantitative transfer of the DASA to the aqueous phase. Conversely, a long alkyl chain

donor (entries 4 and 8) results in DASA cyclization; however, these derivatives fail to transfer to the aqueous phase. Efforts to thermally revert the cyclopentenone to the triene and transfer the adduct from the aqueous layer back to the aromatic organic layer were unsuccessful. However, separation of the resultant aqueous solution and extraction with DCM enabled recovery of the triene forms (entries 1-3, 6 and 7) in 10% to quantitative yield, again highlighting the critical role of the amine donor in this process.

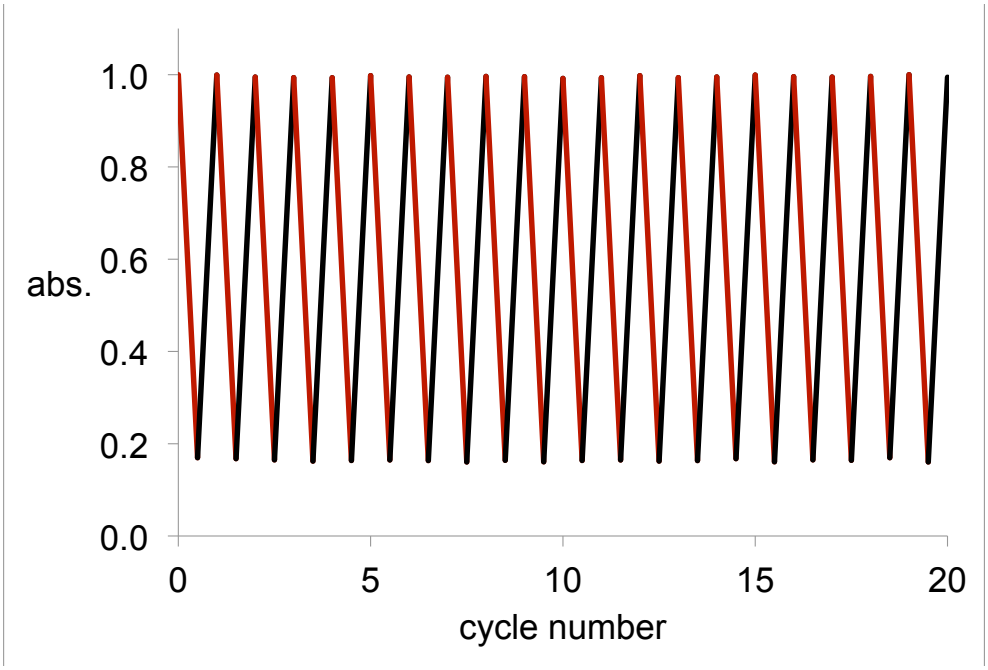

Figure 11. Fatigue testing of **36** in PhMe (0.16 mM), alternative irradiation at 570 nm (red) and dark (black).

Fatigue resistance is a key characteristic for gauging the potential of photochromic materials, thus the performance of DASA photoswitches was tested (Figure 11).[56] Rapid and complete switching of **36** was consistently observed when irradiating with visible light centered at the λ_{max} of our DASA with negligible material degradation (<0.05% loss per cycle), as measured by the intensity of absorbance.[2] As a comparison, when cycled with a broadband light source, a ~0.25% loss in efficiency was observed per cycle due to unfiltered UV light from the broadband source. Fatigue experiments were conducted in ambient conditions

without the need to exclude oxygen or water, demonstrating the robust nature of this process.

Further structural characterization of the two isomeric DASA states was provided by single-crystal X-ray diffraction, which revealed the triene form to be a conjugated, linear, hydrophobic material with an amine "donor" and a 1,3- dicarbonyl "acceptor" (see below in Figure 15). Our assignment of the cyclopentenone form as a zwitterion comes from the observation that these materials are water-soluble and further from bond length measurements in their crystal structures. We have found that one of the ester (or amide) functionalities in the 1,3-dicarbonyl moiety displays bond lengths more appropriate for a β-enolic ester (or amide) than a β-dicarbonyl (Figure 12).

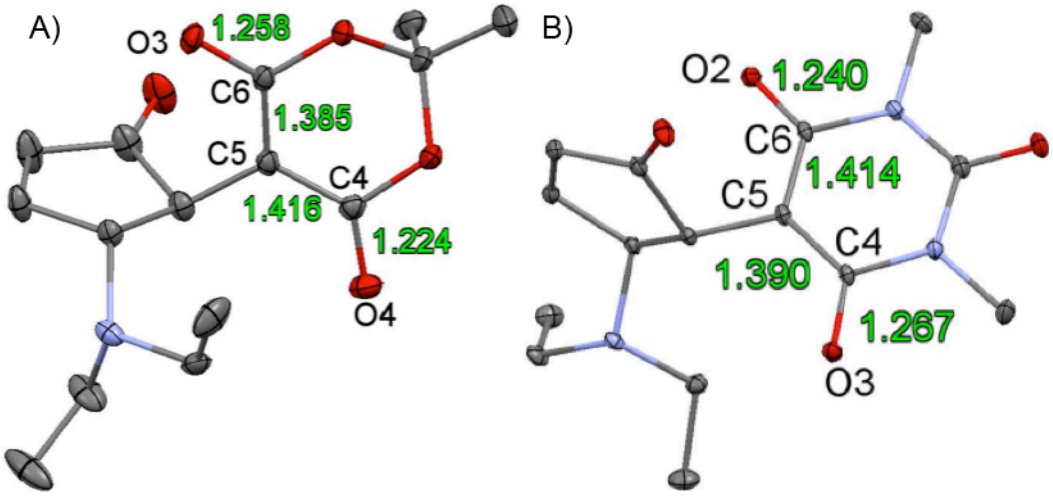

Figure 12. ORTEP renderings of A) derivative **39** and B) derivative **37**, showing atomic distance measurements used to initially assign the cyclopentenone form as a zwitterion (Distances in Å, 50% probability ellipsoids, hydrogen atoms omitted for clarity.

While we felt that both the hydrophilicity of the closed isomer and the data provided from our X-ray crystallographic studies gave nearly conclusive evidence that the closed isomer was indeed a zwitterion, we sought to unambiguously confirm protonation of the donor amine, in the cyclized state. X-ray photoelectron spectroscopy (XPS), is perhaps the

most powerful technique for the characterization of a surface[57] or crystal.[58–62] In an XPS measurement, X-rays of known energy are irradiated onto a surface or crystal, resulting in the emission of core electrons from the elements present. In turn the kinetic energy of the ejected electrons is quantified in relation to the energy of the incident X-ray beam. Thereby the ejected electrons binding energy is determined, which is dependent on the identity and electronic nature of the element from which they were emitted. In this way chemical changes in the material analyzed can be followed. For our purposes, we sought to track conversion of the neutral tertiary amine donor of the triene to the protonated ammonium of the proposed zwitterion. In high resolution X-ray photoelectron spectroscopy (HRXPS), these two states can be distinguished as neutral amines exhibit binding energy of ~400 eV, while ammonium species display binding energy of ~402 eV.

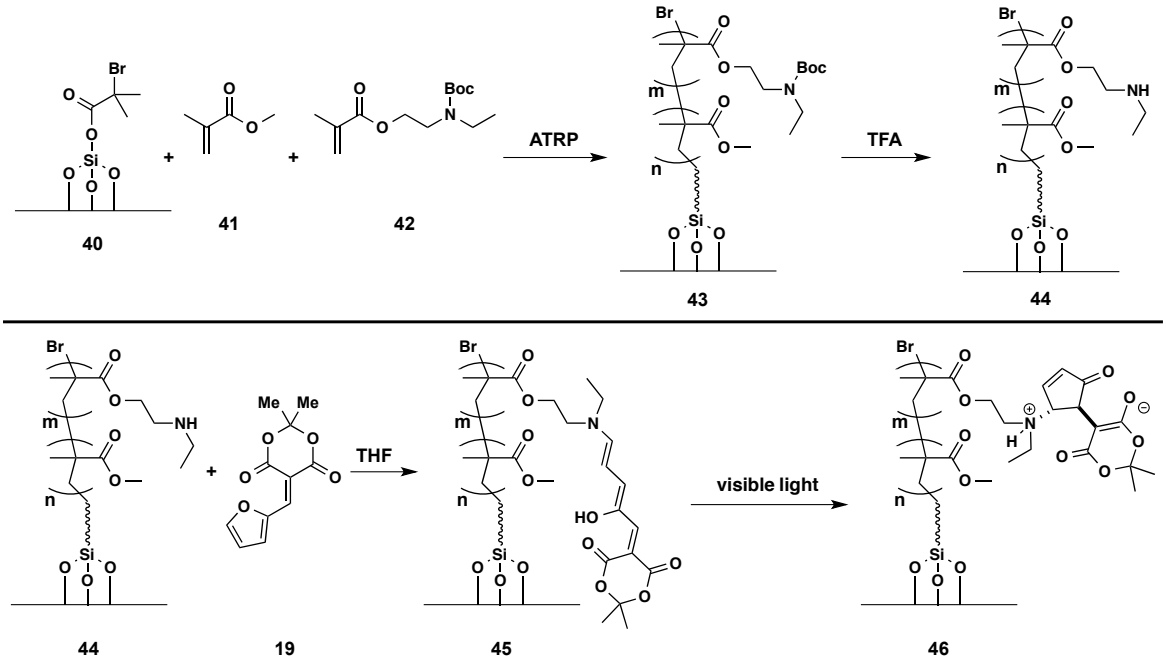

Figure 13. Preparation of DASA functionalized surface for XPS studies.

To accomplish this goal we designed and prepared a secondary amine functionalized polymer covalently bound to a silicon surface, which was reacted with activated furan **19** to

generate DASA functionalized surface **45**, Figure 13. DASA functionalized surface **45** was then exposed to visible light to presumably form surface **46**. We then analyzed surfaces **44** and **46** by HRXPS. Importantly, the choice of monomers and the use of activated furan **19**, ensure that any nitrogen signature in the XPS spectrum will arise solely from the amine donor of the appended DASA. If our hypothesis, that the cyclized form is a zwitterion, was correct we should clearly see this difference in the HRXPS spectra of the two substrates, where surface **44** should only show a peak at ~400 eV, and surface **46** at ~402 eV.

Indeed as can be seen in Figure 14A, surface **44** generates the expected single HRXPS peak centered at ~400 eV. In contrast surface **46** exhibits a broadened HRXPS signature centered at ~402 eV, Figure 14B. Deconvolution and peak fitting of this spectrum indicates that the nitrogen content of the surface is composed of 70% ammonium species. We are therefore confident based on solubility, single crystal X-ray diffraction, and HRXPS that the structure of the colorless cyclized isomer is a zwitterion.

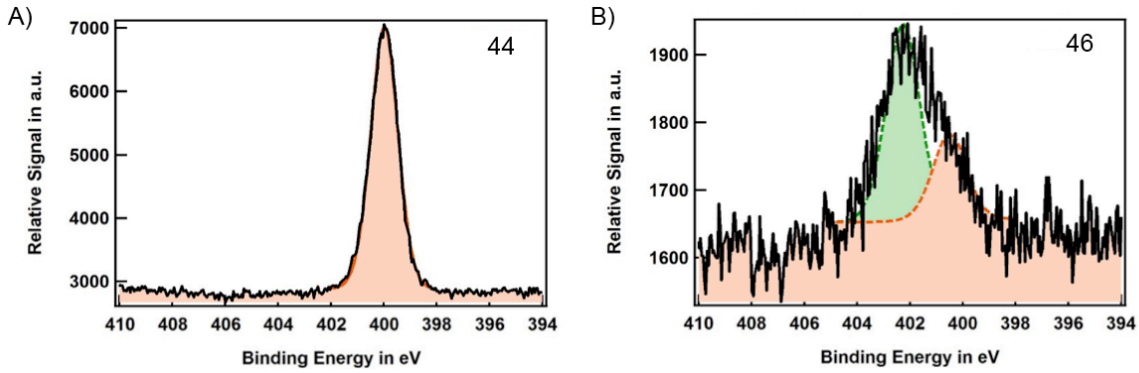

Figure 14. A) HRXPS spectra of surface **44**, B) HRXPS spectra of surface **46**.

The large molecular contraction these materials exhibit upon switching is clearly evident in their crystal structures (Figure 15). Atomic distance measurements identify a 52% molecular contraction of the DASA upon switching as measured from the nitrogen donor to the carbon at the 5 position of the acceptor (7.34/7.40 Å for the open derivative, 3.55/3.53 Å for

the closed). This distance is significantly greater than that observed for other privileged photoswitches, including the spiropyran[63,64] or azobenzene[65,66] systems, (~20% and 30% molecular contraction based on distance (Å) in published crystal structures, respectively).

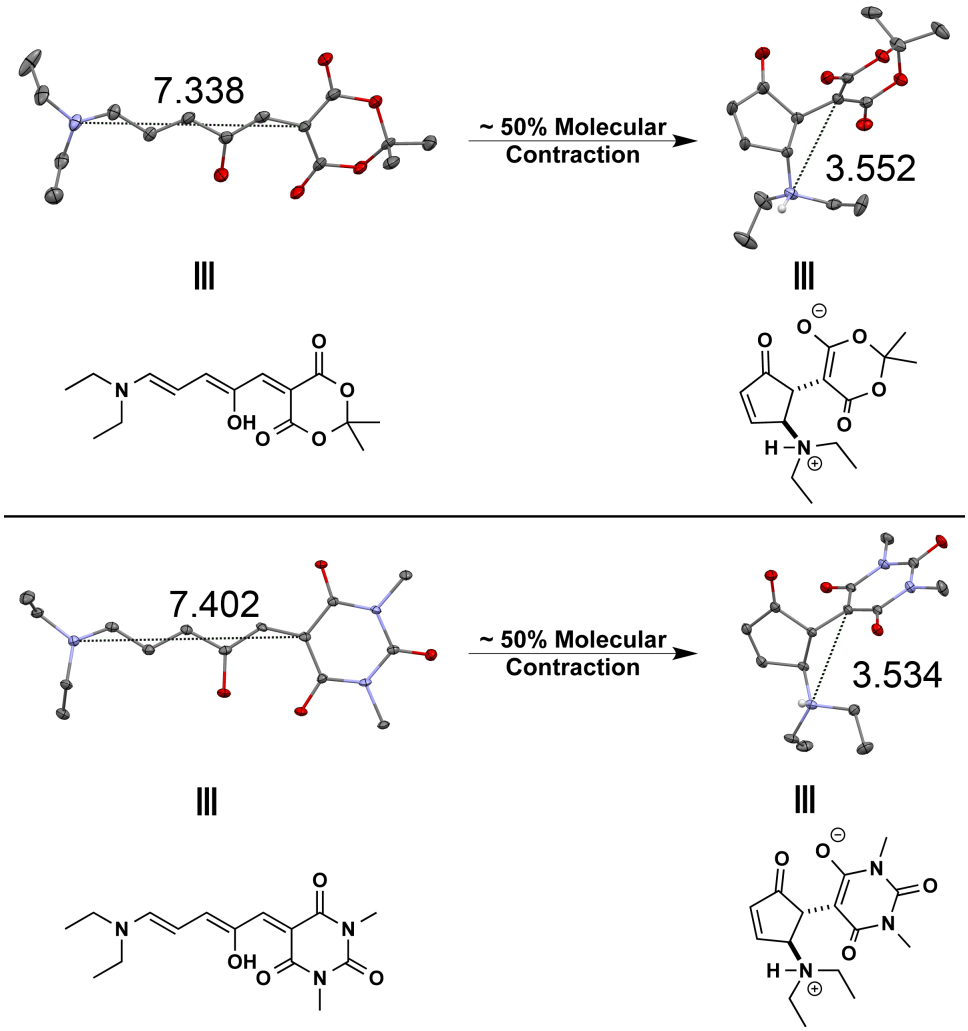

Figure 15: ORTEP renderings of **38** and **39** (top) and **36** and **37** (bottom) (Distances in Å, 50% probability ellipsoids, hydrogen atoms omitted for clarity).

2.4. Closing Remarks

With the ever increasing desire for on demand changes in material properties controlled by environmentally benign triggers, there exists a need for novel molecular switches capable of engaging in these functions. With the limited efforts towards the development of new organic negative photochromic compounds, fulfillment of this need has relied on tailoring

known systems to specific applications. We have developed a novel class organic photochromic compound, donor acceptor Stenhouse adducts, derived from renewable feedstocks, and prepared through a mild, rapid and operationally simple synthesis and purification. We have successfully identified conditions for the reversible and quantitative switching of these compounds in the solution phase. This new class of photoswitchable molecules is synthetically versatile and exhibits a unique combination of physical and chemical properties. These DASAs show reverse photochromism under visible light, which is complementary to previous classes of photoswitches, and display excellent fatigue resistance under ambient conditions.

2.5. References

(1) *Molecular switches*, 2nd, completely rev. and enl. ed.; Feringa, B. L., Browne, W. R., Eds.; Wiley-VCH: Weinheim, Germany, 2011.

(2) Kumpfer, J. R.; Rowan, S. J. *J. Am. Chem. Soc.* **2011**, *133* (32), 12866.

(3) Velema, W. A.; Szymanski, W.; Feringa, B. L. *J. Am. Chem. Soc.* **2014**, *136* (6), 2178.

(4) Spruell, J. M.; Hawker, C. J. *Chem Sci* **2011**, *2* (1), 18.

(5) Rau, H. In *Photochromism*; Elsevier, 2003; pp 165–192.

(6) Mourot, A.; Kienzler, M. A.; Banghart, M. R.; Fehrentz, T.; Huber, F. M. E.; Stein, M.; Kramer, R. H.; Trauner, D. *ACS Chem. Neurosci.* **2011**, *2* (9), 536.

(7) Tian, H.; Yang, S. *Chem. Soc. Rev.* **2004**, *33* (2), 85.

(8) Klajn, R. *Chem Soc Rev* **2014**, *43* (1), 148.

(9) Lee, H.; Wu, W.; Oh, J. K.; Mueller, L.; Sherwood, G.; Peteanu, L.; Kowalewski, T.; Matyjaszewski, K. *Angew. Chem. Int. Ed.* **2007**, *46* (14), 2453.

(10) Sendai, T.; Biswas, S.; Aida, T. *J. Am. Chem. Soc.* **2013**, *135* (31), 11509.

(11) Beharry, A. A.; Sadovski, O.; Woolley, G. A. *J. Am. Chem. Soc.* **2011**, *133* (49), 19684.

(12) Bléger, D.; Schwarz, J.; Brouwer, A. M.; Hecht, S. *J. Am. Chem. Soc.* **2012**, *134* (51), 20597.

(13) Cnossen, A.; Hou, L.; Pollard, M. M.; Wesenhagen, P. V.; Browne, W. R.; Feringa, B. L. *J. Am. Chem. Soc.* **2012**, *134* (42), 17613.

(14) Yang, Y.; Hughes, R. P.; Aprahamian, I. *J. Am. Chem. Soc.* **2012**, *134* (37), 15221.

(15) Hatano, S.; Horino, T.; Tokita, A.; Oshima, T.; Abe, J. *J. Am. Chem. Soc.* **2013**, *135* (8), 3164.

(16) Samanta, S.; Babalhavaeji, A.; Dong, M.; Woolley, G. A. *Angew. Chem. Int. Ed.* **2013**, *52* (52), 14127.

(17) Samanta, S.; Beharry, A. A.; Sadovski, O.; McCormick, T. M.; Babalhavaeji, A.; Tropepe, V.; Woolley, G. A. *J. Am. Chem. Soc.* **2013**, *135* (26), 9777.

(18) Arai, K.; Kobayashi, Y.; Abe, J. *Chem Commun* **2015**, *51* (15), 3057.

(19) Fujita, K.; Hatano, S.; Kato, D.; Abe, J. *Org. Lett.* **2008**, *10* (14), 3105.

(20) Harada, Y.; Hatano, S.; Kimoto, A.; Abe, J. *J. Phys. Chem. Lett.* **2010**, *1* (7), 1112.

(21) Hatano, S.; Fujita, K.; Tamaoki, N.; Kaneko, T.; Nakashima, T.; Naito, M.; Kawai, T.; Abe, J. *J. Phys. Chem. Lett.* **2011**, *2* (21), 2680.

(22) Iwahori, F.; Hatano, S.; Abe, J. *J. Phys. Org. Chem.* **2007**, *20* (11), 857.

(23) Kishimoto, Y.; Abe, J. *J. Am. Chem. Soc.* **2009**, *131* (12), 4227.

(24) Muyoh, K.; Hatano, S.; Abe, J. *J. Photopolym. Sci. Technol.* **2010**, *23* (3), 301.

(25) Blanco-Lomas, M.; Campos, P. J.; Sampedro, D. *Org. Lett.* **2012**, *14* (17), 4334.

(26) Blanco-Lomas, M.; Funes-Ardoiz, I.; Campos, P. J.; Sampedro, D. *Eur. J. Org. Chem.* **2013**, *2013* (29), 6611.

(27) Chen, J.-J.; Li, K.-T.; Yang, D.-Y. *Org. Lett.* **2011**, *13* (7), 1658.

(28) Li, K.-T.; Lin, Y.-B.; Yang, D.-Y. *Org. Lett.* **2012**, *14* (5), 1190.

(29) Lin, C.-H.; Yang, D.-Y. *Org. Lett.* **2013**, *15* (11), 2802.

(30) Veits, G. K.; Wenz, D. R.; Read de Alaniz, J. *Angew. Chem. Int. Ed.* **2010**, *49* (49), 9484.

(31) Palmer, L. I.; Read de Alaniz, J. *Angew. Chem. Int. Ed.* **2011**, *50* (31), 7167.

(32) Palmer, L. I.; de Alaniz, J. R. *Org. Lett.* **2013**, *15* (3), 476.

(33) Palmer, L. I.; Veits, G. K.; Read de Alaniz, J. *Eur. J. Org. Chem.* **2013**, *2013* (28), 6237.

(34) Yu, D.; Thai, V. T.; Palmer, L. I.; Veits, G. K.; Cook, J. E.; Read de Alaniz, J.; Hein, J. E. *J. Org. Chem.* **2013**, *78* (24), 12784.

(35) Fisher, D.; Palmer, L. I.; Cook, J. E.; Davis, J. E.; Read de Alaniz, J. *Tetrahedron* **2014**, *70* (27-28), 4105.

(36) Honda, K.; Komizu, H.; Kawasaki, M. *J. Chem. Soc. Chem. Commun.* **1982**, No. 4, 253.

(37) Stenhouse, J. *Ann. Chem. Pharm.* **1870**, *156* (2), 197.

(38) Schiff, H. *Justus Liebigs Ann. Chem.* **1887**, *239* (3), 349.

(39) Vanderwal, C. D. *J. Org. Chem.* **2011**, *76* (23), 9555.

(40) Henary, M.; Levitz, A. *Dyes Pigments* **2013**, *99* (3), 1107.

(41) Mishra, A.; Behera, R. K.; Behera, P. K.; Mishra, B. K.; Behera, G. B. *Chem. Rev.* **2000**, *100* (6), 1973.

(42) D'Arcy, B.; Lewis, K.; Mulquiney, C. *Aust. J. Chem.* **1985**, *38* (6), 953.

(43) Lewis, K. G.; Mulquiney, C. E. *Tetrahedron* **1977**, *33* (5), 463.

(44) Li, S.-W.; Batey, R. A. *Chem. Commun.* **2007**, No. 36, 3759.

(45) Šafář, P.; Považanec, F.; Prónayová, N.; Baran, P.; Kickelbick, G.; Kožíšek, J.; Breza, M. *Collect. Czechoslov. Chem. Commun.* **2000**, *65* (12), 1911.

(46) Irie, M.; Sayo, K. *J. Phys. Chem.* **1992**, *96* (19), 7671.

(47) Murugan, N. A.; Chakrabarti, S.; Ågren, H. *J. Phys. Chem. B* **2011**, *115* (14), 4025.

(48) Reichardt, C. *Chem. Rev.* **1994**, *94* (8), 2319.

(49) Kulinich, A. V.; Derevyanko, N. A.; Ishchenko, A. A. *Russ. J. Gen. Chem.* **2006**, *76* (9), 1441.

(50) Liu, G.; Wang, J. *Angew. Chem. Int. Ed.* **2010**, *49* (26), 4425.

(51) Bergbreiter, D. E. *Chem. Rev.* **2002**, *102* (10), 3345.

(52) Yoshida, J.; Itami, K. *Chem. Rev.* **2002**, *102* (10), 3693.

(53) Fan, Q.-H.; Li, Y.-M.; Chan, A. S. C. *Chem. Rev.* **2002**, *102* (10), 3385.

(54) Dickerson, T. J.; Reed, N. N.; Janda, K. D. *Chem. Rev.* **2002**, *102* (10), 3325.

(55) Curran, D. P. *Angew. Chem. Int. Ed.* **1998**, *37* (9), 1174.

(56) Bertelson, R. C. In *Organic Photochromic and Thermochromic Compounds*; Crano, J. C., Guglielmetti, R. J., Eds.; Kluwer Academic Publishers: Boston, 2002; pp 11–83.

(57) Strother, T. *Nucleic Acids Res.* **2000**, *28* (18), 3535.

(58) Stevens, J. S.; Newton, L. K.; Jaye, C.; Muryn, C. A.; Fischer, D. A.; Schroeder, S. L. M. *Cryst. Growth Des.* **2015**, *15* (4), 1776.

(59) Stevens, J. S.; de Luca, A. C.; Pelendritis, M.; Terenghi, G.; Downes, S.; Schroeder, S. L. M. *Surf. Interface Anal.* **2013**, *45* (8), 1238.

(60) Stevens, J. S.; Byard, S. J.; Schroeder, S. L. M. *J. Pharm. Sci.* **2010**, *99* (11), 4453.

(61) Stevens, J. S.; Byard, S. J.; Seaton, C. C.; Sadiq, G.; Davey, R. J.; Schroeder, S. L. M. *Angew. Chem. Int. Ed.* **2011**, *50* (42), 9916.

(62) Stevens, J. S.; Byard, S. J.; Muryn, C. A.; Schroeder, S. L. M. *J. Phys. Chem. B* **2010**, *114* (44), 13961.

(63) Clegg, W.; Norman, N. C.; Flood, T.; Sallans, L.; Kwak, W. S.; Kwiatkowski, P. L.; Lasch, J. G. *Acta Crystallogr. C* **1991**, *47* (4), 817.

(64) Hobley, J.; Malatesta, V.; Millini, R.; Montanari, L.; O Neil Parker, Jr, W. *Phys. Chem. Chem. Phys.* **1999**, *1* (14), 3259.

(65) Harada, J.; Ogawa, K.; Tomoda, S. *Acta Crystallogr. B* **1997**, *53* (4), 662.

(66) Mostad, A.; Rømming, C.; Rømming, C.; Hammarström, S.; Lousberg, R. J. J. C.; Weiss, U. *Acta Chem. Scand.* **1971**, *25*, 3561.

3. Synthetic Scope

3.1. Background and Motivation

Having succeeded in our efforts to prepare DASAs,[1] we sought to determine the limits of diversity in terms of the scope of acceptors, donors and methods to effect cyclization. Among the factors motivating us to probe structural diversity, our primary interests were focused on the ability to tune the wavelength of activation and functional group tolerance. While our interest in alternate methods to effect cyclization were driven by a desire to provide access to the cyclopentenone isomer for those applications where thermochromism was desired.

In recent decades, significant effort has been devoted to the chemistry of organic photochromic systems. Their ability to undergo reversible spectral and physical property changes has led to applications ranging from energy production,[2] chemical sensing,[3] and molecular actuators[4] to biological systems.[5–9] The driving force for this focus is the abundant and versatile nature of light as a stimulus which enables both temporal and spatial resolution. However, for a photochromic compound to be applied it is often necessary that it be chemically ligated to a macromolecular system. As such, it is critical to know which functional groups, which can be exploited for this chemical ligation, are tolerated in the synthetic methodology used to prepare the photochromic molecule.

The ability to tune wavelength of activation without the need to modify the synthetic methodology would constitute a significant advance over the accepted practices widely employed for tuning azobenzenes,[10–12] spiropyrans[13] and diarylethenes.[14,15] Specifically, with the discovery that the acceptor moiety has a direct effect on the wavelength of activation, we were interested in examining not only what properties of the acceptor lead to a change in

triene absorbance, but also in attempting to prepare derivatives activated by near infrared (NIR) radiation (650-900 nm). In the realm of biomedical applications, photo-therapeutics are most effective when activated by NIR.[16] The superior performance of NIR in biomedical applications is a result of the spectral absorbance of tissues and fluids; hemoglobin (which absorbs visible light) along with water and lipids (which absorb infrared light) have their lowest absorption coefficient in the NIR.[17,18]

Finally, as a T-type photochromic system,[19] the ability to use heat (ambient or elevated) to revert the metastable DASA cyclopentenone isomer to the more thermodynamically stable triene allows for potential thermochromic applications. As has been shown, photochromic cyclization of DASA triene occurs at dilute concentrations, preventing isolation of the colorless isomer. Accordingly, we sought to develop chemical methods for the cyclization of the triene that also facilitated isolation of the cyclopentenone isomer.

3.2. Donors

3.2.1. Meldrum's Acid Derived DASAs

Having developed optimized conditions for the selective formation and isolation of the triene isomer, we proceeded to evaluate the generality of this process with a range of amine nucleophiles. We found that a broad array of secondary aliphatic amines are competent reaction partners. As can be seen in Figure 1, employing Meldrum's acid activated furan **1**, the desired DASA trienes were obtained in good to excellent yield. We were gratified to find that cyclic secondary amines, including those that bear heteroatoms, and acyclic secondary amines were well tolerated. It is of not that while amino-esters **9** are compatible, the corresponding amino acid, proline, returns only unreacted **1**. Diallylamine, which can be employed as a reaction partner in thiol-ene "click" reactions, was also effective for producing

triene **16**.[20] The broad applicability and widespread adoption of the copper catalyzed azide-alkyne cycloaddition (CuAAC) "click" reaction, prompted us to prepare derivative **15**.[21,22] With an interest in potential applications in polymer settings, derivatives **17** and **18** were prepared with amine donors that could serve as an acrylate monomer and ATRP initiator, respectively. Further, benzylic amines, both cyclic and acyclic were well tolerated, again providing the expected DASA trienes in excellent yield. Finally, secondary anilines were found to participate in the ring opening reaction, though with significantly diminished yield. In the course of this investigation we found that the reaction of **1** with primary aliphatic amines and primary anilines resulted in decomposition.

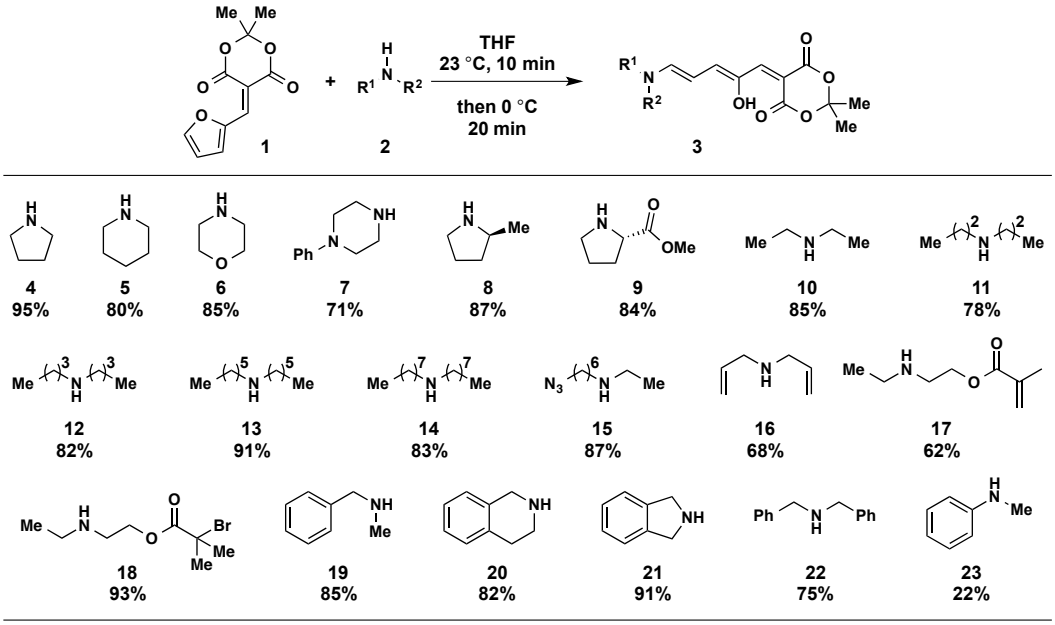

Figure 1. Synthesis of Meldrum's acid derived DASAs, isolated yields.

3.2.2. 1,3-Dimethylbarbituric Acid Derived DASAs

With these results in hand, we proceeded to evaluate this selection of amine donors towards ring opening of 1,3-dimethylbarbituric acid activated furan **24**, Figure 2. We were pleased to find that the desired Stenhouse adducts were formed in good yield and had nearly equal scope as the Meldrum's acid derivatives with respect to the compatibility of the amine

nucleophile with few exceptions. In the case of morpholine (**28**) and phenylpiperazine (**29**) decomposition of **24** is observed, whereas for isoindoline (**43**), dibenzylamine (**44**), and *N*-methylaniline (**45**) the starting material is recovered. Again here, as was seen for activated furan **1**, the reaction of **24** with primary aliphatic amines and primary anilines resulted in decomposition.

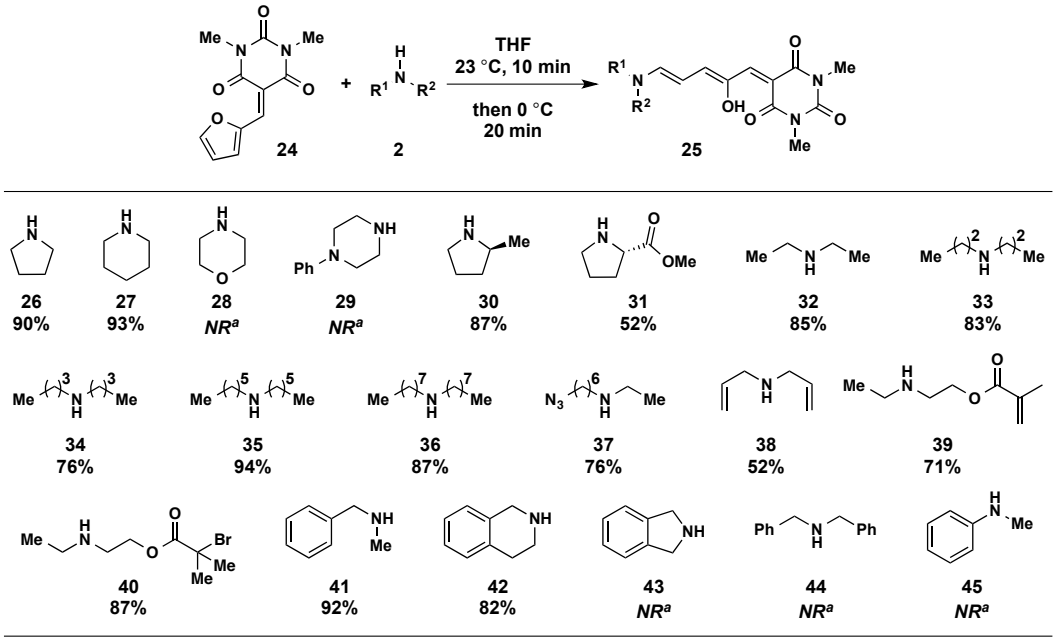

Figure 2. Synthesis of 1,3-dimethylbarbituric acid derived DASAs, isolated yields. [a]*NR*: no reaction.

With a broad and versatile scope of amine nucleophiles established, we sought to determine what effect, if any, the nature of the donor would have on the photochromism of the obtained adducts. We have found that a subset of the triene adducts synthesized do not undergo photoisomerization under the conditions described in Chapter 2. These include adducts derived from amines bearing two benzylic carbons, isoindoline (**21**) and dibenzylamine (**30**), or from amines bearing an electron-withdrawing group, proline methyl ester (**9** and **31**). Interestingly, the adducts derived from either the acrylate monomer (**17** and **39**) or

the ATRP initiator (**18** and **40**) engage in the photochromic transformation to produce the corresponding zwitterionic cyclopentenone.

3.3. Acceptors

3.3.1. Exploration of Cyclic Active Methylene Acceptors

In our initial studies we found that both Meldrum's acid and 1,3-dimethylbarbituric acid were effective activating groups for the ring opening reaction, where acyclic β-diketones and β-diesters or cyclic β-diketones were not. Further, we observed several significant differences in the photophysical properties of the photochromes obtained from these two acceptors. First, there is a bathochromic shift of 25 nm in the λ_{max} of the triene isomer on changing the acceptor from Meldrum's acid to 1,3-dimethylbarbituric acid. Second, there is a marked difference in their rates of thermal reversion, where the zwitterionic cyclopentenone of the 1,3-dimethylbarbituric acid derived DASA recolors approximately twice as fast as its Meldrum's acid derived counterpart.

To probe the limits of diversity in the structure and nature of the acceptor, and ultimately determine its effect on the photochromism of any DASA adducts obtained, we evaluated a wider selection of cyclic and heterocyclic β-dicarbonyl active methylene compounds.[23–25] As outlined in Scheme 1, these potential acceptors were condensed with furfural and the resulting Knoevenagel adducts were then treated with diethylamine.[26,27]

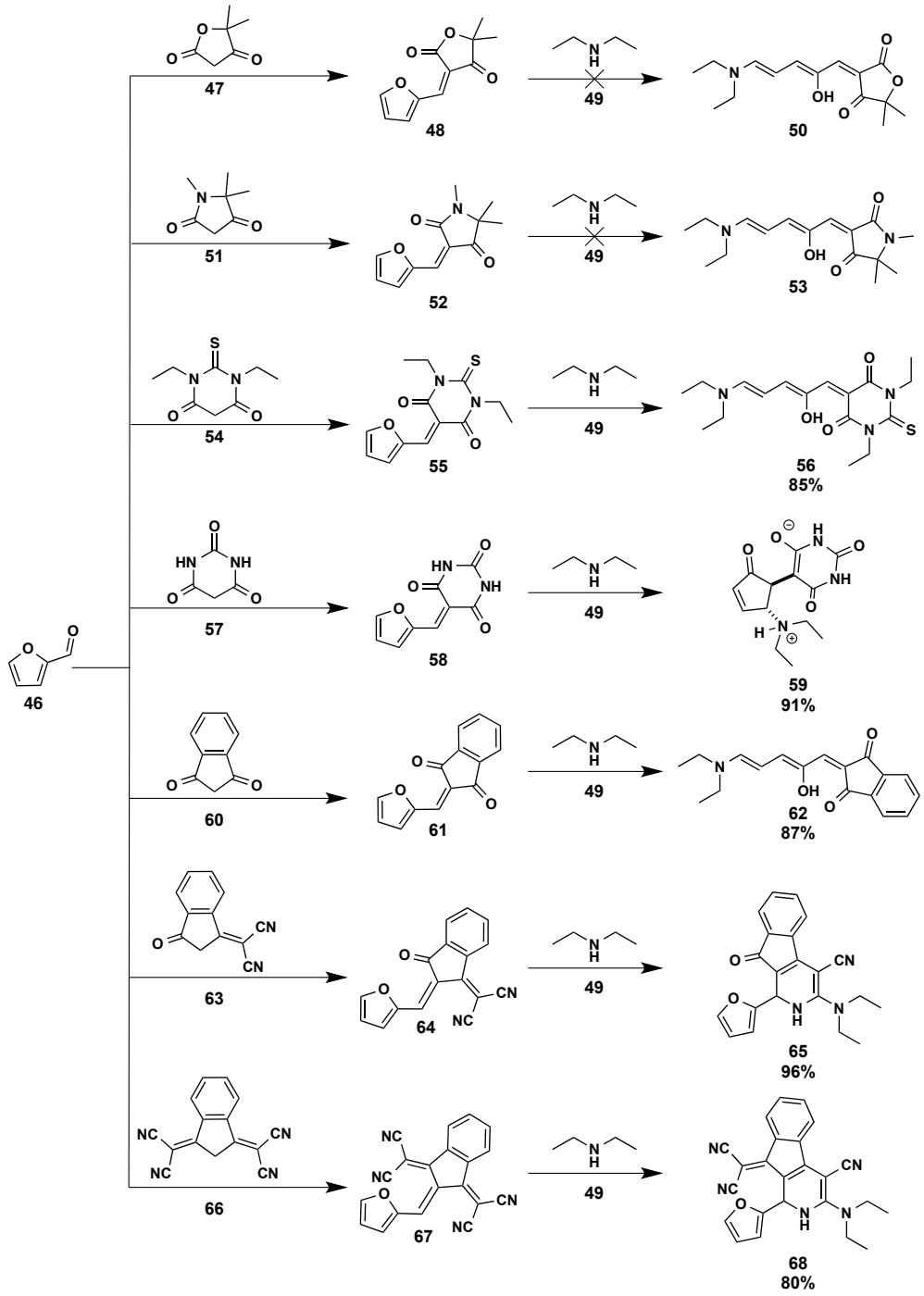

Scheme 1. Expanded evaluation of the scope of active methylene activating groups.

The use of tetronic acid **47** or tetramic acid **51** provided the desired Knoevenagel adduct, however, these activated furans failed to react with diethylamine, and decomposed under the established reactions conditions. 1,3-Diethylthiobarbituric acid **54** was successful at activat-

ing the furan providing the desired DASA triene **56** in 85% yield. This adduct has a λ_{max} of 605 nm, and exhibits the expected photochromic behavior. It is of note that while this derivative behaves as expected, the triene decomposes when stored under ambient conditions. Interestingly, the use of barbituric acid **57** as an activating group provides only the corresponding zwitterionic cyclopentenone **59**. All efforts to access the corresponding triene isomer, either thermally or chemically, were unsuccessful. Similar to 1,3-Diethylthiobarbituric acid **54**, the use of 1,3-indandione **60** provided DASA adduct **62** with a λ_{max} of 600 nm. However, this derivative was not observed to engage in photochromism under the currently optimized conditions. Finally, the use of 1,1-dicyanomethylene-3-indanone **63** and 1,3-bis(dicyanomethylene)-indan **66**, did not produce the desired triene, instead giving the expanded ring dihydroindenopyridine carbonitrile derivatives **65** and **68**, respectively.[28] We have found that these derivatives (**65** and **68**) oxidize in air to the corresponding pyridine adduct. This oxidation can also be affected synthetically with either the mild oxidizing agent chloranil for **65**, or the much stronger $KMnO_4$ for **68**. While we had expected that the use of activating groups **63** and **66** would provide a further bathochromic shift in the absorbance of the triene, however, the isolation of **65** and **68** demonstrate that this strategy was not effective. Thus the continued exploration of activating groups to determine the properties that control the absorbance of the triene remains as a challenge in the further development of DASA photoswitches, particularly if they are to be successfully and widely adopted in biological or biomedical applications.

3.3.2. Diversity in 1,3-Disubsituted Barbituric Acids

Considering the limited success of these efforts we chose to refocus and probe the potential diversity of substituents on the barbituric acid group. This would provide evidence that

the *N*-group could serve as a functional handle for the incorporation of these molecules into materials. We thus prepared several 1,3-disubstituted barbituric acids with various alkyl and aryl substituents. After condensation with furfural, reaction with diethylamine resulted in ring opening to give the anticipated colored trienes in high yield (Scheme 2).

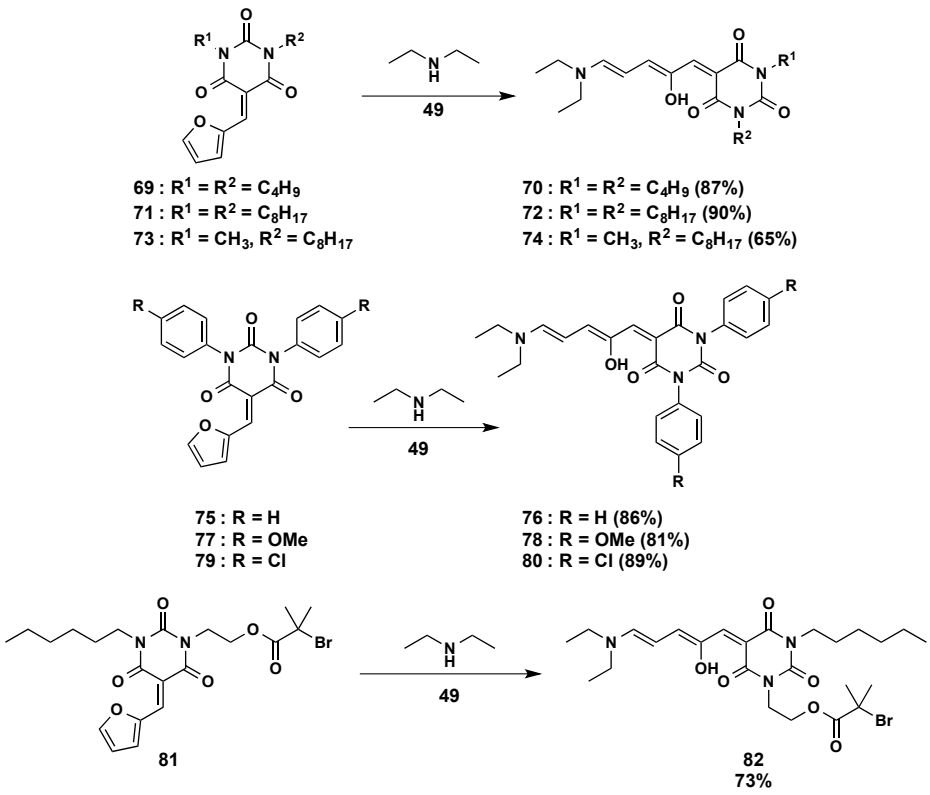

Scheme 2. Synthesis of 1,3-disubstituted barbituric acid derived DASAs.

All of the DASA derivatives shown in Scheme 2 display the expected λ_{max} of ~570 nm that was observed for those derived from 1,3-dimethylbarbituric acid, demonstrating that the nature of substituents on the nitrogen atoms of the barbituric acid group do not affect the absorbance of the triene. On examining the photochromic behavior of these derivatives, we were gratified to find that all engage in fully reversible T-type photochromism, under the conditions previously established. Further, we were particularly pleased to obtain derivative **82**, which bears an ATRP initiator allowing for this DASA (and the activated furan it was

derived from) to serve as complement to secondary amine donor used to prepared DASA adducts **18** and **40**.

3.4. Cyclization by Chemical Catalysis

3.4.1. Background

In accord with Safar's work, we found that furan substrates bearing a substituent at the 3-postion, did not afford Stenhouse adducts, providing only the cyclopentenone products (Scheme 3).

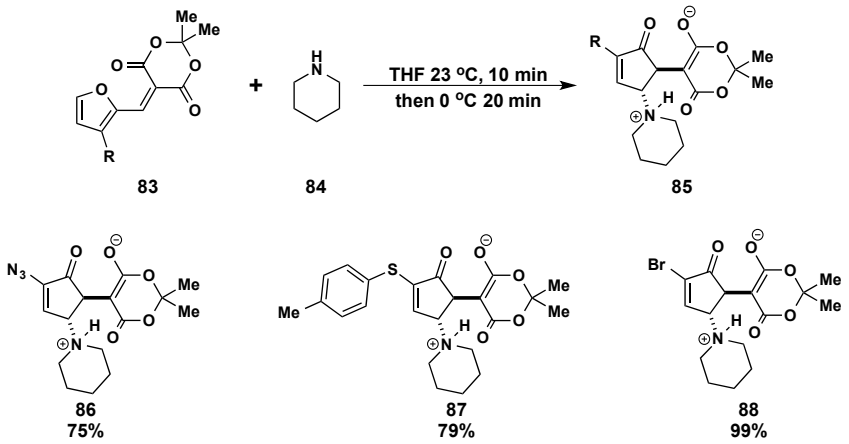

Scheme 3. Effect of substitution of on the furan nucleus.

We hypothesized that this result is due to $A^{1,3}$ strain in the 2*E*,4*E* conformation of the substituted Stenhouse intermediate (Figure 3). Isomerization to the 2*E*,4*Z* conformation relieves this strain and place the molecule in the appropriate conformation for the electrocyclization to occur. Based on this we reasoned that a catalyst capable of alkene isomerization would facilitate isomerization and subsequent electrocyclization to provide the desired cyclopentenone isomers.

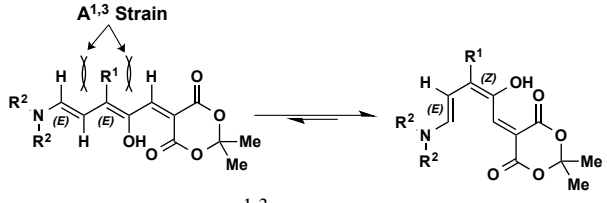

Figure 3. Alkene isomerization due to $A^{1,3}$ strain.

3.4.2. Development and Scope

A number of catalysts known to induce alkene isomerization were evaluated (Table 1). Although, DMAP, DABCO and PPh_3 all mediated the cyclization, PPh_3 was identified as the ideal catalyst due to its reduced toxicity in comparison to DMAP. As with the Stenhouse adducts, these products are easily isolated by filtration and washing with cold diethyl ether. While initial experiments were conducted using a stoichiometric quantity of catalyst, further testing revealed that loading could be reduced as low as 5 mol %. Importantly, this mild procedure allows for isolation of these materials without the use of concentrated HBr, as previously developed by Safar.[29]

Table 1. Optimization of cyclopentenone formation by chemical catalysis.

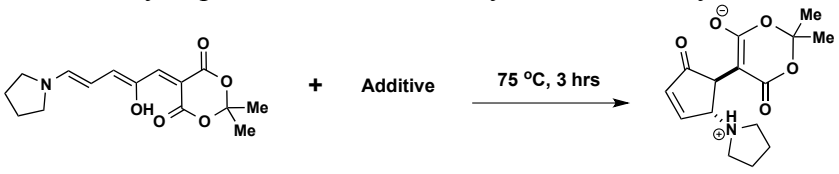

4 89

Catalyst	mol %	Solvent	% Yield
DMAP	100	Acetonitrile	90
DABCO	100	Acetonitrile	70
PPh_3	100	CH_2Cl_2	80
PPh_3	100	Acetonitrile	90
PPh_3	25	Acetonitrile	97
PPh_3	5	Acetonitrile	93

The triphenylphosphine catalyzed cyclization conditions were then applied to a selection of the Meldrum's acid derived Stenhouse adducts. To our delight, we found that nearly all adducts were converted to the desired cyclopentenones in good yield (Figure 4). Notable

exceptions were the adduct derived from diallylamine (**98**), which decomposed under the reaction conditions, and substrates that either contained an electron-withdrawing group on the amine component (**95**) or possessed two benzylic carbon on the amine (**101** and **102**) where the starting triene was recovered.

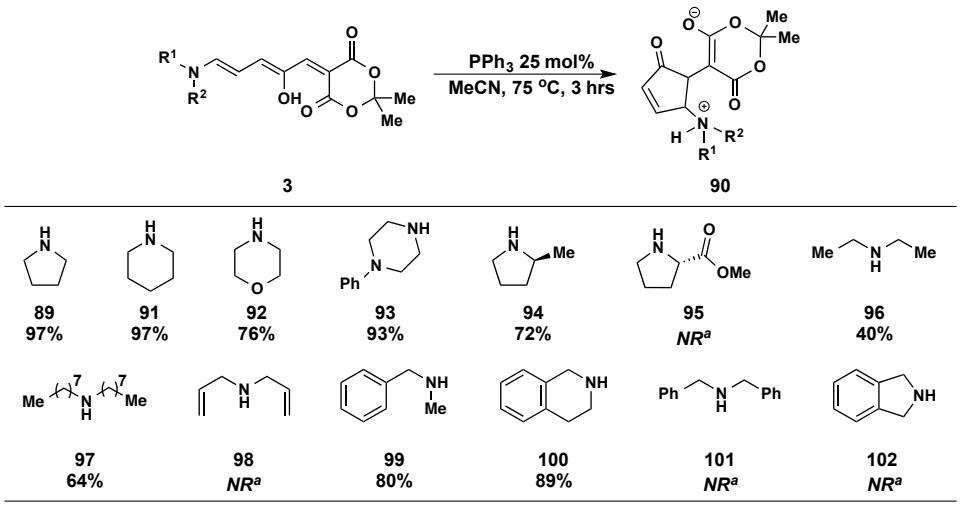

Figure 4. Triphenylphosphine catalyzed cyclization of Meldrum's acid derived DASAs, isolated yields. [a]*NR*: no reaction.

Encouraged by these results, we evaluated if visible light alone could be employed, as an environmentally benign method, to convert the deeply colored Stenhouse adducts to the colorless cyclopentenones. As discussed in Chapter 2, protic solvents stabilize the cyclopentenone isomer. Thus we irradiated methanolic solutions of the same selection of Meldrum's acid derived DASA trienes with a commercially available GE crystal clear 200 bulb. Application of these conditions gratifyingly provided the cyclopentenones in good to excellent yield, including the diallylamine adduct **98**. Again, those substrates with an electron-withdrawing group **94** or two benzylic carbons in the amine component (**101** and **102**) failed to convert to the cyclopentenone (Figure 5).

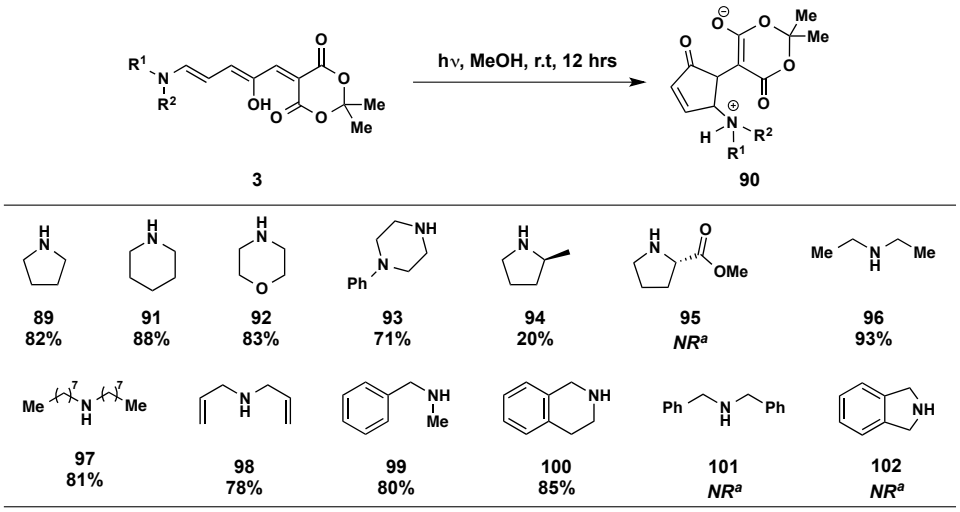

Figure 5. Photo-cyclization of Meldrum's acid derived DASAs, isolated yields. [a]*NR*: no reaction.

We then proceeded to evaluate the efficacy of the PPh_3 protocol to a selection of the 1,3-dimethylbarbituric acid derived DASAs (Figure 6). We found that the corresponding zwitterions were formed in good to excellent yield. Here as with the Meldrum's acid based DASAs, the adduct derived from diallylamine (**110**) decomposed and the substrate bearing an electron-withdrawing group on the amine component (**107**) returned only unconverted starting material.

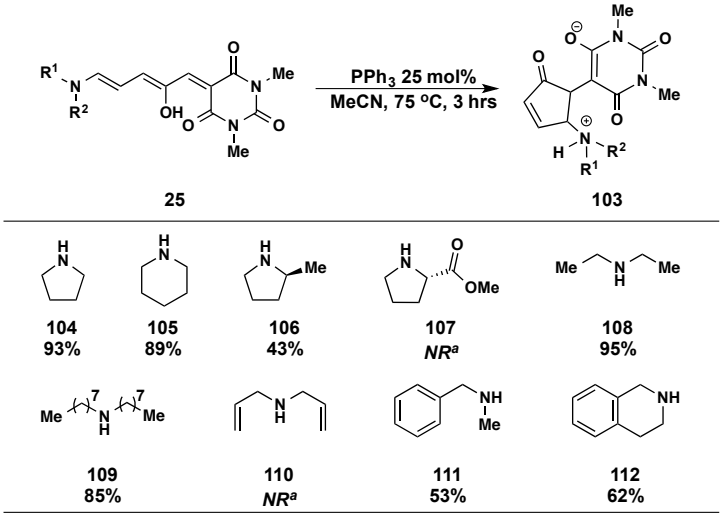

Figure 6. Triphenylphosphine catalyzed cyclization of 1,3-dimethylbarbituric acid derived DASAs, isolated yields. [a]*NR*: no reaction.

Finally, we subjected the same selection of 1,3-dimethylbarbituric acid derived DASAs to the photo-cyclization conditions (Figure 7). A similar trend was again observed, here the 1,3-dimethylbarbituric acid/diallylamine cyclopentenone **110** was obtained in 77% yield, while the adduct bearing an electron-withdrawing group **107** returned only starting material.

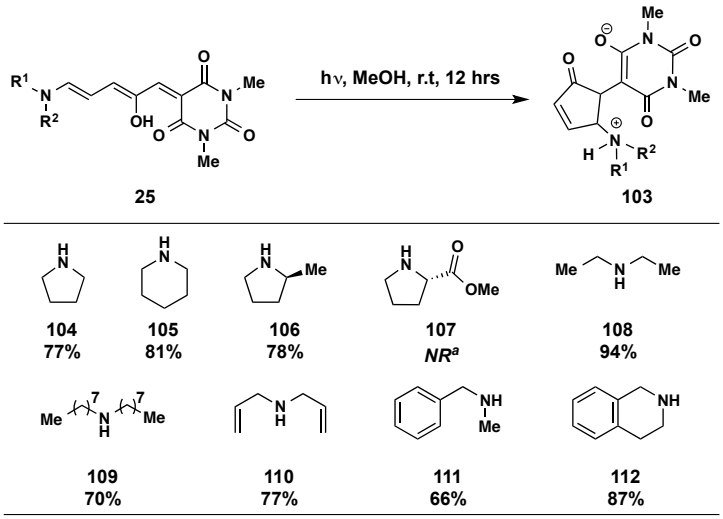

Figure 7. Photo-cyclization of 1,3-dimethylbarbituric acid derived DASAs, isolated yields. [a]*NR*: no reaction.

3.5. Advances in Synthetic Methodology

Having explored the scope of the donors and acceptors, we sought to probe the synthetic methodology used to prepare both the DASA trienes and zwitterionic cyclopentenones, with a primary interest in developing one-pot procedures. Domino reactions have become a flourishing field in organic synthesis, as they hold the promise of greener and more efficient methods for the synthesis of chemical building blocks.[30–32] Further, the ability to conduct organic reaction in aqueous media is highly attractive. There several potential advantages of replacing traditional organic solvents with water. Among the myriad of reason the three most pressing are: (1) Cost. No organic solvent can compete on a fiscal level. (2) Safety. The overwhelming majority of organic solvents commonly employed in laboratories come with significant risks including: flammability, explosion or the formation of explosives on

prolonged storage, and toxicity. (3) Environmental considerations: the chemical industry is a major contributor to pollution leading to regulatory and social pressures focusing on organic solvents.[33–37]

Initially, we evaluated the practicality of developing a one-pot synthesis of the DASA cyclopentenones beginning from the activated furan. We were gratified to find that the cascade can be achieved in a one-pot fashion on a multigram scale without affecting yield using either the photo-cyclization protocol (Scheme 4, Method A) or the PPh_3 procedure (Scheme 4, method B).

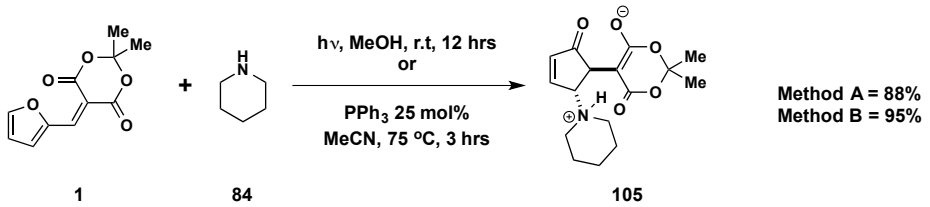

Scheme 4. One-pot cascade reaction for the synthesis of DASA cyclopentenones.

With this success we then proceeded to develop a one-pot preparation of DASA trienes. We considered that the first step in preparing DASA adducts is the "on-water" Knoevenagel condensation of the acceptor with furfural.[26,27] Further, based on the phase transfer behavior of DASA photoswitches (Chapter 2, Section 2.3.) we reasoned that when employing amine donors with eight carbons or more it should be possible to prepare the triene in aqueous media. We were pleased to find that the two-step synthesis of the organic photochromic molecules can be achieved in a one-pot fashion **"**on water**"** without affecting yield.[38] As shown in Scheme 5, Knoevenagel condensation between furfural and either Meldrum**'**s acid or 1,3-dimethylbarbituric acid is complete within 2 h. Direct addition of the amine nucleophile results in formation of the Stenhouse adduct, which then can be isolated by extraction with dichloromethane. The facile nature of this process further highlights the practicality and user-friendly protocol to access these novel organic photochromic materials.

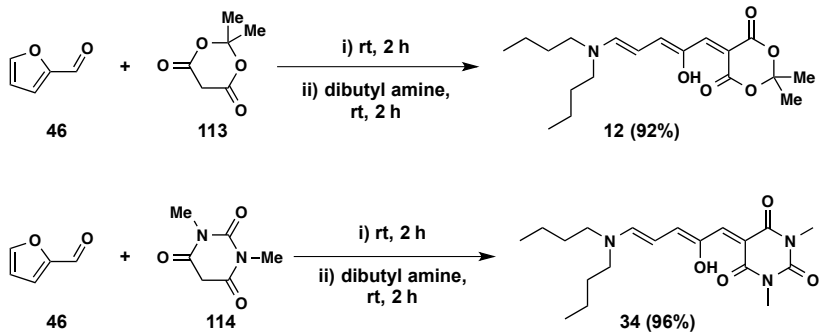

Scheme 5. One-pot **"**on water**"** synthesis of DASA trienes.

3.6. Closing Remarks

In summary, we have developed general conditions for the ring opening of furfural derivatives activated with cyclic β-dicarbonyl compounds by a wide variety of secondary amines to provide 1-dicarbonylmethylene-2-hydroxy-5-(dialkylamino)pentadienes. This strategy provides unprecedented synthetic modularity and tunability in the preparation of visible light activated photoswitches. We have further demonstrated that this process can be performed in a one-pot fashion in water from commercially available starting materials. We have further identified which of the trienes obtained undergo reversible photochromism to give stable, colorless 4-aminocyclopentenone zwitterions. Specifically we have found trienes where the amine donor bears an electron withdrawing group (such as proline methyl ester) or two benzylic carbons off the nitrogen atom of the donor, fail to engage in photochromism. We have further demonstrated mild, efficient and practical conditions for their subsequent cyclization to 4-amino-cyclopentenones using either catalytic PPh_3 or visible light, which facilitated isolation of the cyclized form of the adduct. This chemical cyclization protocol provided nearly identical results to the photo-cyclization protocol, with the exception that diallylamine derived DASAs trienes do not decompose providing the corresponding cyclopentenones in good yield. Finally, either of these cyclization protocols can be executed in a one-pot fashion, beginning from the activated furan, to furnish the desired cy-

clopentenones without affecting yield. Combined these results demonstrate the diversity and practicality of DASA syntheses, providing a versatile platform with unique properties that are synthetically accessible to a wide range of researchers.

3.7. References

(1) Helmy, S.; Leibfarth, F. A.; Oh, S.; Poelma, J. E.; Hawker, C. J.; Read de Alaniz, J. *J. Am. Chem. Soc.* **2014**, *136* (23), 8169.

(2) Castagna, R.; Garbugli, M.; Bianco, A.; Perissinotto, S.; Pariani, G.; Bertarelli, C.; Lanzani, G. *J. Phys. Chem. Lett.* **2012**, *3* (1), 51.

(3) Xie, X.; Mistlberger, G.; Bakker, E. *J. Am. Chem. Soc.* **2012**, *134* (41), 16929.

(4) Terao, F.; Morimoto, M.; Irie, M. *Angew. Chem. Int. Ed.* **2012**, *51* (4), 901.

(5) Kienzler, M. A.; Reiner, A.; Trautman, E.; Yoo, S.; Trauner, D.; Isacoff, E. Y. *J. Am. Chem. Soc.* **2013**, *135* (47), 17683.

(6) *Molecular switches*, 2nd, completely rev. and enl. ed.; Feringa, B. L., Browne, W. R., Eds.; Wiley-VCH: Weinheim, Germany, 2011.

(7) Velema, W. A.; Szymanski, W.; Feringa, B. L. *J. Am. Chem. Soc.* **2014**, *136* (6), 2178.

(8) Kumpfer, J. R.; Rowan, S. J. *J. Am. Chem. Soc.* **2011**, *133* (32), 12866.

(9) Spruell, J. M.; Hawker, C. J. *Chem Sci* **2011**, *2* (1), 18.

(10) Beharry, A. A.; Sadovski, O.; Woolley, G. A. *J. Am. Chem. Soc.* **2011**, *133* (49), 19684.

(11) Bléger, D.; Schwarz, J.; Brouwer, A. M.; Hecht, S. *J. Am. Chem. Soc.* **2012**, *134* (51), 20597.

(12) Yang, Y.; Hughes, R. P.; Aprahamian, I. *J. Am. Chem. Soc.* **2012**, *134* (37), 15221.

(13) Klajn, R. *Chem Soc Rev* **2014**, *43* (1), 148.

(14) Tian, H.; Yang, S. *Chem. Soc. Rev.* **2004**, *33* (2), 85.

(15) Cnossen, A.; Hou, L.; Pollard, M. M.; Wesenhagen, P. V.; Browne, W. R.; Feringa, B. L. *J. Am. Chem. Soc.* **2012**, *134* (42), 17613.

(16) Weissleder, R.; Ntziachristos, V. *Nat. Med.* **2003**, *9* (1), 123.

(17) Samanta, S.; Babalhavaeji, A.; Dong, M.; Woolley, G. A. *Angew. Chem. Int. Ed.* **2013**, *52* (52), 14127.

(18) Samanta, S.; Beharry, A. A.; Sadovski, O.; McCormick, T. M.; Babalhavaeji, A.; Tropepe, V.; Woolley, G. A. *J. Am. Chem. Soc.* **2013**, *135* (26), 9777.

(19) Bouas-Laurent, H.; Dürr, H. *Pure Appl. Chem.* **2001**, *73* (4).

(20) Kade, M. J.; Burke, D. J.; Hawker, C. J. *J. Polym. Sci. Part Polym. Chem.* **2010**, *48* (4), 743.

(21) Kolb, H. C.; Sharpless, K. B. *Drug Discov. Today* **2003**, *8* (24), 1128.

(22) Kolb, H. C.; Finn, M. G.; Sharpless, K. B. *Angew. Chem. Int. Ed.* **2001**, *40* (11), 2004.

(23) Piancatelli, G.; D'Auria, M.; D'Onofrio, F. *Synthesis* **1994**, *1994* (09), 867.

(24) Piutti, C.; Quartieri, F. *Molecules* **2013**, *18* (10), 12290.

(25) Palmer, L.; Read de Alaniz, J. *Synlett* **2013**, *25* (01), 08.

(26) Deb, M. L.; Bhuyan, P. J. *Tetrahedron Lett.* **2005**, *46* (38), 6453.

(27) Bigi, F.; Carloni, S.; Ferrari, L.; Maggi, R.; Mazzacani, A.; Sartori, G. *Tetrahedron Lett.* **2001**, *42* (31), 5203.

(28) Landmesser, T.; Linden, A.; Hansen, H.-J. *Helv. Chim. Acta* **2008**, *91* (2), 265.

(29) Šafář, P.; Považanec, F.; Prónayová, N.; Baran, P.; Kickelbick, G.; Kožíšek, J.; Breza, M. *Collect. Czechoslov. Chem. Commun.* **2000**, *65* (12), 1911.

(30) Wasilke, J.-C.; Obrey, S. J.; Baker, R. T.; Bazan, G. C. *Chem. Rev.* **2005**, *105* (3), 1001.

(31) Tietze, L. F. *Chem. Rev.* **1996**, *96* (1), 115.

(32) Walji, A.; MacMillan, D. *Synlett* **2007**, *2007* (10), 1477.

(33) Alonso, D. A.; Kobayashi, S. *Water in organic synthesis*; 2012.

(34) Simon, M.-O.; Li, C.-J. In *Green Techniques for Organic Synthesis and Medicinal Chemistry*; Zhang, W., Cue, B. W., Eds.; John Wiley & Sons, Ltd: Chichester, UK, 2012; pp 263–295.

(35) *Handbook of green chemistry*; Anastas, P. T., Crabtree, R. H., Eds.; Wiley-VCH: Weinheim, 2009.

(36) Chanda, A.; Fokin, V. V. *Chem. Rev.* **2009**, *109* (2), 725.

(37) Lindström, U. M. *Chem. Rev.* **2002**, *102* (8), 2751.

(38) Helmy, S.; Oh, S.; Leibfarth, F. A.; Hawker, C. J.; Read de Alaniz, J. *J. Org. Chem.* **2014**, *79* (23), 11316.

4. Applications

4.1. Introduction

Any new development in chemical technology necessitates application to ensure it is not relegated as merely a curiosity. This is particularly important in the field of photochromism as without demonstrating the applicability of a new photochromic architecture, a potentially powerful tool can easily be overlooked. As a recent addition to the selection of organic photochromic materials, the potential applications of DASAs are still being explored and developed. However, the dramatic solubility inversion they undergo upon irradiation has been exploited for organo-catalyst recycling and micellar disassembly for cargo delivery.

A fundamental challenge in the field of homogeneous catalysis is the difficulties inherent in recovery of the molecular catalyst. This problem is exacerbated by the fact that increasingly sophisticated organo-catalysts result in high costs and therefore losses. To overcome this problem, several methods have been developed to solve the problem of catalyst/product separation including to immobilize them on polymer resins,[1–3] metal-oxides,[4–6] or textiles.[7] An alternate approach relies on manipulation of the solubility properties of the catalyst by employing so-called phase-tags.[8] Based on the solubility inversion that DASAs undergo upon photoswitching we sought to develop their use as a visible light activated phase-tag for the recycling of a homogeneous organo-catalyst (described in section 4.2.).

Traditional treatments used to combat illnesses typically access their targets *via* blood circulation. However, these medicines are usually plagued by challenges such as low aqueous solubility, poor selectivity, and high toxicity. To combat these challenges researchers have investigated drug delivery systems for decades. Specifically, drug delivery systems that respond to light have received great attention as they offer both spatial and temporal resolu-

tion for drug release, offering the ability to limit side effects and generate considerable therapeutic levels of the drug that may otherwise be unattainable.[9] With these advantages in mind, we sought to develop a polymeric micellar system that disassembles *via* a one-photon process to deliver a hydrophobic cargo with both spatial and temporal resolution (described in section 4.3.).

4.2. Catalyst Recycling

4.2.1. Background

Organic catalysts have become increasingly important in the field of synthetic chemistry for their ability to catalyze a range of valuable transformations.[10,11] As the field has matured, modern developments in organocatalysis look toward increasingly complex chiral catalysts that come at high synthetic or monetary cost.[12] To date, this increasing complexity has not been met with a robust effort to engineer solutions for recycling these valuable moieties and making organocatalysis more sustainable.[13] Broadly, all techniques that separate a catalyst from a reagent mixture involve either liquid-solid or liquid/liquid phase separation. The most common method for reusing homogeneous organic catalysts has been to support them on polymer resins,[1–3] metal-oxides,[4–6] or even textiles and separate the catalyst post-reaction by filtration.[7] Although promising, supported homogeneous catalysts have not proven to be a general solution for catalyst recycling due to the adverse effects supported systems can have on catalyst activity and selectivity.[14]

Another common approach to catalyst recycling, referred to as phase tagging, relies on differential catalyst solubility and is an important tool for recycling organic catalysts. Generally, the phase tag has some intrinsic property that enables easy phase separation from the organic product. For catalyst recycling, fluorous[15–17] and ionic liquid[18–21] tags have proven

effective in a variety of systems. However, drawbacks associated with these methods, such as cost, solvent leaching, and environmental persistence of the phase tag have shifted attention toward the development of separation techniques where the phase tag properties can be controlled by a benign and inexpensive external stimuli. As such, redox- and light-controlled phase tags have been developed and applied to the recycling of the Grubbs-Hoveyda catalyst.[22–24]

Recently, we reported a new class of modular photoswitches termed donor-acceptor Stenhouse adducts (DASAs).[25,26] These systems are easily accessible from furfural, a commodity chemical derived from nonedible biomass, and their modular synthesis enables adoption into a number of functional materials. Upon irradiation, DASAs switch from a conjugated, colored, and hydrophobic form to a ring-closed, colorless, and zwitterionic structure. Most importantly, their switching is stimulated by low-energy visible light, which is non-invasive to many reagents in typical chemical reactions. In collaboration with Frank Leibfarth of the Hawker group, we envisioned the differential solubility imparted by the photoswitching of DASAs and their activation by an external, abundant, and non-transformative stimulus would provide an ideal platform for application in the recycling of organic catalysts (Figure 1).[22]

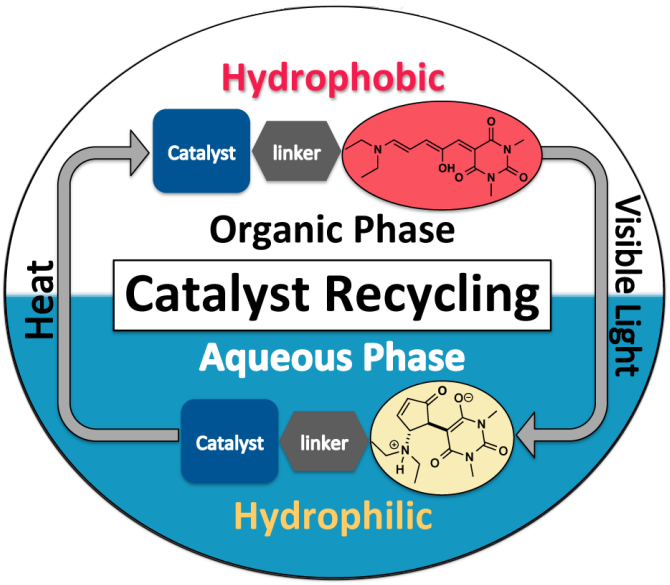

Figure 1. Application of DASA photoswitch as a phase tag for catalyst recycling using visible light and heat.

The ubiquity and broad utility of privileged thiourea organocatalysts make them an ideal target for recycling.[12,27] Further, many of the more complex thiourea derivatives are non-trivial to synthesize and are typically used at high catalyst loadings; thus, catalyst recycling would provide a distinct advantage. To begin our studies, we chose to pursue thiourea catalyzed lactide polymerization.[28,29] This industrially important transformation would not only benefit from catalyst recycling, but a light-mediated separation of catalyst from the polymer product is advantageous to reduce deleterious transesterification reactions and polymer degradation that occur from residual catalyst left in the final material.[30,31]

The modular nature of the DASA photoswitch, broad utility of the thiourea organic catalyst, and benign nature of the stimulus for recycling make this an attractive concept for further application. An easily accessed DASA-appended thiourea catalyst is shown to effectively polymerize lactide with control over polymer molecular weight and dispersity. The photoswitch-organocatalyst construct can subsequently be separated from the reactant mixture by irradiation with visible light, recovered and reused. This process can be repeated numer-

ous times with negligible affect on catalyst activity or performance. Lastly, mechanistic studies demonstrating the advantages and limitations of the reported system and providing valuable insights into future recyclable catalyst design principles are presented.

4.2.2. Catalyst Synthesis

The exceptional properties of DASA photoswitches, including their activation by visible light and their solubility, color, and shape change upon irradiation, make them excellent candidates to interface with catalytic moieties. The ease and modularity of DASA synthesis enabled preparation of thiourea catalyst **4** in a convergent manner, as outlined in Figure 2. We chose to use the barbituric acid-derived DASA photoswitch for its superior performance in control experiments compared to its Meldrum's acid based counterpart. First, an alkyne-functionalized thiourea was prepared from 4-aminocyclohexanol through Boc-protection of the amine, alkylation with propargyl bromide, and subsequent Boc-deprotection. The free amine was reacted with 3,5-di(trifluoromethyl)phenyl isothiocyanate in dichloromethane to generate an alkyne-functionalized variant of the well-known electron deficient thiourea catalyst **1** (Figure 2, top). An azide-bearing DASA was prepared from activated furan **2** and an azide-containing secondary amine to provide the azide terminated DASA **3** (Figure 2, center). Finally, the catalyst and photoswitch were coupled though the copper catalyzed azide-alkyne cycloaddition to yield the DASA-catalyst conjugate **4** as a dark purple solid (Figure 2, bottom).

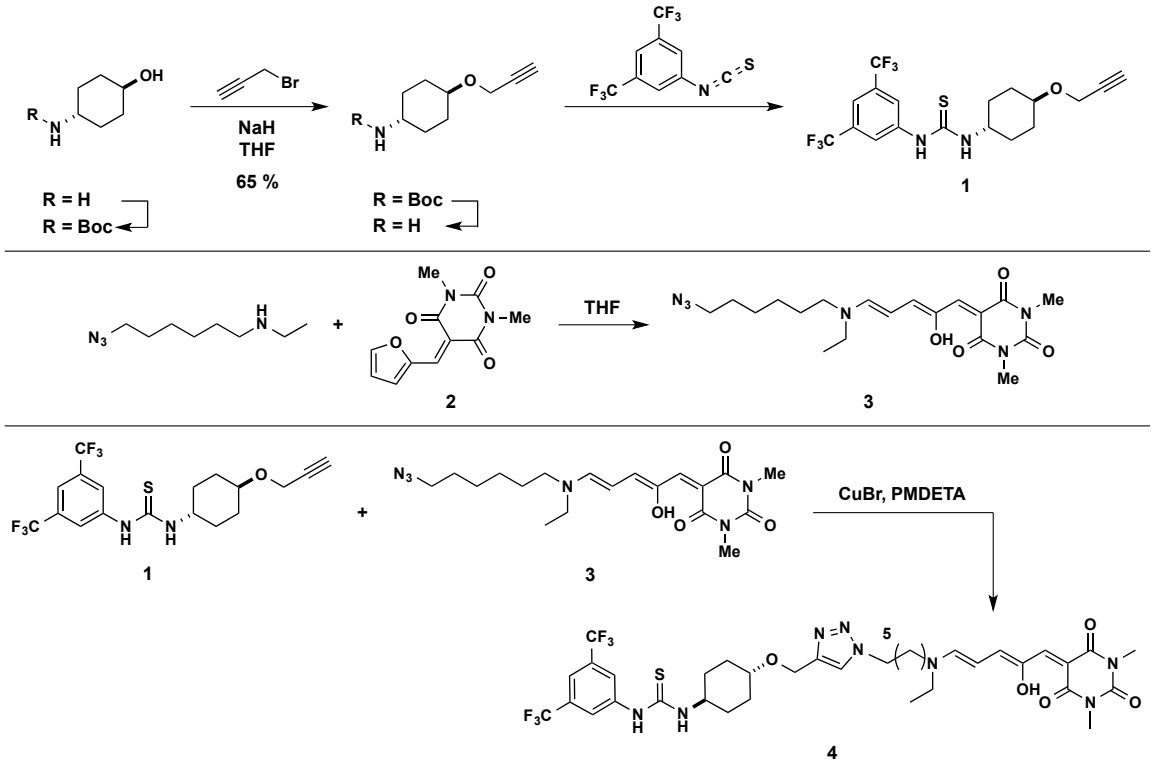

Figure 2. Synthesis of thiourea-photoswitch adduct **4**.

4.2.3. Catalyst Photochromism and Phase-Transfer

The utility of DASA photoswitches for catalyst recycling is dependent on its ability to undergo reversible phase-change upon irradiation with visible light. To confirm this behavior for the thiourea-photoswitch adduct, **4** was dissolved in toluene at a concentration of 0.05 M and the dark purple solution was layered over water. We chose water as the polar solvent for the phase transfer studies because it is widely employed in liquid/liquid extractions. The bi-phasic mixture was irradiated with visible light (550-750 nm) for ten minutes, after which the purple color had disappeared from the organic layer and **4** resided in the aqueous layer in its zwitterionic form. To quantify the phase transfer, the same experiment was performed and aliquots from the organic phase were taken at intervals throughout the photoswitching. The results in Figure 3 demonstrate the characteristic decrease in absorbance at ~570 nm that accompanies photoswitching from the linear, conjugated form **4** to the cyclic, zwitteri-

onic form, resulting in 98% photoswitching efficiency in ten minutes. The transfer of the catalyst-photoswitch construct to the aqueous phase was confirmed by employing deuterated solvents in the experiment, where the diagnostic ^{1}H-NMR peaks of the zwitterionic moiety are evident in the D_2O phase after photoswitching and no observable peaks are left in the toluene-D_8 layer.

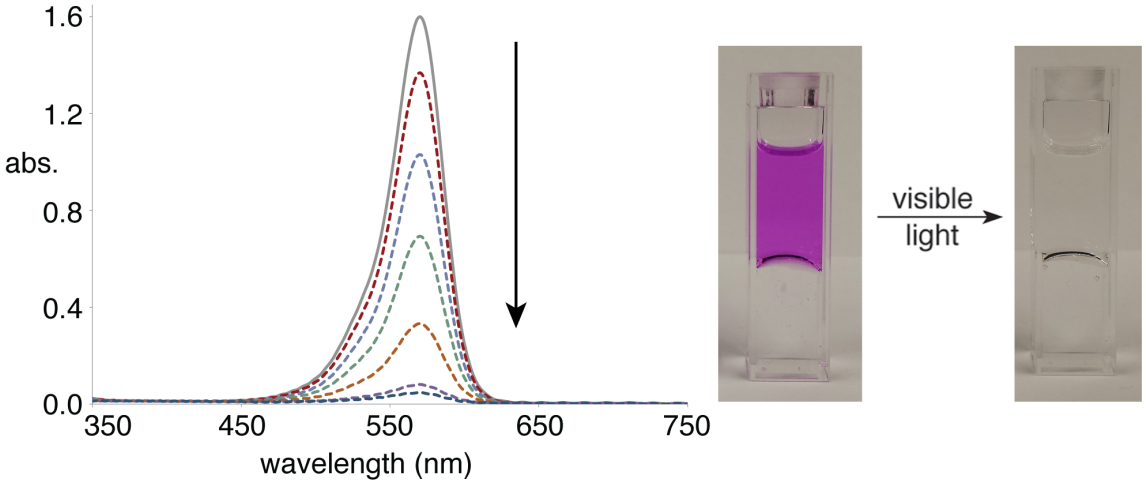

Figure 3. The photoswitching of catalyst **4** under visible light irradiation displays characteristic decrease in absorbance at 568 nm (left), which can be visualized in a biphasic system (right).

Reclaiming the DASA-catalyst conjugate from the aqueous phase is imperative for a functioning catalyst recycling system. After phase transfer into the water layer, heating the biphasic mixture results in ca. 20% recovery of the catalyst into the toluene layer. Screening solvents for catalyst recovery, led to the discovery that chlorinated solvents, such as methylene chloride and chloroform, allow far superior catalyst recovery. Therefore, dissolving **4** in toluene, layering the solution over water, and irradiating with visible light provides complete transfer of the catalyst to the aqueous layer. Separating the aqueous phase, layering it over methylene chloride, and heating the mixture to ~40 ºC for two minutes results in near quantitative isolation of the catalyst. This process of catalyst recycling compares favorably

to a previously reported light-controlled catalyst recycling protocol based on a spiropyran phototag.[22]

4.2.4. Catalyst Performance and Recycling

To demonstrate the utility of recycling a thiourea catalyst, we chose to employ **4** for the ring opening polymerization of lactide. The parent thiourea catalyst is well established to provide controlled polymerization of lactide, resulting in polymers with predictable molecular weight and low polydispersity (PDI).[28,29] Assuming the photoswitch would not interfere with polymerization, we hypothesized that polymerization of lactide by adduct **4** would provide well-controlled polymerization to afford polylactide (PLA). Subsequently, visible light irradiation of the polymerization solution in the presence of water would prompt photoswitching and concurrent transfer of **4** to the aqueous phase. Phase transfer of **4** would provide multiple benefits. First, this would fully remove the transesterification catalyst from the PLA product; thus, preventing undesired scrambling of PLA by residual catalyst during polymer processing or device fabrication which is a known problem.[31] Further, the reversibility of DASA photoswitching would allow the catalyst to be recovered from the aqueous phase of the mixture for reuse.

The catalyst-photoswitch adduct **4** was effective for polymerizing lactide. Polymerizations were initiated by pyrene butanol targeting a degree of polymerization (DP) of 100, employing 10 mol% of 4 and 20 mol% of pentamethyldiethylenetriamine (PMDETA) as the amine co-catalyst.[32] After 48 hours, polymerizations provided PLA with a molecular weight of 11.2 kg/mol at 70% conversion (as determined by ^{1}H-NMR) and a PDI of 1.12. Control experiments excluding **4**, excluding PMDETA, and excluding both resulted in no polymer formation. The polymerization catalyzed by **4** displayed the characteristics of a living sys-

tem, similar to previous thiourea catalysts, with good agreement between theoretical and calculated molecular weight and a linear relationship between molecular weight and conversion being observed (Figure 4A). Further, comparing the refractive index (RI) and absorbance spectra obtained from the size-exclusion chromatogram of the crude polymerization mixture confirms the successful polymerization of lactide by **4**. As shown in Figure 4B, the RI peak of the polymer centered at a retention time of ~15.2 minutes overlaps with the characteristic absorbance for the initiator pyrene butanol. This demonstrates the chain-end fidelity of the polymerization and confirms (along with control experiments and characterization of the purified polymer) that **4** is not incorporated into the polymer. The peak at a longer retention time of ~18.5 min has the characteristic absorbance profile of the catalyst-photoswitch adduct **4**, with a strong absorbance centered at ~570 nm, confirming that **4** both catalyzes the polymerization and survives the reaction.

Upon conclusion of the polymerization, the DASA photoswitch assumes its role in recycling the thiourea catalyst. The reaction mixture is taken up in benzene, layered over water, and exposed to visible light for 1 hour. Irradiation triggers photoswitching of the DASA and thus a drastic change in its solubility properties. The catalyst-photoswitch adduct transfers to the aqueous phase, separating it from the polymer product that remains in the organic layer and enabling its recovery. The PLA, free of catalyst, can be precipitated into methanol yielding pure product. The aqueous phase, containing the thiourea, can be extracted with dichloromethane to recover **4** in its linear, hydrophobic form for reuse in subsequent polymerizations. After passing recovered **4** through a short silica plug to remove base-line impurities, the catalyst-photoswitch adduct is recovered in 70% yield.

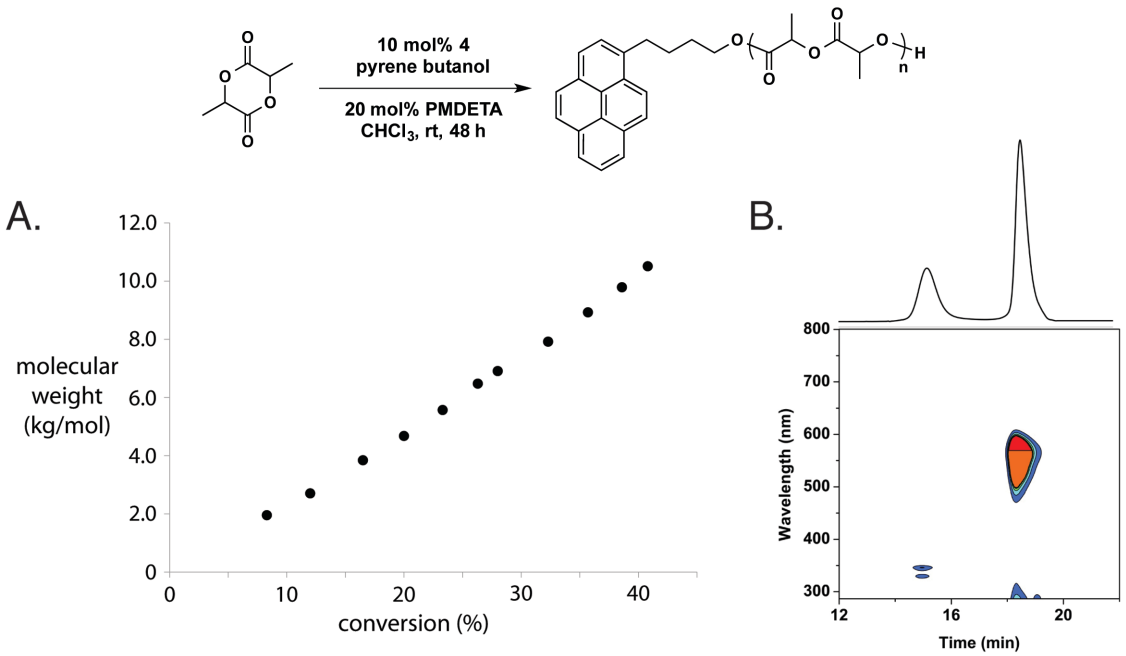

Figure 4. A) Polymerization of lactide catalyzed by **4** demonstrates good agreement between molecular weight and conversion. B) Crude GPC spectrum including both RI and UV-vis detectors show end-group fidelity and stability of the photoswitch to the reaction conditions.

To our gratification, the catalyst was analytically unchanged by the polymerization/recovery process and retained its activity. Employing the recycled catalyst for the polymerization of lactide under identical polymerization conditions to those used previously provided PLA with a molecular weight of 8.10 kg/mol and PDI of 1.24 at 60% conversion (Table 1). Repeating the visible light-mediated recovery procedure provided separation and re-isolation of the catalyst-photoswitch adduct in 65% yield. The catalyst was employed a third time to yield PLA with a molecular weight of 9.14 kg/mol and PDI of 1.31. These iterative reaction, separation, and reuse cycles demonstrate the robust nature of the DASA-organocatalyst construct and demonstrate its utility in both substrate purification and catalyst recovery. Accomplishing this unique function using a non-invasive and benign stimulus such as visible light makes this method attractive to a wide range of catalytic systems that could be applicable in polymer or small molecule synthesis.

Table 1. Recycling of **4** over three catalytic cycles. [a]Molecular weight determined by ^{1}H-NMR.

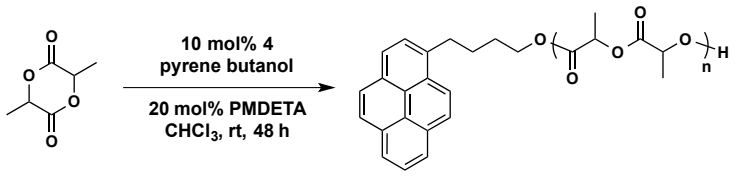

Entry	Time	Conversion	Molecular Weight[a]	PDI
Catalyst **4**	48 h	70%	11.2 kg/mol	1.12
1st Reuse	48 h	60%	8.10 kg/mol	1.24
2nd Reuse	48 h	63%	9.14 kg/mol	1.31

4.2.5. Mechanistic Studies

Mechanistic studies of the polymerization employing the catalyst–photoswitch construct are critical to aid in the future design of visible light recyclable catalysts. Initially, the rate of polymerization was determined for reactions employing the parent thiourea catalyst as well as the catalyst–photoswitch construct **4**. The rates were determined by running polymerizations in $CDCl_3$ (1.2 M) targeting a DP of 100 with 10 mol% thiourea and 20 mol% PMDETA, recording ^{1}H-NMR spectra every 30 minutes. The reactions were monitored to conversions under 60% where viscosity and undesired side-reactions are unlikely to have an effect. We assume that the alcohol concentration, as initially determined by the concentration of the pyrene butanol initiator, remains constant throughout the polymerization. These experiments produced three-dimensional NMR data (Figure 5A), which show the doublet of the lactide methyl group at 1.65 ppm decreasing over time and the commensurate growth of the polymer methyl group signal at 1.62 ppm. Integration of the individual spectra over time and fitting the data to a first-order kinetic model provides the plots shown in Figure 5B.

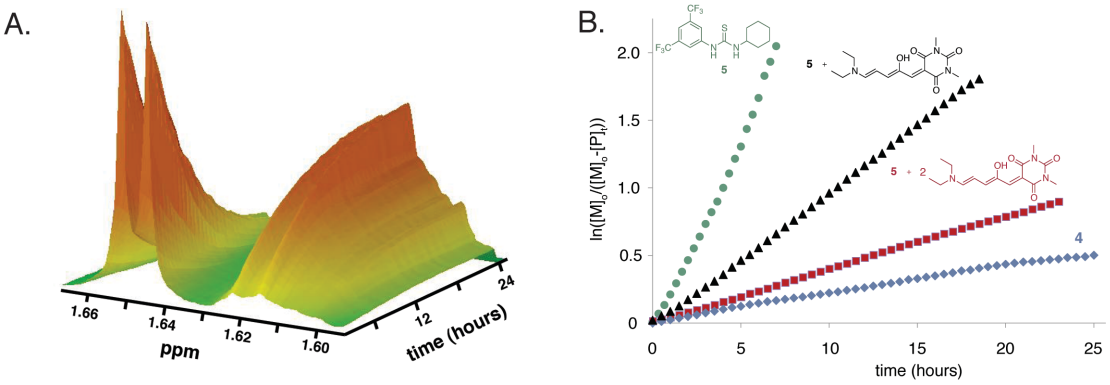

Figure 5. A) Three dimensional ^{1}H-NMR data of lactide polymerization. B) Kinetic data for polymerization catalyzed by parent thiourea **5** (green circles), **5** + one equivalent of diethyl DASA photoswitch (black triangles), **5** + two equivalents of diethyl DASA photoswitch (red squares), and catalyst-photoswitch construct **4** (blue diamonds).

As shown in Figure 5B, the polymerization catalyzed by **4** (blue diamonds) is considerably slower that the same polymerization catalyzed by the parent thiourea catalyst (green circles). Mechanistically, hydrogen bonding between the thiourea and lactide is proposed to activate the lactide ester for transesterification in this polymerization. We hypothesized that the slower rate of the catalyst–photoswitch construct **4** may be due to competitive binding of the thiourea between lactide and the electron-rich carbonyls of the barbituric acid. To test this hypothesis, we measured the rate of polymerization employing the parent thiourea catalyst while including both one (black triangles) and two (red squares) equivalents of an intermolecular inhibitor in the form of the diethylamine-derived DASA photoswitch. The reactions exhibit first-order kinetics and clearly illustrate the inhibitory affect of the DASA, as each equivalent of photoswitch decreased the reaction rate by approximately three-fold. To gain further insight on the relative strength of thiourea binding to cyclic esters verses our DASA photoswitch, NMR titration experiments were undertaken, tracking the chemical shift of the thiourea N–H protons in the presence increasing amounts of binding partner. The magnitude of downfield shift of the N–H protons corresponds to the relative strength of the hydrogen-bonded complex being formed.[33,34] A plot of chemical shift verses equivalents of

carbonyl is shown in Figure 6. To ensure 1:1 binding of thiourea to cyclic ester, caprolactone was employed in place of lactide. As evidenced by the significantly larger chemical shift change when titrated with the DASA photoswitch, the thiourea binds the barbituric acid carbonyls much stronger than the carbonyl of the cyclic ester.

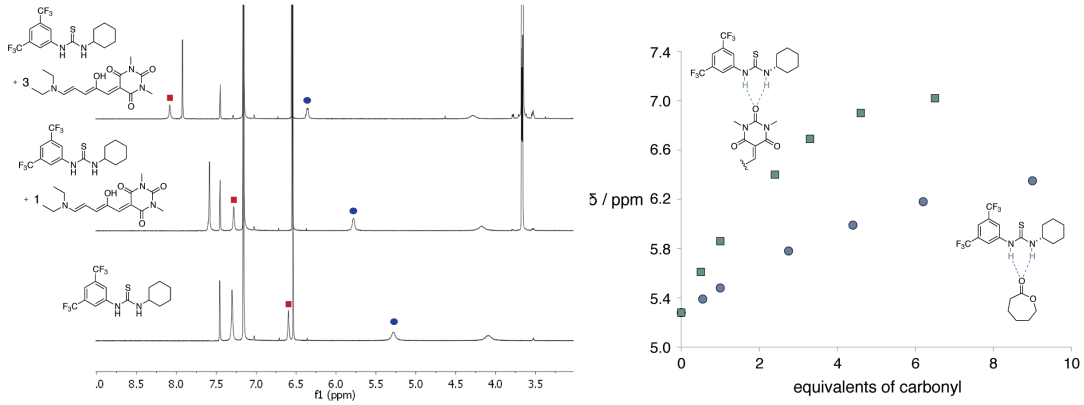

Figure 6. A) Example of ^{1}H-NMR data obtained for the titration of the thiourea catalyst with a cyclic carbonyl. B) A plot depicting the change in the ^{1}H-NMR chemical shift of one N–H proton of the thiourea upon titration with caprolactone (blue circles) or the diethyl DASA photoswitch (green squares). Titrations were carried out in C_6D_6 with the concentration of thiourea between 0.05 and 0.01 M.

To the best of our knowledge, this is the first example of employing visible light as a stimulus to recycle a homogeneous catalyst[35] and represents a rare example of catalyst recycling in a polymer application. The challenge for this and any complex catalytic system is that each function, catalysis and recycling in this instance, works independently and one does not compromise the other. The mechanistic studies undertaken herein demonstrate that while the presence of the DASA photoswitch decreases the rate of polymerization, the presence of the thiourea does not seem to affect the photoswitching and phase transfer of the DASA moiety. From the data presented, we surmise that the intramolecular binding of the barbituric acid to the thiourea competes with the activation of lactide, causing the rate decrease. Despite this decrease in rate, the DASA-catalyst conjugate was effective for the con-

trolled polymerization of lactide, providing PLA with predictable molecular weights and narrow PDIs even after repeated use and recycling.

4.3. Micellar Cargo Delivery

4.3.1. Background

Polymeric micelle drug delivery systems offer tremendous potential for the effective and safe treatment of human diseases due to their ability to minimize harmful side effects, increase drug bioavailability, and carry drugs with prolonged circulation time.[36–39] To gain greater control over the delivery process, on-demand triggered release of therapeutic agents has garnered enormous interest, specifically light-activated systems.[40–42] As a non-invasive and readily available resource, light offers precise control over the nanocarrier system by releasing the encapsulated payload at a specific time and specific location. The ability to exert precise control over the delivery of a therapeutic cargo is highly desired as this level of control may serve as a method to significantly reduce or ultimately eliminate potential side effects of indiscriminate chemotherapeutics (e.g., paclitaxel or docetaxel).[36–39,43] These "smart" drug delivery systems have been made possible by the development of photoresponsive compounds, such as o-nitrobenzyl ester,[42,44] azobenzene[40] and spiropyran.[45] However, an inherent challenge arises from their reliance on ultraviolet (UV) light, which not only has the potential to harm healthy cells but also suffers from poor tissue penetration, thereby limiting their applicability.

To address this issue, researchers have shifted their attention to systems that are activated by light sources of longer wavelengths (600–1200 nm), which have minimal effect on cells and penetrate deeper through human tissue.[46,47] While emerging technologies like two-photon excitation,[42,48,49] and upconverted UV light[50,51] have enabled the use of near infrared

(NIR) spectral window of tissues, similar approaches have proven challenging to adapt to polymeric micelles. The most significant challenge is inefficient micelle disruption, which necessitates prolonged irradiation and the use of high laser power (3–5 W), both of which can lead to heat-induced cell toxicity. These limitations are rooted in the properties of the photoresponsive compounds used to control the micelle disruption and highlight the need for the development of new photochromic material for light-triggered drug delivery system. We therefore envisioned the development of a polymeric micelle system that could be controlled by a one-photon visible light process, thereby enhancing the drug delivery efficiency, simplifying the synthetic strategy, and improving the therapeutic efficacy.

A powerful aspect of the modular design of DASAs is the ability to rapidly modify their structure, critical for the adoption of these photoswitches into complex systems that require on-demand property changes.[26] Accordingly, we sought to develop a functional polymer system to exploit the visible-light-mediated solubility switch of DASAs.[25] The development of a general, stimuli-responsive micellar system with external control over assembly has been a long-standing goal in polymer chemistry with potential applications in biological settings.[52–54] The characteristics of DASA photoswitches are therefore perfectly suited to provide such a function, as visible light mediates structural and property changes from the hydrophobic, linear derivative to the fully hydrophilic, cyclic derivative.

4.3.2. Initial Efforts

The facile and modular synthesis of DASA photoswitches enabled the generation of a DASA-functionalized amphiphilic polymer. In collaboration with Saemi Polema, a DASA bearing a terminal azide and 1,3-di-n-octyl barbituric acid, was coupled to alkyne terminated monomethyl poly(ethylene glycol) (PEG) (M_w = 3000 g/mol, PDI = 1.1) to form the desired

end-functionalized polymer, **6a** (Figure 7A). The amphiphilic nature of **6a** induced micelle formation in aqueous environments (Figure 7B), as determined by Nile Red encapsulation experiments and dynamic light scattering, confirming that Nile Red is successfully encapsulated and solubilized in water and that the critical micelle concentration for this system is 49 µM (Figure 7C). Upon visible light irradiation, the absorption peak of **6a** at 550 nm decreased steadily, indicating the photoswitching of the DASA to its cyclic, hydrophilic state. Concurrently, the fluorescence emission of encapsulated Nile Red showed a sharp decrease in intensity and red shift, indicating that the hydrophobic dye was released into the aqueous phase (Figure 7D).[48,55–57] These results are consistent with a disruption in the micellar structure and a release of hydrophobic cargo caused by the light-induced photoswitching of **6a** to the fully hydrophilic derivative **6b**. This simple but powerful application of DASAs illustrates the significant potential of these photochromic compounds.

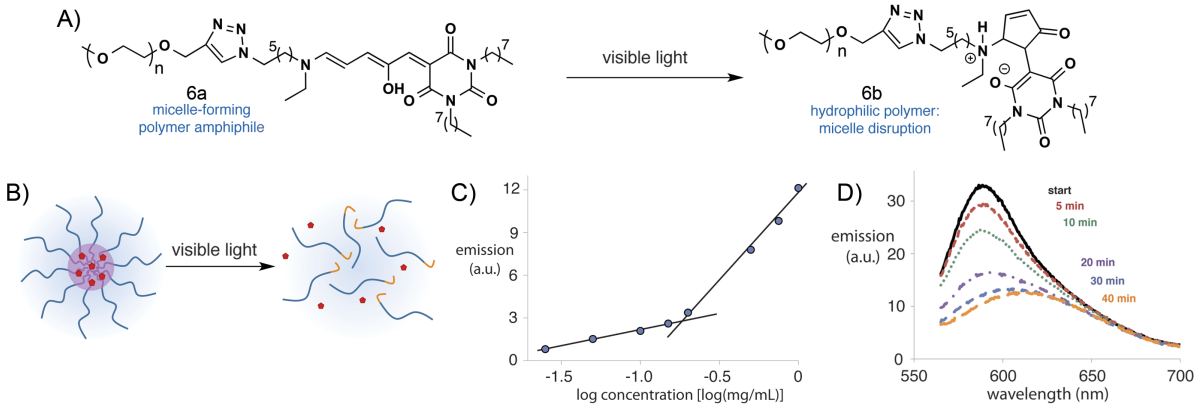

Figure 7. A) Photoswitching of micelle-forming polymer amphiphile. B) Schematic of micelle formation and hydrophobic cargo encapsulation by functional amphiphile **6a** and micelle disruption and cargo release on visible light irradiation. C) Fluorescence intensity (Em at 588 nm) vs log concentration (mg/mL) of **6a**. D) Fluorescence emission spectra of Nile Red in 0.50 mg/mL **6a** in water at various times of visible light irradiation.

Based on these results and our interest in exploring the potential of this new class of photochromic material, we sought to explore their use in selective drug release to mammalian cells. To the best of our knowledge, this work would be the first example of controlled

drug release to living cells by property change of a photochromic component to control the structural disassembly of a micelle. Moreover, this offers a new approach to drug delivery that does not rely on a metal or a two-photon process.

4.3.3. Second Generation: Micelle Formation and Cargo Release

Donor-acceptor Stenhouse adducts are photochromic compounds that respond to visible light. These materials are easily prepared by a two-step process: an "on-water" Knoevenagel condensation of a barbituric acid derivative with furfural to produce an activated furan, which is then treated with a secondary amine (which can bear tailored functionalities) to provide the highly colored DASA in good yield. This simple and modular synthesis of DASAs facilitates their incorporation into visible light-responsive systems. As an example, we explored visible light-induced drug release based on functional amphiphiles. Specifically, a DASA was functionalized with an azide and reacted with alkyne-functionalized monomethyl poly(ethylene glycol) (PEG) under "click" reaction conditions to prepare amphiphilic DASA-PEG conjugate (DPC) **7** (Scheme 1A, left). Triggered by visible light, the hydrophobic triene form of the DASA moiety photoisomerizes into its hydrophilic zwitterionic form. This significant change in polarity and solubility of the DASA moiety leads to **8**, which is doubly hydrophilic (Scheme 1A, right).

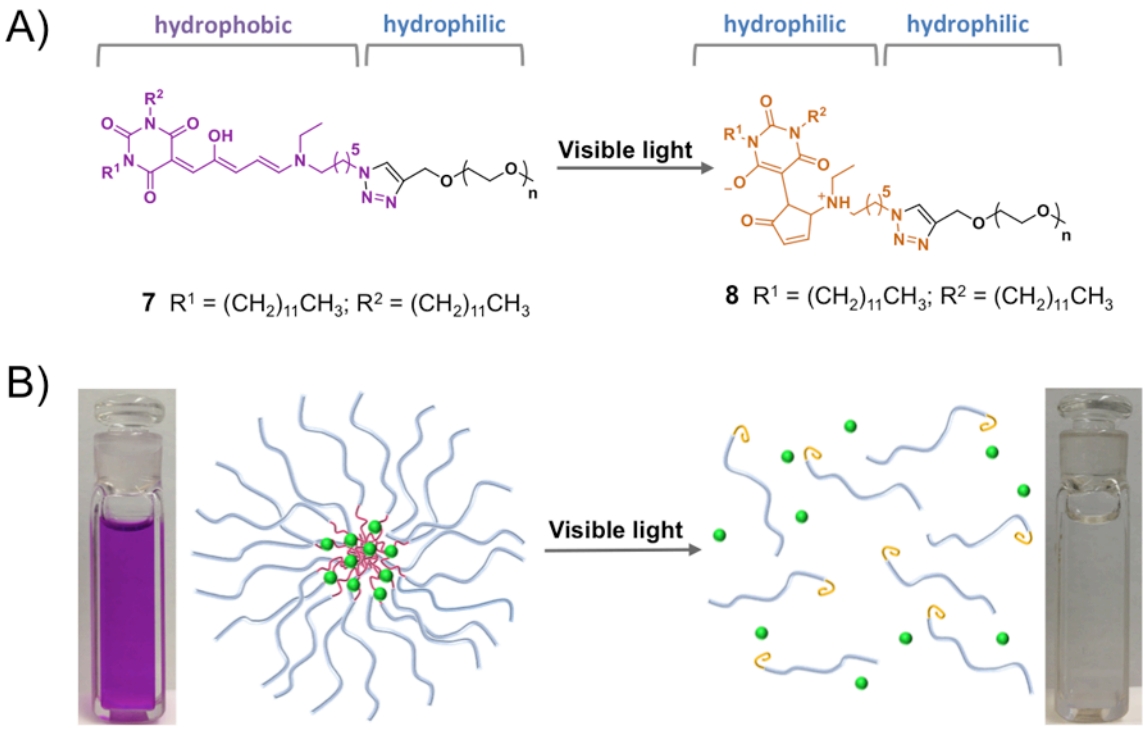

Scheme 1. A) Amphiphilic DPC **7** with hydrophobic and hydrophilic segments loses its amphiphilic character once irradiated with visible light. B) left: DPC **7** self-assembles into micelles in an aqueous media encapsulating hydrophobic cargo, portrayed by the highly colored micelle solution; right: Disruption of micelles and release of cargo molecules, colorless solution indicates complete photoisomerization of **7** to **8**.

Visible light irradiation on aqueous samples of DPC **7** induces isomerization of the DASA to its hydrophilic form, which leads to disassembly of the micelles. This process can be monitored by the naked eye as the strongly colored solution of DPC **7** indicates the hydrophobic DASA form and its subsequent photoisomerization to the zwitterion **8** is implied by the colorless solution. Based on this functional DPC **7**, a visible light-responsive micellar system that can release hydrophobic cargo to an aqueous environment becomes viable (Scheme 1B). In an aqueous medium, self-assembly of DPC **7** into micelles is expected where hydrophilic PEG (blue) comprises the corona and hydrophobic DASAs (purple) constitute the core.

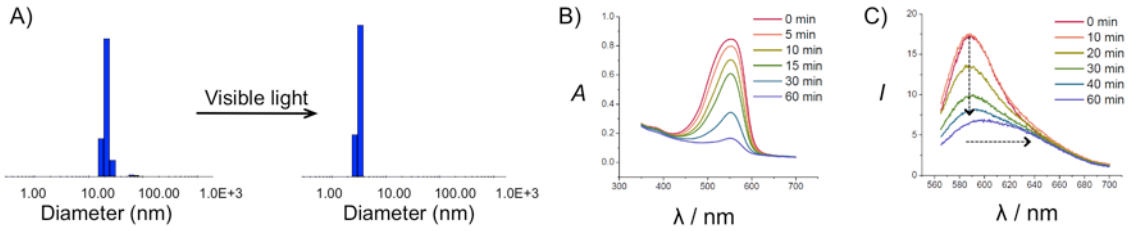

Figure 8. A) DLS measurements of aqueous solution of DPC **7** (0.5 mg/mL) before (left) and after (right) irradiation. B) UV-Vis spectra of DPC **7** (0.5 mg/mL) in water after varying times of visible light irradiation. C) Fluorescence emission spectra of initially encapsulated Nile Red in aqueous solution of DPC **7** (0.5 mg/mL) after varying times of visible light irradiation.

Dynamic light scattering (DLS) measurements of **7** were employed to verify the light-induced micellar disruption. Prior to light irradiation, solutions of DPC **7** above the CMC (0.5 mg/mL) successfully formed micelles, whose average size was ~22 nm in diameter (Figure 8A, left). Upon irradiation with visible light, the micelles rapidly disassembled due to destabilization of micellar core caused by isomerization of the DASA moieties into hydrophilic zwitterions. After irradiation no particle greater than 3 nm could be detected by DLS (Figure 8A, right).

To verify that the disruption of micelle is being induced by the photoisomerization of the DASA segments, UV-Vis spectroscopy was employed (Figure 8B). A micellar solution was prepared and the change in absorbance of the DASA moiety (λ_{max} = 553 nm) was monitored at different time intervals of visible light irradiation. After 1 hour of irradiation, the absorbance decreased by ~80%. This observation confirms that the primary reason for micelle disruption is indeed the visible light-triggered photoisomerization of the DASA segments from **7** to **8**. As the triene form of the DASA is isomerized to a hydrophilic zwitterion by visible light, the amphiphilic character of the DPC is lost, and thus the micellar structure disintegrates.

In order to demonstrate the disassembly of the micelles with visible light, fluorescence spectroscopy was used to monitor the release of cargo with respect to irradiation time. Nile Red, a solvatochromic and hydrophobic dye that fluoresces at 660 nm with weak emission intensity in water and at < 600 nm with enhanced emission intensity in hydrophobic environments, was chosen as an ideal cargo.[55,58] Accordingly, a micelle-encapsulated solution of Nile Red was prepared, and the micellar disruption by visible light was observed by monitoring the fluorescence emission of Nile Red (Figure 8C). At 0 min of irradiation, the micelles remained intact and provided a hydrophobic environment for Nile Red, as indicated by the emission λ_{max} at 590 nm. As irradiation was continued, the intensity of fluorescence steadily decreased with a concurrent bathochromic shift of the emission λ_{max}. This confirms that Nile Red is slowly released into the aqueous solution from the micelle core as the DASA segments of DPC **7** isomerize to their hydrophilic form of DPC **8** in response to visible light.

Working with Seung Soo Oh, we visualized the selective unloading of the hydrophobic dye into cells by micelle disassembly in response to irradiation with visible light (Figure 9). The CMC was pre-determined using Nile Red as a fluorescent probe. Initially, we incubated 0.5 mg/mL of DPC **7** containing 10 μM Nile Red with MCF-7 human breast cancer epithelial cells for 1 hour in the presence or absence of visible light. Nile Red easily penetrates cell membranes and subsequently stains intracellular lipids, emitting strong fluorescence at 530 nm.[56] To monitor the delivery of Nile Red into the cells, we performed live-cell imaging via a fluorescence microscopy immediately after cell washing. In the absence of irradiation, the Nile Red remained in the micelles, and its delivery into the cells was suppressed, as evidenced by the negligible levels of fluorescence (Figure 9A, left). In contrast, irradiation by

visible light induced the disruption of micelles and allowed successful cargo delivery into the cells, as evidenced by the strong fluorescence of Nile Red observed from the interior of the cells (Figure 9A, right).

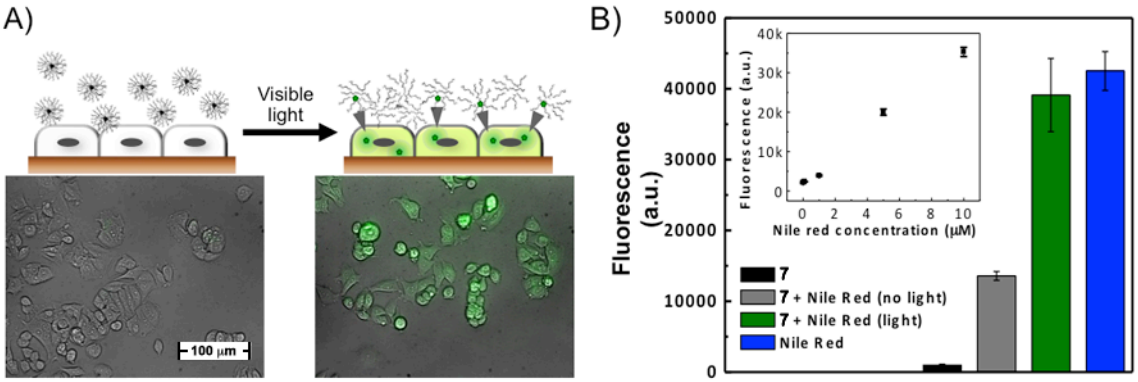

Figure 9. Visible light mediated cargo delivery of Nile Red into MCF-7 cells. A) Schematic of experimental process (top), corresponding fluorescence microscopy images of MCF-7 before irradiation (bottom left), after irradiation (bottom right). B) Linear relationship of cell fluorescence to Nile Red concentration (inset), and visible light mediated release of Nile red and relevant controls.

To further verify that cargo delivery is triggered by visible light, we measured the amount of delivered cargo through the fluorescence of cell-internalized Nile Red. As shown in the inset of Figure 9B, cell fluorescence after incubation with free Nile Red and subsequent washing was proportional to the concentration of Nile Red (0.1 μM to 10 μM). From this linear relationship, we found that compared to the absence of visible light (grey), visible light irradiation (green) induced an approximately 3-fold increase in intensity, confirming light-mediated cargo delivery to the cells. Moreover, the intensity of cells incubated with free Nile Red (blue) was comparable to that of the cells incubated with Nile Red encapsulating DPC **7** after visible light irradiation (green). This result suggests that DPC **8** does not interfere with intracellular diffusion of the unloaded cargo, achieving highly efficient delivery. Note that the visible light-induced cargo delivery requires the self-assembly of amphiphiles and their subsequent disassembly triggered by visible light. Below the CMC of the

amphiphiles, we observed no evidence of light-induced cargo delivery, implying that the cargo freely diffuses into the cells in the absence of micelle formation.

4.3.4. Micellar Delivery of a Chemotheraputic

Finally, in collaboration with Saemi Polema and Seung Soo Oh the capability of light-mediated cell death was explored by unloading hydrophobic chemotherapy drugs (Figure 10). As a model drug, we chose paclitaxel, which is widely used as a mitotic inhibitor that interferes with cell division for the treatment of tumors including breast cancers.[59,60] We prepared 0.5 mg/mL solutions of DPC **7** containing 1 μM of paclitaxel and incubated MCF-7 cells with this solution for an hour in both the presence and absence of visible light irradiation. Following thorough washing, the cells were further incubated at 37 °C for 4 days, and cell viability was measured every 24 hours by live/dead cell viability assay. It is noteworthy that DPC **7** is not inherently toxic to the cells, and thus only the drug was responsible for the decrease in cell viability. Regardless of light irradiation, cells previously incubated with DPC **7** did not show any notable decrease of cell viability over 4 days (Figure 10, black and red). In addition, the viability of the cells directly exposed to DPC **7** for 24 hours without washing did not change significantly, which supports that DPC **7** is biocompatible. Compared to cells incubated with paclitaxel-loaded DPCs and not irradiated with visible light (Figure 10, orange), similarly incubated cells exposed to visible light irradiation (Figure 10, green) displayed a significantly greater decrease in cell viability over 4 days. Within 48 hours, the viability of cells irradiated with visible light decreased by 47%, approximately 3 times more than did non-irradiated cells, resulting from light-enhanced drug delivery. While preparing micelles with a higher loading of paclitaxel provided larger decrease in cell viability by light irradiation, the degree of enhanced cytotoxicity became smaller, which is pre-

sumably related to the effective concentration of paclitaxel to inhibit the cell growth. Once again, the viability of the cells treated with paclitaxel alone (Figure 10, blue) was comparable to that of the cells incubated with paclitaxel-loaded DPC **7** micelles and irradiated with visible light (green), indicating the efficient drug release mediated by visible light.

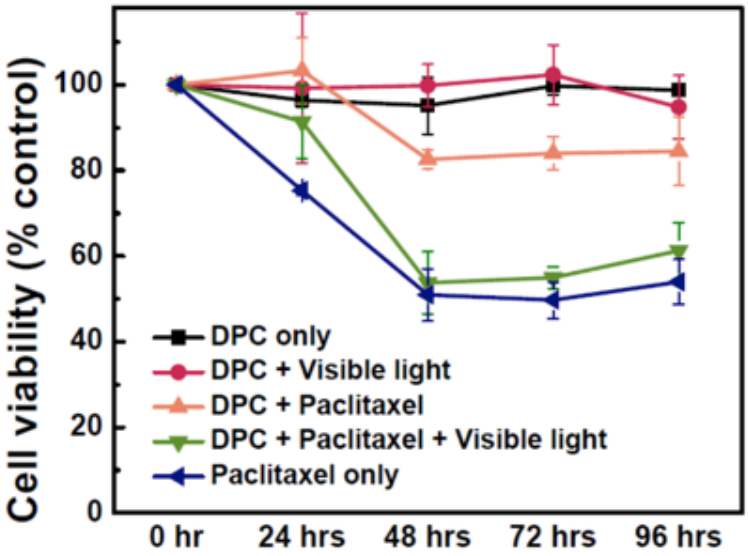

Figure 10. Visible light-mediated cytotoxicity of cancer cells by paclitaxel loaded DPC **7** micelles, and relevant controls.

4.4. Closing Remarks

We have demonstrated the considerable potential of employing DASA photoswitches for the visible light-initiated recycling of homogeneous organic catalysts. Catalyst development was enabled by modular and simple methods to generate functional thiourea and DASA coupling partners. The catalyst-photoswitch construct effectively polymerized lactide with control over molecular weight and a low PDI. The visible-light mediated phase transfer and subsequent recovery of the thiourea catalyst allowed recycling of the organocatalyst. The photoswitch-catalyst construct was shown to be effective over numerous polymerization cycles with negligible effect on efficiency. Detailed mechanistic studies provided valuable insight into future catalyst design for visible light-mediated recycling. The prevalence of or-

ganocatalysis in modern synthetic chemistry coupled with the mild and benign nature of the recycling stimulus and procedure make this an attractive concept for further development.

We have also developed a one-photon visible light-responsive micellar system for efficient, on-demand drug delivery. The efficiency and effectiveness of this system was demonstrated in an in-vitro setting, delivering the chemotherapeutic paclitaxel only on exposure to visible light. Particularly, this is facilitated by the use of a novel class of photochromic material, donor-acceptor Stenhouse adducts, which overcome challenges associated with UV light and multi-photon processes. This system offers promising new directions in phototherapy and controlled release applications.

4.5. References

(1) Edward, J. A.; Kiesewetter, M. K.; Kim, H.; Flanagan, J. C. A.; Hedrick, J. L.; Waymouth, R. M. *Biomacromolecules* **2012**, *13* (8), 2483.

(2) Lipshutz, B. H.; Ghorai, S. *Org. Lett.* **2012**, *14* (1), 422.

(3) Gruttadauria, M.; Giacalone, F.; Noto, R. *Chem. Soc. Rev.* **2008**, *37* (8), 1666.

(4) He, W.; Zhang, F.; Shi, X.; Li, H. *Eur. J. Org. Chem.* **2012**, *2012* (20), 3753.

(5) Puglisi, A.; Annunziata, R.; Benaglia, M.; Cozzi, F.; Gervasini, A.; Bertacche, V.; Sala, M. C. *Adv. Synth. Catal.* **2009**, *351* (1-2), 219.

(6) Yu, P.; He, J.; Guo, C. *Chem. Commun.* **2008**, No. 20, 2355.

(7) Lee, J.-W.; Mayer-Gall, T.; Opwis, K.; Song, C. E.; Gutmann, J. S.; List, B. *Science* **2013**, *341* (6151), 1225.

(8) Yoshida, J.; Itami, K. *Chem. Rev.* **2002**, *102* (10), 3693.

(9) Alvarez-Lorenzo, C.; Bromberg, L.; Concheiro, A. *Photochem. Photobiol.* **2009**, *85* (4), 848.

(10) MacMillan, D. W. C. *Nature* **2008**, *455* (7211), 304.

(11) Dalko, P. I.; Moisan, L. *Angew. Chem. Int. Ed.* **2004**, *43* (39), 5138.

(12) Doyle, A. G.; Jacobsen, E. N. *Chem. Rev.* **2007**, *107* (12), 5713.

(13) Hernández, J. G.; Juaristi, E. *Chem. Commun.* **2012**, *48* (44), 5396.

(14) Cole-Hamilton, D. J. *Science* **2003**, *299* (5613), 1702.

(15) Chu, Q.; Yu, M. S.; Curran, D. P. *Org. Lett.* **2008**, *10* (5), 749.

(16) Miura, T.; Nishida, S.; Masuda, A.; Tada, N.; Itoh, A. *Tetrahedron Lett.* **2011**, *52* (32), 4158.

(17) Vuluga, D.; Legros, J.; Crousse, B.; Bonnet-Delpon, D. *Chem. - Eur. J.* **2010**, *16* (6), 1776.

(18) Miao, W.; Chan, T. H. *Adv. Synth. Catal.* **2006**, *348* (12-13), 1711.

(19) Ni, B.; Headley, A. D. *Chem. - Eur. J.* **2010**, *16* (15), 4426.

(20) Luo, S.; Mi, X.; Zhang, L.; Liu, S.; Xu, H.; Cheng, J.-P. *Angew. Chem. Int. Ed.* **2006**, *45* (19), 3093.

(21) Ni, B.; Zhang, Q.; Headley, A. D. *Green Chem.* **2007**, *9* (7), 737.

(22) Liu, G.; Wang, J. *Angew. Chem. Int. Ed.* **2010**, *49* (26), 4425.

(23) Liu, G.; He, H.; Wang, J. *Adv. Synth. Catal.* **2009**, *351* (10), 1610.

(24) Süßner, M.; Plenio, H. *Angew. Chem. Int. Ed.* **2005**, *44* (42), 6885.

(25) Helmy, S.; Leibfarth, F. A.; Oh, S.; Poelma, J. E.; Hawker, C. J.; Read de Alaniz, J. *J. Am. Chem. Soc.* **2014**, *136* (23), 8169.

(26) Helmy, S.; Oh, S.; Leibfarth, F. A.; Hawker, C. J.; Read de Alaniz, J. *J. Org. Chem.* **2014**, *79* (23), 11316.

(27) Taylor, M. S.; Jacobsen, E. N. *Angew. Chem. Int. Ed.* **2006**, *45* (10), 1520.

(28) Dove, A. P.; Pratt, R. C.; Lohmeijer, B. G. G.; Waymouth, R. M.; Hedrick, J. L. *J. Am. Chem. Soc.* **2005**, *127* (40), 13798.

(29) Pratt, R. C.; Lohmeijer, B. G. G.; Long, D. A.; Lundberg, P. N. P.; Dove, A. P.; Li, H.; Wade, C. G.; Waymouth, R. M.; Hedrick, J. L. *Macromolecules* **2006**, *39* (23), 7863.

(30) Fernández, J.; Etxeberría, A.; Sarasua, J. R. *Polym. Degrad. Stab.* **2013**, *98* (7), 1293.

(31) Coulembier, O.; Moins, S.; Raquez, J.-M.; Meyer, F.; Mespouille, L.; Duquesne, E.; Dubois, P. *Polym. Degrad. Stab.* **2011**, *96* (5), 739.

(32) Coady, D. J.; Engler, A. C.; Horn, H. W.; Bajjuri, K. M.; Fukushima, K.; Jones, G. O.; Nelson, A.; Rice, J. E.; Hedrick, J. L. *ACS Macro Lett.* **2012**, *1* (1), 19.

(33) Kelly, T. R.; Kim, M. H. *J. Am. Chem. Soc.* **1994**, *116* (16), 7072.

(34) Lohmeijer, B. G. G.; Pratt, R. C.; Leibfarth, F.; Logan, J. W.; Long, D. A.; Dove, A. P.; Nederberg, F.; Choi, J.; Wade, C.; Waymouth, R. M.; Hedrick, J. L. *Macromolecules* **2006**, *39* (25), 8574.

(35) Osorio-Planes, L.; Rodríguez-Escrich, C.; Pericàs, M. A. *Org. Lett.* **2014**, *16* (6), 1704.

(36) Li, Y.; Xiao, W.; Xiao, K.; Berti, L.; Luo, J.; Tseng, H. P.; Fung, G.; Lam, K. S. *Angew. Chem. Int. Ed.* **2012**, *51* (12), 2864.

(37) Gillies, E. R.; Fréchet, J. M. J. *Bioconjug. Chem.* **2005**, *16* (2), 361.

(38) Nasongkla, N.; Shuai, X.; Ai, H.; Weinberg, B. D.; Pink, J.; Boothman, D. A.; Gao, J. *Angew. Chem. Int. Ed.* **2004**, *43* (46), 6323.

(39) Bae, Y.; Fukushima, S.; Harada, A.; Kataoka, K. *Angew. Chem. Int. Ed.* **2003**, *42* (38), 4640.

(40) Zhao, Y. *Macromolecules* **2012**, *45* (9), 3647.

(41) Bédard, M. F.; De Geest, B. G.; Skirtach, A. G.; Möhwald, H.; Sukhorukov, G. B. *Adv. Colloid Interface Sci.* **2010**, *158* (1-2), 2.

(42) Fomina, N.; McFearin, C.; Sermsakdi, M.; Edigin, O.; Almutairi, A. *J. Am. Chem. Soc.* **2010**, *132* (28), 9540.

(43) Li, Y.-L.; Zhu, L.; Liu, Z.; Cheng, R.; Meng, F.; Cui, J.-H.; Ji, S.-J.; Zhong, Z. *Angew. Chem. Int. Ed.* **2009**, *48* (52), 9914.

(44) Yesilyurt, V.; Ramireddy, R.; Thayumanavan, S. *Angew. Chem. Int. Ed.* **2011**, *50* (13), 3038.

(45) Lee, H.; Wu, W.; Oh, J. K.; Mueller, L.; Sherwood, G.; Peteanu, L.; Kowalewski, T.; Matyjaszewski, K. *Angew. Chem. Int. Ed.* **2007**, *46* (14), 2453.

(46) Bansal, A.; Zhang, Y. *Acc. Chem. Res.* **2014**, *47* (10), 3052.

(47) Velema, W. A.; Szymanski, W.; Feringa, B. L. *J. Am. Chem. Soc.* **2014**, *136* (6), 2178.

(48) Goodwin, A. P.; Mynar, J. L.; Ma, Y.; Fleming, G. R.; Fréchet, J. M. J. *J. Am. Chem. Soc.* **2005**, *127* (28), 9952.

(49) Lin, Q.; Huang, Q.; Li, C.; Bao, C.; Liu, Z.; Li, F.; Zhu, L. *J. Am. Chem. Soc.* **2010**, *132* (31), 10645.

(50) Yan, B.; Boyer, J.-C.; Branda, N. R.; Zhao, Y. *J. Am. Chem. Soc.* **2011**, *133* (49), 19714.

(51) Viger, M. L.; Grossman, M.; Fomina, N.; Almutairi, A. *Adv. Mater.* **2013**, *25* (27), 3733.

(52) Rodriguezhernandez, J.; Checot, F.; Gnanou, Y.; Lecommandoux, S. *Prog. Polym. Sci.* **2005**, *30* (7), 691.

(53) Joralemon, M. J.; McRae, S.; Emrick, T. *Chem. Commun.* **2010**, *46* (9), 1377.

(54) Malic, N.; Evans, R. A. *J. Polym. Sci. Part Polym. Chem.* **2012**, *50* (7), 1434.

(55) Fowler, S. D.; Greenspan, P. *J. Histochem. Cytochem.* **1985**, *33* (8), 833.

(56) Greenspan, P. *J. Cell Biol.* **1985**, *100* (3), 965.

(57) Amir, E.; Amir, R. J.; Campos, L. M.; Hawker, C. J. *J. Am. Chem. Soc.* **2011**, *133* (26), 10046.

(58) Krishna, M. M. G. *J. Phys. Chem. A* **1999**, *103* (19), 3589.

(59) Nehate, C.; Jain, S.; Saneja, A.; Khare, V.; Alam, N.; Dubey, R.; Gupta, P. *Curr. Drug Deliv.* **2014**, *11* (6), 666.

(60) Zhang, Z.; Mei, L.; Feng, S.-S. *Expert Opin. Drug Deliv.* **2013**, *10* (3), 325.

5. Future Directions

5.1. Introduction

In the course of any scientific endeavor it is only natural that certain efforts will be initially explored but ultimately abandoned. The intention in this chapter is to present some of these efforts as a guidance to future researchers who choose to apply their efforts in this field. Specifically, I will first outline our efforts towards the development of an "intramolecular" DASA, where the donor amine is covalently appended to the activated furan. Second, our attempt to bathochromicaly shift the absorbance λ_{max} of DASA trienes by extending conjugation of the activated furan precursor will be presented. Next we will outline our efforts towards the synthesis of γ-alkylidene butenolides form Meldrum's acid derived DASA trienes. Following this will be our work on developing DASA dimers, where two of the photochromic moieties are linked through either the donor or the acceptor group. Finally, we will present our investigations on the formation and properties of (dihydro)indenopyridinecarbonitriles, derived from heterocyclic aldehydes activated by either 1,1-dicyanomethylene-3-indanone or 1,3-bis(dicyanomethylene)-indane. Combined, all of these exploratory efforts were aimed at expanding the utility of our new class of photochromic material.

5.2. Structural Variations and Synthetic Manipulations

5.2.1. Intramolecular Variant

Aza-spirocycles are important synthetic building blocks in alkaloid chemistry because such ring skeletons are present in many naturally occurring substances of biological properties.[1] In 2010 Read de Alaniz and co-workers developed the aza-Piancatelli rearrangement, a powerful method for the highly diastereoselective formation of 4-aminocyclopentenones.[2] In

the following year this discovery was expanded by their report of an intramolecular aza-Piancatelli rearrangement, which provides aza-spirocycles in unprecedented yields and diastereoselectivity.[3] In the coming years these efforts were further expanded to methods for forming spirocyclic ethers,[4] and fused oxabicycles,[5] as well as fully substituted all-carbon stereocenters.[6] Our general interest in the domino and cascade reactions of activated furans combined with our success in developing DASA photoswitches prompted us to consider if an intramolecular variant of these materials could be prepared, and what effect if any this structural variation would have on the photophysical properties of the resulting compounds.[2–5,7–10,6,11]

Using procedures previously established by our group, we began from ethyl 3-(furan-2-yl)propanoate **1**, Figure 1. Saponification of the ester followed by coupling with benzyl amine **3**, cleanly provided amide **4**, which was reduced to give secondary amine **5**. Boc protection of the amine functionality enabled Vilsmeier-Haack formylation to afford furfuraldehyde derivative **7** (81% yield from **1**).

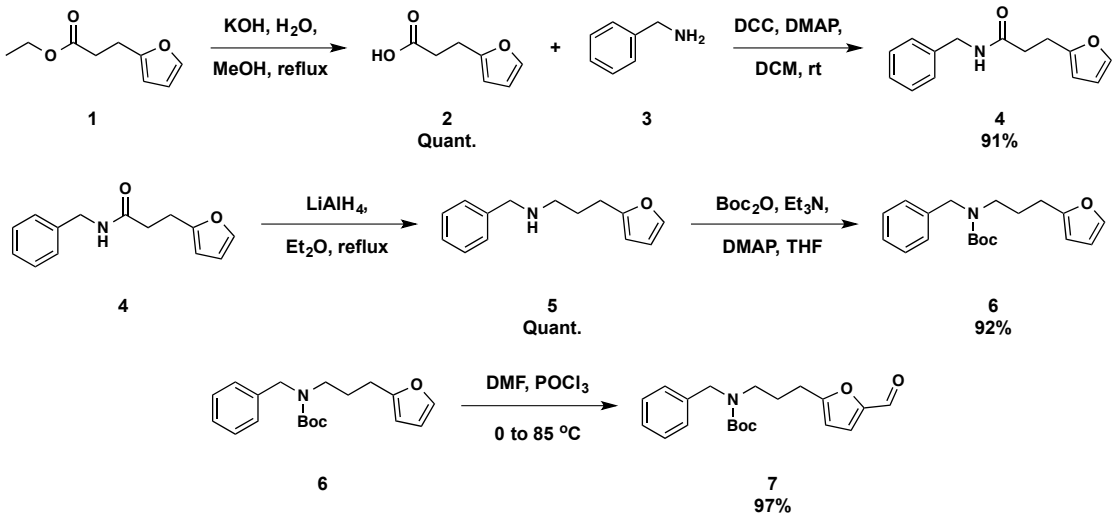

Figure 1. Preparation of furaldehyde precursor **7**.

With precursor **7** in hand, we proceeded to attempt formation of the activated furan, Figure 2. Repeated attempts to condense Meldrum's acid **8** with **7**, were met with varying degrees of success. At best we could isolate, activated furan **9** in only 10% yield, always with concomitant formation of DASA adduct **10** in up to 20% yield. The structure of DASA triene **10** was confirmed by ^{1}H NMR, and has a similar spectral absorption to other Meldrum's acid derived DASA trienes. We propose that after the initial condensation, the highly acidic nature of Meldrum's acid, serves as a catalyst to remove the Boc protecting group from **9**, which then undergoes ring opening to provide **10**.

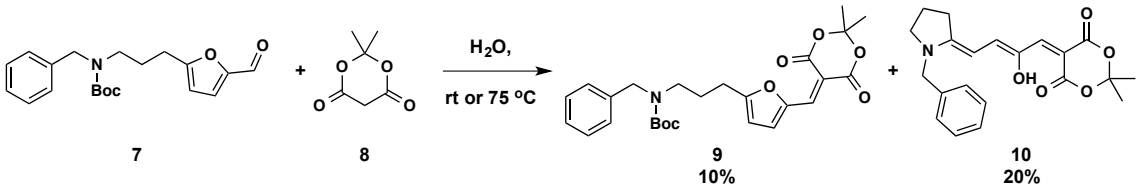

7 8 **9** 10% **10** 20%

Figure 2. Initial attempts towards formation of activated furan **9**.

Intrigued, but undaunted, by this result, we continued our efforts, finding that under prolonged exposure to the reaction conditions we could isolate the DASA adduct **10** in up to 50% yield (Figure 3, top). With DASA adduct **10** in hand we next sought to evaluate its ability to undergo cyclization by either photochromic reaction or the PPh_3 mediated conditions described in Chapter 3 (Figure 3, bottom). To our dismay, both of the developed conditions failed to provide the desired zwitterion **11**, and **10** was recovered unchanged.

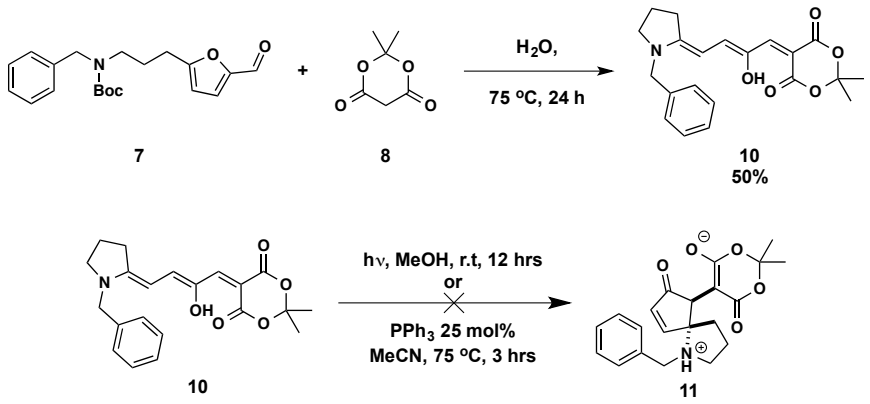

Figure 3. Improved synthesis of DASA adduct **10** (top), and attempted cyclization to zwitterion **11** (bottom).

5.2.2. Extending Conjugation

In Chapter 3 we outlined our investigations to bathochromically shift the absorbance λ_{max} of DASA trienes to the NIR region by employing different acceptor moieties. In addition to these efforts we also considered if this goal could be achieved by extending conjugation in the activated furan precursor.[12,13] To this end we prepared activated furans **13** and **15**, from 3-(2-furyl)acrolein **12** (Figure 4).

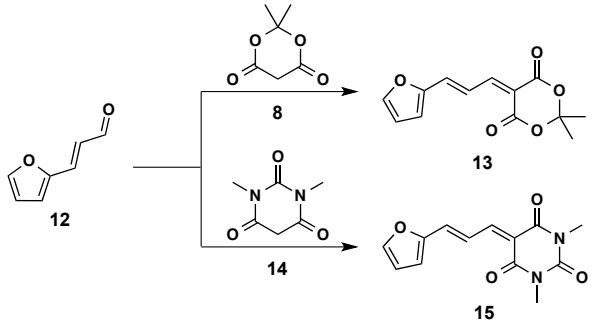

Figure 4. Preparation of activated furans **13** and **15** with extended conjugation.

On reaction with secondary amines, both activated furans curiously only provided the DASA trienes **17** and **19** in poor yield, Figure 5. Repeated efforts to form or isolate DASA tetraenes **16** or **18**, continued to provide similar results.

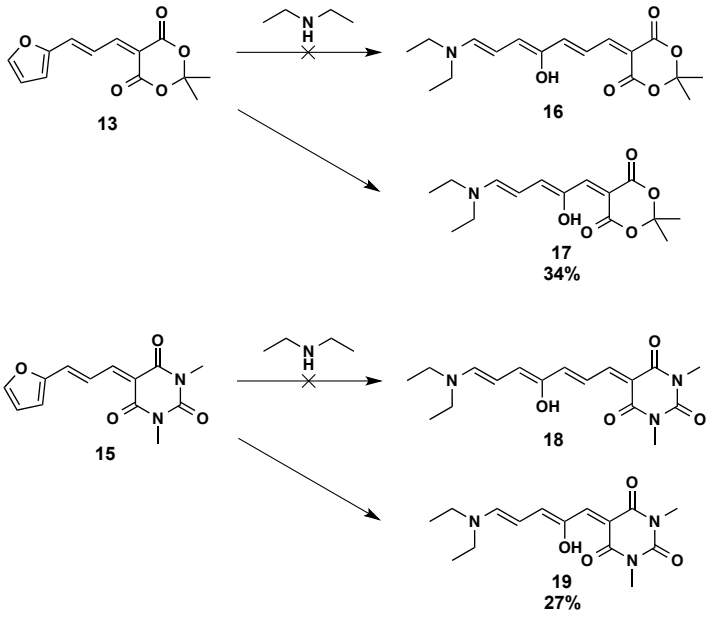

Figure 5. Ring opening reaction of activated furans **13** and **15**.

While disheartening, this result prompted us to consider what may be occurring to inhibit formation of the tetraene. After careful consideration, we hypothesize that the tetraenes are initially formed, however, convert to the triene after their formation. As shown in Figure 6, it is believed that nucleophilic attack by amine **20** leads to the ring opened tetraene **23**. We propose that following alkene isomerization, iminium mesomer **24** undergoes intramolecular [2+2] cycloaddition to form cyclobutene intermediate **25**. Cyclobutene **25** is believed to decompose *via* [2+2] cycloreversion, releasing acetylene **26** and ultimately producing DASA triene **27**.

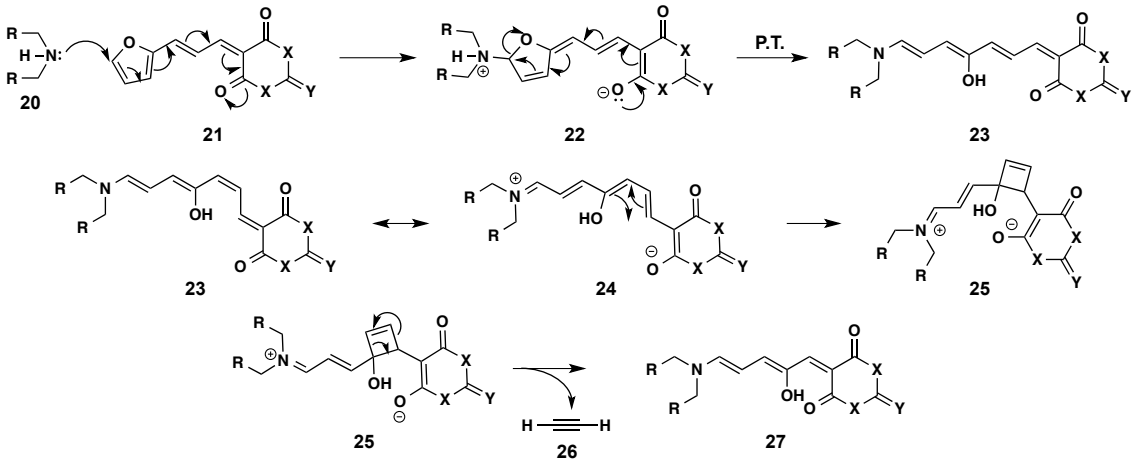

Figure 6. Proposed mechanism for formation of DASA trienes from activated furans with extended conjugation.

5.2.3. γ-Alkylidene Butenolides

Over one hundred years ago, in 1908, Scottish chemist Andrew Norman Meldrum synthesized a substance that years later would bear his name.[14] Today, Meldrum's acid **8** is one of the most useful reagents in the synthesis of heterocycles. In his first independent publication, he studied the reaction between malonic acid **28** and acetone **29** and, following the suggestion of Prof. Japp, employed a mixture of acetic anhydride and sulfuric acid as condensing agent.[15] From elemental analysis data, in conjunction with previous results and the acidic properties of the final compound, he formulated the structure of the product to be β-lactone of β-hydroxyisopropylmalonic acid **31** (Scheme 1).

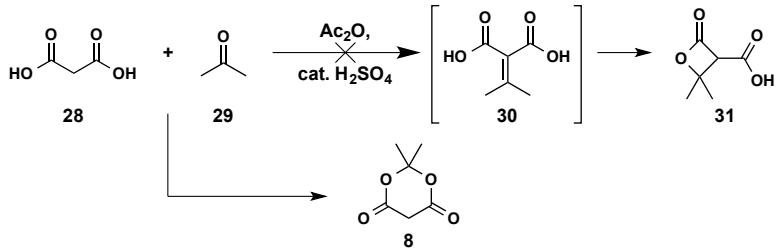

Scheme 1. Synthesis of Meldrum's acid.

Clearly, back then it was difficult to assign the correct chemical structure of the product isolated from this reaction. For example, the unusual C–H acidity of Meldrum's acid (pK_a

4.83 in water) continues to be the focus of attention for research.[16,17] However, it was not until 1948, when more experimental data on the chemistry of this product were collected, that its correct structure was determined to be 2,2-dimethyl-4,6-diketo-1,3-dioxane **8**.[14] The first review on the chemistry of Meldrum's acid by McNab describes mostly the synthesis of derivatives via functionalization of the methylene group, and only a few reactions are mentioned where the 1,3-dioxane moeity is the reaction site.[18] A more detailed literature survey shows an enormous interest in Meldrum's acid chemistry in the 1980s that continues to this century.[19] Thus, recent reviews focused on more specialized subjects such as the role of Meldrum's acid in multicomponent reactions,[20] flash vacuum pyrolysis (FVP) techniques,[21] and more recently in synthesis of natural products.[22,23]

One of the most valuable manipulations of Meldrum's acid derivatives is their thermolysis or pyrolysis to form highly reactive ketene intermediates, Scheme 2. Specifically, 5,5-dialkyl (**32**) or 5-methylene (**35**) Meldrum's acids decompose at high temperatures (> 200 °C) liberating acetone **28** and carbon dioxide **34**, to generate dialkyl ketenes (**33**) or methylene ketenes (**36**), respectively (Scheme 2A). In recent years this transformation has also been applied materials chemistry. The Hawker group have pioneered this field demonstrating the versatility of ketenes in polymer chemistry in a number of advanced applications, including patterning of substrates,[24,25] crosslinking of polyolefins,[26] and the preparation of robust, solvent–stable nanostructured materials.[27] Further, Leibfarth and co-workers have demonstrated, both computationally and experimentally, that the thermolysis temperature can be significantly lowered through inter- or intramolecular hydrogen bonding of a Bronsted acid (specifically a hydroxyl group) to one of the carbonyls of the Meldrum's acid moiety (Scheme 2B).[28]

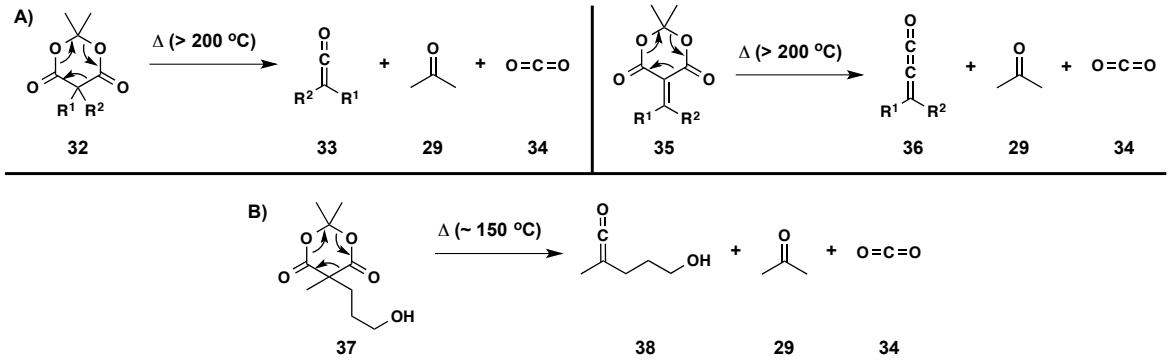

Scheme 2. Formation of ketenes from Meldrum's acid derivatives.

Single crystal X-ray diffraction studies of our Meldrum's acid derived DASA trienes, revealed that the enolic hydroxyl proton engages in hydrogen bonding to a carbonyl oxygen in the Meldrum's acid acceptor group, Scheme 3. Based on this observation and the works of Leibfarth[28] and McNabb,[18,21] we reasoned that thermolysis of Meldrum's acid derived DASA trienes may provide access to methylene ketene intermediates, and further what products would arise from this process.

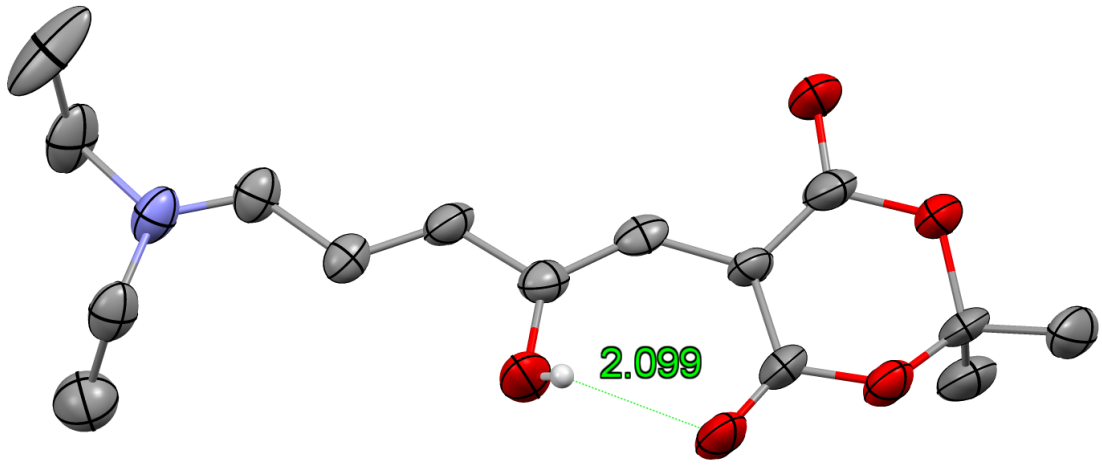

Scheme 3. ORTEP rendering of DASA triene **17** highlighting intramolecular hydrogen bonding (50% probability ellipsoids, distance in Å, hydrogen atoms omitted for clarity).

We began our study by examining the thermal decomposition of DASA triene **17** by thermogravimetric analysis/mass spectrometry (TGA/MS). As is shown in Figure 7, compound **17** experiences a dramatic loss of mass at ~ 170 °C. Mass spectrometry analysis of

the effluent gas targeting CO_2 and acetone, m/z 44 and 58 respectively, confirmed decomposition of the Meldrum's acid group in the solid state at this temperature, implying ketene formation.

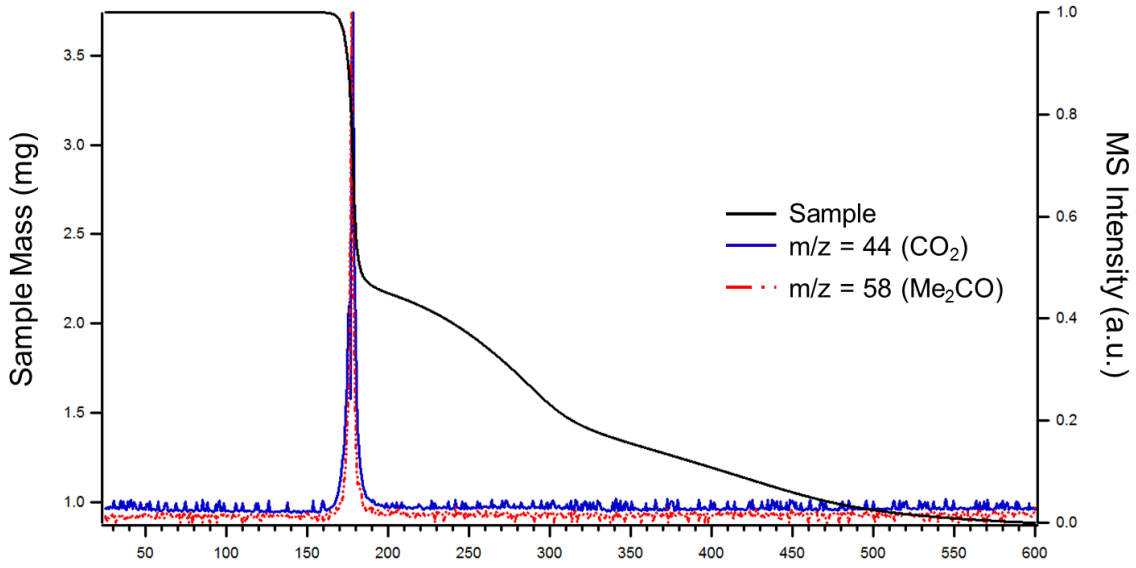

Figure 7. TGA/MS of DASA triene **17**.

Based on this result we proceeded to subject compound **17** to solution state thermolysis. Considering the high temperature needed to generate the ketene intermediate we chose to forgo conventional heating and opted to examine thermolysis under microwave irradiation. Based on the work of Vanderwal, we selected *o*-dicholorbenzene as the solvent for the reaction, as it is both non-nucleophilic and is known to tolerate high temperatures.[29,30] Following optimization of the temperature and time of the reaction, we were pleased to find that we could isolate γ-alkylidene butenolide **39** in up to 33% yield, Figure 8A. We propose that thermolysis of **17**, leads to formation of methylene ketene **40**, which then undergoes intramolecular cyclization and proton transfer to afford butenolide **39**, Figure 8B.

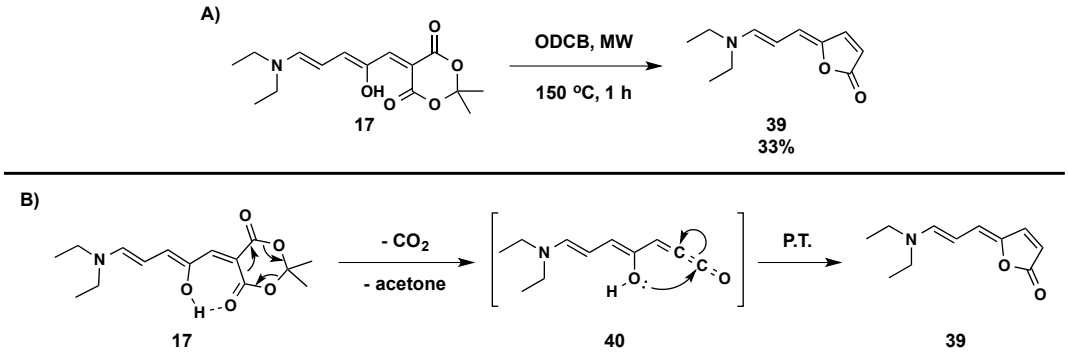

Figure 8. A) Optimized synthesis of butenolide **39**, B) Proposed mechanism of formation.

With the ubiquity of the butenolide motif in many natural products and biologically relevant compounds, this methodology allows for rapid access to these materials in as little as 3 steps. This constitutes a significant advance in the synthesis of these compounds, which has historically been plagued by the use of highly toxic reagents, lengthy procedures and low yields.[31–34] Further, Vanderwal has shown that 5-aminopentadienals can be treated with trialkyl tin species, resulting in the exchange of the amine component for the trialkyl tin.[35] We believe that our conjugated butenolides can undergo the same exchange reaction; enabling the use of these materials in Stille cross coupling reactions for the synthesis of complex polyenes and natural products.

5.3. DASA Dimers

The ability to reversibly alter the geometry of macromolecules has been exploited for the elaboration of guest-encapsulation structures,[36,37] and opto-mechanical materials,[38–42] which enable direct conversion of photon energy into mechanical work. To prepare efficient structures and materials however, it is desirable to design macromolecules apt to dramatically change shape and dimensions upon exposure to light.[43] The groups of Aida,[44] and in particular McGrath,[45–48] and later on also Mullen and co-workers,[49] introduced azobenzene photochromes into the core of rather spherical dendrimers, resulting in (quasi)isotropic nanoobjects that display significant changes in hydrodynamic volume upon photoirradiation, with

contractions as high as ΔV_h= 37%, as evaluated by gel permeation chromatography (GPC). In 2011, Hecht and co-workers reported the synthesis of rigid-rod polymers consisting of azobenzene photochromes in the main chain and the dramatic change of their shape induced upon irradiation.[50] The embedded photo-switches act as hinges, which upon light-induced isomerization lead to reversible shrinking and stretching of the polymer backbone. Based on these works and the dramatic change in molecular length that DASAs undergo upon irradiation,[9] we began a program to prepare DASA oligomers and polymers, wherein the backbone of the macromolecule was composed of DASA trienes.

At the outset we sought to evaluate the feasibility of generating DASA dimers. We began by examining linking two DASA units through the acceptor. To this end we prepared Meldrum's acid dimer **42**, where a cyclohexane group links the two acceptors, Figure 9. Knoevenagel condensation of **42** with furfural **43** provided activated furan dimer **44**. Treatment of **44** with diethylamine **45** cleanly provided the anticipated DASA **46**. When we irradiated a toluene solution of dimer **46**, we observed an incomplete decrease in the absorbance attributed to the DASA triene by UV-Vis spectroscopy. Further, when irradiation was ceased, we observed only incomplete recovery of the triene absorbance. Based on these results, we believe that the highly rigid spirocyclic dimer may not have the conformational freedom necessary for both photochromic units to isomerize. Thus this strategy was not pursued further.

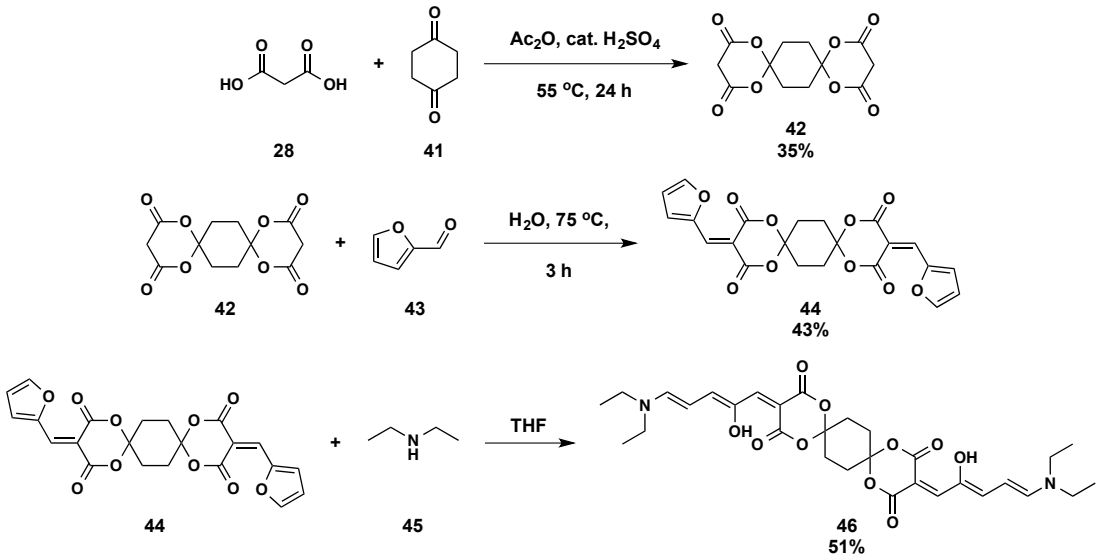

Figure 9. Synthesis of acceptor linked DASA dimer **46**.

Following this effort we chose to pursue linking two DASAs through a single bifunctional amine donor. For our initial attempt at this strategy, we selected piperazine **48**. To our gratification reacting Meldrum's acid activated furan **47** with piperazine **48**, provided donor linked DASA dimer **49** in 67% yield, Figure 10. Further, this protocol was equally proficient when applied to 1,3-dimethyl barbituric acid activated furan **50**, generating the corresponding dimer **51** in 73% yield.

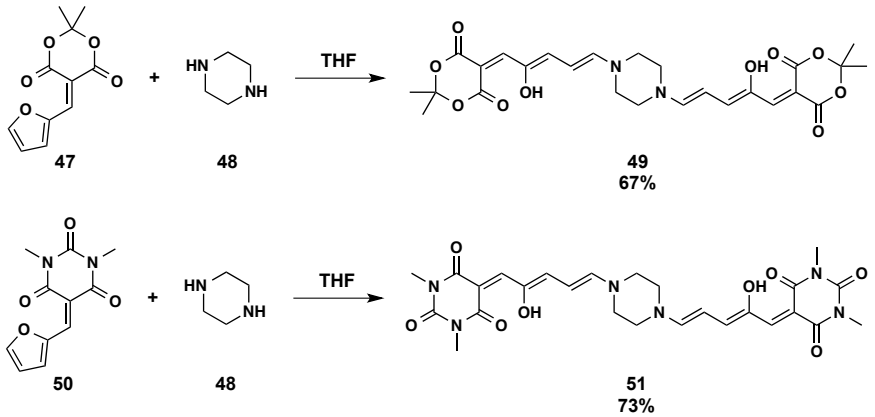

Figure 10. Synthesis of first generation donor linked DASA dimers.

Unfortunately, we observed similar incomplete photoswitching of these derivatives as was observed for acceptor linked DASA **46**. We thus probed, whether an extended linking donor may provide greater conformational freedom, to allow for complete and fully reversi-

ble photochromism. To that end we substituted *N,N`*-dibutyl hexanediamine **52** for piperazine **48**, reasoning that the hexyl linker would provide greater conformational freedom while the butyl substituents would enhance solubility. We were gratified to find that not only were DASA dimers **53** and **54** obtained in excellent yield, but that both derivatives were observed to undergo complete and fully reversible photochromism under the developed conditions, Figure 11.

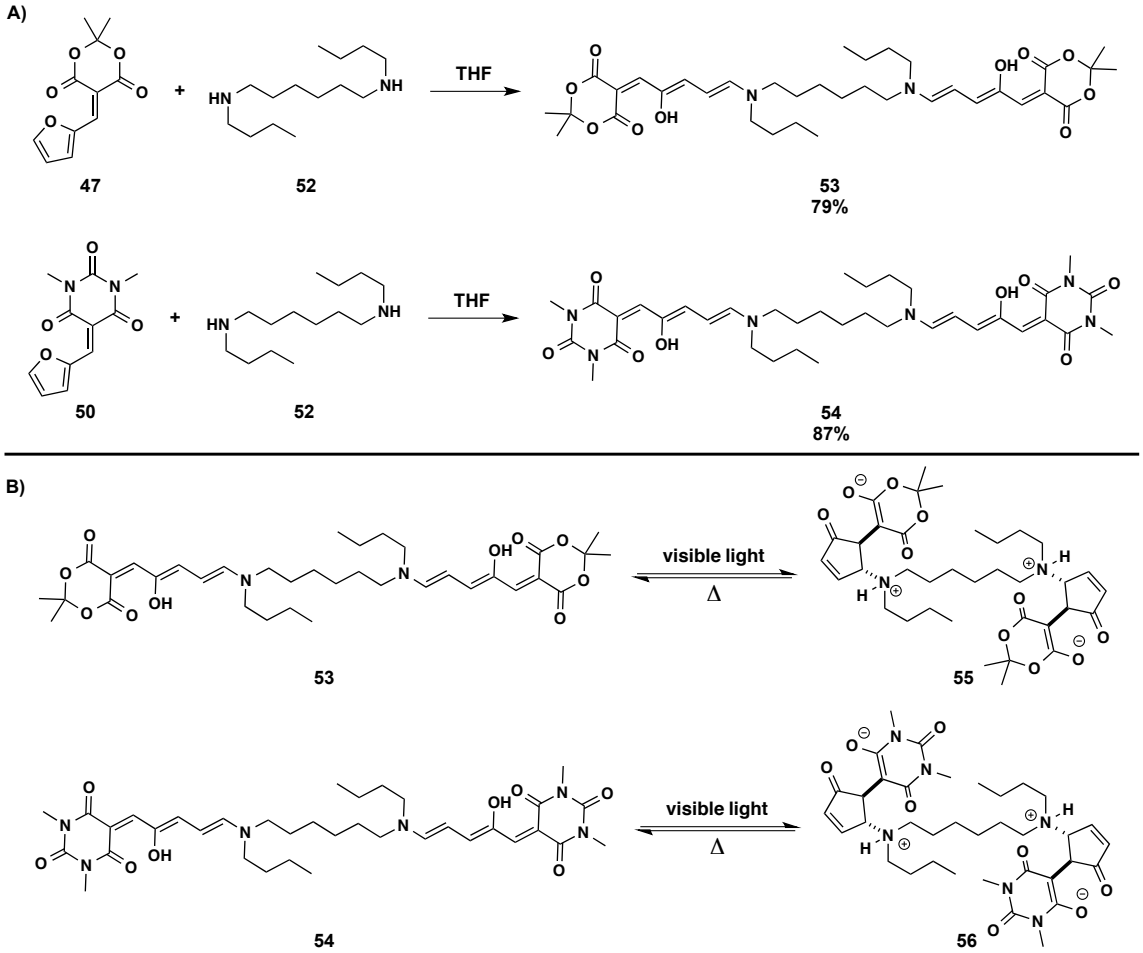

Figure 11. A) Synthesis and B) Photochromism of 2nd generation donor linked DASA dimers.

As a final effort towards the development of an acceptor linked dimer, we employed our experience in the synthesis of complex and functionalized 1,3-disubstituted barbituric acids to prepare barbituric acid dimer **61**, Figure 12. Briefly, 4,4′-methylenebis(phenyl isocyanate)

57 was treated with 2 equivalents of butylamine **58** to provide bis-urea **59** in 96% yield, which was reacted with 2 equivalents of malonyl chloride **60** to afford the desired barbituric acid dimer **61** in 91% yield.

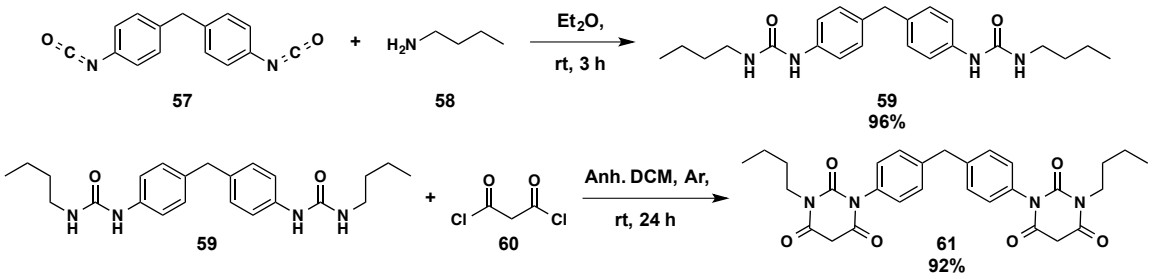

Figure 12. Synthesis of barbituric acid dimer **61**.

With dimer **61** in hand, we were able to prepare acceptor linked bis-activated furan **62** in 67% yield (unoptimized), and were pleased to find that reaction of **62** with 2 equivalents of diethylamine **43** provided acceptor linked DASA dimer **63** in 52% yield, Figure 13A. Further, encouraged by these results we proceeded to prepare acceptor linked DASA dimer **65** substituting diethylamine **43** with 6-azido-*N*-ethylhexan-1-amine **64**, which we had previously employed for preparation of our micelle forming polymer amphiphiles and recyclable thiourea catalyst, Figure 13B. We were gratified to find that both derivatives **63** and **65**, engage in complete and fully reversible photochromism.

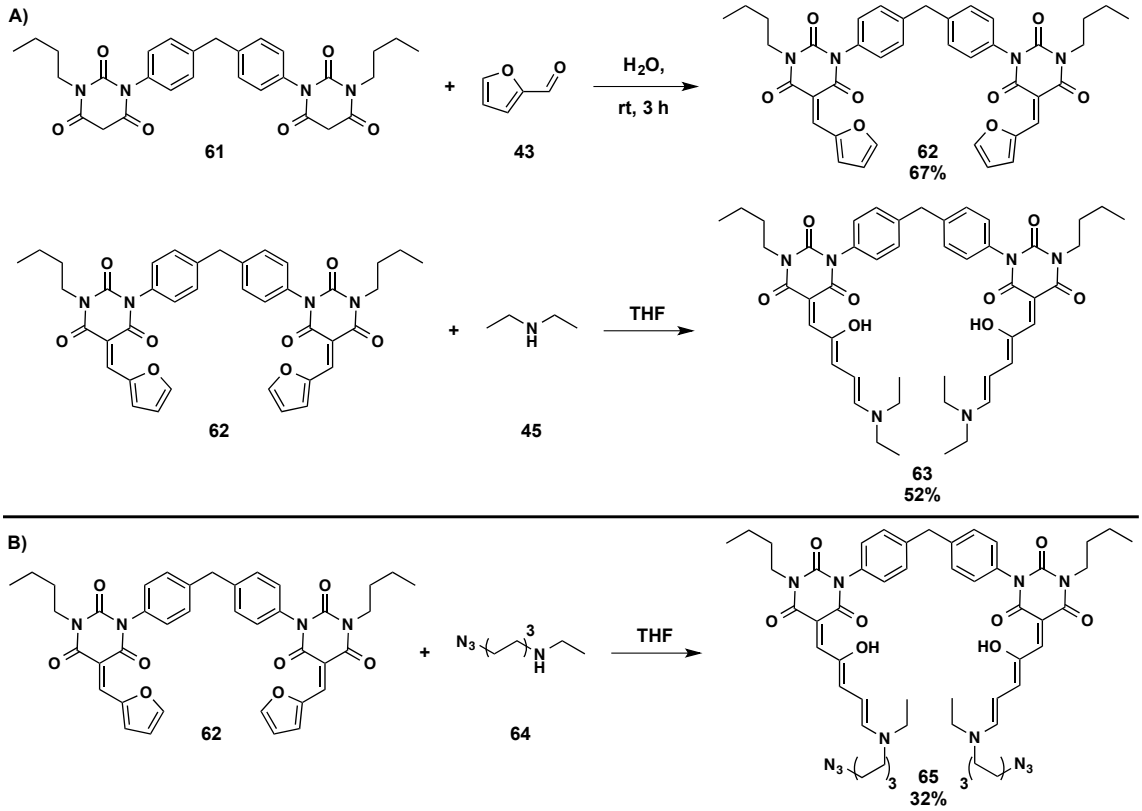

Figure 13. Synthesis of 2nd generation acceptor linked DASA dimers.

We believe that these results lay the foundation for the preparation of DASA oligomers and polymers. As has been demonstrated, in future efforts a key design principle will be ensuring that the resulting oligomers and polymers have the conformational flexibility needed to ensure complete and reversible photoisomerization of all incorporated DASA units. Further, it has been demonstrated that rigid conjugated polymers typically exhibit poor solubility in traditional organic solvents.[50–54] It is therefore clear that this feature cannot be overlooked in future developments. We propose that solubilizing groups can be introduced in two strategic locations without affecting the photochromic properties. First, in the preparation of acceptor linked activated furan dimers, similar to derivative **62**, we advise that opposed to the use of butylamine **58**, it would be beneficial to employ branched, acyclic alkylamines such as 2-ethylhexylamine. Second, we advise that any donor amine employed in-

clude branched acyclic alkyl chains, as well. With these considerations in mind we believe that DASA-backbone oligomers and polymers can be realized in the near future.

5.4. Indenopyridine Carbonitriles

5.4.1. Synthesis

As discussed in Chapter 3, when we attempted to employ 1,1-dicyanomethylene-3-indanone **66** or 1,3-bis(dicyanomethylene)-indan **69**, we failed to obtain the desired DASA trienes instead we isolated expanded ring dihydroindenopyridine carbonitrile derivatives **68** and **71**, respectively, Figure 14.[55] We then prepared thiophene analog **74** to determine if this phenomenon was limited to furans or if it was applicable to other 5-membered heterocycles as well. It should be noted that while we were successful in preparing a thiophene analog with 1,1-dicyanomethylene-3-indanone **66**, both the Knoevenagel adduct and corresponding dihydroindenopyridine were unstable and decomposed rapidly in air.

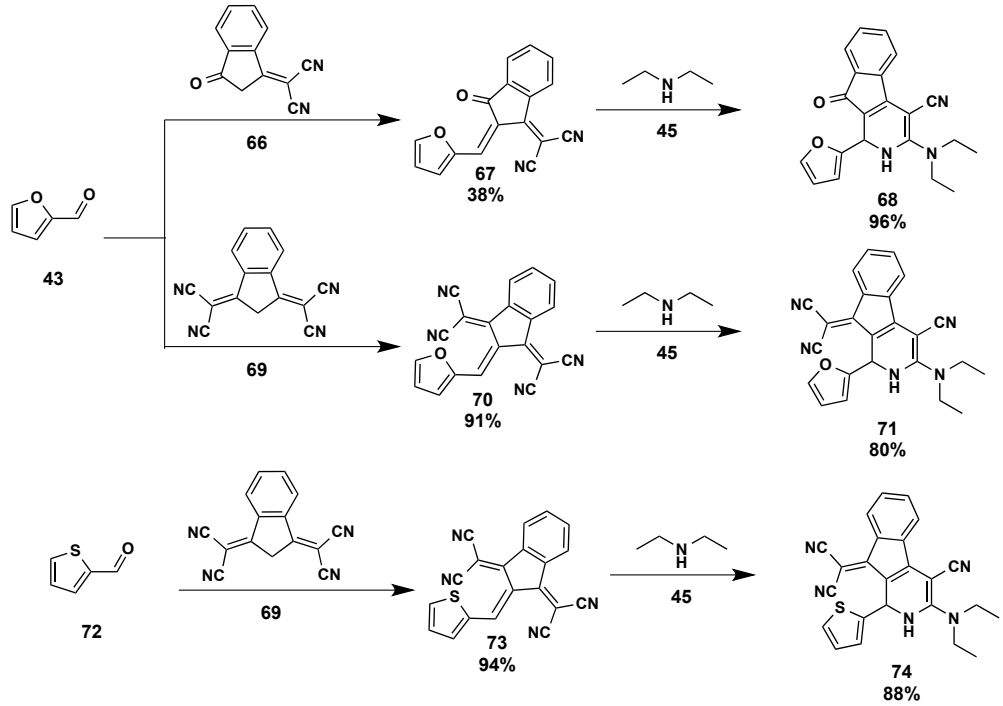

Figure 14. Synthesis of dihydroindenopyridine carbonitrile derivatives.

As discussed previously (Chapter 3, Section 3.3.1.), these dihydroindenopyridine carbonitriles oxidize on standing in air to the corresponding pyridines. We have subsequently found that the pyridines can also be accessed via chemical oxidation. As shown in Figure 15, the mild oxidizing agent chloranil afforded pyridine **75** in 47% yield, however, it was ineffective at oxidizing derivatives **71** and **74**. We were pleased to find that **71** and **74** could be oxidized synthetically, albeit with the use of the much stronger $KMnO_4$ affording pyridines **76** and **77** in 52% and 39% yield respectively.

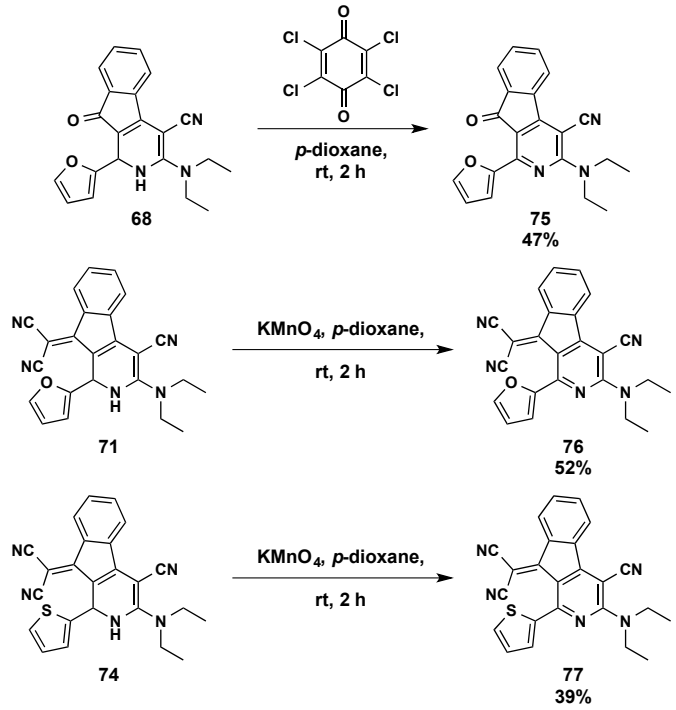

Figure 15. Oxidation of dihydroindenopyridine carbonitriles to indenopyridine carbonitriles.

We believe that with some optimization, these synthetic manipulations can provide facile access to either dihydroindenopyridine carbonitriles or indenopyridine carbonitriles. Further, the generality of this process will allow for the rapid introduction of structural diversity, both in the heterocyclic moiety appended to the (dihydro)pyridine moiety and the amine group employed.

5.4.2. Electrochemical Properties

Intrigued by these materials we sought to determine their electrochemical properties, as a first step to determining what if any application they may have. As such, we contacted Danisha M. Rivera-Nazario and Luis Echegoyen of University of Texas at El Paso who graciously conducted the experiments discussed below. The electrochemical properties of the samples were studied by cyclic voltammetry (CV) and square wave voltammetry (SWV) using 0.1 M $TBAPF_6$ in anhydrous DCM at a scan rate of 100 mV/s. The sample concentrations were 0.5 mM for all samples.

5.4.2.1. Dihydroindenopyridines

All compounds exhibited similar behavior with the exception of **68** (Figure 16). On the anodic scan two irreversible waves were observed for **68** and one irreversible wave for both **71** and **74**. These waves could be attributed to the oxidation of the dihydropyridine (DHP) moiety.

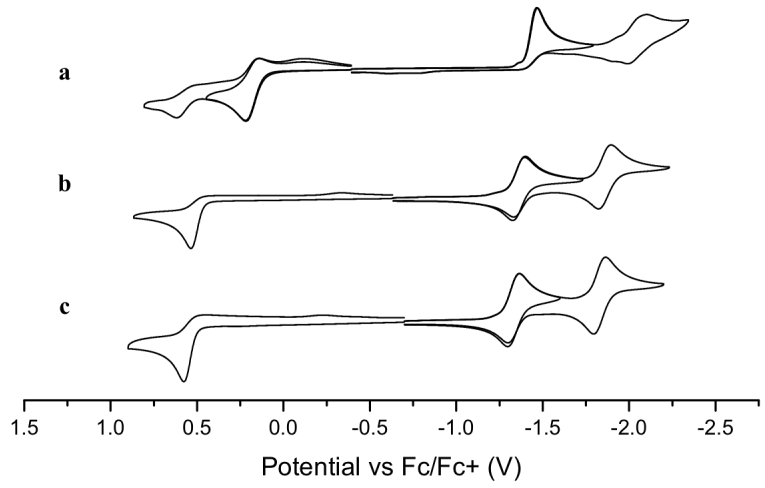

Figure 16. Cyclic voltammograms in 0.1 M $TBAPF_6$/DCM of 0.5 mM **a**) **68**, **b**) **71** and **c**) **74**.

It has been reported that the oxidation of DHP follows a two-electron pathway leading to the formation of neutral pyridine.[56,57] Scheme 4 shows the proposed mechanism involving the loss of two electrons and two hydrogen atoms, however, the mechanism has been proposed only for 1,4-dihydropyridine not for 1,2-dihydropyridine containing compounds.[58]

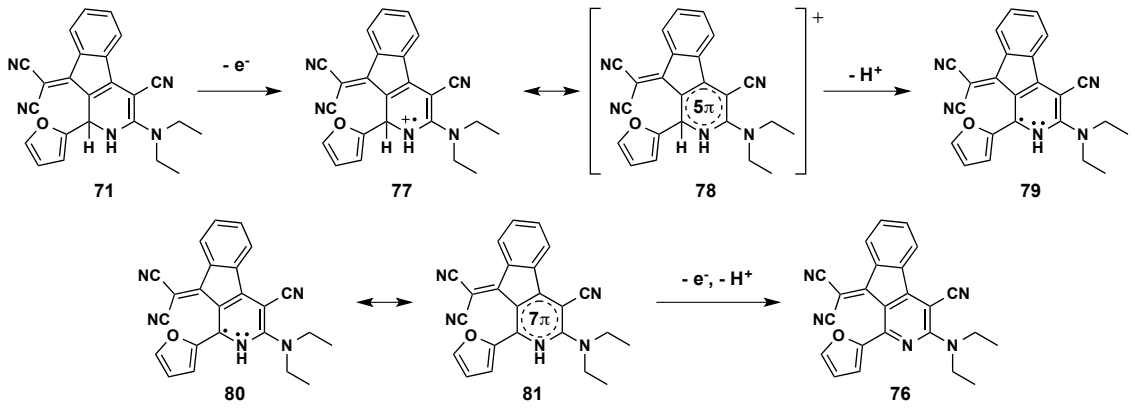

Scheme 4. Proposed mechanism for the oxidation of 1,2-dihydropyridines following the proposed mechanism reported by Srividya *et al*. Note: This is the proposed mechanism for all three compounds, **71** was used as example.

Interestingly, the cathodic scan exhibits one irreversible and one reversible wave for **68**, but two reversible waves upon incorporation of the dicyano moiety on both **71** and **74**. The first reduction waves at -1.47, -1.37 and -1.34 V for **68**, **71** and **74**, respectively, are tentatively assigned to a possible DHP radical anion. Structurally, the compounds are similar to fluorene compounds and can be considered modified fluorenes. We thus assigned the second reversible reduction waves to the reduction of the fluorene-like portion of the molecule (highlighted in Figure 17) since similar reduction potentials have been reported for this system.[59]

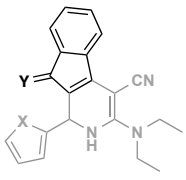

Figure 17. Fluorene-like portion of the compounds under study.

5.4.2.2. Pyridines

In the pyridine series, all compounds exhibit similar electrochemical behavior (Figure 18). No oxidation processes were observed due to the absence of oxidizable groups such as the DHP.

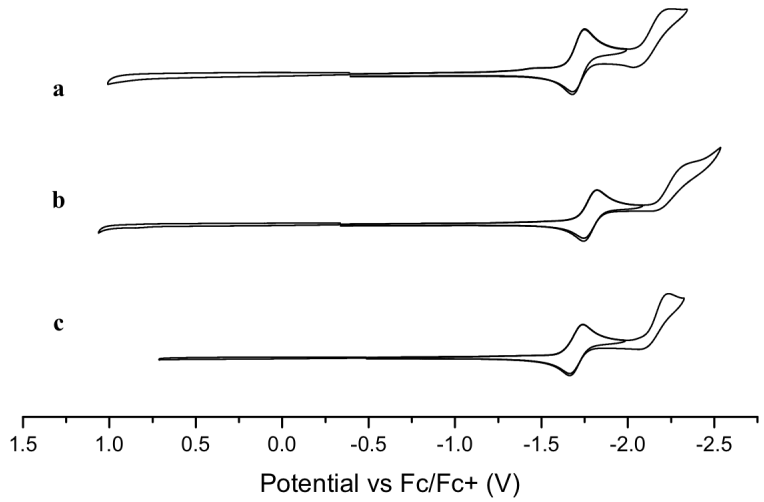

Figure 18. Cyclic voltammograms in 0.1 M $TBAPF_6$/DCM of 0.5 mM **a**) **75**, **b**) **76** and **c**) **77**.

Interestingly, the cathodic processes of **75** are very different than those for **68**. The first reduction wave at -1.72 V is reversible and cathodically shifted 250 mV when compared to that for **68**. Therefore, we assigned the first reduction waves to the reduction of the fluorene-like portion of the molecules (Figure 17) which are in the potential range for similar systems.[59] It is known that pyridines can be reduced in proton-rich media to hydrogenated pyridines, but as the experiments were conducted under neutral conditions we tentatively assigned the second reduction waves to a radical anion localized in the pyridine moiety.[60]

Table 1. Electrochemical potentials (E/V) from cyclic voltammetry experiments vs Fc/Fc^+ and electrochemical HOMO/LUMO levels.

Compound	E_2^{ox} (V)	E_1^{ox} (V)	E_1^{red} (V)	E_2^{red} (V)	E_{onset}^{ox} (V)	HOMO (eV)[b]	E_{onset}^{red} (V)	LUMO (eV)[c]
68	+0.619[a]	+0.222	-1.47[a]	-2.05	-0.039	-4.34	-1.23	-3.15
75	-	-	-1.72	-2.24	-	-	-1.51	-2.87
71	-	+0.537[a]	-1.37	-1.86	+0.292	-4.67	-1.16	-3.22
76	-	-	-1.78	-2.35[a]	-	-	-1.61	-2.77
74	-	+0.576[a]	-1.34	-1.83	+0.331	-4.71	-1.13	-3.25
77	-	-	-1.70	-2.23[a]	-	-	-1.51	-2.87

[a] Peak potentials.
[b] Calculated from $E_{HOMO} = -q(E_{onset}^{ox} + 4.38)$ eV.
[c] Calculated from $E_{LUMO} = -q(E_{onset}^{red} + 4.38)$ eV.

Table 2. Electrochemical potentials (E/V) from square wave voltammetry experiments vs Fc/Fc^+.

Compound	E_2^{ox} (V)	E_1^{ox} (V)	E_1^{red} (V)	E_2^{red} (V)
68	+0.590	+0.194	-1.42	-2.02
75	-	-	-1.71	-2.16
71	-	+0.551	-1.33	-1.83
76	-	-	-1.73	-2.23
74	-	+0.565	-1.32	-1.82
77	-	-	-1.71	-2.17

While we currently have not determined a potential application for these materials we believe that they should continue to be studied, as it is clear the structural variations have a direct impact on their electrochemical properties.

5.5. Closing Remarks

In summary, we have demonstrated that there are still a number of potentially promising avenues of exploration for DASA photo switches. Specifically, we believe that our efforts towards the preparation of γ-alkylidene butenolides from Meldrum's acid derived DASA

trienes has significant potential to impact natural product synthesis. Further, our work on DASA dimers lays the foundation for the development of oligomeric and polymeric materials that can undergo dramatic changes in size and volume. Finally, our investigations on the formation and properties of (dihydro)indenopyridine-carbonitriles, derived from heterocyclic aldehydes activated by either 1,1-dicyanomethylene-3-indanone or 1,3-bis(dicyanomethylene)-indane, provides rapid access to these unique materials. We hope that the work presented here will serve as an inspiration to further the applications of donor-acceptor Stenhouse adducts.

5.6. References

(1) Dake, G. *Tetrahedron* **2006**, *62* (15), 3467.

(2) Veits, G. K.; Wenz, D. R.; Read de Alaniz, J. *Angew. Chem. Int. Ed.* **2010**, *49* (49), 9484.

(3) Palmer, L. I.; Read de Alaniz, J. *Angew. Chem. Int. Ed.* **2011**, *50* (31), 7167.

(4) Palmer, L. I.; de Alaniz, J. R. *Org. Lett.* **2013**, *15* (3), 476.

(5) Palmer, L. I.; Veits, G. K.; Read de Alaniz, J. *Eur. J. Org. Chem.* **2013**, *2013* (28), 6237.

(6) Wenz, D. R.; Read de Alaniz, J. *Org. Lett.* **2013**, *15* (13), 3250.

(7) Fisher, D.; Palmer, L. I.; Cook, J. E.; Davis, J. E.; Read de Alaniz, J. *Tetrahedron* **2014**, *70* (27-28), 4105.

(8) Helmy, S.; Leibfarth, F. A.; Oh, S.; Poelma, J. E.; Hawker, C. J.; Read de Alaniz, J. *J. Am. Chem. Soc.* **2014**, *136* (23), 8169.

(9) Helmy, S.; Oh, S.; Leibfarth, F. A.; Hawker, C. J.; Read de Alaniz, J. *J. Org. Chem.* **2014**, *79* (23), 11316.

(10) Palmer, L.; Read de Alaniz, J. *Synlett* **2013**, *25* (01), 08.

(11) Yu, D.; Thai, V. T.; Palmer, L. I.; Veits, G. K.; Cook, J. E.; Read de Alaniz, J.; Hein, J. E. *J. Org. Chem.* **2013**, *78* (24), 12784.

(12) Woodward, R. B. *J. Am. Chem. Soc.* **1941**, *63* (4), 1123.

(13) Fieser, L. F.; Fieser, M.; Rajagopalan, S. *J. Org. Chem.* **1948**, *13* (6), 800.

(14) Davidson, D.; Bernhard, S. A. *J. Am. Chem. Soc.* **1948**, *70* (10), 3426.

(15) Meldrum, A. N. *J. Chem. Soc. Trans.* **1908**, *93*, 598.

(16) Byun, K.; Mo, Y.; Gao, J. *J. Am. Chem. Soc.* **2001**, *123* (17), 3974.

(17) Arnett, E. M.; Harrelson, J. A. *J. Am. Chem. Soc.* **1987**, *109* (3), 809.

(18) McNab, H. *Chem. Soc. Rev.* **1978**, *7* (3), 345.

(19) Chen, B.-C. *HETEROCYCLES* **1991**, *32* (3), 529.

(20) Gerencsér, J.; Dormán, G.; Darvas, F. *QSAR Comb. Sci.* **2006**, *25* (5-6), 439.

(21) Gaber, A. E.-A. M.; McNab, H. *Synthesis* **2001**, *2001* (14), 2059.

(22) Ivanov, A. S. *Chem. Soc. Rev.* **2008**, *37* (4), 789.

(23) Dumas, A. M.; Fillion, E. *Acc. Chem. Res.* **2010**, *43* (3), 440.

(24) Leibfarth, F. A.; Kang, M.; Ham, M.; Kim, J.; Campos, L. M.; Gupta, N.; Moon, B.; Hawker, C. J. *Nat. Chem.* **2010**, *2* (3), 207.

(25) Spruell, J. M.; Wolffs, M.; Leibfarth, F. A.; Stahl, B. C.; Heo, J.; Connal, L. A.; Hu, J.; Hawker, C. J. *J. Am. Chem. Soc.* **2011**, *133* (41), 16698.

(26) Leibfarth, F. A.; Schneider, Y.; Lynd, N. A.; Schultz, A.; Moon, B.; Kramer, E. J.; Bazan, G. C.; Hawker, C. J. *J. Am. Chem. Soc.* **2010**, *132* (42), 14706.

(27) Miyamura, Y.; Park, C.; Kinbara, K.; Leibfarth, F. A.; Hawker, C. J.; Aida, T. *J. Am. Chem. Soc.* **2011**, *133* (9), 2840.

(28) Leibfarth, F. A.; Wolffs, M.; Campos, L. M.; Delany, K.; Treat, N.; Kade, M. J.; Moon, B.; Hawker, C. J. *Chem Sci* **2012**, *3* (3), 766.

(29) Steinhardt, S. E.; Silverston, J. S.; Vanderwal, C. D. *J. Am. Chem. Soc.* **2008**, *130* (24), 7560.

(30) Steinhardt, S. E.; Vanderwal, C. D. *J. Am. Chem. Soc.* **2009**, *131* (22), 7546.

(31) Tasi, M.; Horvath, I. T.; Andreeti, G. D.; Palyi, G. *J. Chem. Soc. Chem. Commun.* **1989**, No. 7, 426.

(32) Rousset, S.; Thibonnet, J.; Abarbri, M.; Duchêne, A.; Parrain, J.-L. *Synlett* **2000**, *2000* (2), 260.

(33) Fiandanese, V.; Bottalico, D.; Marchese, G. *Tetrahedron* **2001**, *57* (51), 10213.

(34) Sorg, A.; Siegel, K.; Brückner, R. *Synlett* **2004**, No. 2, 0321.

(35) Michels, T. D.; Rhee, J. U.; Vanderwal, C. D. *Org. Lett.* **2008**, *10* (21), 4787.

(36) Archut, A.; Azzellini, G. C.; Balzani, V.; De Cola, L.; Vögtle, F. *J. Am. Chem. Soc.* **1998**, *120* (47), 12187.

(37) Nguyen, T.-T.-T.; Türp, D.; Wang, D.; Nölscher, B.; Laquai, F.; Müllen, K. *J. Am. Chem. Soc.* **2011**, *133* (29), 11194.

(38) Morimoto, M.; Irie, M. *J. Am. Chem. Soc.* **2010**, *132* (40), 14172.

(39) Hosono, N.; Kajitani, T.; Fukushima, T.; Ito, K.; Sasaki, S.; Takata, M.; Aida, T. *Science* **2010**, *330* (6005), 808.

(40) Harris, K. D.; Cuypers, R.; Scheibe, P.; van Oosten, C. L.; Bastiaansen, C. W. M.; Lub, J.; Broer, D. J. *J. Mater. Chem.* **2005**, *15* (47), 5043.

(41) Yu, Y.; Nakano, M.; Ikeda, T. *Nature* **2003**, *425* (6954), 145.

(42) Hugel, T. *Science* **2002**, *296* (5570), 1103.

(43) Bléger, D.; Yu, Z.; Hecht, S. *Chem. Commun.* **2011**, *47* (45), 12260.

(44) Jiang, D.-L.; Aida, T. *Nature* **1997**, *388* (6641), 454.

(45) Junge, D. M.; McGrath, D. V. *Chem. Commun.* **1997**, No. 9, 857.

(46) Junge, D. M.; McGrath, D. V. *J. Am. Chem. Soc.* **1999**, *121* (20), 4912.

(47) Li, S.; McGrath, D. V. *J. Am. Chem. Soc.* **2000**, *122* (28), 6795.

(48) Liao, L.-X.; Stellacci, F.; McGrath, D. V. *J. Am. Chem. Soc.* **2004**, *126* (7), 2181.

(49) Grebel-Koehler, D.; Liu, D.; De Feyter, S.; Enkelmann, V.; Weil, T.; Engels, C.; Samyn, C.; Müllen, K.; De Schryver, F. C. *Macromolecules* **2003**, *36* (3), 578.

(50) Bléger, D.; Liebig, T.; Thiermann, R.; Maskos, M.; Rabe, J. P.; Hecht, S. *Angew. Chem. Int. Ed.* **2011**, *50* (52), 12559.

(51) Coffin, R. C.; Peet, J.; Rogers, J.; Bazan, G. C. *Nat. Chem.* **2009**, *1* (8), 657.

(52) Mei, J.; Kim, D. H.; Ayzner, A. L.; Toney, M. F.; Bao, Z. *J. Am. Chem. Soc.* **2011**, *133* (50), 20130.

(53) Mei, J.; Bao, Z. *Chem. Mater.* **2014**, *26* (1), 604.

(54) Cheng, Y.-J.; Yang, S.-H.; Hsu, C.-S. *Chem. Rev.* **2009**, *109* (11), 5868.

(55) Landmesser, T.; Linden, A.; Hansen, H.-J. *Helv. Chim. Acta* **2008**, *91* (2), 265.

(56) LudvíK, J.; Tureček, F.; Volke, J. *J. Electroanal. Chem. Interfacial Electrochem.* **1985**, *188* (1-2), 105.

(57) Ludvik, J.; Volke, J.; Klima, J. *Electrochimica Acta* **1987**, *32* (7), 1063.

(58) Srividya, N.; Ramamurthy, P.; Shanmugasundaram, P.; Ramakrishnan, V. T. *J. Org. Chem.* **1996**, *61* (15), 5083.

(59) Cao, Y.; Zhang, S.-C.; Zhang, M.; Shen, G.-B.; Zhu, X.-Q. *J. Org. Chem.* **2013**, *78* (14), 7154.

(60) Cisak, A.; Elving, P. J. *Electrochimica Acta* **1965**, *10* (9), 935.

6. Experimental Procedures and Analytical Data

6.1. Chapter 2

General Methods:

All commercially obtained solvents and reagents were used without further purification. Analytical thin-layer chromatography (TLC) was carried out on Merck silica gel 60 F_{254} glass plates and flash column chromatography was performed on Merck silica gel 60 (70 – 230 mesh) or on a Biotage SP1 Flash Purification System using FLASH 40+M cartridges and FLASH 40+ sample cartridges. Dry column vacuum chromatography was performed on Merck silica gel 60 (15 – 40 mesh). ^{1}H and ^{13}C solution-state NMR were recorded on a Varian VNMRS 600 (600 MHz for ^{1}H and 150 MHz for ^{13}C) spectrometer or Varian Inova-500 (500 MHz for ^{1}H, and 125 MHz for ^{13}C). Chemical shifts are reported relative to residual solvent peaks (δ 7.26 for $CDCl_3$ in ^{1}H NMR and δ 77.2 for $CDCl_3$ in ^{13}C NMR). IR spectra were recorded on a Perkin Elmer Spectrum 2 FT/IR or a Perkin Elmer Spectrum 100 employing a Universal ATR Sampling Accessory and are reported in terms of frequency of absorption (cm^{-1}). X-Ray analysis was obtained from the UC Santa Barbara X-Ray Facilities. Mass spectral data were collected on a Micromass QTOF2 Quadrupole/Time-of Flight Tandem mass spectrometer (ESI-MS). UV-vis spectral and kinetic data were collected on a Shimadzu UV-3600 UV-Vis-NIR Spectrophotometer with a quartz spectrasil UV-vis cuvette (1 x 1 x 4 cm) using direct detection at a slit width of 2 nm. Fluorescence measurements were obtained using a Cary Eclipse spectrophotometer (Varian, Inc.) with a quartz fluorescence cuvette (1 x 1 x 0.2 cm) with the following settings: excitation wavelength of 550 nm, excitation slit width = 5 nm, emission slit width = 10 nm, range = 560 nm to 700 nm and scan speed = 30 nm/min.

Synthetic Methods

5-(furan-2-ylmethylene)-2,2-dimethyl-1,3-dioxane-4,6-dione (19):

2,2-dimethyl-1,3-dioxane-4,6-dione (1.51 g, 10.5 mmol) and 2-furaldehyde (961 mg, 10 mmol) were added sequentially to 30 mL H_2O. The heterogeneous mixture was heated to 75 ^oC and stirred at that temperature for 2 h. During the course of the reaction a yellow precipitate formed. At the completion of the reaction (as monitored by TLC, 3:1 hexane:ethyl acetate) the mixture was cooled to room temperature. The precipitated solid was collected by vacuum filtration and washed twice with 30 mL cold H_2O. The collected solid was dissolved in dichloromethane, washed sequentially with 30 mL saturated aqueous $NaHSO_3$, 30 mL H_2O, 30 mL saturated aqueous $NaHCO_3$, and 30 mL brine. The organic layer was dried over $MgSO_4$, filtered and the solvent removed by rotary evaporation to give 2.19 g (99%) of 5-(furan-2-ylmethylene)-2,2-dimethyl-1,3-dioxane-4,6-dione (a known compound) as a bright yellow powder. All spectroscopic data match reported values.[1]

5-(furan-2-ylmethylene)-1,3-dimethylpyrimidine-2,4,6(1*H*,3*H*,5*H*)-trione (35):

1,3-dimethylpyrimidine-2,4,6(1*H*,3*H*,5*H*)-trione (1.56 g, 10 mmol) and 2-furaldehyde (961 mg, 10 mmol) were added sequentially to 40 mL H_2O. The heterogeneous mixture was stirred at room temperature for 2 h. During the course of the reaction a yellow precipitate formed. At the completion of the reaction (as monitored by TLC, 3:1 hexane:ethyl acetate) the precipitated solid was collected by vacuum filtration and washed twice with 30 mL cold H_2O. The collected solid was dissolved in dichloromethane (75 mL), washed sequentially with 30 mL saturated aqueous $NaHSO_3$, 30 mL H_2O, 30 mL saturated aqueous $NaHCO_3$, and 30 mL brine. The organic layer was dried over $MgSO_4$, filtered and the solvent removed by rotary evaporation to give 2.26 g (96%) of 5-(furan-2-ylmethylene)-1,3-

dimethylpyrimidine-2,4,6(1*H*,3*H*,5*H*)-trione (a known compound) as a bright yellow powder. All spectroscopic data match reported values.[2]

5-((2Z,4E)-5-(diethylamino)-2-hydroxypenta-2,4-dien-1-ylidene)-2,2-dimethyl-1,3-dioxane-4,6-dione (38): 5-(furan-2-ylmethylene)-2,2-dimethyl-1,3-dioxane-4,6-dione (1 gram, 4.5 mmol, 1 eq) was dissolved in 10 ml tetrahydrofuran. To this solution was added diethylamine (466 μL, 329 mg, 4.5 mmol, 1 eq). The mixture was stirred at 23 ^{o}C for 10 min followed by cooling at 0 ^{o}C for 20 min. The reaction mixture was then filtered to collect the precipitated solid, the solid was washed with cold diethyl ether, and dried *in vacuo* to afford Stenhouse adduct **38** (1.13g, 85%) as a red solid. ^{1}H NMR (600 MHz, cd_2cl_2) δ 11.37 – 11.34 (m, 1H), 7.33 (d, *J* = 12.2 Hz, 1H), 6.96 (s, 1H), 6.80 (dd, *J* = 12.5, 1.3 Hz, 1H), 6.08 (t, *J* = 12.4 Hz, 1H), 3.54 – 3.45 (m, 4H), 1.68 (s, 6H), 1.31 (dt, *J* = 18.1, 7.3 Hz, 6H). ^{13}C NMR (151 MHz, cd_2cl_2) δ 167.0, 164.6, 157.6, 151.4, 144.5, 137.8, 103.0, 102.2, 89.8, 52.0, 44.2, 26.4, 14.1, 12.1. IR (KBR) 3071, 2996, 2938, 1681, 1634, 1603, 1573, 1510, 1463, 1414, 1369, 1340, 1264, 1235, 1196, 1172, 1139, 1128, 1096, 1083, 1059, 1015 cm^{-1}. HRMS (ESI+) *m/z* 318.1313 (318.1317 calc'd for $C_{15}H_{21}NO_5Na^+$ $[M + Na]^+$). Crystal structure data for **5-((2Z,4E)-5-(diethylamino)-2-hydroxypenta-2,4-dien-1-ylidene)-2,2-dimethyl-1,3-dioxane-4,6-dione** can be obtained free of charge from the Cambridge Crystallographic Data Centre via www.ccdc.cam.ac.uk/data_request/cif CCDC# 865315

5-((2*Z*,4*E*)-5-(diethylamino)-2-hydroxypenta-2,4-dien-1-ylidene)-1,3-dimethylpyrimidine-2,4,6-(1*H*,3*H*,5*H*)-trione (36): 5-(furan-2-ylmethylene)-1,3-dimethylpyrimidine-2,4,6(1*H*,3*H*,5*H*)-trione (234 mg, 1 mmol) was suspended in 10 ml tetrahydrofuran. To this suspension was added diethylamine (104 μL, 1 mmol). The mixture

was stirred at 23 ^{o}C for 10 min followed by cooling at 0 ^{o}C for 20 min. The reaction mixture was then filtered to collect the precipitated solid, the solid was washed with cold diethyl ether, and dried *in vacuo* to afford Stenhouse adduct **36** (283 mg, 92%) as a purple solid. ^{1}H NMR (Methylene Chloride-d2) δ: 12.50 (s, 1H), 7.30 (d, J = 12.2 Hz, 1H), 7.06 (s, 1H), 6.82 (dd, J = 12.3, 1.5 Hz, 1H), 6.10 (t, J = 12.3 Hz, 1H), 3.50 (dq, J = 25.4, 7.2 Hz, 4H), 3.29 (s, 3H), 3.27 (s, 3H), 1.31 (dt, J = 13.0, 7.2 Hz, 6H). ^{13}C NMR (151 MHz, cd2cl2) δ 165.7, 163.6, 157.8, 151.8, 146.7, 138.2, 103.3, 98.1, 52.6, 44.8, 28.6, 28.5, 14.8, 12.7. IR (KBr) 3365, 2944, 2486, 1685, 1618, 1592, 1566, 1509, 1460, 1418, 1373, 1328, 1309, 1286, 1270. HRMS (ESI+) *m/z* 330.1433 (330.1430 calc'd for $C_{15}H_{21}N_3O_4Na^+$ $[M+Na]^+$).

5-(2-(diethylammonio)-5-oxocyclopent-3-en-1-yl)-2,2-dimethyl-4-oxo-4H-1,3-dioxin-6-olate (39): Stenhouse adduct **38** (148 mg, 0.5 mmol) was suspended in 10 mL methanol. The reaction mixture was irradiated with a GE Crystal Clear 200 bulb (200 watt, 3780 lumens) placed approximately 10 inches from the reaction vessel at ambient temperature with stirring for 12 h. The reaction mixture was cooled to 0 ^{o}C for 20 min, then filtered to collect the precipitated solid; the solid was washed with cold diethyl ether, and dried *in vacuo* to afford **39** (140 mg, 95%) as a white solid. ^{1}H NMR (600 MHz, d_2o) δ 7.68 (dd, *J* = 6.1, 1.9 Hz, 1H), 6.55 (dt, *J* = 6.1, 1.4 Hz, 1H), 4.72 – 4.69 (m, 1H), 3.49 (d, *J* = 3.6 Hz, 1H), 3.24 (b, *J* = 72.0 Hz, 4H), 1.54 (s, 6H), 1.22 (t, *J* = 7.3 Hz, 6H). ^{13}C NMR (151 MHz, d_2o) δ 208.2, 155.1, 138.0, 103.7, 72.6, 66.6, 44.1, 24.5, 9.3. IR (KBr) 3409, 3071, 2992, 2956, 2916, 2589, 2439, 1714, 1673, 1572, 1513, 1487, 1475, 1460, 1416, 1376, 1339, 1287, 1261, 1233, 1215, 1198, 1182, 1161, 1148, 1121, 1047, 1030 cm^{-1}. HRMS (ESI) *m/z* 318.1313 (318.1317 calc'd for $C_{15}H_{21}NO_5Na^+$ $[M + Na]^+$). Crystal structure data for **5-(2-(diethylammonio)-5-oxocyclopent-3-en-1-yl)-2,2-dimethyl-4-oxo-4H-1,3-dioxin-6-olate**

can be obtained free of charge from the Cambridge Crystallographic Data Centre via www.ccdc.cam.ac.uk/data_request/cif CCDC# 977459

5-(2-(diethylammonio)-5-oxocyclopent-3-en-1-yl)-1,3-dimethyl-2,6-dioxo-1,2,3,6-tetrahydropyrimidin-4-olate (37): Stenhouse adduct **36** (154 mg, 0.5 mmol) was suspended in 10 mL methanol. The reaction mixture was irradiated with a GE Crystal Clear 200 bulb (200 watt, 3780 lumens) placed approximately 10 inches from the reaction vessel at ambient temperature with stirring for 12 h. The reaction mixture was cooled to 0 ^{o}C for 20 min, then filtered to collect the precipitated solid; the solid was washed with cold diethyl ether, and dried *in vacuo* to afford **37** (142 mg, 92%) as a white solid. ^{1}H NMR (600 MHz, Deuterium Oxide) δ 7.84 (dd, *J* = 6.1, 1.9 Hz, 1H), 6.71 (ddd, *J* = 6.1, 1.9, 0.8 Hz, 1H), 4.83 (d, *J* = 1.8 Hz, 1H), 3.88 (d, *J* = 3.6 Hz, 1H), 3.39 (dq, *J* = 14.6, 7.4 Hz, 2H), 3.36 – 3.21 (m, 6H), 3.18 (s, 2H), 1.30 (t, *J* = 7.3 Hz, 6H). ^{13}C NMR (151 MHz, d_2o) δ 208.5, 164.6, 163.7, 154.0, 138.0, 85.6, 66.5, 66.5, 46.4, 44.4, 44.4, 28.0, 27.2, 9.2. IR (KBr) 3052, 2986, 2972, 2919, 2742, 2660, 2502, 1727, 1674, 1667, 1614, 1599, 1578, 1517, 1477, 1435, 1397. HRMS (ESI+) *m/z* 330.1433 (330.1430 calc'd for $C_{15}H_{21}N_3O_4Na^+$ $[M+Na]^+$).

Representative NMR Spectra:

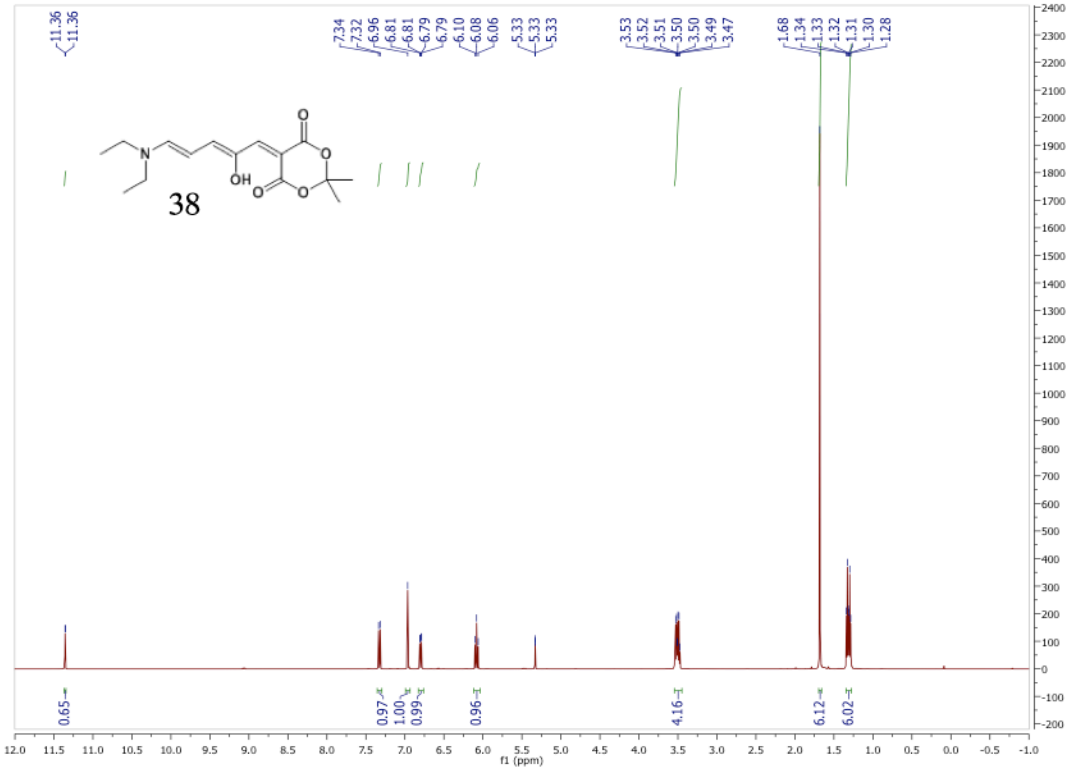

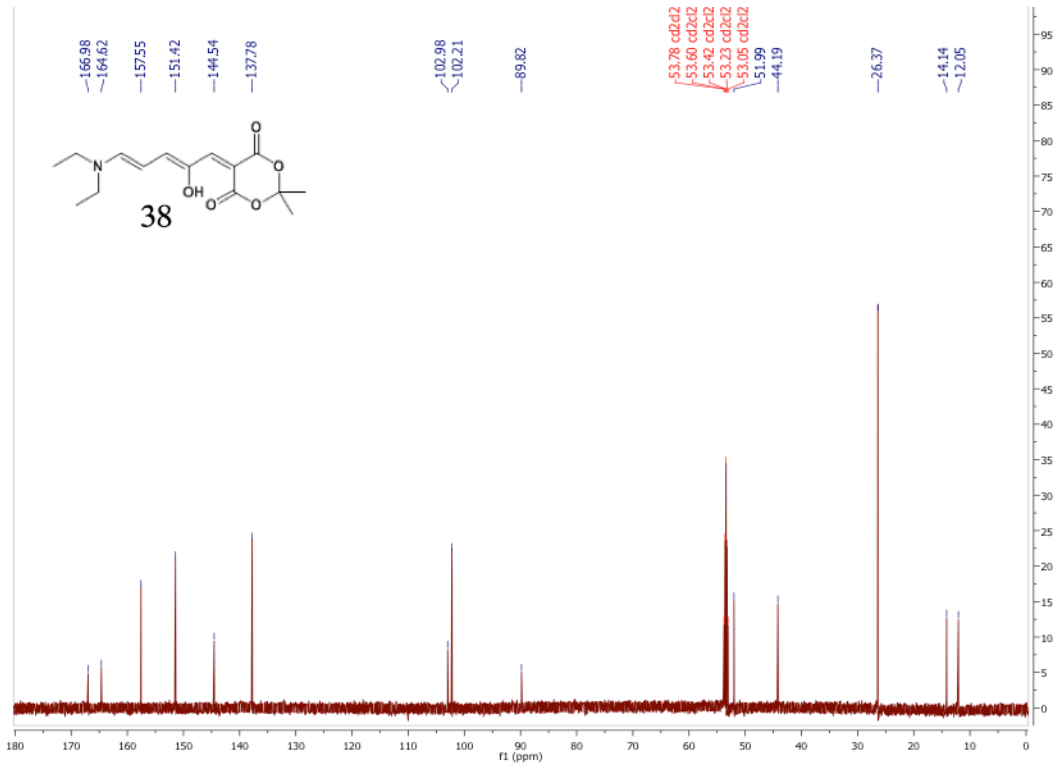

^{1}H NMR (Methylene Chloride-d2) δ: 12.50 (s, 1H), 7.30 (d, J = 12.2 Hz, 1H), 7.06 (s, 1H), 6.82 (dd, J = 12.3, 1.5 Hz, 1H), 6.10 (t, J = 12.3 Hz, 1H), 3.50 (dq, J = 25.4, 7.2 Hz, 4H), 3.29 (s, 3H), 3.27 (s, 3H), 1.31 (dt, J = 13.0, 7.2 Hz, 6H)

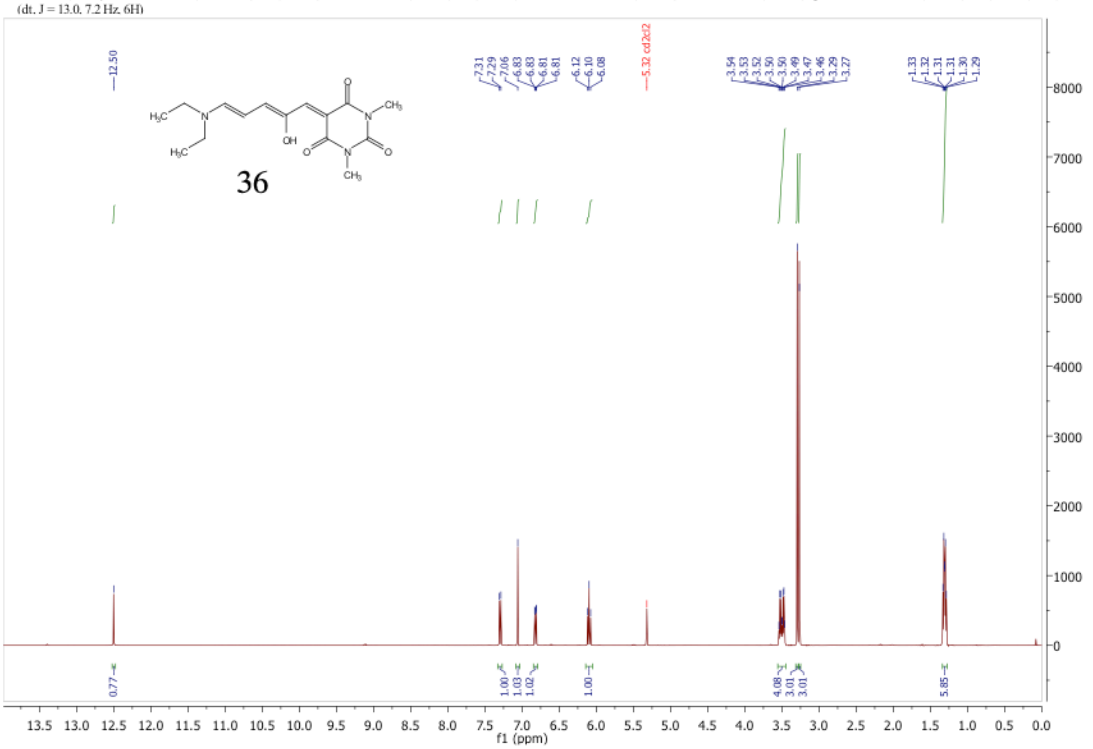

^{13}C NMR (151 MHz, cd_2cl_2) δ 165.65, 163.55, 157.75, 151.84, 146.73, 138.20, 103.31, 98.15, 52.55, 44.78, 28.60, 28.49, 14.76, 12.68.

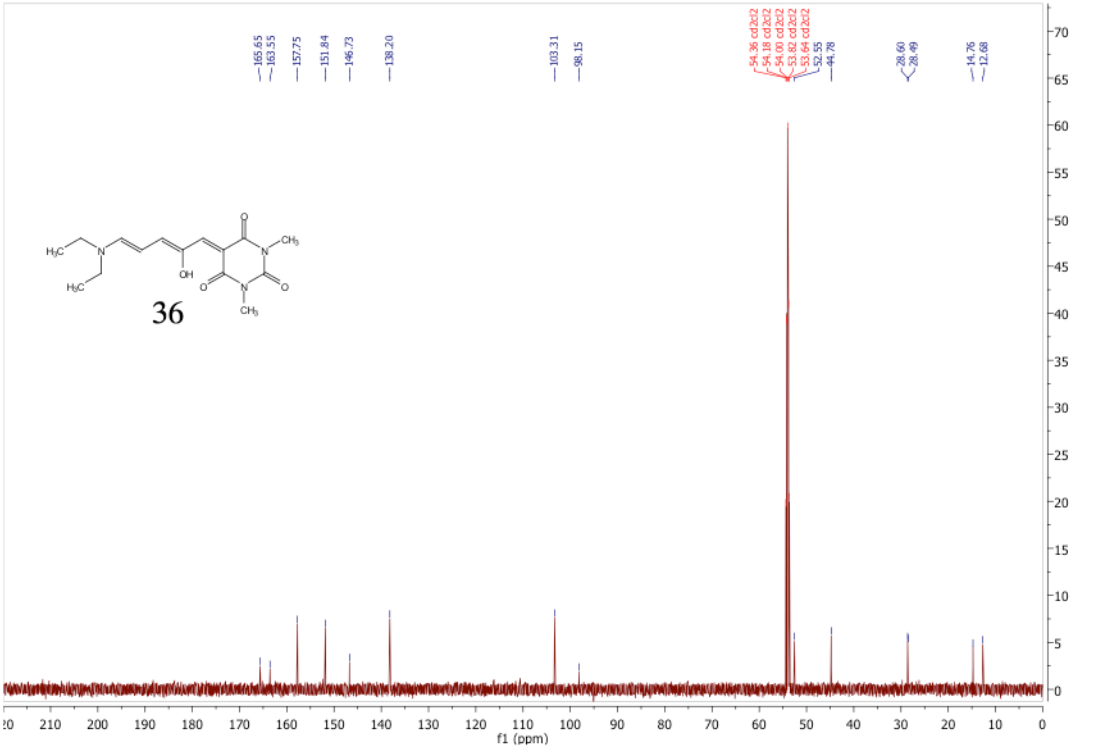

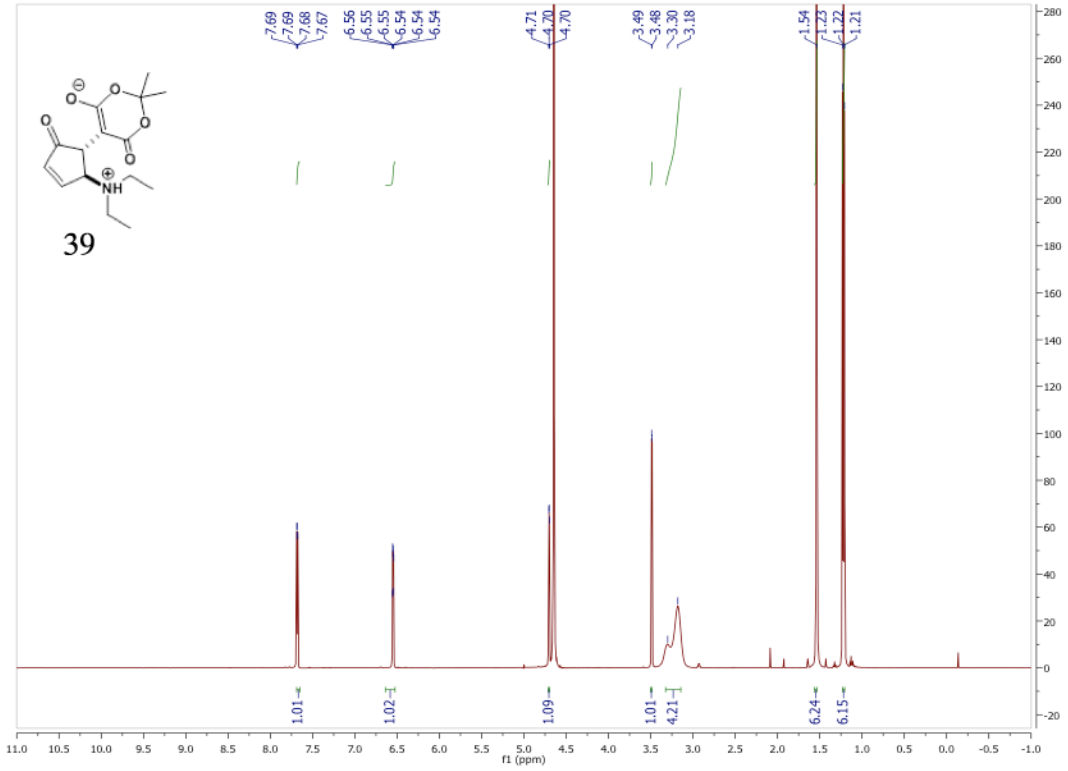
7.69
7.69
7.68
7.67
6.56
6.55
6.55
6.54
6.54
6.54
4.71
4.70
4.70
3.49
3.48
3.30
3.18
1.54
1.23
1.22
1.21
1.01
1.02
1.09
1.01
4.21
6.24
6.15
f1 (ppm)

39

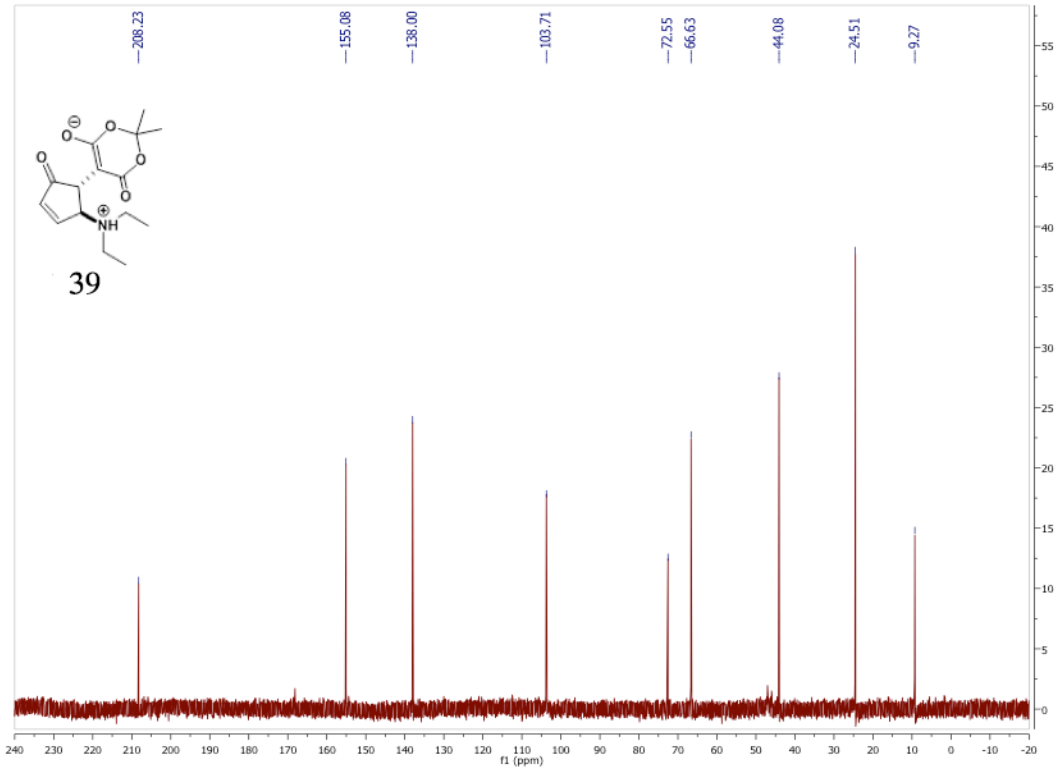
208.23
155.08
138.00
103.71
72.55
66.63
44.08
24.51
9.27
f1 (ppm)

39

^{1}H NMR (600 MHz, Deuterium Oxide) δ 7.84 (dd, J = 6.1, 1.9 Hz, 1H), 6.71 (ddd, J = 6.1, 1.9, 0.8 Hz, 1H), 4.83 (d, J = 1.8 Hz, 1H), 3.88 (d, J = 3.6 Hz, 1H), 3.39 (dq, J = 14.6, 7.4 Hz, 2H), 3.36 – 3.21 (m, 6H), 3.18 (s, 2H), 1.30 (t, J = 7.3 Hz, 6H).

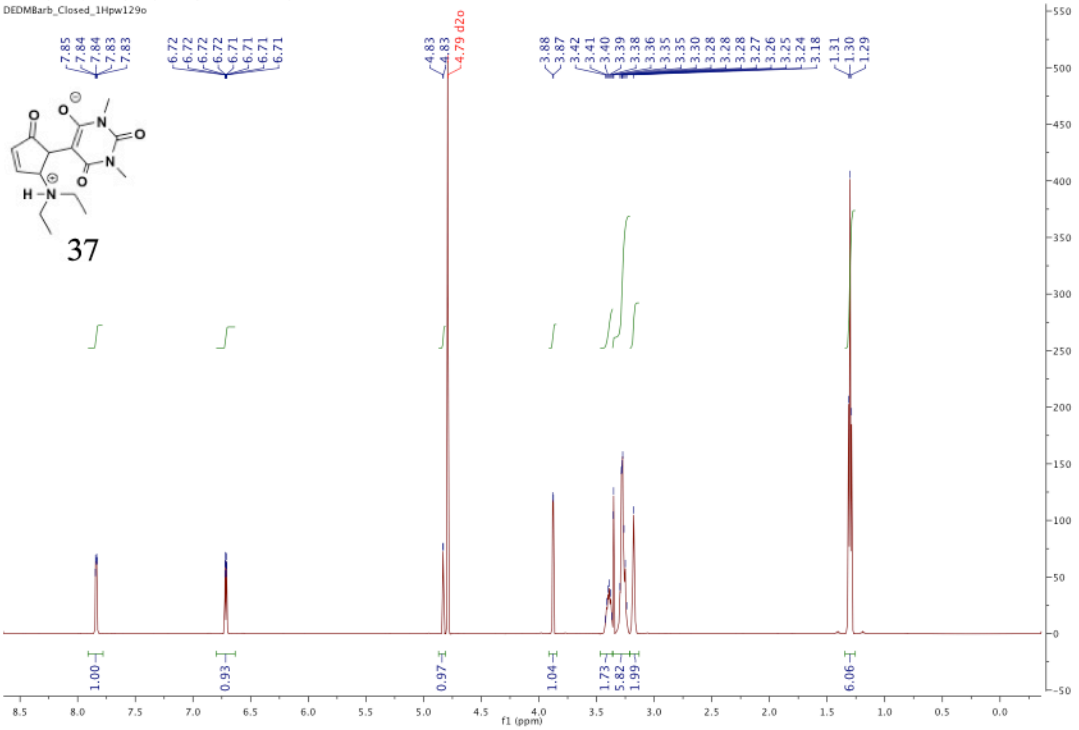

37

^{13}C NMR (151 MHz, d-ω) δ 208.51, 164.59, 163.74, 154.01, 137.95, 85.61, 66.54, 66.51, 46.41, 44.40, 44.38, 28.00, 27.24, 9.19.

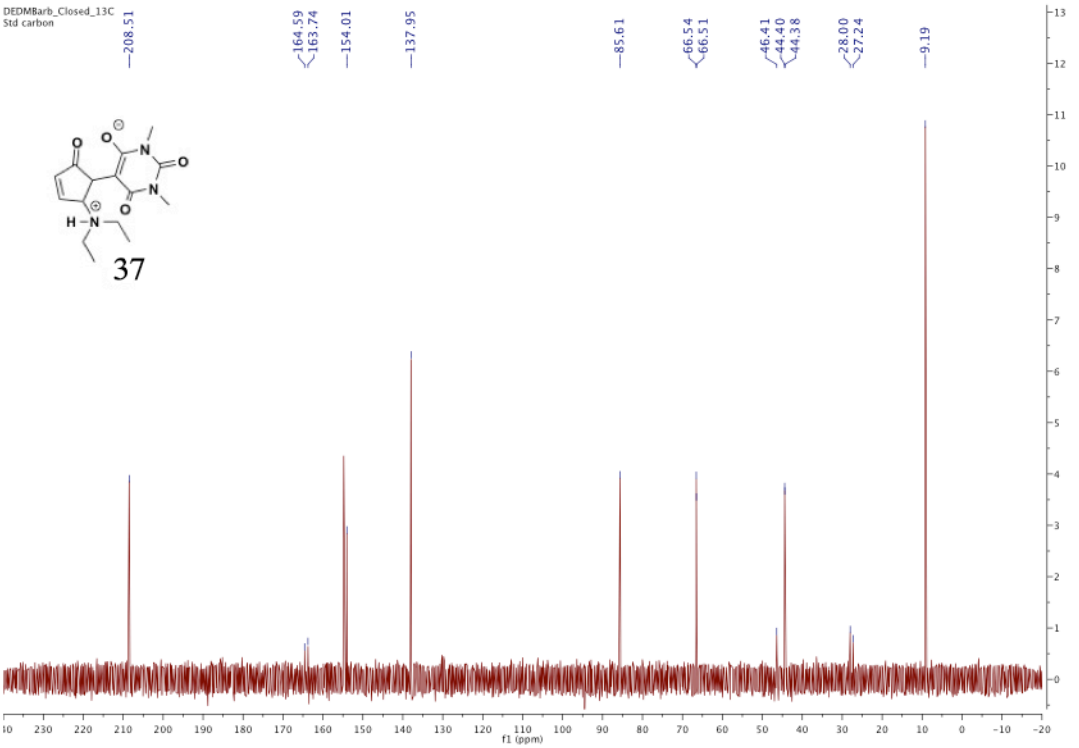

37

Uv-vis Spectral Data:

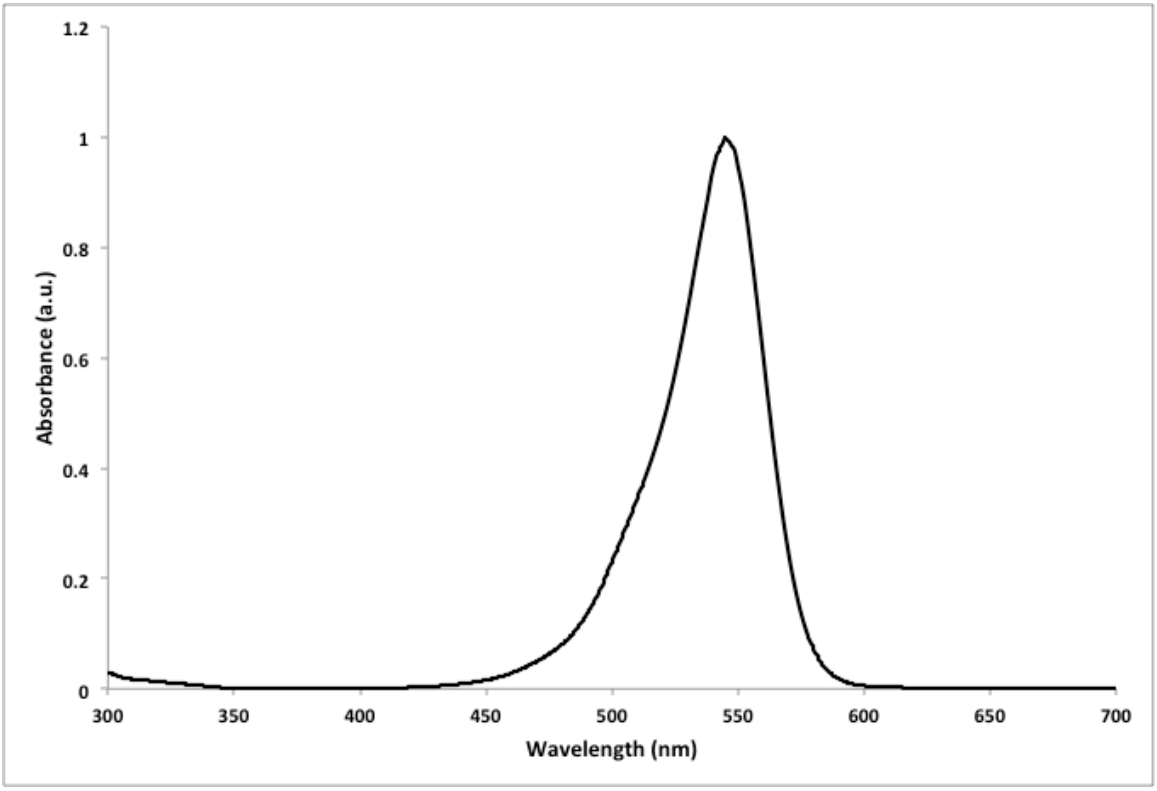

Figure S1: Normalized of UV/vis absorption spectrum of **38** in toluene**,** λ_{max} = 545 nm.

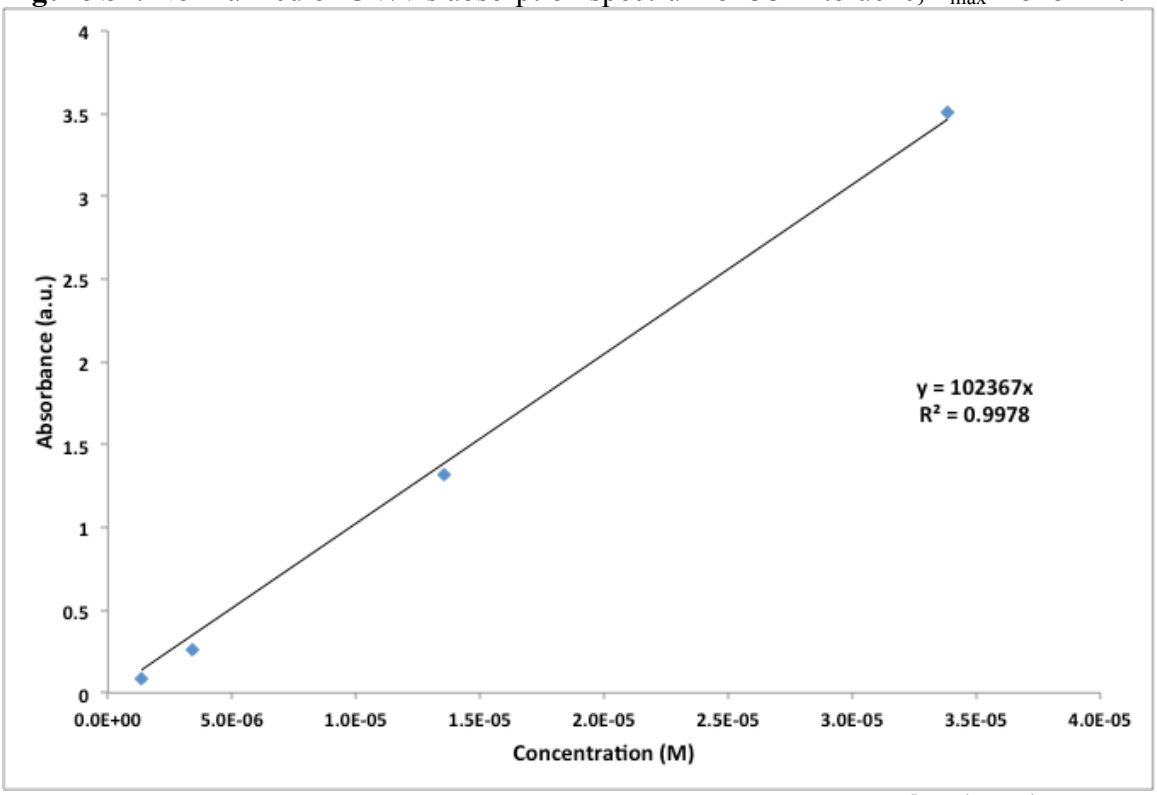

Figure S2: UV/vis concentration vs. absorbance curve for **38**, ε= $1x10^5$ M^{-1} cm^{-1}.

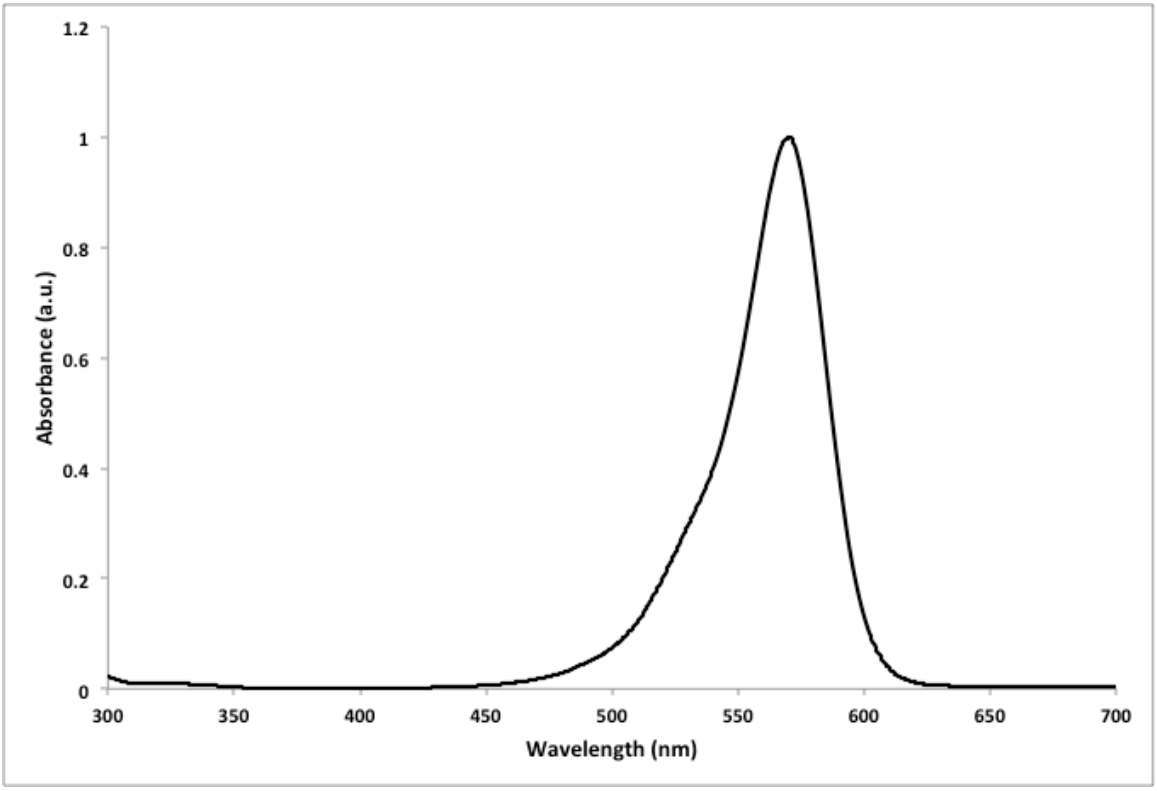

Figure S3: Normalized of UV/vis absorption spectrum of **36** in toluene, λ_{max} = 570 nm.

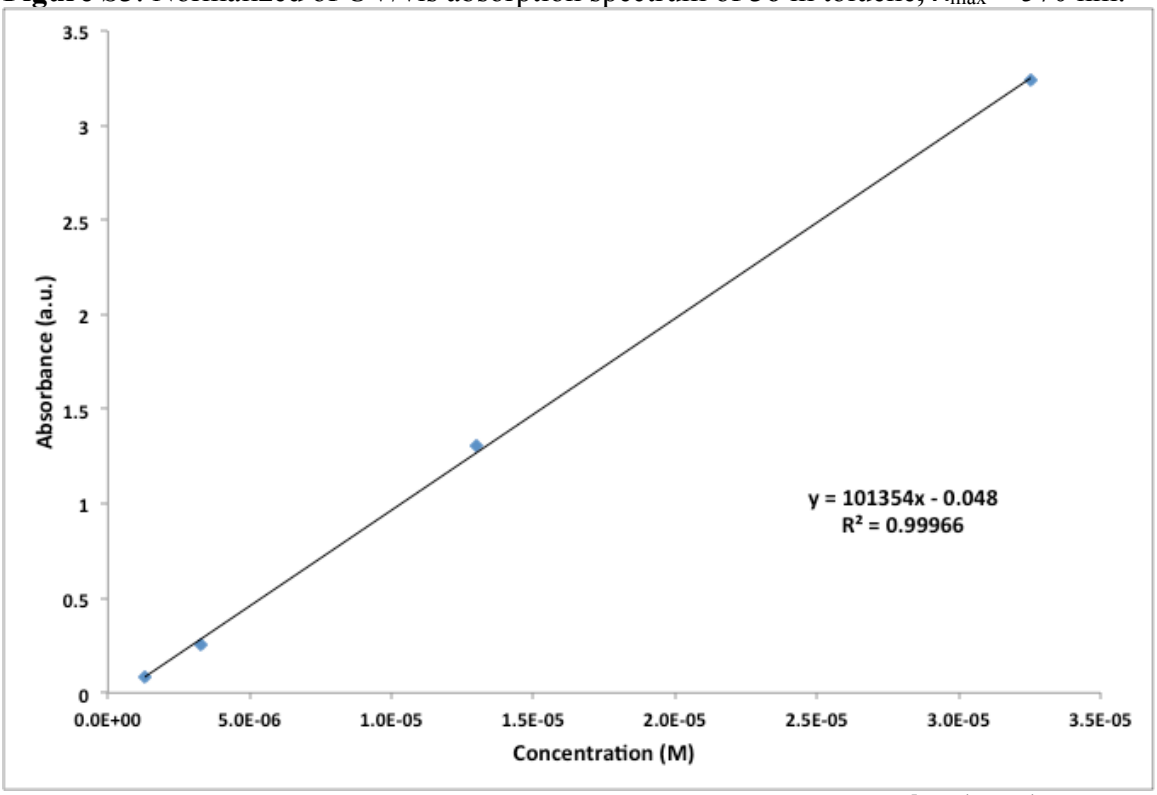

Figure S4: UV/vis concentration vs. absorbance curve for **36**, $\varepsilon = 1 \times 10^5\ M^{-1}\ cm^{-1}$.

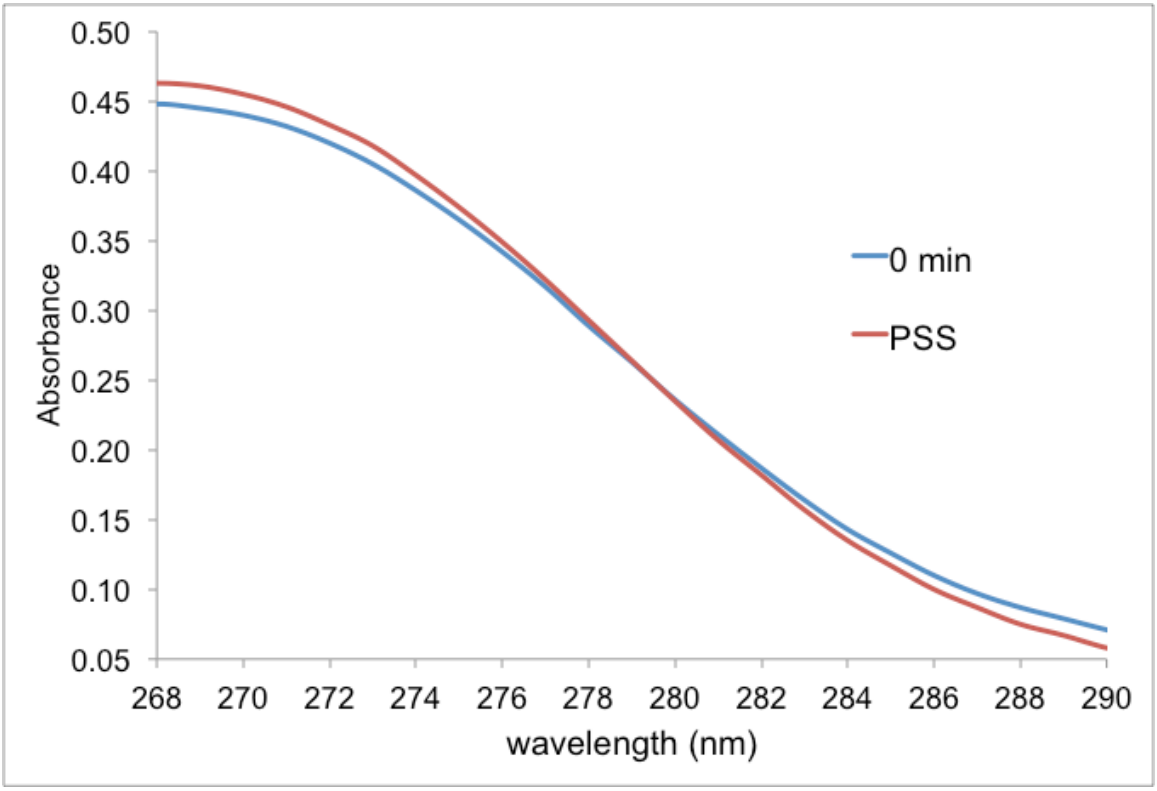

Figure S5: Determination of Isosbestic Point for **38** in methanol, which occurs at 280 nm.

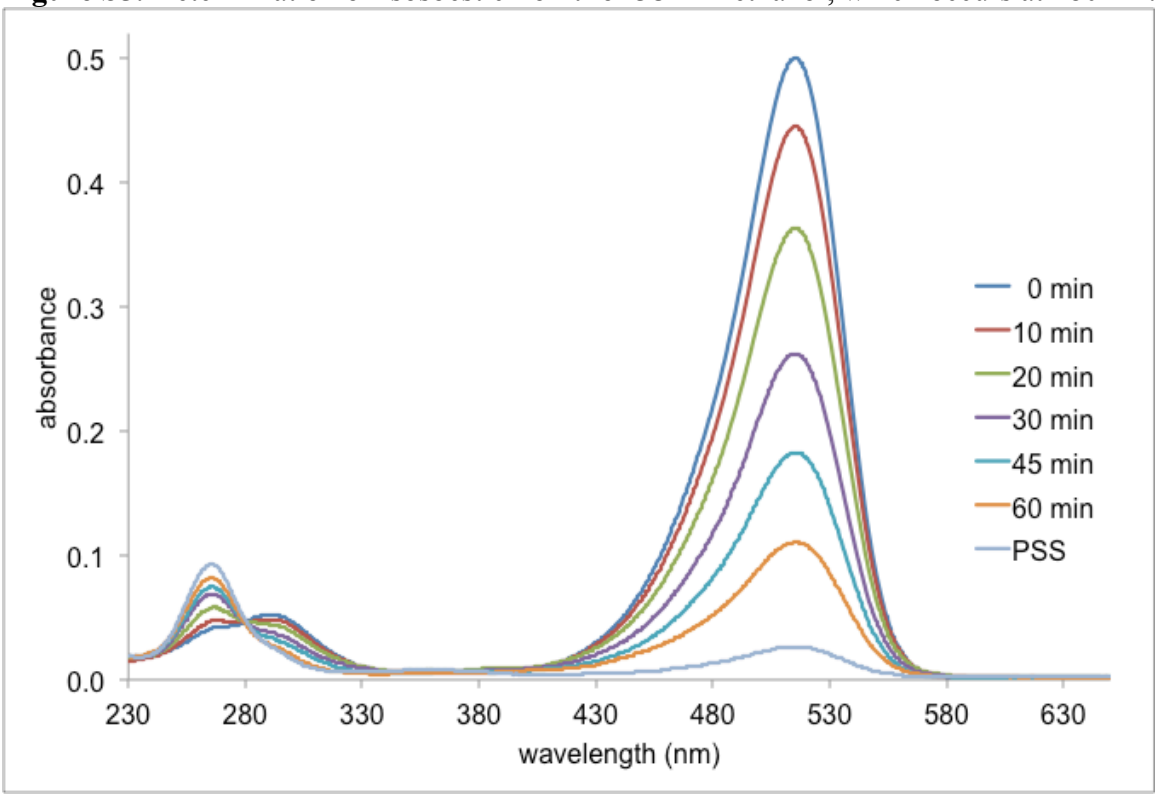

Figure S6: Absorption spectra of the photoisomerization **38** to **39** on irradiation with unfiltered, high intensity visible light in methanol, λ_{max} = 515 nm. Isosbestic point occurs at 280 nm.

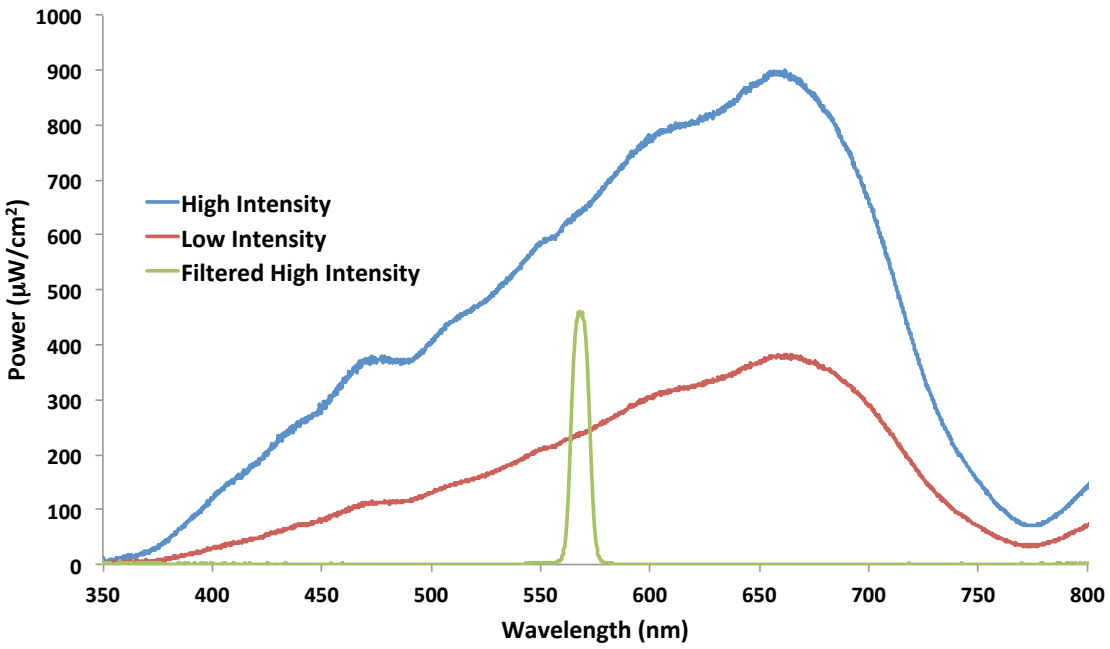

Figure S7: Comparison of light source intensities.

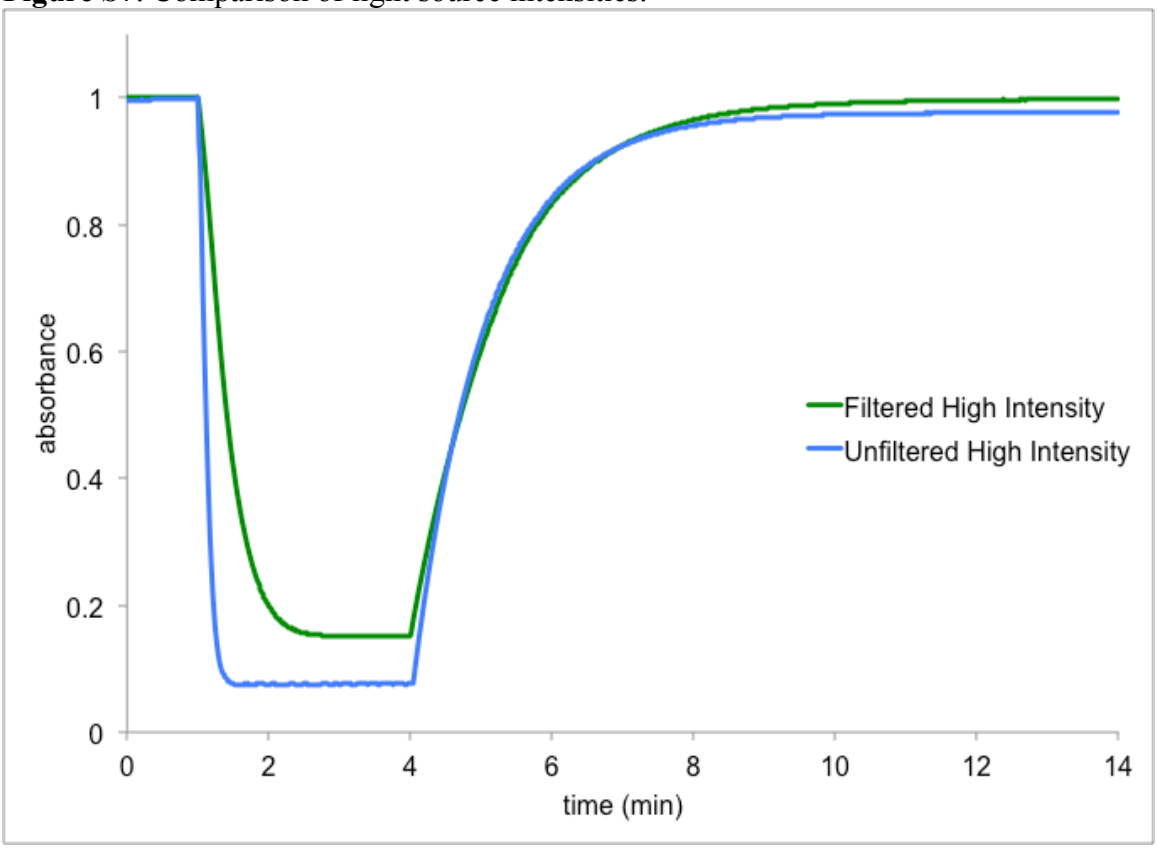

Figure S8: Effect of light source intensity on photoswitching rates of **36** in toluene.

6.2. Chapter 3

General Methods Unless stated otherwise, reactions were conducted in flame dried glass-ware under an atmosphere of air using reagent grade solvents. All commercially obtained reagents were used as received. Reaction temperatures were controlled using automated temperature modulator, and unless stated otherwise, reactions were performed at room temperature (rt, approximately 23 ºC). Thin-layer chromatography (TLC) was conducted with E. Merck silica gel 60 F254 pre-coated plates (0.25 mm) and visualized by exposure to UV light (254 nm) or stained with anisaldehyde or potassium permanganate. Flash column chromatography was performed using normal phase silica gel (60 Å, 230-240 mesh, Merck KGA). ^{1}H NMR spectra were recorded at 500 or 600 MHz and are reported relative to deuterated solvent signals. Data for ^{1}H NMR spectra are reported as follows: chemical shift (δ ppm), multiplicity, coupling constant (Hz) and integration. ^{13}C NMR spectra were recorded at 125 or 150 MHz. Data for ^{13}C NMR spectra are reported as follows: shift (δ ppm). High-resolution mass spectra (HRMS) were obtained using a TOF mass spectrometer, whereas infrared (IR) spectra were obtained using a Fourier transform infrared spectrometer.

General Procedure A: preparation of Stenhouse adducts: The activated furan (1.0 equiv.) is added to tetrahydrofuran (0.4 M). To this solution at 23 ºC is added 1.0 equiv. of secondary amine. The reaction mixture is stirred at 23 ^{o}C for 10 minutes followed by cooling at 0 ^{o}C for 20 minutes. The reaction mixture is then filtered to collect the precipitated solid; the solid is washed with cold diethyl ether, and dried *in vacuo* to afford the title compounds.

5-((2Z,4E)-2-hydroxy-5-(pyrrolidin-1-yl)penta-2,4-dien-1-ylidene)-2,2-dimethyl-1,3-dioxane-4,6-dione (4): Following General Procedure A, the title compound was obtained as a red solid (1.25g, 95%). ^{1}H NMR (600 MHz, CD_2Cl_2) δ 11.36 (s, 1H), 7.53 (d, *J* = 12.0 Hz, 1H), 6.95 (s, 1H), 6.77 (d, *J* = 12.6 Hz, 1H), 5.97 (t, *J* = 12.3 Hz, 1H), 3.71 (t, *J* = 6.5 Hz, 2H), 3.54 (t, *J* = 6.6 Hz, 2H), 2.14 – 2.08 (m, 2H), 2.05 – 1.98 (m, 2H), 1.68 (s, 6H). ^{13}C NMR (150 MHz, CD_2Cl_2) δ 167.0, 164.6, 155.0, 150.7, 144.7, 137.7, 103.6, 103.0, 89.8, 54.1, 48.7, 26.4, 24.9, 24.9. IR (KBr) 2986, 2874, 1689, 1643, 1640, 1574, 1521, 1453, 1391, 1371, 1344, 1308, 1263, 1228, 1200, 1152, 1104, 1004 cm^{-1}. HRMS (ESI+) *m/z* 316.1154 (316.1161 calculated for $C_{15}H_{19}NO_5Na^+$ $[M + Na]^+$).

5-((2Z,4E)-2-hydroxy-5-(piperidin-1-yl)penta-2,4-dien-1-ylidene)-2,2-dimethyl-1,3-dioxane-4,6-dione (5): Following General Procedure A, the title compound was obtained as a red solid (1.10g, 80%). ^{1}H NMR (600 MHz, CD_2Cl_2) δ 11.38 (s, 1H), 7.32 (d, *J* = 12.2 Hz, 1H), 6.93 (s, 1H), 6.85 – 6.79 (m, 1H), 6.14 (t, *J* = 12.3 Hz, 1H), 3.58 (d, *J* = 23.3 Hz, 4H), 1.75 (s, 6H), 1.68 (s, 6H). ^{13}C NMR (150 MHz, CD_2Cl_2) δ 167.0, 164.7, 157.5, 151.6, 144.5, 137.0, 102.9, 101.7, 57.0, 47.9, 26.7, 26.4, 25.4, 23.5. IR (KBr) 3855, 3841, 3678, 3446, 3075, 2987, 2941, 1720, 1681, 1639, 1599, 1571, 1524, 1469, 1452, 1412, 1372, 1263, 1244, 1201, 1149, 1024 cm^{-1}. HRMS (ESI+) *m/z* 330.1318 (330.1317 calculated for $C_{16}H_{21}NO_5Na^+$ $[M + Na]^+$).

5-((2Z,4E)-2-hydroxy-5-morpholinopenta-2,4-dien-1-ylidene)-2,2-dimethyl-1,3-dioxane-4,6-dione (6): Following General Procedure A, the title compound was obtained as a red solid (1.19g, 85%). ^{1}H NMR (600 MHz, CD_2Cl_2) δ 11.27 (s, 1H), 7.22 (d, *J* = 12.4 Hz, 1H), 7.10 (s, 1H), 6.76 (d, *J* = 12.2 Hz, 1H), 6.09 (t, *J* = 12.3 Hz, 1H), 3.80 – 3.78 (m, 4H),

3.58 (s, 4H), 1.69 (s, 6H). ^{13}C NMR (150 MHz, CD_2Cl_2) δ 161.7, 156.1, 156.1, 149.8, 140.5, 140.5, 140.5, 134.3, 100.9, 69.3, 67.0, 49.6, 46.1, 44.7, 28.0, 26.8, 26.5. IR (KBr) 2988, 2934, 2857, 1688, 1633, 1604, 1569, 1520, 1442, 1392, 1371, 1354, 1301, 1278, 1258, 1244, 1204, 1162, 1139, 1114, 1067, 1025, 1009 cm^{-1}. HRMS (ESI+) *m/z* 332.1105 (332.1110 calculated for $C_{15}H_{19}NO_6Na^+$ $[M + Na]^+$). Crystal structure data for **5-((2Z,4E)-2-hydroxy-5-morpholinopenta-2,4-dien-1-ylidene)-2,2-dimethyl-1,3-dioxane-4,6-dione (6)** can be obtained free of charge from the Cambridge Crystallographic Data Centre via www.ccdc.cam.ac.uk/data_request/cif CCDC 844844

5-((2Z,4E)-2-hydroxy-5-(4-phenylpiperazin-1-yl)penta-2,4-dien-1-ylidene)-2,2-dimethyl-1,3-dioxane-4,6-dione (7): Following General Procedure A, the title compound was obtained as a red solid (273 mg, 71%). ^{1}H NMR (600 MHz, CD_2Cl_2) δ 11.22 (s, 1H), 7.24 – 7.14 (m, 4H), 7.00 (s, 1H), 6.89 – 6.83 (m, 4H), 6.73 – 6.66 (m, 1H), 6.06 (t, *J* = 12.3 Hz, 1H), 3.65 (s, 4H), 3.24 (t, *J* = 5.2 Hz, 4H), 1.61 (s, 6H). ^{13}C NMR (150 MHz, CD_2Cl_2) δ 164.4, 156.0, 150.2, 150.0, 140.1, 134.2, 129.3, 129.0, 121.0, 119.6, 116.8, 116.0, 103.3, 101.1, 93.9, 69.0, 49.4, 49.2, 46.3, 44.8, 28.0, 26.8, 26.5. IR (KBr) 3055, 2995, 2930, 2829, 1689, 1634, 1601, 1568, 1523, 1503, 1443, 1389, 1374, 1362, 1283, 1258, 1249, 1230, 1208, 1163, 1095, 1051, 1015 cm^{-1}. HRMS (ESI+) *m/z* 407.1581 (407.1583 calculated for $C_{21}H_{24}N_2O_5Na^+$ $[M + Na]^+$).

5-((2Z,4E)-2-hydroxy-5-((R)-2-methylpyrrolidin-1-yl)penta-2,4-dien-1-ylidene)-2,2-dimethyl-1,3-dioxane-4,6-dione (8): Following General Procedure A, the title compound was obtained as a red solid (1.21g, 87%). ^{1}H NMR (600 MHz, CD_2Cl_2) δ 11.28 (s, 1H), 7.42 (d, *J* = 12.0 Hz, 1H), 6.85 (s, 1H), 6.72 (d, *J* = 12.6 Hz, 1H), 5.90 (t, *J* = 12.3 Hz, 1H),

3.83 (d, *J* = 6.5 Hz, 1H), 3.56 – 3.47 (m, 2H), 2.17 – 1.87 (m, 4H), 1.59 (s, 6H), 1.28 (d, *J* = 6.5 Hz, 3H). ^{13}C NMR (150 MHz, CD_2Cl_2) δ 167.0, 164.7, 153.9, 150.9, 144.6, 137.3, 103.9, 102.9, 89.6, 60.4, 49.2, 32.7, 26.4, 26.4, 22.8, 20.1. IR (KBr) 3065, 2996, 2877, 1676, 1599, 1509, 1466, 1441, 1369, 1345, 1311, 1259, 1232, 1191, 1135, 1004 cm^{-1}. HRMS (ESI+) *m/z* 330.1320 (330.1317 calculated for $C_{16}H_{21}NO_5Na^+$ $[M + Na]^+$).

(S)-methyl-1-((1E,3Z)-5-(2,2-dimethyl-4,6-dioxo-1,3-dioxan-5-ylidene)-4-hydroxypenta-1,3-dien-1-yl) pyrrolidine-2-carboxylate (9): Following General Procedure A, the title compound was obtained as a **g**reen solid (1.33g, 84%). ^{1}H NMR (600 MHz, CD_2Cl_2) δ 11.14 (s, 1H), 7.29 (d, *J* = 12.5 Hz, 1H), 7.05 (s, 1H), 6.63 (d, *J* = 12.3 Hz, 1H), 5.89 (t, *J* = 12.3 Hz, 1H), 4.37 – 4.32 (m, 1H), 3.70 (s, 3H), 2.24 – 2.17 (m, 2H), 2.07 – 1.98 (m, 2H), 1.74 (d, *J* = 3.6 Hz, 2H), 1.61 (d, *J* = 2.0 Hz, 6H). ^{13}C NMR (150 MHz, CD_2Cl_2) δ 166.8, 164.2, 161.6, 153.6, 149.0, 141.8, 134.5, 110.0, 103.4, 103.1, 65.0, 62.9, 51.8, 48.8, 46.5, 29.7, 29.5, 26.5, 26.5, 23.9, 23.7, 23.5. IR (KBr) 3068, 2990, 2953, 2880, 1742, 1688, 1627, 1485, 1450, 1407, 1391, 1362, 1340, 1274, 1244, 1234, 1200, 1141, 1118, 1043, 1006 cm^{-1}. HRMS (ESI+) *m/z* 374.1212 (374.1216 calculated for $C_{17}H_{21}NO_7Na^+$ $[M + Na]^+$). Crystal structure data for **(S)-methyl 1-((1E,3Z)-5-(2,2-dimethyl-4,6-dioxo-1,3-dioxan-5-ylidene)-4-hydroxypenta-1,3-dien-1-yl)pyrrolidine-2-carboxylate (9)** can be obtained free of charge from the Cambridge Crystallographic Data Centre via www.ccdc.cam.ac.uk/data_request/cif CCDC 844843

5-((2*Z*,4*E*)-5-(dipropylamino)-2-hydroxypenta-2,4-dien-1-ylidene)-2,2-dimethyl-1,3-dioxane-4,6-dione (11): Following General Procedure A, the title compound was obtained as a red solid (252 mg, 78%). ^{1}H NMR (500 MHz, CD_2Cl_2) δ: 11.35 (s, 1H), 7.31 (d, J =

12.2 Hz, 1H), 6.96 (s, 1H), 6.78 (d, J = 12.4 Hz, 1H), 6.06 (t, J = 12.3 Hz, 1H), 3.38 (q, J = 7.4 Hz, 4H), 1.72 (dq, J = 9.6, 7.5 Hz, 4H), 1.67 (s, 6H), 0.96 (dt, J = 25.4, 7.4 Hz, 6H). ^{13}C NMR (125 MHz, CD_2Cl_2) δ 167.6, 165.3, 159.0, 152.0, 145.2, 138.5, 103.6, 102.9, 59.9, 51.8, 27.0, 22.8, 21.1, 11.6, 11.2. IR (KBr) 3150, 2993, 2917, 2696, 1644, 1589, 1548, 1501, 1447, 1403, 1359, 1315, 1278, 1232, 1196, 1145, 1122 cm^{-1}. HRMS (ESI+) *m/z* 346.1620 (346.1630 calculated for $C_{17}H_{25}NO_5Na^+$ $[M + Na]^+$).

5-((2*Z*,4*E*)-5-(dibutylamino)-2-hydroxypenta-2,4-dien-1-ylidene)-2,2-dimethyl-1,3-dioxane-4,6-dione (12): Following General Procedure A, the title compound was obtained as a red solid (288 mg, 82%). ^{1}H NMR (500 MHz, CD_2Cl_2) δ: 11.34 (s, 1H), 7.31 (d, J = 12.3 Hz, 1H), 6.95 (s, 1H), 6.78 (dd, J = 12.5, 1.5 Hz, 1H), 6.06 (t, J = 12.3 Hz, 1H), 3.41 (q, J = 7.0 Hz, 4H), 1.67 (s, 10H), 1.37 (dh, J = 29.9, 7.4 Hz, 4H), 0.97 (q, J = 7.5 Hz, 6H). ^{13}C NMR (125 MHz, CD_2Cl_2) δ 167.6, 165.2, 159.0, 152.0, 145.2, 138.2, 103.6, 103.0, 58.1, 50.1, 31.4, 29.7, 27.0, 20.7, 20.2, 14.0, 140. IR (KBr) 3157, 2991, 2923, 1691, 1645, 1592, 1544, 1498, 1446, 1404, 1357, 1311, 1274, 1228, 1191, 1136, 1116 cm^{-1}. HRMS (ESI+) *m/z* 374.1947 (374.1943 calculated for $C_{19}H_{29}NO_5Na^+$ $[M + Na]^+$).

5-((2*Z*,4*E*)-5-(dihexylamino)-2-hydroxypenta-2,4-dien-1-ylidene)-2,2-dimethyl-1,3-dioxane-4,6-dione (13): Following General Procedure A, the title compound was obtained as a red solid (371 mg, 91%). ^{1}H NMR (500 MHz, CD_2Cl_2) δ: 11.34 (s, 1H), 7.31 (d, J = 12.2 Hz, 1H), 6.94 (s, 1H), 6.78 (dd, J = 12.5, 1.5 Hz, 1H), 6.06 (t, J = 12.3 Hz, 1H), 3.41 (q, J = 6.7 Hz, 5H), 1.67 (s, 10H), 1.38 – 1.25 (m, 16H), 0.90 (ddt, J = 10.8, 7.6, 4.4 Hz, 6H). ^{13}C NMR (125 MHz, CD_2Cl_2) δ 167.6, 165.3, 159.0, 152.0, 145.2, 138.2, 103.6, 103.0, 58.3, 50.3, 31.9, 31.9, 31.9, 29.4, 27.6, 27.1, 27.0, 26.6, 23.1, 23.1, 23.0, 14.3. IR (KBr)

3163, 2996, 2921, 1694, 1639, 1585, 1537, 1487, 1435, 1395, 1344, 1297, 1260, 1223, 1183, 1125, 1109 cm^{-1}. HRMS (ESI+) *m/z* 430.2573 (430.2569 calculated for $C_{23}H_{37}NO_5Na^+$ $[M + Na]^+$).

5-((2Z,4E)-5-(dioctylamino)-2-hydroxypenta-2,4-dien-1-ylidene)-2,2-dimethyl-1,3-dioxane-4,6-dione (14): Following General Procedure A, the title compound was obtained as a red solid (1.75g, 83%). ^1H NMR (600 MHz, CD_2Cl_2) δ 11.36 (s, 1H), 7.30 (d, *J* = 12.2 Hz, 1H), 6.96 (s, 1H), 6.78 (d, *J* = 12.4 Hz, 1H), 6.07 (t, *J* = 12.3 Hz, 1H), 3.41 (q, *J* = 7.2 Hz, 4H), 1.68 (s, 6H), 1.41 – 1.18 (m, 24H), 0.90 (t, *J* = 6.8 Hz, 6H). ^{13}C NMR (150 MHz, CD_2Cl_2) δ 167.0, 164.6, 158.3, 151.3, 144.6, 137.7, 103.0, 102.3, 89.8, 57.7, 49.7, 31.7, 31.7, 29.1, 29.1, 29.0, 28.8, 27.3, 27.0, 26.9, 26.4, 26.4, 22.6, 13.8. IR (KBr) 2924, 2855, 1719, 1676, 1575, 1503, 1462, 1416, 1391, 1346, 1287, 1262, 1231, 1199, 1142, 1117, 1047, 1029 cm^{-1}. HRMS (ESI+) *m/z* 486.3181 (486.3195 calculated for $C_{27}H_{45}NO_5Na^+$ $[M + Na]^+$).

5-((2Z,4E)-5-(diallylamino)-2-hydroxypenta-2,4-dien-1-ylidene)-2,2-dimethyl-1,3-dioxane-4,6-dione (16): Following General Procedure A, the title compound was obtained as a purple solid (968 mg, 68%). ^1H NMR (600 MHz, CD_2Cl_2) δ 11.17 (s, 1H), 7.23 (d, *J* = 12.4 Hz, 1H), 7.00 (s, 1H), 6.65 (d, *J* = 12.3 Hz, 1H), 5.96 (t, *J* = 12.3 Hz, 1H), 5.75 (dt, *J* = 13.8, 7.6 Hz, 2H), 5.32 – 5.15 (m, 4H), 3.94 (dd, *J* = 16.9, 5.0 Hz, 4H), 1.60 (s, 6H). ^{13}C NMR (150 MHz, CD_2Cl_2) δ 166.9, 164.4, 157.1, 150.1, 145.1, 140.5, 131.2, 129.4, 120.5, 119.1, 119.0, 103.3, 102.0, 91.9, 59.1, 51.3, 26.5. IR (KBr) 3071, 3003, 2943, 1698, 1646, 1612, 1561, 1499, 1446, 1368, 1299, 1283, 1242, 1207, 1164 cm^{-1}. HRMS (ESI+) *m/z* 342.1324 (342.1317 calculated for $C_{17}H_{21}NO_5Na^+$ $[M +Na]^+$).

5-((2Z,4E)-5-(benzyl(methyl)amino)-2-hydroxypenta-2,4-dien-1-ylidene)-2,2-dimethyl-1,3-dioxane-4,6-dione (19): Following General Procedure A, the title compound was obtained as a purple solid (1.31g, 85%). ^{1}H NMR (600 MHz, CD_2Cl_2) δ 11.32 (d, *J* = 1.6 Hz, 1H), 7.53 (d, *J* = 12.2 Hz, 1H), 7.42 (qd, *J* = 7.8, 7.2, 3.7 Hz, 3H), 7.31 – 7.18 (m, 2H), 7.08 (s, 1H), 6.82 (dd, *J* = 12.5, 1.6 Hz, 1H), 6.14 (dt, *J* = 93.0, 12.3 Hz, 1H), 4.61 (d, *J* = 18.0 Hz, 2H), 3.13 (d, *J* = 122.7 Hz, 3H), 1.68 (d, *J* = 5.1 Hz, 6H). ^{13}C NMR (150 MHz, CD_2Cl_2) δ 166.9, 164.5, 158.8, 158.0, 150.7, 150.4, 145.1, 139.9, 139.5, 134.0, 129.2, 129.1, 128.8, 128.7, 128.5, 128.4, 127.8, 127.4, 103.2, 102.1, 102.0, 62.9, 53.8, 53.6, 53.4, 53.3, 53.1, 36.3, 26.5. IR (KBr) 3082, 3028, 2990, 2940, 1695, 1610, 1565, 1502, 1447, 1401, 1386, 1356, 1276, 1260, 1239, 1200, 1150, 1065, 1032, 1003 cm^{-1}. HRMS (ESI+) *m/z* 366.1320 (366.1317 calculated for $C_{19}H_{21}NO_5Na^+$ $[M+Na]^+$).

5-((2Z,4E)-5-(3,4-dihydroisoquinolin-2(1H)-yl)-2-hydroxypenta-2,4-dien-1-ylidene)-2,2-dimethyl-1,3-dioxane-4,6-dione (20): Following General Procedure A, the title compound was obtained as a red solid (1.32 g, 82%). ^{1}H NMR (600 MHz, CD_2Cl_2) δ 11.24 (s, 1H), 7.36 (d, *J* = 12.4 Hz, 1H), 7.25 – 6.90 (m, 7H), 6.71 (d, *J* = 12.3 Hz, 1H), 6.06 (d, *J* = 12.5 Hz, 1H), 4.64 (s, 2), 3.75 – 3.64 (m, 2H), 2.96 (d, *J* = 18.9 Hz, 2H), 1.60 (s, 6H). ^{13}C NMR (150 MHz, CD_2Cl_2) δ 166.9, 164.4, 156.7, 156.6, 150.1, 150.0, 140.1, 128.7, 128.6, 127.3, 127.1, 127.1, 127.0, 126.5, 126.4, 125.6, 101.5, 101.4, 52.4, 48.3, 29.3, 26.5. IR (KBr) 3469, 3062, 2992, 2937, 1690, 1632, 1609, 1561, 1500, 1458, 1440, 1364, 1283, 1267, 1234, 1203, 1153, 1051 cm^{-1}. HRMS (ESI+) *m/z* 378.1314 (378.1317 calculated for $C_{20}H_{21}NO_5Na^+$ $[M+Na]^+$).

5-((2Z,4E)-2-hydroxy-5-(isoindolin-2-yl)penta-2,4-dien-1-ylidene)-2,2-dimethyl-1,3-dioxane-4,6-dione (21): Following General Procedure A, the title compound was obtained as a red solid (870 mg, 91%). ^{1}H NMR (600 MHz, CD_2Cl_2) δ 11.21 (s, 1H), 7.48 (d, *J* = 12.2 Hz, 1H), 7.27 (d, *J* = 26.5 Hz, 4H), 7.05 (s, 1H), 6.69 (d, *J* = 12.2 Hz, 1H), 5.96 (t, *J* = 12.3 Hz, 1H), 4.97 (s, 2H), 4.78 (s, 2H), 1.61 (s, 6H). ^{13}C NMR (150 MHz, CD_2Cl_2) δ 153.6, 149.0, 141.1, 128.4, 128.2, 122.8, 122.5, 103.3, 103.0, 58.3, 54.5, 26.5. IR (KBr) 3063, 2985, 2958, 1688, 1637, 1611, 1565, 1505, 1468, 1451, 1368, 1349, 1284, 1268, 1235, 1223, 1198, 1180, 1151, 1114, 1025, 1006 cm^{-1}. HRMS (ESI+) *m/z* 364.1163 (364.1161 calculated for $C_{19}H_{19}NO_5Na^+$ $[M+Na]^+$). Crystal structure data for **5-((2Z,4E)-2-hydroxy-5-(isoindolin-2-yl)penta-2,4-dien-1-ylidene)-2,2-dimethyl-1,3-dioxane-4,6-dione (21)** can be obtained free of charge from the Cambridge Crystallographic Data Centre via www.ccdc.cam.ac.uk/data_request/cif CCDC 846378

5-((2Z,4E)-5-(dibenzylamino)-2-hydroxypenta-2,4-dien-1-ylidene)-2,2-dimethyl-1,3-dioxane-4,6-dione (22): Following General Procedure A, the title compound was obtained as a green solid (1.42g, 75%). ^{1}H NMR (600 MHz, CD_2Cl_2) δ 11.25 (s, 1H), 7.59 (d, *J* = 12.4 Hz, 1H), 7.40 (tt, *J* = 14.8, 6.6 Hz, 6H), 7.22 (dd, *J* = 12.8, 7.3 Hz, 4H), 7.13 (s, 1H), 6.83 (d, *J* = 12.2 Hz, 1H), 6.23 (t, *J* = 12.3 Hz, 1H), 4.56 (d, *J* = 5.5 Hz, 4H), 1.68 (s, 6H). ^{13}C NMR (150 MHz, CD_2Cl_2) δ 166.9, 164.4, 157.7, 150.2, 145.2, 140.8, 134.1, 133.8, 129.2, 129.1, 128.8, 128.8, 128.4, 128.3, 128.1, 127.5, 127.3, 103.4, 102.0, 92.2, 60.0, 54.5, 51.7, 26.6, 26.5. IR (KBr) 3469, 3058, 3027, 2992, 2932, 1696, 1626, 1553, 1489, 1476, 1449, 1391, 1365, 1346, 1291, 1261, 1231, 1197, 1139, 1111, 1030, 1016, 1003 cm^{-1}. HRMS (ESI+) *m/z* 442.1637 (442.1630 calculated for $C_{25}H_{25}NO_5Na^+$ $[M + Na]^+$). Crystal structure data for **5-((2Z,4E)-5-(dibenzylamino)-2-hydroxypenta-2,4-dien-1-ylidene)-2,2-**

dimethyl-1,3-dioxane-4,6-dione (22) can be obtained free of charge from the Cambridge Crystallographic Data Centre via www.ccdc.cam.ac.uk/data_request/cif CCDC 844842

5-((2*Z*,4*E*)-2-hydroxy-5-(methyl(phenyl)amino)penta-2,4-dien-1-ylidene)-2,2-dimethyl-1,3-dioxane-4,6-dione (23): Following general procedure A, the title compound was obtained as a purple solid (74 mg, 22%). ^{1}H NMR (600 MHz, CD_2Cl_2) δ 7.67 (d, *J* = 5.5 Hz, 1H), 7.24 (t, *J* = 7.8 Hz, 2H), 6.84 (d, *J* = 8.1 Hz, 2H), 6.78 (t, *J* = 7.3 Hz, 1H), 6.43 (d, *J* = 4.6 Hz, 1H), 5.52 (s, 1H), 4.00 (s, 1H), 3.50 – 3.43 (d, *J* = 3.4 Hz, 1H), 2.79 (s, 3H), 1.70 (s, 6H). ^{13}C NMR (125 MHz, CD_2Cl_2) δ 163.8, 149.9, 134.7, 130.4, 130.0, 118.9, 114.1, 106.2, 63.6, 48.4, 45.0, 32.8, 28.4, 27.2, 27.2. IR (ATR) 3060, 2999, 2921, 1780, 1742, 1710, 1596, 1503, 1470, 1382, 1324, 1269, 1197, 1147, 1104, 1015, 990, 927, 871, 791, 749, 694 cm^{-1}. HRMS (ESI+) *m/z* 352.1147 (352.1161 calculated for $C_{18}H_{19}NO_5Na^+$ $[M + Na]^+$).

2-((2*Z*,4*E*)-5-(diethylamino)-2-hydroxypenta-2,4-dien-1-ylidene)-1*H*-indene-1,3(2*H*)-dione (62): Following General Procedure A the title compound was obtained as a dark blue solid (259 mg, 87%). ^{1}H NMR (600 MHz, CD_2Cl_2) δ 11.51 (s, 1H), 7.60 (dt, *J* = 19.4, 2.6 Hz, 2H), 7.57 – 7.52 (m, 2H), 7.24 (d, *J* = 12.2 Hz, 1H), 6.71 (d, *J* = 12.3 Hz, 1H), 6.64 (s, 1H), 6.04 (t, *J* = 12.3 Hz, 1H), 3.46 (dq, *J* = 28.1, 7.2 Hz, 4H), 1.27 (dt, *J* = 7.9, 4.5 Hz, 6H). ^{13}C NMR (125 MHz, CD_2Cl_2) δ 193.2, 190.8, 156.4, 147.8, 147.3, 141.2, 140.9, 133.5, 133.2, 132.0, 121.3, 121.1, 114.5, 102.6, 52.3, 44.5, 14.8, 12.6. IR (ATR): 3007, 2971, 2924, 2869, 1674, 1613, 1583, 1483, 1439, 1373, 1353, 1331, 1262, 1163, 1146, 1110, 974, 905, 765 cm^{-1}. HRMS (ESI+) *m/z* 320.1262 (320.1263 calculated for $C_{18}H_{19}NO_3Na^+$ $[M + Na]^+$).

5-((2*Z*,4*E*)-2-hydroxy-5-(pyrrolidin-1-yl)penta-2,4-dien-1-ylidene)-1,3-dimethylpyrimidine-2,4,6(1*H*,3*H*,5*H*)-trione (26): Following General Procedure A, the title compound was obtained as a purple solid (275 mg, 90%). ^{1}H NMR (600 MHz, $CDCl_3$) δ 12.53 (s, 1H), 7.43 (d, *J* = 12.2 Hz, 1H), 7.14 (s, 1H), 6.72 (d, *J* = 12.4 Hz, 1H), 5.98 (t, *J* = 12.3 Hz, 1H), 3.70 (t, *J* = 6.8 Hz, 3H), 3.52 (t, *J* = 7.0 Hz, 3H), 3.35 (d, *J* = 6.2 Hz, 7H), 3.21 (s, 2H), 2.13 (p, *J* = 6.8 Hz, 4H), 2.04 (p, *J* = 6.6 Hz, 4H). ^{13}C NMR (150 MHz, $CDCl_3$) δ 163.3, 153.6, 150.0, 146.7, 139.4, 104.0, 70.0, 53.8, 48.4, 28.4, 28.3, 25.0, 22.7. IR (KBr) 2961, 2915, 2763, 1693, 1617, 1580, 1559, 1491, 1454, 1419, 1370, 1343, 1266, 1226, 1177, 1105, 1043, 967, 941, 924, 829, 754 cm^{-1}. HRMS (ESI+) *m/z* 328.1263 (328.1273 calculated for $C_{15}H_{19}N_3O_4Na^+$ $[M + Na]^+$).

5-((2*Z*,4*E*)-2-hydroxy-5-(piperidin-1-yl)penta-2,4-dien-1-ylidene)-1,3-dimethylpyrimidine-2,4,6(1*H*,3*H*,5*H*)-trione (27): Following General Procedure A, the title compound was obtained as a purple solid (297mg, 93%). ^{1}H NMR (500 MHz, CD_2Cl_2) δ: 12.52 (s, 1H), 7.32 (d, J = 12.1 Hz, 1H), 7.01 (s, 1H), 6.85 (d, J = 12.5 Hz, 1H), 6.16 (t, J = 12.3 Hz, 1H), 3.71 – 3.65 (m, 2H), 3.61 – 3.58 (m, 2H), 3.55 (bs, 2H), 3.29 (s, 3H), 3.26 (s, 3H), 3.17 (bs, 2H), 1.84 – 1.79 (m, 2H). ^{13}C NMR (125 MHz, CD_2Cl_2) δ 165.0, 163.0, 157.3, 151.6, 146.1, 136.7, 102.4, 67.7, 57.0, 27.9, 25.5, 23.6. IR (KBr) 2964, 2915, 2832, 1694, 1616, 1578, 1557, 1488, 1452, 1419, 1369, 1345, 1260, 1217, 1164, 1105, 1043, 967, 941, 924, 829, 754 cm^{-1}. HRMS (ESI+) *m/z* 342.1426 (342.1430 calculated for $C_{16}H_{21}N_3O_4Na^+$ $[M + Na]^+$).

5-((2*Z*,4*E*)-2-hydroxy-5-((*R*)-2-methylpyrrolidin-1-yl)penta-2,4-dien-1-ylidene)-1,3-dimethylpyrimidine-2,4,6(1*H*,3*H*,5*H*)-trione (30): Following General Procedure A, the

title compound was obtained as a purple solid (278 mg, 87%). ^{1}H NMR (600 MHz, $CDCl_3$) δ 12.53 (s, 1H), 7.38 (d, *J* = 12.2 Hz, 1H), 7.15 (s, 1H), 6.75 (d, *J* = 12.6 Hz, 1H), 5.99 (t, *J* = 12.3 Hz, 1H), 3.89 (q, *J* = 6.5 Hz, 1H), 3.58 (q, *J* = 6.7 Hz, 2H), 3.35 (d, *J* = 5.8 Hz, 7H), 2.32 – 1.95 (m, 5H), 1.71 (dq, *J* = 12.9, 6.6 Hz, 1H), 1.37 (d, *J* = 6.5 Hz, 3H). ^{13}C NMR (150 MHz, $CDCl_3$) δ 165.1, 152.3, 152.0, 150.2, 146.7, 139.2, 104.2, 59.9, 49.0, 32.9, 28.4, 28.3, 22.9, 20.5. IR (KBr) 2965, 2913, 2821, 1694, 1616, 1576, 1557, 1487, 1452, 1421, 1369, 1346, 1260, 1219, 1166, 1109, 1050, 976, 968, 924, 829, 754 cm^{-1}. HRMS (ESI+) *m/z* 342.1430 (342.1430 calculated for $C_{16}H_{21}N_3O_4Na^+$ $[M + Na]^+$).

(S)-methyl-1-((1E,3Z)-5-(1,3-dimethyl-2,4,6-trioxotetrahydropyrimidin-5(2*H*)-ylidene)-4-hydroxypenta-1,3-dien-1-yl) pyrrolidine-2-carboxylate (31): Following General Procedure A, the title compound was obtained as a purple solid (189 mg, 52%). ^{1}H NMR (500 MHz, CD_2Cl_2) δ: 12.35 (s, 1H), 7.37 (d, J = 12.1 Hz, 1H), 7.18 (s, 1H), 6.72 (d, J = 12.5 Hz, 1H), 5.96 (t, J = 12.3 Hz, 1H), 4.43 (dd, J = 7.7, 4.3 Hz, 1H), 3.76 (s, 3H), 3.71 – 3.58 (m, 2H), 3.28 (s, 3H), 3.25 (s, 3H), 2.32 – 2.18 (m, 2H), 2.07 (tdd, J = 12.8, 8.0, 5.9 Hz, 2H). ^{13}C NMR (125 MHz, CD_2Cl_2) δ 171.3, 165.8, 163.3, 153.9, 152.2, 149.4, 147.5, 141.9, 135.0, 104.3, 65.6, 53.5, 49.4, 30.1, 28.7, 28.6, 24.1. IR (KBr) 2966, 2912, 2813, 1694, 1615, 1573, 1557, 1486, 1452, 1425, 1369, 1347, 1260, 1222, 1180, 1126, 1071, 1004, 968, 924, 829, 754 cm^{-1}. HRMS (ESI+) *m/z* 386.1321 (386.1328 calculated for $C_{17}H_{21}N_3O_6Na^+$ $[M + Na]^+$).

5-((2*Z*,4*E*)-5-(dipropylamino)-2-hydroxypenta-2,4-dien-1-ylidene)-1,3-dimethylpyrimidine-2,4,6(1*H*,3*H*,5*H*)-trione (33): Following General Procedure A, the title compound was obtained as a purple solid (278 mg, 83%). ^{1}H NMR (500 MHz,

CD_2Cl_2) δ: 12.50 (s, 1H), 7.31 (d, J = 12.2 Hz, 1H), 7.05 (s, 1H), 6.83 (d, J = 12.5 Hz, 1H), 6.09 (t, J = 12.3 Hz, 1H), 3.39 (dt, J = 11.8, 7.8 Hz, 4H), 3.29 (s, 3H), 3.26 (s, 3H), 1.72 (dh, J = 16.8, 9.6, 8.1 Hz, 4H), 0.97 (dt, J = 28.8, 7.4 Hz, 6H). ^{13}C NMR (125 MHz, CD_2Cl_2) δ 165.6, 163.6, 158.8, 151.9, 146.8, 138.1, 103.4, 59.8, 51.8, 28.6, 28.5, 22.8, 21.1, 11.7, 11.5, 11.2. IR (KBr) 2972, 2920, 2813, 1695, 1614, 1569, 1558, 1485, 1451, 1424, 1386, 1346, 1260, 1221, 1176, 1122, 1078, 1009, 977, 936, 836, 757 cm^{-1}. HRMS (ESI+) *m/z* 358.1740 (358.1743 calculated for $C_{17}H_{25}N_3O_4Na^+$ $[M + Na]^+$).

5-((2*Z*,4*E*)-5-(dibutylamino)-2-hydroxypenta-2,4-dien-1-ylidene)-1,3-dimethylpyrimidine-2,4,6(1*H*,3*H*,5*H*)-trione (34): Following General Procedure A, the title compound was obtained as a purple solid (276 mg, 76%). ^{1}H NMR (500 MHz, CD_2Cl_2) δ: 12.49 (s, 1H), 7.29 (d, J = 12.2 Hz, 1H), 7.04 (s, 1H), 6.81 (d, J = 12.4 Hz, 1H), 6.08 (t, J = 12.3 Hz, 1H), 3.42 (dt, J = 12.2, 7.7 Hz, 4H), 3.29 (s, 3H), 3.26 (s, 3H), 1.71 – 1.62 (m, 4H), 1.37 (dh, J = 30.1, 7.4 Hz, 4H), 0.97 (dt, J = 11.4, 7.4 Hz, 6H). ^{13}C NMR (125 MHz, CD_2Cl_2) δ 165.1, 163.0, 158.0, 151.2, 146.2, 137.4, 102.9, 57.4, 49.5, 30.9, 29.1, 28.0, 27.9, 20.2, 19.6, 13.4, 13.3. IR (KBr) 2971, 2919, 2813, 1695, 1613, 1586, 1558, 1484, 1451, 1423, 1370, 1339, 1257, 1221, 1176, 1122, 1063, 1007, 977, 936, 836, 759 cm^{-1}. HRMS (ESI+) *m/z* 386.2049 (386.2056 calculated for $C_{19}H_{29}N_3O_4Na^+$ $[M + Na]^+$).

5-((2*Z*,4*E*)-5-(dihexylamino)-2-hydroxypenta-2,4-dien-1-ylidene)-1,3-dimethylpyrimidine-2,4,6(1*H*,3*H*,5*H*)-trione (35): Following General Procedure A, the title compound was obtained as a purple solid (394 mg, 94%). ^{1}H NMR (500 MHz, CD_2Cl_2) δ: 12.49 (s, 1H), 7.30 (d, J = 12.2 Hz, 1H), 7.03 (s, 1H), 6.82 (d, J = 12.1 Hz, 1H), 6.08 (t, J = 12.3 Hz, 1H), 3.41 (dt, J = 10.8, 7.8 Hz, 4H), 3.29 (s, 3H), 3.26 (s, 3H), 1.69 – 1.65 (m,

4H), 1.34 – 1.30 (m, 12H), 0.91 – 0.89 (m, 6H). ^{13}C NMR (125 MHz, CD_2Cl_2) δ 165.0, 163.0, 158.0, 151.3, 146.2, 137.3, 103.0, 57.7, 49.7, 31.3, 31.3, 28.8, 28.0, 27.9, 27.0, 26.5, 26.4, 26.0, 22.5, 22.4, 13.7. IR (KBr) 2971, 2919, 2818, 1699, 1613, 1568, 1553, 1484, 1457, 1423, 1369, 1343, 1264, 1220, 1173, 1123, 1075, 1009, 979, 944, 848, 766 cm^{-1}. HRMS (ESI+) *m/z* 442.2681 (442.2682 calculated for $C_{23}H_{37}N_3O_4Na^+$ $[M + Na]^+$).

5-((2*Z*,4*E*)-5-(dioctylamino)-2-hydroxypenta-2,4-dien-1-ylidene)-1,3-dimethylpyrimidine-2,4,6(1*H*,3*H*,5*H*)-trione (36): Following General Procedure A, the title compound was obtained as a purple solid (414 mg, 87%). ^{1}H NMR (500 MHz, CD_2Cl_2) δ: 12.49 (s, 1H), 7.29 (d, J = 12.2 Hz, 1H), 7.03 (s, 1H), 6.82 (d, J = 12.5 Hz, 1H), 6.08 (t, J = 12.3 Hz, 1H), 3.41 (dt, J = 11.0, 7.7 Hz, 4H), 3.29 (s, 3H), 3.26 (s, 3H), 1.70 – 1.65 (m, 4H), 1.32 – 1.27 (m, 20H), 0.90 – 0.87 (m, 6H). ^{13}C NMR (125 MHz, CD_2Cl_2) δ 165.0, 163.0, 158.0, 151.3, 146.2, 137.3, 102.9, 57.7, 49.7, 31.7, 31.7, 31.7, 29.1, 29.1, 29.1, 29.1, 28.9, 28.0, 27.9, 27.1, 26.9, 26.4, 22.6, 13.8. IR (KBr) 2969, 2917, 2806, 1693, 1616, 1576, 1557, 1487, 1453, 1425, 1360, 1342, 1267, 1226, 1180, 1124, 1073, 1006, 978, 941, 851, 761 cm^{-1}. HRMS (ESI+) *m/z* 498.3296 (498.3308 calculated for $C_{27}H_{45}N_3O_4Na^+$ $[M + Na]^+$).

5-((2*Z*,4*E*)-5-(diallylamino)-2-hydroxypenta-2,4-dien-1-ylidene)-1,3-dimethylpyrimidine-2,4,6(1*H*,3*H*,5*H*)-trione (38): Following General Procedure A, the title compound was obtained as a purple solid (315 mg, 95%). ^{1}H NMR (500 MHz, CD_2Cl_2) δ: 12.40 (s, 1H), 7.31 (d, J = 12.4 Hz, 1H), 7.15 (s, 1H), 6.78 – 6.75 (m, 2H), 6.06 (t, J = 12.3 Hz, 1H), 5.40 – 5.33 (m, 2H), 5.31 – 5.24 (m, 2H), 4.07 – 3.96 (m, 4H), 3.36 (m, 2H), 3.29 (s, 3H), 3.27 (s, 3H). ^{13}C NMR (125 MHz, CD_2Cl_2) δ 165.8, 163.5, 157.4, 152.2, 150.6,

147.2, 140.7, 131.9, 130.1, 121.1, 119.6, 103.2, 59.7, 50.8, 30.3, 28.7, 28.6. IR (KBr) 2967, 2911, 2809, 1694, 1610, 1552, 1459, 1428, 1361, 1348, 1263, 1222, 1174, 1116, 1060, 991, 965, 931, 836, 758 cm^{-1}. HRMS (ESI+) *m/z* 354.1426 (354.1430 calculated for $C_{17}H_{21}N_3O_4Na^+$ $[M + Na]^+$).

5-((2*Z*,4*E*)-5-(benzyl(methyl)amino)-2-hydroxypenta-2,4-dien-1-ylidene)-1,3-dimethylpyrimidine-2,4,6(1*H*,3*H*,5*H*)-trione (41): Following General Procedure A, the title compound was obtained as a purple solid (327 mg, 92%). ^1H NMR (500 MHz, CD_2Cl_2) δ: 12.44 (s, 1H), 7.46 (d, J = 12.3 Hz, 1H), 7.40 (dd, J = 13.8, 7.2 Hz, 3H), 7.24 (d, J = 7.4 Hz, 2H), 7.18 (s, 1H), 6.82 (d, J = 12.3 Hz, 1H), 6.06 (t, J = 12.3 Hz, 1H), 4.58 (s, 2H), 3.30 (s, 3H), 3.27 (s, 3H), 3.03 (s, 3H). ^{13}C NMR (150 MHz, CD_2Cl_2) δ 165.8, 163.5, 157.8, 152.3, 150.4, 147.3, 140.7, 134.7, 129.7, 129.4, 128.3, 128.0, 102.9, 63.4, 36.9, 28.7, 28.6. IR (KBr) 2961, 2918, 2816, 1692, 1614, 1573, 1559, 1486, 1456, 1421, 1369, 1341, 1261, 1221, 1179, 1118, 1062, 994, 968, 932, 841, 752 cm^{-1}. HRMS (ESI+) *m/z* 378.1428 (378.1430 calculated for $C_{19}H_{21}N_3O_4Na^+$ $[M + Na]^+$).

5-((2*Z*,4*E*)-5-(3,4-dihydroisoquinolin-2(1*H*)-yl)-2-hydroxypenta-2,4-dien-1-ylidene)-1,3-dimethylpyrimidine-2,4,6(1*H*,3*H*,5*H*)-trione (42): Following General Procedure A, the title compound was obtained as a purple solid (301 mg, 82%). ^1H NMR (500 MHz, CD_2Cl_2) δ: 12.48 (s, 1H), 7.45 (d, J = 12.9 Hz, 1H), 7.30 – 7.10 (m, 6H), 6.84 (d, J = 12.3 Hz, 1H), 6.17 (d, J = 11.9 Hz, 1H), 4.73 (s, 2H), 3.81 (s, 2H), 3.30 (s, 3H), 3.26 (s, 3H), 3.09 – 2.99 (m, 2H). ^{13}C NMR (125 MHz, CD_2Cl_2) δ 165.7, 163.6, 157.0, 152.3, 150.6, 140.3, 129.5, 129.3, 128.5, 127.7, 127.1, 102.7, 68.3, 52.6, 45.4, 42.4, 29.9, 28.7, 28.6, 26.1, 25.9. IR (KBr) 2965, 2913, 2814, 1697, 1619, 1573, 1556, 1481, 1456, 1426, 1362, 1345, 1269,

1228, 1175, 1120, 1065, 998, 972, 933, 838, 759 cm^{-1}. HRMS (ESI) *m/z* 390.1425 (390.1430 calculated for $C_{20}H_{21}N_3O_4Na^+$ $[M + Na]^+$).

1,3-dibutyl-5-((2*Z*,4*E*)-5-(diethylamino)-2-hydroxypenta-2,4-dien-1-ylidene)pyrimidine-2,4,6(1*H*,3*H*,5*H*)-trione (70): Following General Procedure A, the title compound was obtained as a purple solid (341 mg, 87%). ^1H NMR (600 MHz, CD_2Cl_2) δ 12.56 (s, 1H), 7.28 (d, *J* = 12.3 Hz, 1H), 7.06 (s, 1H), 6.80 (d, *J* = 11.5 Hz, 1H), 6.07 (t, *J* = 12.3 Hz, 1H), 3.87 (dt, *J* = 14.9, 7.5 Hz, 4H), 3.49 (dq, *J* = 24.8, 7.2 Hz, 4H), 1.55 (m, 4H), 1.40 – 1.23 (m, 10H), 0.93 (q, *J* = 7.3 Hz, 6H). ^{13}C NMR (126 MHz, CD_2Cl_2) δ 165.5, 163.3, 157.4, 151.9, 151.3, 146.8, 138.7, 103.0, 98.7, 52.5, 44.7, 41.8, 41.7, 30.9, 30.9, 20.8, 20.8, 14.8, 14.2, 14.2, 12.7. IR (ATR): 2958, 2932, 2873, 1691, 1622, 1596, 1556, 1497, 1405, 1373, 1339, 1261, 1205, 1143, 1076, 990, 907, 779 cm^{-1}. HRMS (ESI+) *m/z* 414.2379 (414.2369 calculated for $C_{21}H_{33}N_3O_4Na^+$ $[M + Na]^+$)

5-((2*Z*,4*E*)-5-(diethylamino)-2-hydroxypenta-2,4-dien-1-ylidene)-1,3-dioctylpyrimidine-2,4,6(1*H*,3*H*,5*H*)-trione (72): Following General Procedure A, the title compound was obtained as a purple solid (453 mg, 90%). ^1H NMR (600 MHz, CD_2Cl_2) δ 12.56 (s, 1H), 7.28 (d, *J* = 12.2 Hz, 1H), 7.06 (s, 1H), 6.79 (d, *J* = 12.4 Hz, 1H), 6.07 (t, *J* = 12.3 Hz, 1H), 3.92 – 3.81 (m, 4H), 3.49 (dq, *J* = 24.7, 7.2 Hz, 4H), 1.57 (dt, *J* = 18.5, 7.4 Hz, 4H), 1.28 (m, 26H), 0.87 (td, *J* = 7.0, 2.1 Hz, 6H). ^{13}C NMR (125 MHz, CD_2Cl_2) δ 165.5, 163.3, 157.4, 151.8, 151.3, 146.8, 138.7, 103.0, 98.8, 52.5, 42.1, 32.4, 30.0, 29.9, 28.8, 27.6, 23.2, 14.4. IR (ATR) 2956, 2923, 2854, 1691, 1620, 1595, 1556, 1492, 1454, 1403, 1370, 1337, 1260, 1198, 1074, 989, 907, 779 cm^{-1}. HRMS (ESI+) *m/z* 526.3612 (526.3621 calculated for $C_{29}H_{49}N_3O_4Na^+$ $[M + Na]^+$).

(E/Z)-5-((2Z,4E)-5-(diethylamino)-2-hydroxypenta-2,4-dien-1-ylidene)-1-methyl-3-octylpyrimidine-2,4,6(1H,3H,5H)-trione (74): Following General Procedure A, the title compound was obtained as a dark purple solid (90 mg, 65 %). ^{1}H NMR (500 MHz, CD_2Cl_2) δ 12.53 (dd, *J* = 28.6, 1.3 Hz, 1H), 7.29 (dd, *J* = 12.2, 1.2 Hz, 1H), 7.06 (s, 1H), 6.81 (ddd, *J* = 12.3, 2.8, 1.5 Hz, 1H), 6.08 (t, *J* = 12.3 Hz, 1H), 3.93 – 3.81 (m, 2H), 3.49 (dq, *J* = 21.1, 7.2 Hz, 4H), 3.27 (d, *J* = 14.2 Hz, 3H), 1.63 – 1.52 (m, 2H), 1.30 (m, 16H), 0.88 (td, *J* = 7.0, 2.0 Hz, 3H). ^{13}C NMR (125 MHz, CD_2Cl_2) δ 165.7, 165.4, 163.6, 163.2, 157.6, 152.1, 151.6, 146.7, 146.7, 138.4, 103.2, 98.4, 52.5, 44.7, 42.1, 42.0, 32.4, 30.0, 29.9, 29.9, 29.8, 28.8, 28.7, 28.5, 28.4, 27.6, 27.5, 23.2, 14.8, 14.4, 12.7. IR (ATR) 2925, 2854, 1692, 1621, 1596, 1557, 1495, 1461, 1425, 1406, 1371, 1352, 1261, 1229, 1203, 1150, 1074, 989, 909, 838, 777, 729, 685. HRMS (ESI+) *m/z* 428.2524 (428.2525 calculated for $C_{22}H_{35}N_3O_4Na^+$ $[M + Na]^+$).

5-((2*Z*,4*E*)-5-(diethylamino)-2-hydroxypenta-2,4-dien-1-ylidene)-1,3-diphenylpyrimidine-2,4,6(1*H*,3*H*,5*H*)-trione (76): Following General Procedure A, the title compound was obtained as a purple solid (371 mg, 86%). ^{1}H NMR (600 MHz, CD_2Cl_2) δ 12.19 (s, 1H), 7.52 – 7.24 (m, 11H), 7.02 (s, 1H), 6.92 (dd, *J* = 12.6, 1.5 Hz, 1H), 6.16 (t, *J* = 12.4 Hz, 1H), 3.50 (dq, *J* = 36.5, 7.3 Hz, 4H), 1.30 (dt, *J* = 10.2, 7.2 Hz, 6H). ^{13}C NMR (150 MHz, CD_2Cl_2) δ 165.1, 163.2, 158.7, 153.2, 151.2, 146.3, 136.7, 136.3, 135.6, 129.0, 129.0, 128.9, 128.8, 128.5, 128.2, 128.0, 103.9, 96.5, 52.2, 44.5, 14.1, 12.2. IR(ATR) 3398, 2976, 2927, 1691, 1623, 1583, 1491, 1453, 1430, 1367, 1348, 1254, 1223, 1181, 1115, 1071, 986, 958, 883, 751, 692 cm^{-1}. HRMS (ESI+) *m/z* 454.1735 (454.1743 calculated for $C_{25}H_{25}N_3O_4Na^+$ $[M + Na]^+$).

5-((2*Z*,4*E*)-5-(diethylamino)-2-hydroxypenta-2,4-dien-1-ylidene)-1,3-bis(4-methoxyphenyl)pyrimidine-2,4,6(1*H*,3*H*,5*H*)-trione (78): Following General Procedure A, the title compound was obtained as a purple solid (398 mg, 81%). ^{1}H NMR (600 MHz, CD_2Cl_2) δ 12.21 (s, 1H), 7.35 (d, *J* = 12.1 Hz, 1H), 7.17 (dd, *J* = 19.5, 8.8 Hz, 4H), 7.03 (s, 1H), 6.97 (t, *J* = 9.1 Hz, 4H), 6.90 (dd, *J* = 12.7, 1.5 Hz, 1H), 6.14 (t, *J* = 12.3 Hz, 1H), 3.83 (d, *J* = 3.4 Hz, 6H), 3.51 (dq, *J* = 28.3, 7.2 Hz, 4H), 1.34 – 1.27 (m, 6H). ^{13}C NMR (125 MHz, CD_2Cl_2) δ 165.3, 163.3, 159.3, 159.1, 158.2, 152.7, 151.6, 146.3, 136.4, 129.9, 129.2, 128.8, 114.1, 103.6, 96.9, 55.4, 52.2, 44.4, 14.1, 12.2. IR(ATR) 3444, 2984, 2928, 2837, 1697, 1587, 1508, 1462, 1432, 1368, 1349, 1244, 1181, 1143, 1117, 1073, 1026, 987, 961, 828, 769, 748 cm^{-1}. HRMS (ESI+) *m/z* 514.1949 (514.1954 calculated for $C_{27}H_{29}N_3O_6Na^+$ $[M + Na]^+$).

1,3-bis(4-chlorophenyl)-5-((2*Z*,4*E*)-5-(diethylamino)-2-hydroxypenta-2,4-dien-1-ylidene)pyrimidine-2,4,6(1*H*,3*H*,5*H*)-trione (80): Following General Procedure A, the title compound was obtained as a purple solid (445 mg, 89%). ^{1}H NMR (600 MHz, CD_2Cl_2) δ 12.08 (s, 1H), 7.44 (dd, *J* = 11.2, 8.5 Hz, 4H), 7.40 (d, *J* = 12.1 Hz, 1H), 7.24 (dd, *J* = 18.5, 8.6 Hz, 4H), 6.97 (s, 1H), 6.93 (dd, *J* = 12.8, 1.4 Hz, 1H), 6.20 (t, *J* = 12.4 Hz, 1H), 3.54 (dq, *J* = 25.9, 7.3 Hz, 4H), 1.32 (dt, *J* = 18.1, 7.2 Hz, 6H). ^{13}C NMR (125 MHz, CD_2Cl_2) δ 163.4, 159.6, 154.4, 151.5, 146.9, 135.5, 134.3, 131.1, 131.0, 129.6, 129.6, 104.9, 96.6, 54.4, 53.0, 45.3, 14.7, 12.8. IR(ATR) 3468, 3007, 2986, 2928, 1701, 1625, 1589, 1489, 1461, 1430, 1366, 1347, 1275, 1258, 1224, 1181, 1142, 1116, 1073, 1014, 959, 824, 810, 765, 750 cm^{-1}. HRMS (ESI+) *m/z* 522.0953 (522.0963 calculated for $C_{25}H_{23}N_3O_4Cl_2Na^+$ $[M + Na]^+$).

General Procedure B: Photo-isomerization of Stenhouse adducts to cyclopentenones: Stenhouse adduct is suspended in methanol (0.04 M). The reaction mixture is irradiated with a GE Crystal Clear 200 bulb (200 watt, 3780 lumens) placed approximately 10 inches from the reaction vessel at ambient temperature with stirring for 12 hours. The reaction mixture is then cooled to 0 ^{o}C for 20 minutes, then filtered to collect the precipitated solid; the solid is washed with cold diethyl ether, and dried *in vacuo* to afford the title compounds.

2,2-dimethyl-4-oxo-5-(2-oxo-5-(pyrrolidin-1-ium-1-yl)cyclopent-3-en-1-yl)-4H-1,3-dioxin-6-olate (89): Following General Procedure B, the title compound was obtained as a white solid (87.8 mg, 82%). ^{1}H NMR (600 MHz, D_2O) δ 7.87 (d, *J* = 6.1 Hz, 1H), 6.67 (d, *J* = 6.0 Hz, 1H), 4.57 (s, 1H), 3.66-3.41 (b, 4H), 3.56 (d, *J* = 3.1 Hz, 1H), 2.12 (b, 4H), 1.68 (s, 6H). ^{13}C NMR (150 MHz, D_2O) δ 208.4, 155.1, 137.6, 103.7, 72.3, 69.1, 52.6, 46.6, 24.5, 22.7. IR (KBr) 3410, 3090, 3036, 2985, 2908, 2584, 2411, 1715, 1667, 1574, 1490, 1471, 1412, 1393, 1371, 1346, 1323, 1289, 1263, 1216, 1198, 1162, 1134, 1116, 1066, 1035, 1006 cm^{-1}. HRMS (ESI+) *m/z* 316.1154 (316.1161 calculated for $C_{15}H_{19}NO_5Na^+$ $[M + Na]^+$).

2,2-dimethyl-4-oxo-5-(2-oxo-5-(piperidin-1-ium-1-yl)cyclopent-3-en-1-yl)-4H-1,3-dioxin-6-olate (91): Following General Procedure B, the title compound was obtained as a white solid (108 mg, 88%). ^{1}H NMR (500 MHz, D_2O) δ 7.86 (dd, *J* = 6.1, 1.8 Hz, 1H), 6.65 (dd, *J* = 6.1, 1.4 Hz, 1H), 4.62 – 4.52 (m, 1H), 3.58 – 2.94 (m, 4H), 2.24 – 1.71 (m, 6H), 1.67 (s, 6H). ^{13}C NMR (125 MHz, D_2O) δ 208.4, 154.5, 137.6, 103.7, 73.0, 70.7, 44.3, 24.5, 23.1, 21.1. IR (KBr) 3420, 3049, 2989, 2968, 2940, 2877, 2645, 2327, 2274, 1717, 1682, 1576, 1521, 1469, 1446, 1413, 1375, 1365, 1345, 1330, 1321, 1291, 1261, 1235, 1215, 1201, 1190, 1179, 1149, 1116, 1081, 1048, 1038, 1005 cm^{-1}. HRMS (ESI+) *m/z* 330.1318

(330.1317 calculated for $C_{16}H_{21}NO_5Na^+$ $[M + Na]^+$). Due to it's sparing solubility in D_2O, and reversion to **17** in organic solvents, the structure of **72** was confirmed by single crystal x-ray analysis. The crystal structure data for **2,2-dimethyl-4-oxo-5-(2-oxo-5-(piperidin-1-ium-1-yl)cyclopent-3-en-1-yl)-4H-1,3-dioxin-6-olate** (**91**) can be obtained free of charge from the Cambridge Crystallographic Data Centre via www.ccdc.cam.ac.uk/data_request/cif CCDC 844845

5-(2-(benzyl(methyl)ammonio)-5-oxocyclopent-3-en-1-yl)-2,2-dimethyl-4-oxo-4H-1,3-dioxin-6-olate (99): Following General Procedure B, the title compound was obtained as a white solid (137 mg, 80%). ^{1}H NMR (500 MHz, D_2O) δ 7.86 (s, 1H), 7.51 (m, 5H), 6.69 (dd, *J* = 6.1, 1.9 Hz, 1H), 4.22 (s, 1H), 3.76 (d, *J* = 3.6 Hz, 1H), 2.87 (s, 3H), 2.73 (s, 2H), 1.67 (m, 6H). ^{13}C NMR (125 MHz, D_2O) δ 208.1, 138.04, 130.6, 130.2, 129.6, 129.6, 129.4, 129.2, 129.0, 105.0, 103.8, 52.3, 32.0, 30.2, 25.1, 24.5. IR (KBr) 3080, 3037, 2988, 2938, 2901, 2646, 2461, 1726, 1717, 1673, 1576, 1498, 1476, 1458, 1415, 1375, 1349, 1290, 1262, 1212, 1199, 1173, 1159, 1120, 1040 cm^{-1}. HRMS (ESI+) *m/z* 366.1320 (366.1317 calculated for $C_{19}H_{21}NO_5Na^+$ $[M +Na]^+$). Due to it's sparing solubility in D_2O, and reversion in organic solvents, the structure of **99** was confirmed by single crystal x-ray analysis. The crystal structure data for **5-(2-(benzyl(methyl)ammonio)-5-oxocyclopent-3-en-1-yl)-2,2-dimethyl-4-oxo-4H-1,3-dioxin-6-olate (99)** can be obtained free of charge from the Cambridge Crystallographic Data Centre via www.ccdc.cam.ac.uk/data_request/cif CCDC 851860

2,2-dimethyl-4-oxo-5-(2-oxo-5-(1,2,3,4-tetrahydroisoquinolin-2-ium-2-yl)cyclopent-3-en-1-yl)-4H-1,3-dioxin-6-olate (100): Following General Procedure B, the title compound

was obtained as a white solid (151 mg, 85%). ^{1}H NMR (500 MHz, D_2O) δ 7.96 (dd, *J* = 6.1, 2.0 Hz, 1H), 7.37 – 7.27 (m, 3H), 7.21 – 7.15 (m, 1H), 6.68 (dd, *J* = 6.2, 1.9 Hz, 1H), 4.71 (s, 1H), 3.70 (d, *J* = 3.4 Hz, 1H), 3.62 (dq, *J* = 12.3, 6.3 Hz, 1H), 3.54 (t, *J* = 6.6 Hz, 1H), 3.21 (q, *J* = 6.4 Hz, 2H), 3.13 (t, *J* = 6.4 Hz, 1H), 3.02 (t, *J* = 6.7 Hz, 1H), 1.67 (s, 6H). ^{13}C NMR (125 MHz, D_2O) δ 207.3, 155.2, 137.6, 133.1, 128.7, 128.2, 128.0, 127.7, 127.0, 126.8, 126.6, 103.7, 69.5, 51.4, 47.9, 44.8, 41.6, 25.1, 24.5. IR (KBr) 3433, 3019, 2994, 2944, 2722, 2509, 2400, 1926, 1726, 1667, 1568, 1504, 1479, 1457, 1440, 1426, 1411, 1394, 1373, 1346, 1323, 1288, 1275, 1259, 1231, 1200, 1181, 1152, 1115, 1087, 1070, 1056, 1026, 1008 cm^{-1}. HRMS (ESI+) *m/z* 378.1314 (378.1317 calculated for $C_{20}H_{21}NO_5Na^+$ $[M+Na]^+$). Due to it's sparing solubility in D_2O, and reversion in organic solvents, the structure of **100** was confirmed by single crystal x-ray analysis. The crystal structure data for **2,2-dimethyl-4-oxo-5-(2-oxo-5-(1,2,3,4-tetrahydroisoquinolin-2-ium-2-yl)cyclopent-3-en-1-yl)-4H-1,3-dioxin-6-olate** (**100**) can be obtained free of charge from the Cambridge Crystallographic Data Centre via www.ccdc.cam.ac.uk/data_request/cif CCDC 844846

1,3-dimethyl-2,6-dioxo-5-(2-oxo-5-(pyrrolidin-1-ium-1-yl)cyclopent-3-en-1-yl)-1,2,3,6-tetrahydropyrimidin-4-olate (104): Following General Procedure B, the title compound was obtained as a white solid (235 mg, 77%). ^{1}H NMR (600 MHz, D_2O) δ 7.85 (dd, *J* = 5.8, 1.8 Hz, 1H), 6.67 (dd, *J* = 6.3, 1.6 Hz, 1H), 4.53 (d, *J* = 1.9 Hz, 1H), 3.78 (d, *J* = 3.4 Hz, 1H), 3.48 (s, 4H), 3.20 (d, *J* = 61.7 Hz, 6H), 2.06 (s, 4H). ^{13}C NMR (125 MHz, D_2O) δ 208.7, 164.4, 163.7, 154.8, 154.1, 137.7, 85.5, 69.1, 52.4, 46.9, 28.0, 27.2, 22.8. IR (ATR) 3006, 2990, 2747, 2619, 1716, 1667, 1567, 1435, 1361, 1275, 1260, 1189, 750 cm^{-1}. HRMS (ESI+) *m/z* 328.1273 (328.1273 calculated for $C_{15}H_{19}N_3O_4Na^+$ $[M+Na]^+$).

1,3-dimethyl-2,6-dioxo-5-(2-oxo-5-(piperidin-1-ium-1-yl)cyclopent-3-en-1-yl)-1,2,3,6-tetrahydropyrimidin-4-olate (105): Following General Procedure B, the title compound was obtained as a white solid (259 mg, 81%). ^{1}H NMR (600 MHz, D_2O) δ 7.69 (dd, *J* = 6.2, 2.0 Hz, 1H), 6.50 (dd, *J* = 6.3, 1.9 Hz, 1H), 4.46 – 4.32 (m, 1H), 3.71 (d, *J* = 3.6 Hz, 1H), 3.49 – 2.85 (m, 10H), 1.93 – 1.24 (m, 6H). ^{13}C NMR (125 MHz, D_2O) δ 208.7, 164.4, 163.8, 154.3, 154.1, 137.5, 86.1, 70.7, 67.8, 50.8, 44.7, 23.0, 22.1, 21.4, 21.1. IR(ATR) 3006, 2989, 2918, 2861, 1718, 1673, 1604, 1575, 1473, 1440, 1370, 1319, 1275, 1260, 1191, 1153, 1117, 1016, 951, 707 cm^{-1}. HRMS (ESI+) *m/z* 342.1424 (324.1430 calculated for $C_{16}H_{21}N_3O_4Na^+$ $[M + Na]^+$).

1,3-dimethyl-2,6-dioxo-5-(2-oxo-5-(1,2,3,4-tetrahydroisoquinolin-2-ium-2-yl)cyclopent-3-en-1-yl)-1,2,3,6-tetrahydropyrimidin-4-olate (112): Following General Procedure B, the title compound was obtained as a white solid (320 mg, 87%). ^{1}H NMR (600 MHz, D_2O) δ 7.84 (dd, *J* = 6.3, 1.9 Hz, 1H), 7.20 – 7.00 (m, 3H), 6.89 – 6.75 (m, 1H), 6.55 (dd, *J* = 6.2, 1.9 Hz, 1H), 4.59 (dt, *J* = 3.8, 2.0 Hz, 1H), 4.45 – 4.29 (m, 2H), 3.78 (d, *J* = 3.6 Hz, 1H), 3.67 (dt, *J* = 11.9, 5.7 Hz, 1H), 3.57 (dt, *J* = 5.5, 2.0 Hz, 1H), 3.19 – 2.78 (m, 8H). ^{13}C NMR (125 MHz, D_2O) δ 208.0, 164.4, 163.6, 153.9, 153.7, 137.8, 130.2, 128.9, 128.7, 128.4, 128.0, 126.8, 126.5, 85.5, 67.8, 51.3, 47.7, 45.8, 28.0, 27.1. IR (ATR) 3006, 2989, 1716, 1668, 1568, 1435, 1374, 1318, 1275, 1260, 1187, 1062, 967, 907, 824, 764, 750 cm^{-1}. HRMS (ESI+) *m/z* 390.1418 (390.1430 calculated for $C_{20}H_{21}N_3O_4Na^+$ $[M + Na]^+$).

2-(2-(furan-2-ylmethylene)-3-oxo-2,3-dihydro-1*H*-inden-1-ylidene)malononitrile (64): Following the procedure out lined by Bello et al.,[3] the title compound was isolated as a bright orange solid (882 mg, 81%). ^{1}H NMR (500 MHz, $CDCl_3$) δ 8.73 – 8.68 (m, 2H), 8.57

(s, 1H), 7.93 (dd, *J* = 7.5, 1.5 Hz, 1H), 7.84 (d, *J* = 1.6 Hz, 1H), 7.82 – 7.74 (m, 2H), 6.80 – 6.75 (m, 1H). ^{13}C NMR (125 MHz, $CDCl_3$) δ 187.1, 160.5, 150.9, 150.2, 139.8, 137.3, 135.3, 134.8, 130.4, 127.3, 125.4, 124.4, 124.0, 115.5, 114.2, 113.8, 71.2. IR (ATR): 3166, 3147, 3129, 3079, 2218, 1708, 1595, 1576, 1543, 1451, 1357, 1231, 1146, 1091, 1025, 933, 764, 718 cm^{-1}. HRMS (EI+) *m/*z 272.0589 (272.0586 calculated for $C_{17}H_8N_2O_2$ $[M]^+$).

3-(diethylamino)-1-(furan-2-yl)-9-oxo-2,9-dihydro-1*H*-indeno[2,1-*c*]pyridine-4-carbonitrile (65): Following General Procedure A the title compound was isolated as a dark blue solid (332 mg, 96%). ^{1}H NMR (600 MHz, CD_2Cl_2) δ 8.36 (d, *J* = 7.6 Hz, 1H), 7.61 – 7.40 (m, 4H), 7.31 (s, 1H), 6.95 (d, *J* = 12.8 Hz, 1H), 6.32 (s, 1H), 5.33 (s, 1H), 3.59 (dq, *J* = 29.4, 7.3 Hz, 4H), 1.36 (dt, *J* = 14.6, 7.3 Hz, 6H). ^{13}C NMR (125 MHz, CD_2Cl_2) δ 191.7, 160.0, 159.8, 152.8, 148.4, 141.1, 136.6, 133.7, 132.2, 127.3, 123.8, 122.1, 118.2, 118.1, 113.4, 106.3, 53.2, 45.7, 14.6, 12.9. IR(ATR): 3325, 2979, 2935, 2874, 2196, 2179, 1666, 1616, 1602, 1579, 1498, 1436, 1367, 1344, 1243, 1185, 1111, 1068, 974, 912, 821, 759, 712 cm^{-1}. HRMS (EI+) *m/*z 345.1483 (345.1477 calculated for $C_{21}H_{19}N_3O_2$ $[M]^+$).

2,2'-(2-(furan-2-ylmethylene)-1*H*-indene-1,3(2*H*)-diylidene)dimalononitrile (67): Following the procedure out lined by Bello et al.,[3] the title compound was isolated as a bright orange solid (1.17 g, 91%). ^{1}H NMR (600 MHz, $CDCl_3$) δ 8.62 (d, *J* = 7.8 Hz, 1H), 8.51 (d, *J* = 7.8 Hz, 1H), 8.21 (s, 1H), 7.91 – 7.70 (m, 3H), 7.24 (d, *J* = 3.6 Hz, 1H), 6.72 (dd, *J* = 3.9, 1.8 Hz, 1H). ^{13}C NMR (150 MHz, $CDCl_3$) δ 161.7, 160.7, 149.7, 148.6, 138.3, 136.6, 135.3, 134.6, 127.8, 127.4, 126.7, 126.2, 125.3, 115.3, 113.3, 113.1, 112.1, 78.8, 71.9. IR(ATR): 3139, 3121, 2222, 1608, 1551, 1527, 1460, 1396, 1349, 1025, 880, 772. 715 cm^{-1}. HRMS (EI+) *m/*z 320.0693 (320.0698 calculated for $C_{20}H_8N_4O$ $[M]^+$).

2-(4-cyano-3-(diethylamino)-1-(furan-2-yl)-1,2-dihydro-9*H*-indeno[2,1-*c*]pyridin-9-ylidene)malononitrile (68): Following General Procedure A the title compound was isolated as a dark blue solid (315 mg, 80%). ^{1}H NMR (600 MHz, CD_2Cl_2) δ 8.19 – 8.09 (m, 2H), 7.42 – 7.34 (m, 3H), 6.49 (s, 1H), 6.36 – 6.30 (m, 2H), 6.20 (d, *J* = 3.3 Hz, 1H), 3.63 (ddt, *J* = 42.7, 15.2, 7.5 Hz, 4H), 1.31 (t, *J* = 7.1 Hz, 6H). ^{13}C NMR (125 MHz, CD_2Cl_2) δ 158.1, 155.6, 155.2, 152.9, 144.0, 137.9, 137.6, 131.4, 130.8, 124.0, 123.1, 119.2, 117.5, 116.9, 111.0, 108.4, 48.0, 46.2, 30.3, 13.6. IR(ATR) 3312, 3108, 2937, 2206, 2188, 1581, 1546, 1504, 1396, 1380, 1347, 1242, 1219, 1164, 1143, 1079, 1015, 920, 882, 749 cm^{-1}. HRMS (EI+) *m/z* 393.1583 (393.1590 calculated for $C_{24}H_{19}N_5O$ $[M]^+$).

1,3-dibutyl-5-(furan-2-ylmethylene)pyrimidine-2,4,6(1H,3H,5H)-trione (69): Following the procedure outlined by Deb and Bhuyan,[2] the title compound was obtained as a pale yellow solid (10.93g, 63%) ^{1}H NMR (500 MHz, $CDCl_3$) δ 8.62 (d, *J* = 3.8 Hz, 1H), 8.41 (d, *J* = 0.7 Hz, 1H), 7.83 (dd, *J* = 1.7, 0.6 Hz, 1H), 6.72 (ddd, *J* = 3.8, 1.6, 0.8 Hz, 1H), 4.04 – 3.87 (m, 4H), 1.75 – 1.51 (m, 4H), 1.50 – 1.29 (m, 4H), 0.95 (td, *J* = 7.4, 3.4 Hz, 6H). ^{13}C NMR (125 MHz, $CDCl_3$) δ 162.4, 160.8, 151.4, 151.1, 150.4, 141.0, 128.0, 115.2, 112.1, 42.5, 41.8, 30.4, 30.3, 20.4, 20.4, 14.0, 14.0. IR (ATR) 3120, 2957, 2933, 2873, 1724, 1659, 1578, 1445, 1428, 1409, 1376, 1308, 1250, 1203, 1157, 1128, 1091, 1036, 1022, 962, 915, 884, 791, 760, 734 cm^{-1}. HRMS (ESI+) *m/z* 341.1479 (341.1477 calculated for $C_{17}H_{22}N_2O_4Na^+$ $[M + Na]^+$).

5-(furan-2-ylmethylene)-1-methyl-3-octylpyrimidine-2,4,6(1H,3H,5H)-trione (73): 1-methyl-3-octylpyrimidine-2,4,6(1H,3H,5H)-trione: A solution of methylamine-HCl (0.12 g, 1.79 mmol) in anhydrous DCM (15 mL) was treated with n-octyl isocyanate (0.30 mL, 1.70

mmol) under argon. Triethylamine (0.35 mL, 2.56 mmol) was then added and the mixture was heated to reflux. After 1 h, malonyl dichloride (0.17 mL, 1.70 mmol) was added under argon and heated to reflux for an additional hour. The mixture was cooled to rt and quenched with 1N HCl. The crude product was extracted with DCM (3 x 10 mL), washed with H_2O (10 mL), dried over $MgSO_4$ and filtered. The solvent was removed in vacuo and the product was purified by column chromatography (hexane:EtOAc= 9:1 to 1:1) to afford clear oil (302 mg, 67%). ^{1}H NMR (500 MHz, $CDCl_3$) δ 3.91 – 3.78 (m, 2H), 3.65 (s, 2H), 3.29 (s, 3H), 1.62 – 1.52 (m, 2H), 1.34 – 1.18 (m, 10H), 0.86 (t, *J* = 7.0 Hz, 3H). ^{13}C NMR (125 MHz, $CDCl_3$) δ 165.0, 164.7, 151.8, 42.4, 39.7, 32.0, 29.4, 29.3, 28.6, 28.2, 27.0, 22.8, 14.3. IR (ATR) 2956, 2924, 2855, 1685, 1519, 1433, 1409, 1389, 1364, 1334, 1268, 1168, 1121, 1005, 936, 758, 723, 685 cm^{-1}. HRMS (EI+) *m/z* 254.1641 (254.1630 calculated for $C_{13}H_{22}N_2O_3^+$ $[M]^+$). This material was subjected to the conditions of Deb and Bhuyan[2] to give the title compound as a pale yellow solid (228 mg, 83%) ^{1}H NMR (500 MHz, $CDCl_3$) δ 8.63 (d, *J* = 3.7 Hz, 1H), 8.42 (s, 1H), 7.84 (d, *J* = 1.5 Hz, 1H), 6.72 (ddd, *J* = 3.9, 1.8, 0.9 Hz, 1H), 3.98 – 3.92 (m, 2H), 3.40 (s, 3H), 1.68 – 1.61 (m, 2H), 1.39 – 1.24 (m, 10H), 0.89 – 0.85 (m, 3H). ^{13}C NMR (125 MHz, $CDCl_3$) δ 162.7, 160.7, 151.4, 151.3, 150.4, 141.1, 128.1, 115.3, 111.9, 42.1, 32.0, 29.5, 29.4, 29.1, 28.3, 27.2, 22.8, 14.3. IR (ATR) 3145, 2915, 2851, 1728, 1658, 1575, 1543, 1450, 1423, 1407, 1366, 1327, 1252, 1201, 1166, 1129, 1115, 1095, 1029, 988, 962, 921, 882, 789, 756, 719 cm^{-1}. HRMS (ESI+) *m/z* 355.1627 (355.1634 calculated for $C_{18}H_{24}N_2O_4Na^+$ $[M + Na]^+$)

5-(furan-2-ylmethylene)-1,3-diphenylpyrimidine-2,4,6(1*H*,3*H*,5*H*)-trione (75): Following the procedure out lined by Deb and Bhuyan,[2] the title compound was isolated as a bright yellow solid (1.22 g, 85%). ^{1}H NMR (600 MHz, $CDCl_3$) δ 8.66 (d, *J* = 3.9 Hz, 1H), 8.59 (s,

1H), 7.88 (d, *J* = 1.5 Hz, 1H), 7.56 – 7.41 (m, 6H), 7.36 – 7.30 (m, 4H), 6.71 (ddd, *J* = 3.9, 1.7, 0.8 Hz, 1H). ^{13}C NMR (150 MHz, $CDCl_3$) δ 162.5, 151.3, 151.1, 142.4, 135.0, 134.7, 129.5, 129.4, 129.2, 129.1, 128.8, 128.6, 115.6, 111.4. IR (ATR) 3348, 3146, 3124, 3070, 1736, 1668, 1570, 1490, 1455, 1416, 1356, 1326, 1236, 1199, 1149, 1030, 948, 882, 786, 691 cm^{-1}. HRMS (ESI+) *m/z* 381.0851 (381.0851 calculated for $C_{21}H_{14}N_2O_4Na^+$ $[M + Na]^+$).

5-(furan-2-ylmethylene)-1,3-bis(4-methoxyphenyl)pyrimidine-2,4,6(1*H*,3*H*,5*H*)-trione (66): Following the procedure out lined by Deb and Bhuyan,[2] the title compound was isolated as a bright yellow solid (1.46 g, 87%). ^{1}H NMR (600 MHz, $CDCl_3$) δ 8.66 (d, *J* = 3.9 Hz, 1H), 8.57 (s, 1H), 7.86 (d, *J* = 1.6 Hz, 1H), 7.25 – 7.20 (m, 4H), 7.04 – 6.98 (m, 4H), 6.70 (ddd, *J* = 4.0, 1.6, 0.8 Hz, 1H), 3.84 (d, *J* = 2.6 Hz, 6H). ^{13}C NMR (150 MHz, $CDCl_3$) δ 162.8, 161.3, 159.9, 159.8, 151.3, 151.2, 151.0, 142.3, 129.7, 129.6, 129.3, 127.6, 127.2, 115.5, 114.8, 114.7, 111.6, 55.6. IR (ATR) 3139, 3116, 3002, 2964, 2835, 1733, 1674, 1607, 1568, 1509, 1455, 1349, 1325, 1239, 1156, 1027, 951, 828, 808, 779, 752 cm^{-1}. HRMS (ESI+) *m/z* 441.1049 (441.1063 calculated for $C_{23}H_{18}N_2O_6Na^+$ $[M + Na]^+$).

1,3-bis(4-chlorophenyl)-5-(furan-2-ylmethylene)pyrimidine-2,4,6(1*H*,3*H*,5*H*)-trione (68): Following the procedure out lined by Deb and Bhuyan,[2] the title compound was isolated as a bright yellow solid (1.32 g, 77%). ^{1}H NMR (600 MHz, $CDCl_3$) δ 8.57 (d, *J* = 3.8 Hz, 1H), 8.49 (s, 1H), 7.81 (d, *J* = 1.5 Hz, 1H), 7.39 (dd, *J* = 13.3, 8.6 Hz, 4H), 7.17 (dd, *J* = 12.5, 8.6 Hz, 4H), 6.70 – 6.61 (m, 1H). ^{13}C NMR (150 MHz, $CDCl_3$) δ 162.2, 160.7, 151.7, 151.2, 150.4, 142.8, 135.2, 135.1, 133.3, 133.0, 130.2, 130.0, 130.0, 129.8, 129.7, 115.8, 110.8. IR(ATR) 3136, 3118, 2925, 2855, 1735, 1672, 1564, 1489, 1454, 1418, 1399, 1346,

1324, 1233, 1154, 1087, 1028, 1014, 949, 920, 826, 801, 783, 751 cm^{-1}. HRMS (ESI+) *m/z* 449.0066 (449.0072 calculated for $C_{21}H_{12}N_2O_4Cl_2Na^+$ $[M + Na]^+$).

"On water" synthesis of DASAs:

General Procedure C: The active methylene compound (1 mmol, 1 eq) was suspended in 20 mL DI H_2O. To this suspension was added 2-furaldehyde (1 mmol, 1 eq). The reaction mixture was stirred at the temperature indicated in Scheme 3 of the main text, for two hours, developing a bright yellow precipitate. The reaction mixture was then cooled to room temperature if necessary. The secondary amine (1 mmol, 1 eq) was then added, neat, to the reaction mixture, rapidly converting the precipitate from yellow to red or purple. This mixture was stirred at room temperature for two hours. The reaction was diluted with 10 mL 1M HCl, and 30 mL of dichloromethane, and stirred for 10 min. The organic layer was separated and the aqueous layer extracted twice with 30 mL fresh dichloromethane. The organics were combined, dried over MgSO4, and evaporated in vacuo to give the target DASA. If necessary the target can be purified by column chromatography (SiO_2) eluting with a gradient from 100% DCM to 9:1 DCM:MeOH.

Considerations: If the amine nucleophile employed contains fewer than 6 carbons, the DASA is prone to adopting its zwitterionic form, hindering isolation as described in **General Procedure C**. In these instances, in lieu of the above work-up procedure, the resulting heterogeneous reaction mixture is stripped of water by evaporation. The resulting residue is dissolved in hot DCM, and after cooling to room temperature, concentrated then purified by chromatography as described above.

5-(3-azido-2-oxo-5-(piperidin-1-yl)cyclopent-3-en-1-yl)-6-hydroxy-2,2-dimethyl-4H-1,3-dioxin-4-one (25): 5-((3-azidofuran-2-yl)methylene)-2,2-dimethyl-1,3-dioxane-4,6-dione (86): 3-azidofuran-2-carbaldehyde, prepared by reaction of sodium azide with 3-bromofuran-2-carbaldehyde according to the procedure of Gronowitz et al.,[4] was reacted with Meldrum's acid according to the procedure of Bigi, et al. to afford 5-((3-azidofuran-2-yl)methylene)-2,2-dimethyl-1,3-dioxane-4,6-dione as a pale yellow solid.[1] According to General Procedure A, 5-((3-azidofuran-2-yl)methylene)-2,2-dimethyl-1,3-dioxane-4,6-dione (42 mg, 0.16 mmol, 1 eq) was dissolved in 5 mL tetrahydrofuran. To this solution was added piperidine (19 mL, 16 mg, 0.2 mmol, 1.2 eq). The mixture was stirred at 23 ^{o}C for 10 minutes followed by cooling at 0 ^{o}C for 20 minutes. The reaction mixture was then filtered to collect the precipitated solid, the solid was washed with cold diethyl ether, and dried *in vacuo* to afford 5-(3-azido-2-oxo-5-(piperidin-1-yl)cyclopent-3-en-1-yl)-6-hydroxy-2,2-dimethyl-4H-1,3-dioxin-4-one **86** (42 mg, 75%) as a white solid. ^{1}H NMR (600 MHz, d_2o) δ 5.85 (d, *J* = 3.0 Hz, 1H), 3.65 (s, 1H), 2.74 (d, *J* = 3.8 Hz, 1H), 2.49 (d, *J* = 12.2 Hz, 1H), 2.11 (d, *J* = 11.3 Hz, 1H), 1.70 (t, *J* = 12.3 Hz, 1H), 0.87 (d, *J* = 13.2 Hz, 2H), 0.73 (s, 0H), 0.66 (d, *J* = 38.1 Hz, 6H), 0.40 – 0.23 (m, 1H). ^{13}C NMR (151 MHz, d_2o) δ 194.42, 169.58, 168.19, 164.52, 163.60, 143.42, 127.34, 106.86, 66.34, 65.27, 64.70, 63.96, 52.07, 47.71, 43.34, 42.29, 21.36. IR (KBr) 3438, 3058, 2988, 2943, 2866, 2661, 2518, 2412, 2119, 1729, 1668, 1632, 1571, 1473, 1457, 1413, 1391, 1375, 1348, 1333, 1295, 1259, 1216, 1198, 1177, 1146, 1121, 1059, 1022 cm^{-1}. MS (ESI) *m/z* 349.16 (349.14 calcd for $C_{16}H_{21}N_4O_5^+$ [M +H]$^+$). **86** was characterized by single crystal x-ray analysis, the crystal structure data for **5-(3-azido-2-oxo-5-(piperidin-1-yl)cyclopent-3-en-1-yl)-6-hydroxy-2,2-dimethyl-4H-1,3-**

dioxin-4-one (86) can be obtained free of charge from the Cambridge Crystallographic Data Centre via www.ccdc.cam.ac.uk/data_request/cif CCDC 851859

5-(3-bromo-2-oxo-5-(piperidin-1-yl)cyclopent-3-en-1-yl)-6-hydroxy-2,2-dimethyl-4H-1,3-dioxin-4-one (88): 3-bromofuran-2-carbaldehyde, prepared by formylation of 3-bromofuran, was reacted with Meldrum's acid according to the procedure of Bigi, et al. to afford 5-((3-bromofuran-2-yl)methylene)-2,2-dimethyl-1,3-dioxane-4,6-dione as a pale yellow solid.[1] According to General Procedure A, 5-((3-bromofuran-2-yl)methylene)-2,2-dimethyl-1,3-dioxane-4,6-dione (151 mg, 0.5 mmol, 1 eq) was dissolved in 5 mL tetrahydrofuran. To this solution was added piperidine (59 mL, 51 mg, 0.6 mmol, 1.2 eq). The mixture was stirred at 23 ^{o}C for 10 minutes followed by cooling at 0 ^{o}C for 20 minutes. The reaction mixture was then filtered to collect the precipitated solid, the solid was washed with cold diethyl ether, and dried *in vacuo* to afford 5-(3-bromo-2-oxo-5-(piperidin-1-yl)cyclopent-3-en-1-yl)-6-hydroxy-2,2-dimethyl-4H-1,3-dioxin-4-one **88** (193 mg, 99%) as a white solid. ^{1}H NMR (600 MHz, d_2o) δ 6.55 – 6.50 (m, 1H), 2.47 (d, *J* = 4.1 Hz, 1H), 2.29 (p, *J* = 2.9, 2.4 Hz, 2H), 2.19 (dd, *J* = 34.6, 11.0 Hz, 2H), 1.86 (t, *J* = 12.0 Hz, 2H), 1.37 (dd, *J* = 12.9, 9.7 Hz, 1H), 0.56 (t, *J* = 14.1 Hz, 3H), 0.33 (d, *J* = 40.0 Hz, 6H). ^{13}C NMR (151 MHz, d_2o) δ 194.52, 169.52, 168.03, 149.04, 130.02, 106.82, 67.44, 66.25, 52.18, 48.19, 42.56, 41.59, 25.39, 23.17, 21.47, 19.09. IR (KBr) 3461, 3072, 2990, 2955, 2867, 2661, 2505, 2405, 1736, 1682, 1661, 1571, 1486, 1446, 1408, 1391, 1375, 1363, 1326, 1299, 1259, 1214, 1199, 1178, 1145, 1119, 1063, 1040, 1020, 1005 cm^{-1}. MS (ESI) *m/z* 386.07/388.07 (385.05/387.05 calcd for $C_{16}H_{21}BrNO_5^+$ $[M+H]^+$).

6-hydroxy-2,2-dimethyl-5-(2-oxo-5-(piperidin-1-yl)-3-(p-tolylthio)cyclopent-3-en-1-yl)-4H-1,3-dioxin-4-one (87): 2-(3-bromofuran-2-yl)-1,3-dioxolane was prepared from 3-bromofuran-2-carbaldehyde by the method of Wishka et al.[5] 3-(p-tolylthio)furan-2-carbaldehyde was prepared from 2-(3-bromofuran-2-yl)-1,3-dioxolane by the method of Hartman et al. followed by dioxolane hydrolysis.[6] 2,2-dimethyl-5-((3-(p-tolylthio)furan-2-yl)methylene)-1,3-dioxane-4,6-dione was prepared from 3-(p-tolylthio)furan-2-carbaldehyde by the method of Bigi et al.[1] According to General Procedure A, 2,2-dimethyl-5-((3-(p-tolylthio)furan-2-yl)methylene)-1,3-dioxane-4,6-dione (95 mg, 0.23 mmol, 1 eq) was dissolved in 5 mL tetrahydrofuran. To this solution was added piperidine (34 mL, 29 mg, 0.34 mmol, 1.5 eq). The mixture was stirred at 23 ^{o}C for 10 minutes followed by cooling at 0 ^{o}C for 20 minutes. The reaction mixture was then filtered to collect the precipitated solid, the solid was washed with cold diethyl ether, and dried *in vacuo* to afford 6-hydroxy-2,2-dimethyl-5-(2-oxo-5-(piperidin-1-yl)-3-(p-tolylthio)cyclopent-3-en-1-yl)-4H-1,3-dioxin-4-one **27** (78 mg, 79%) as a white solid. ^{1}H NMR (600 MHz, d_2o) δ 6.21 – 5.99 (m, 2H), 5.99 – 5.89 (m, 2H), 5.21 (d, *J* = 1.3 Hz, 1H), 3.35 (s, 1H), 2.59 (d, *J* = 4.0 Hz, 1H), 2.49 – 2.36 (m, 2H), 2.16 (d, *J* = 8.5 Hz, 2H), 1.71 (t, *J* = 12.6 Hz, 1H), 1.25 (dd, *J* = 23.6, 12.0 Hz, 1H), 0.99 (s, 3H), 0.85 (d, *J* = 1.4 Hz, 2H), 0.62 (d, *J* = 14.9 Hz, 2H), 0.47 (d, *J* = 37.6 Hz, 6H). ^{13}C NMR (151 MHz, d_2o) δ 196.54, 169.82, 168.37, 164.70, 163.73, 151.24, 150.65, 140.19, 132.88, 132.73, 129.53, 121.26, 106.78, 67.25, 66.44, 66.33, 47.46, 44.70, 44.57, 43.55, 23.25, 18.35, 18.26. IR (KBr) 3432, 3058, 2946, 2864, 2661, 2508, 1724, 1679, 1575, 1492, 1449, 1413, 1389, 1373, 1327, 1297, 1261, 1201, 1180, 1149, 1121, 1064, 1019 cm^{-1}. MS (ESI) *m/z* 430.17 (430.16 calcd for $C_{23}H_{28}NO_5S^+$ $[M+H]^+$).

6.4. Chapter 4

General Methods:

All commercially obtained solvents and reagents were used without further purification. Analytical thin-layer chromatography (TLC) was carried out on Merck silica gel 60 F_{254} glass plates and flash column chromatography was performed on Merck silica gel 60 (70 – 230 mesh) or on a Biotage SP1 Flash Purification System using FLASH 40+M cartridges and FLASH 40+ sample cartridges. ^{1}H and ^{13}C solution-state NMR were recorded on a Varian VNMRS 600 (600 MHz for ^{1}H and 150 MHz for ^{13}C) spectrometer or Varian Inova-500 (500 MHz for ^{1}H, and 125 MHz for ^{13}C). Chemical shifts are reported relative to residual solvent peaks (δ 7.26 for $CDCl_3$ in ^{1}H NMR and δ 77.2 for $CDCl_3$ in ^{13}C NMR). IR spectra were obtained using a Thermo-Nicholet Avatar-330 IR spectrometer with ^{1}single-bounce attenuated total reflection (ATR) (Ge crystal) accessory (Smart MIRacle). Gel permeation chromatography (GPC) was performed in chloroform (with 0.25% triethylamine) on a Waters 2695 Separation Module equipped with a Waters 2414 Refractive Index Detecter and a Waters 2996 Photodiode Array Detector. Molecular weights of polymers were calculated relative to linear polystyrene standards unless otherwise noted. Mass spectral data were collected on a Micromass QTOF2 Quadrupole/Time-of Flight Tandem mass spectrometer (ESI-MS).

Synthetic methods

***tert*-butyl (4-(prop-2-yn-1-yloxy)cyclohexyl)carbamate:** To a flame dried 250 mL round bottom flask equipped with a magnetic stir bar was added 1.80 g (8.37 mmols) of *tert*-butyl (4-hydroxycyclohexyl)carbamate and 100 mL dry THF. The solution was cooled to 0 °C and 301 mg (12.6 mmols) of NaH was added slowly. The solution was subsequently allowed to

warm to room temperature and stir for 1 hour. The solution was cooled back to 0 °C and potassium iodide (1.66 g, 10.0 mmols) and catalytic 18-crown-6 were added before the dropwise addition of propargyl bromide (1.12 mL of 80 wt. % solution in toluene, 12.6 mmols). The solution was allowed to warm to room temperature and stirred for 12 hours. The reaction was quenched into 100 mL of 1.0 M HCl and extracted ×3 with 40 mL EtOAc. The organic layers were combined, washed with brine and dried over anhydrous Na_2SO_4. Column chromatography on silica gel (0 to 10 % EtOAc:Hexane) yielded the product as a crystalline solid (1.38 g, 65 % yield). ^{1}H NMR (600 MHz, $CDCl_3$) δ 4.39 (m, 1H), 4.15 (d, 2H, *J*=6 Hz), 3.43 (m, 1H), 2.38 (t, 1H, *J*=6 Hz), 2.01 (m, 4H), 1.41 (s, 9H), 1.34 (q, 2H, *J*=12 Hz), 1.14 (q, 2H, *J*=12 Hz); ^{13}C-NMR (150 MHz, $CDCl_3$) δ 155.4, 80.4, 79.4, 76.1, 74.1, 55.4, 49.1, 31.1, 30.4, 28.6; IR (ATR) 3305, 3285, 2979, 2939, 2862, 1694, 1670, 1534, 1454, 1364, 1314, 1274, 1174, 1082, 1051, 992, 895, 670 cm^{-1}; MS (TOF-ESI) calcd for $C_{14}H_{23}NO_3Na$ $[M+Na]^+$: 276.1576, found $[M+Na]^+$: 276.1582.

4-(prop-2-yn-1-yloxy)cyclohexaneamine: To a 100 mL round bottom flask equipped with a magnetic stir bar was added 30 mL of dry dichloromethane and 690 mg (2.73 mmols) of *tert*-butyl (4-(prop-2-yn-1-yloxy)cyclohexyl)carbamate. The solution was cooled to 0 °C and 1.25 mL (16.4 mmols) trifluoroacetic acid was added dropwise. The reaction mixture was allowed to warm to room temperature and stirred until all starting material was consumed as judged by TLC (~5 hours). The reaction mixture was quenched into 20 mL 1.0 M HCl and extracted ×2 with EtOAc. The aqueous layer was made basic by the addition of $NaHCO_3$, 20 mL brine was added, and extracted ×3 with dichloromethane. The organic layers were combined, dried with anhydrous Na_2SO_4, and the solvent removed to yield the desired product as a crystalline solid (310 mg, 74 % yield). ^{1}H NMR (600 MHz, $CDCl_3$) δ 4.14 (d, 2H, *J*=6

Hz), 3.41 (m, 1H), 2.66 (m, 1H), 2.37 (t, 1H, *J*=6Hz), 2.00 (m, 2H), 1.85 (m, 2H), 1.38 (s, 2H), 1.27 (q, 2H, *J*=12 Hz), 1.11 (q, 2H, *J*=12 Hz); ^{13}C-NMR (150 MHz, $CDCl_3$) δ 80.5, 76.7, 73.9, 55.4, 49.9, 34.5, 30.59; IR (ATR) 3286, 2930, 2858, 2112, 1575, 1452, 1356, 1260, 1084, 1013, 931, 799 cm^{-1}; MS (TOF-EI) calcd for $C_9H_{14}NO$ $[M-H]^+$: 152.1075, found $[M-H]^+$: 152.1072.

1-(3,5-bis(trifluoromethyl)phenyl)-3-(4-(prop-2-yn-1-yloxy)cyclohexyl)thiourea (1): To a 50 mL round bottom flask equipped with a magnetic stir bar was added 10 mL of dry dichloromethane and 205 mg (1.33 mmols) of 4-(prop-2-yn-1-yloxy)cyclohexaneamine. The solution was cooled to 0 °C and 0.243 mL (1.33 mmols) of 3,5-bis(trifluoromethyl) phenylisothiocyanate was added dropwise. The reaction mixture was allowed to warm to room temperature and stirred for 12 hours. The solvent was removed and the solid was recrystallized from a hexanes:DCM mixture to yield the product as a crystalline solid (537 mg, 95 % yield). ^{1}H NMR (600 MHz, $CDCl_3$) δ 8.30 (bs, 1H), 7.75 (s, 2H), 7.70 (s, 1H), 5.99 (bs, 1H), 4.21 (m, 1H), 4.18 (d, 2H, *J*=6 Hz), 3.49 (m, 2H), 2.40 (t, 1H, *J*=6 Hz), 2.18 (m, 2H), 2.05 (m, 2H), 1.44 (q, 2H, *J*=12 Hz), 1.27 (q, 2H, *J*=12 Hz); ^{13}C-NMR (150 MHz, $CDCl_3$) δ 179.8, 139.0, 133.3 (q, *J*=33 Hz), 124.1, 122.9 (q, *J*=271.5 Hz), 119.7, 80.2, 75.6, 74.4, 55.6, 53.5, 30.1, 30.0; IR (ATR) 3273, 3218, 3044, 2947, 2859, 2112, 1543, 1531, 1455, 1379, 1273, 1165, 1127, 1076, 896, 699, 681 cm^{-1}; MS (TOF-ESI) calcd for $C_{18}H_{18}F_6N_2OSNa$ $[M+Na]^+$: 447.0942, found $[M+Na]^+$: 447.0916.

Azide-dimethylbarbitiuc acid DASA photoswitch (3): To a 20 mL scintillation vial equipped with a magnetic stir bar was added 463 mg (2.72 mmols) of 6-azido-*N*-ethylhexan-1-amine and 1.50 mL THF. A solution of 5-(furan-2-ylmethylene)-1,3-dimethylbarbitiuc

acid (637 mg, 2.72 mmols) in 1.50 mL THF was added dropwise at room temperature. The reaction mixture was allowed to stir for 6 hours. The THF was removed and column chromatography (3 % MeOH:DCM) provided the product as a purple solid (837 mg, 76 % yield). ^{1}H NMR (600 MHz, $CDCl_3$) δ 12.51 (d, 1H, *J*=6 Hz), 7.22 (m, 1H), 7.11 (d, 1H, *J*=6 Hz), 6.73 (d, 1H, *J*=12 Hz), 6.04 (dt, 1H, *J*=12 & 12 Hz), 3.46 (qn, 2H, *J*=6 Hz), 3.40 (q, 2H, *J*=12 Hz), 3.33 (s, 3H), 3.32 (s, 3H), 3.27 (t, 2H, *J*=6 Hz), 1.67 (m, 2H), 1.58 (m, 2H), 1.42-1.30 (m, 4H), 1.31 (t, 3H, *J*=6 Hz); ^{13}C-NMR (150 MHz, $CDCl_3$) δ 165.0, 163.3, 156.8, 156.7, 151.9, 150.9, 146.5, 139.2, 139.0, 102.8, 102.5, 98.4,57.0, 52.1, 51.1, 49.1, 44.3, 28.9, 28.6, 28.4, 28.2, 27.0, 26.5, 26.3, 26.2, 26.0 14.5, 12.2; IR (ATR) 3288, 3047, 2937, 2861, 2094, 1691, 1615, 1594, 1559, 1495, 1462, 1412, 1364, 1203, 1135, 1076, 968, 775 cm^{-1}; MS (TOF-ESI) calcd for $C_{19}H_{28}N_6O_4Na$ $[M+Na]^+$: 427.2070, found $[M+Na]^+$: 427.2065.

DASA-thiourea organic catalyst (4): To a 50 mL round bottom flask equipped with a magnetic stir bar was added 10 mL of THF, 312 mg (0.771 mmols) of azide-dimethylbarbitiuc acid DASA photoswitch, 327 mg alkyne thiourea (0.771 mmols), and 7.0 mg (0.386 mmols) of pentamethyldiethyltriamine. The reaction mixture was subjected to three freeze-pump-thaw cycles, backfilled with argon, and 5 mg CuBr was added. The reaction mixture was stirred for 5 hours, the solvent removed, and column chromatography (5 % MeOH:DCM) provided the product as a purple solid (423 mg, 67 % yield). ^{1}H NMR (600 MHz, $CDCl_3$) δ 12.51 (d, 1H, *J*=24 Hz); 9.12 (s, 1H), 8.07 (d, 2H, *J*=6 Hz), 7.59 (d, 1H, *J*=24 Hz), 7.55 (s, 1H), 7.42 (bs, 1H), 7.28 (m, 1H), 6.98 (d, 1H, *J*=6 Hz), 6.72 (dd, 1H, *J*=6 & 12 Hz), 6.04 (dt, 1H, *J*=12 & 24 Hz), 4.63 (s, 2H), 4.35 (q, 2H, *J*=6 Hz), 4.27 (bs, 2H), 3.46 (q, 2H, *J*=6 Hz), 3.44-3.35 (m, 4H), 3.32 (s, 6H), 2.19 (bs, 2H), 2.04 (bs, 2H), 1.90 (q,

2H, *J*=12 Hz), 1.64 (m, 2H), 1.42-1.28 (m, 12H), 1.26 (t, 3H, *J*=6 Hz); ^{13}C-NMR (150 MHz, $CDCl_3$) δ 180.1, 164.9, 163.6, 158.0, 157.6, 152.1, 151.8, 151.7, 146.5, 145.8, 140.8, 137.4, 131.6 (q, *J*=33 Hz), 123.1 (q, *J*=271.5 Hz), 123.1, 122.7, 103.4, 103.3, 97.6, 61.7, 56.9, 53.4, 52.4, 50.2, 50.1, 49.1, 44.5, 30.9, 30.5, 30.0, 29.9, 29.8, 28.6, 28.5, 28.3, 26.8, 26.0, 25.9, 25.9, 25.7, 14.4, 12.2; IR (ATR) 3293, 3053, 2927, 2856, 1692, 1609, 1594, 1557, 1458, 1412, 1348, 1273, 1201, 1115, 1070, 960, 880, 773, 679 cm^{-1}; MS (TOF-ESI) calcd for $C_{37}H_{46}F_6N_8O_5SNa$ $[M+Na]^+$: 851.3114, found $[M+Na]^+$: 851.3098.

1,3-dioctylpyrimidine-2,4,6(1*H*,3*H*,5*H*)-trione: To a solution of n-octyl amine (2.00 g, 15.48 mmol) in 100 mL dichloromethane was added a solution of n-octyl isocyanate (2.73 mL, 15.48 mmol) in 30 mL dichloromethane under argon. The mixture was stirred at room temperature for 1 h. After malonyl chloride (1.51 mL, 15.48 mmol) was added, the mixture was heated at reflux for 1 h. The mixture was allowed to cool to room temperature and was quenched with 1 N HCl (60 mL). The crude product was extracted with dichloromethane (3 x 70 mL) and the combined organic phases were washed with H_2O (1 x 50 mL), dried over $MgSO_4$ and filtered. Solvent was removed under vacuo. Purification by flash column chromatography (hexane:EtOAc = 9:1 to 4:1) gave 4.80 g (88% yield) of the product as yellow oil. ^{1}H NMR (500 MHz, Methylene Chloride-d_2) δ 3.84 – 3.81 (m, 4H), 3.61 (s, 2H), 1.68 – 1.48 (m, 4H), 1.40 – 1.19 (m, 20H), 0.88 (t, *J* = 6.6 Hz, 6H); ^{13}C NMR (126 MHz, cd_2cl_2) δ 165.2, 152.0, 42.5, 40.4, 32.4, 29.8, 29.8, 28.5, 27.4, 23.2, 14.4. IR (NaCl) 2957, 2926, 2856, 1707, 1682, 1443, 1413, 1369, 1320, 1286, 1227, 1167, 937, 760, 723 cm^{-1}. HRMS (EI+) *m/z* 352.2725 (352.2726 calc'd for $C_{20}H_{36}N_2O_3^+$ $[M]^+$).

5-(Furan-2-ylmethyl)-1,3-dioctylpyrimidine-2,4,6(1*H*,3*H*,5*H*)-trione: 1,3-dioctylpyrimidine-2,4,6(1*H*,3*H*,5*H*)-trione (4.80 g, 13.6 mmol) in H_2O (27 mL) was treated with 2-furaldehyde (1.13 mL, 13.6 mmol). The mixture was stirred at room temperature for 2 h. The yellow waxy solid was extracted by dichloromethane (3 x 30 mL). Combined organic phases was dried over $MgSO_4$, filtered and the solvent was removed in vacuo to give 1.55 g (26 % yield) of 5-(Furan-2-ylmethyl)-1,3-dioctylpyrimidine-2,4,6(1*H*,3*H*,5*H*)-trione as a light yellow powder. ^{1}H NMR (500 MHz, Methylene Chloride-d_2) δ 8.52 (d, J = 4.0 Hz, 1H), 8.27 (s, 1H), 7.77 (dd, J = 1.7, 0.6 Hz, 1H), 6.66 (ddd, J = 3.8, 1.7, 0.8 Hz, 1H), 3.87 – 3.82 (m, 4H), 1.53 (m, 4H), 1.33 – 1.11 (m, 20H), 0.85 – 0.73 (m, 6H). ^{13}C NMR (126 MHz, cd_2cl_2) δ 162.6, 161.2, 151.8, 150.7, 140.7, 127.8, 115.5, 112.8, 42.9, 32.4, 29.9, 29.8, 28.6, 27.5, 23.2, 14.4. IR (NaCl) 3145, 3115, 2955, 2922, 2853, 1725, 1670, 1660, 1580, 1466, 1449, 1432, 1410, 1386, 1361, 1334, 1297, 1270, 1256, 1201, 1164, 1128, 1095, 1031, 883, 792, 754 cm^{-1}. HRMS (EI+) *m/z* 430.2834 (430.2832 calc'd for $C_{25}H_{38}N_2O_4$ $[M]^+$).

(Z)-5-((2Z,4E)-5-((6-azidohexyl)(ethyl)amino)-2-hydroxypenta-2,4-dien-1-ylidene)-1,3-dioctylpyrimidine-2,4,6(1*H*,3*H*,5*H*)-trione: To a solution of 5-(Furan-2-ylmethyl)-1,3-dioctylpyrimidine-2,4,6(1*H*,3*H*,5*H*)-trione (1.00 g, 2.32 mmol) in 2.6 mL tetrahydrofuran was added a solution of 6-azido-N-ethylhexan-1-amine (0.43 mL, 2.44 mmol) in 2.0 mL tetrahydrofuran. The mixture was stirred at room temperature for 17 h. Purification by flash column chromatography gave 1.09 g of (Z)-5-((2Z,4E)-5-((6-azidohexyl)(ethyl)amino)-2-hydroxypenta-2,4-dien-1-ylidene)-1,3-dioctylpyrimidine-2,4,6(1*H*,3*H*,5*H*)-trione as purple viscous oil in 78 % yield. ^{1}H NMR (500 MHz, Methylene Chloride-d_2) δ 12.54 (s, 1H), 7.26 (dd, J = 27.9, 12.2 Hz, 1H), 7.08 (s, 1H), 6.79 (dd, J = 12.4, 1.4 Hz, 1H), 6.06 (t, J = 12.3 Hz, 1H), 3.99 – 3.75 (m, 4H), 3.56 – 3.34 (m, 4H), 3.28 (m, 2H), 1.70 (m, 2H), 1.65 – 1.51

(m, 6H), 1.41 (m, 4H), 1.37 – 1.19 (m, 23H), 0.88 (m, 6H). ^{13}C NMR (126 MHz, cd_2cl_2) δ 165.5, 157.6, 151.8, 151.1, 146.9, 139.1, 139.0, 102.8, 42.1, 42.0, 32.4, 32.2, 30.0, 29.8, 29.2, 28.8, 28.7, 28.7, 27.6, 27.2, 23.2, 23.2, 14.4, 14.4. IR (NaCl) 2956, 2930, 2857, 2096, 1694, 1623, 1599, 1557, 1498, 1459, 1429, 1407, 1368, 1341, 1266, 1226, 1204, 1144, 1110, 1088, 970, 907, 839, 780, 760, 730, 687 cm^{-1}. HRMS (ESI+) *m/z* 623.4234 (623.4261 calc'd for $C_{33}H_{56}N_6O_4Na^+$ $[M + Na]^+$).

Donor-Acceptor Stenhouse Adduct appended to poly(ethylene glycol) (DASA-PEG) (6a): To a stirring mixture of poly(ethylene glycol) (112 mg, 0.037 mmol), $CuSO_4$-$5H_2O$ (1.0 mg, 0.0037 mmol) and sodium ascorbate (1.5 mg, 0.0074 mmol) in 1.0 mL water was added (Z)-5-((2Z,4E)-5-((6-azidohexyl)(ethyl)amino)-2-hydroxypenta-2,4-dien-1-ylidene)-1,3-dioctylpyrimidine-2,4,6(1*H*,3*H*,5*H*)-trione (67 mg, 0.112 mmol) dissolved in minimum amount of acetone. The mixture was heated to 50 ^{0}C in a water bath for 19 h. After the mixture was cooled to room temperature, the product was extracted with dichloromethane (4 x 20 mL). The crude product was precipitated twice into diethyl ether, yielding 83 mg (62 % yield) of DASA-PEG **6a** as a purple solid. ^{1}H NMR (600 MHz, Methylene Chloride-d_2) δ 12.54 (d, *J* = 11.2 Hz, 1H), 7.67 (s, 1H), 7.24 (dd, *J* = 28.9, 12.2 Hz, 1H), 7.09 (s, 1H), 6.77 (dd, *J* = 12.4, 4.6 Hz, 1H), 6.10 – 5.99 (m, 1H), 4.62 (dd, *J* = 4.8, 2.1 Hz, 2H), 4.34 (dd, *J* = 8.7, 6.9 Hz, 2H), 3.86 (dt, *J* = 15.0, 7.6 Hz, 4H), 3.60 (s, 259H), 3.34 (s, 3H), 2.92 (s, 2H), 2.80 (s, 2H), 2.07 – 1.86 (m, 8H), 1.36 – 1.19 (m, 27H), 0.87 (dt, *J* = 7.2, 3.4 Hz, 6H). IR (NaCl) 2879, 2095, 1679, 1467, 1359, 1343, 1279, 1147, 1113, 1061, 842, 597 cm^{-1}.

Polymerization:

To a dry 1 dram vial equipped with a magnetic stir bar and a Teflon cap was added D,L-lactide (30 mg, 0.208 mmols), **4** (17 mg, 0.0208 mmols), and pyrene butanol (0.5 mg,

0.00208 mmols) and evacuated and backfilled with argon. Dry $CDCl_3$ (175 μL, 1.2 M) and dry pentamethyldiethylenetriamine (9 μL, 0.0416 mmols) were added under inert atmosphere and the reaction mixture was allowed to stir for 48 hours at 30 °C.

Recycling procedure:

The $CDCl_3$ was removed under vacuum and the mixture was dissolved in 0.2 mL THF and diluted with 4.8 mL benzene. The solution was layered over 10 mL deionized H_2O, placed in a light box and irradiated for 1 hour with visible light (578 nm peak wavelength) while stirring. The water layer was removed, 10 mL fresh DI water was added, and the solution was again irradiated for one hour. The water layer was removed and combined with the previous extraction, made acidic by the addition of 5 mL 1 N HCl, and extracted ×3 with 20 mL dichloromethane. The organic layers were combined, washed with brine, dried over Na_2SO_4, concentrated, and run over a plug of silica (5% MeOH:DCM) to yield the pure catalyst as a dark red solid (11.6 mg, 70% recovery).

^{1}H-NMR titration experiments

This procedure constitutes a slightly modified version from previous studies.[7] C_6D_6 was stirred over CaH_2 for 24 hours and distilled. Stock solutions of thiourea, caprolactone, and the diethyl DASA photoswitch were prepared in dry C_6D_6. The chemical shift of the thiourea N–H protons was found to be independent of concentration between 0.05 and 0.01 M; thus, those all spectra were obtained within that concentration range.

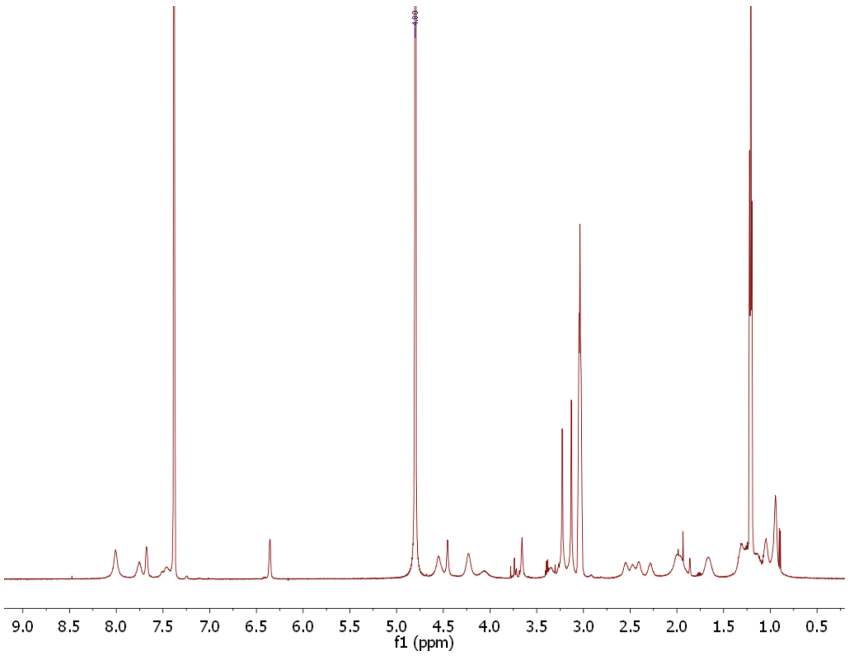

Figure S9. NMR spectra of D_2O layer after photoswitching and phase transfer of **4**

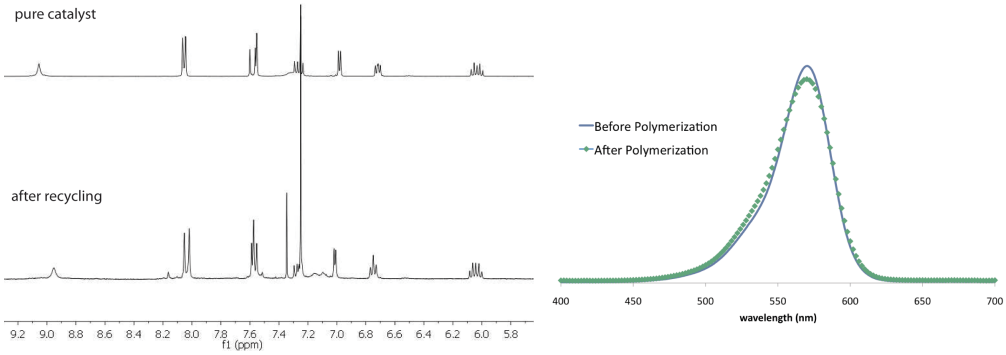

Figure S10. Comparison of **4** before and after recycling.

Preparation of micelle solutions with Nile Red:

The stock solutions were prepared according to the procedure used by Fréchet and coworkers.[8] Briefly, 12.5 µL of Nile Red stock solution in dichloromethane (0.05 mg/mL) was added to a 4 mL vial. This vial was placed under vacuum until the solvent was completely removed. An aqueous DASA-PEG amphiphile **(6a)** stock solution at concentration of 2 mg/mL was prepared and added to this vial. Deionized water was added to dilute the solution to 2 mL with desired concentration. This solution was stirred vigorously for 10 minutes and then allowed to equilibrate at room temperature for 1 hour.

Critical Micelle Concentration Studies:

Fluorescence measurements were obtained using a Cary Eclipse spectrophotometer (Varian, Inc.) with a quartz fluorescence cuvette (1 x 1 x 0.2 cm) with the following settings: excitation wavelength of 550 nm, excitation slit width = 5 nm, emission slit width = 10 nm, range = 560 nm to 700 nm and scan speed = 30 nm/min.

Kinetic Studies:

A set of micelle solutions of same concentration containing Nile Red was prepared as described above and transferred to vials. All vials were transferred to a Rayonet photoreactor RPR-200, irradiated at 575 nm for desired amounts of time and taken out for fluorescence measurement. Same settings were used for fluorescence measurement.

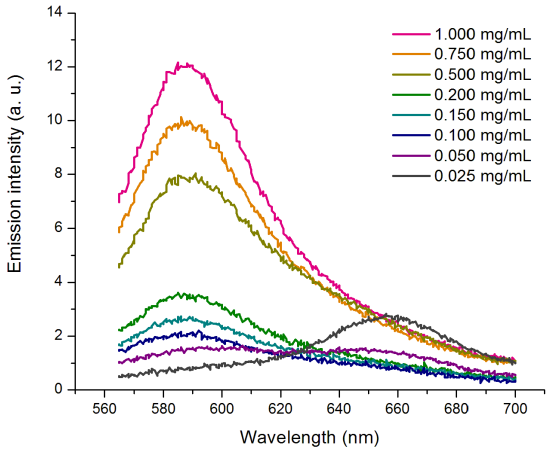

Figure S11. Fluorescence emission spectrum of Nile red with varying concentrations of DASA-PEG amphiphile **(6a)** in water. At low concentrations, maximum emission occurs around 660 nm. As concentrations increase, maximum emission blue shifts indicating encapsulation of Nile red within the core of micelles.

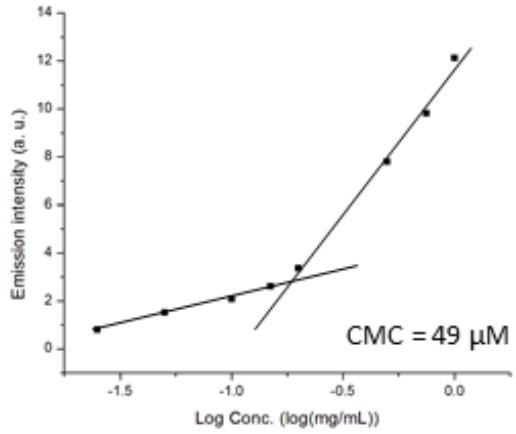

Figure S12. A plot of relative intensity as a function of log of concentration of **6a**. Non-linear relationship suggests that the inflection point (28 µM) is the critical micelle concentration (CMC).

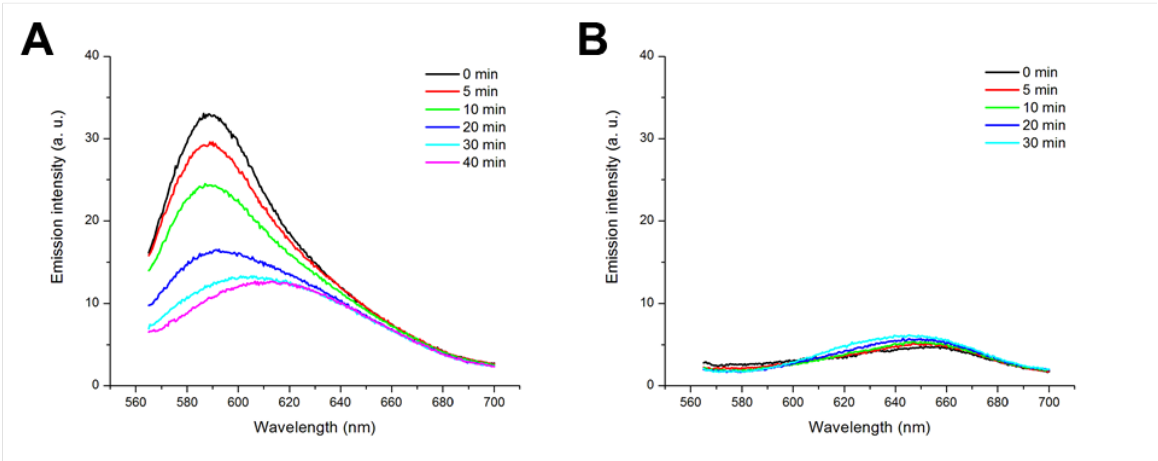

Figure S13. Fluorescence emission spectra of Nile Red in (A) 0.50 mg/mL and (B) 0.05 mg/mL of **6a** in water at various times of visible light irradiation. A noticeable red shift and decrease in emission intensity were observed as light irradiation continued (left), whereas minimum change occurred at the concentration below CMC (right).

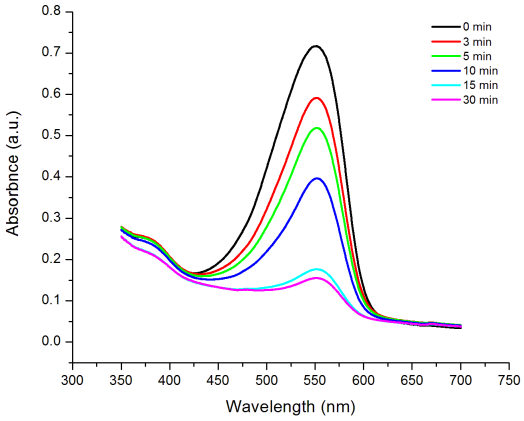

Figure S14. UV-Vis spectra of **6a** at 0.50 mg/mL in water at various time points of visible light (570 nm) irradiation Almost complete structural conversion from the extended form to the closed form is observed after 30 minutes of irradiation, This data corresponds to the minimum change that occurred in the emission spectrum of Nile red after the same time of irradiation.

6.5. References

(1) Bigi, F.; Carloni, S.; Ferrari, L.; Maggi, R.; Mazzacani, A.; Sartori, G. *Tetrahedron Lett.* **2001**, *42* (31), 5203.

(2) Deb, M. L.; Bhuyan, P. J. *Tetrahedron Lett.* **2005**, *46* (38), 6453.

(3) Bello, K. A.; Cheng, L.; Griffiths, J. *J. Chem. Soc. Perkin Trans. 2* **1987**, No. 6, 815.

(4) Gronowitz, S.; Westerlund, C.; Hörnfeldt, A.-B.; Wahren, R.; Schroll, G.; Altona, C. *Acta Chem. Scand.* **1975**, *29b*, 224.

(5) Wishka, D. G.; Walker, D. P.; Yates, K. M.; Reitz, S. C.; Jia, S.; Myers, J. K.; Olson, K. L.; Jacobsen, E. J.; Wolfe, M. L.; Groppi, V. E.; Hanchar, A. J.; Thornburgh, B. A.; Cortes-Burgos, L. A.; Wong, E. H. F.; Staton, B. A.; Raub, T. J.; Higdon, N. R.; Wall, T. M.; Hurst, R. S.; Walters, R. R.; Hoffmann, W. E.; Hajos, M.; Franklin, S.; Carey, G.; Gold, L. H.; Cook, K. K.; Sands, S. B.; Zhao, S. X.; Soglia, J. R.; Kalgutkar, A. S.; Arneric, S. P.; Rogers, B. N. *J. Med. Chem.* **2006**, *49* (14), 4425.

(6) Hartman, G. D.; Halczenko, W.; Smith, R. L.; Sugrue, M. F.; Mallorga, P. J.; Michelson, S. R.; Randall, W. C.; Schwam, H.; Sondey, J. M. *J. Med. Chem.* **1992**, *35* (21), 3822.

(7) Lohmeijer, B. G. G.; Pratt, R. C.; Leibfarth, F.; Logan, J. W.; Long, D. A.; Dove, A. P.; Nederberg, F.; Choi, J.; Wade, C.; Waymouth, R. M.; Hedrick, J. L. *Macromolecules* **2006**, *39* (25), 8574.

(8) Goodwin, A. P.; Mynar, J. L.; Ma, Y.; Fleming, G. R.; Fréchet, J. M. J. *J. Am. Chem. Soc.* **2005**, *127* (28), 9952.